



THE UNIVERSITY OF  
**WAIKATO**  
*Te Whare Wānanga o Waikato*

Research Commons

<http://researchcommons.waikato.ac.nz/>

## Research Commons at the University of Waikato

### Copyright Statement:

The digital copy of this thesis is protected by the Copyright Act 1994 (New Zealand).

The thesis may be consulted by you, provided you comply with the provisions of the Act and the following conditions of use:

- Any use you make of these documents or images must be for research or private study purposes only, and you may not make them available to any other person.
- Authors control the copyright of their thesis. You will recognise the author's right to be identified as the author of the thesis, and due acknowledgement will be made to the author where appropriate.
- You will obtain the author's permission before publishing any material from the thesis.

**DEVELOPMENTAL GENE EXPRESSION PROFILE OF  
*VMO1* IN THE MOUSE AUDITORY SYSTEM**

A thesis submitted in partial fulfilment  
of the requirements for the degree

of

**Masters of Science  
in Biological Sciences**

at

**The University of Waikato**

by

**Blaise Kelly Erin Forrester-Gauntlett**

---

The University of Waikato

2013



THE UNIVERSITY OF  
**WAIKATO**  
*Te Whare Wānanga o Waikato*

# ABSTRACT

Hearing loss (HL) is a sensory disorder that affects an estimated 250 million people worldwide and can greatly affect quality of life. In New Zealand, more than 10% of the population is affected by HL with the Māori population being overrepresented among all age groups. Therefore, understanding the mechanism of HL is extremely important for the development of new pharmaceuticals for the prevention or treatment of HL disorders.

The main aim of the research undertaken in this thesis was to characterise the function of the *Mus musculus* (mouse) vitelline membrane outer layer one (*Vmo1*) gene. This gene is considered an excellent candidate for being involved in human HL and/or balance disorders. Our hypothesis is based on its restricted gene localisation within the mouse inner ear and the postulated function of Reissner's membrane.

Two methods were used to address this aim. Firstly, comparative genomics was used to determine the level of nucleotide and amino acid conservation of *VMO1* across mammalian species, and to search for DNA motifs that may imply a biological function. Secondly, molecular biology and histochemical techniques were used to DNA sequence the *Vmo1* gene, detect the expression of 22 kDa VMO1 protein within mouse tissues, and to localise the expression of VMO1 protein within the mouse inner ear.

Comparative genomics results showed *VMO1* to be highly conserved across 36 species. An in-depth analysis of the differences and similarities between the mouse, human and chicken indicated a high level of gene conservation with an even greater degree of identity and similarity seen at a proteomic level. In addition, a high level of conservation across amino acids involved in the formation and stabilisation of the three dimensional structure. Thus, results suggest an important function for the VMO1 protein.

Two commercial VMO1 antibodies were purchased to determine the localisation of the mouse VMO1 protein. They were validated for specificity using western

blot analysis of protein lysates dissected from postnatal day 28 mice (P28). VMO1 was identified within the inner ear protein lysate and tear gland protein lysate of an expected molecular weight size of 20-37kDa with additional binding observed in the ear sample at 250kDa.

Immunohistochemistry detected high concentrations of VMO1 protein within the tectorial membrane (TM) and inner pillar cells (IPC) in inner ear sections from the mouse at P5. In agreement with the comparative genomics analysis, VMO1 is a secreted protein.

The movement of the hair cells (HC) relative to the TM is essential for the transduction of sound into electrical signals. The IPC act as supporting cells for the hair cells, and help to couple movement of the basilar membrane to the HC. In conclusion, the importance of the TM and IPC in hearing function, and the localisation of the VMO1 protein within these structures implies an important role for VMO1 in hearing function. We recommend further studies to examine the specificity of the VMO1 antibody, and the development of a *Vmo1* knockout mouse to support the functional analysis of *Vmo1* in the auditory system.



# ACKNOWLEDGEMENTS

First and foremost I would like to acknowledge my supervisor Dr. Linda Peters. Thank you for taking me on as a student and for all of your knowledge and enthusiasm in the lab and in the writing of this thesis. Your encouragement and your calm and patient attitude has made me a more confident researcher and a better mother. Without your support and guidance this wouldn't have been possible. From myself and my family a huge heartfelt thank you.

Thank you to Olivia Patty for answering all of my questions and proofreading my thesis and for all of your technical help, advice and training in the lab.

Thank you to Greg Jacobson, Ray Cursons, Judith Burrows, Barry O'Brien, Emma Summers, Jo Hobbs, Bruce Patty, Logan Voss and Steve Bird for their training and expertise. To everyone else in the Molecular Genetics lab thank you for your help and for keeping me company. Thank you to Kevin Eastwood and Yvonne Taura for your support through, and employment with, the Māori Mentoring unit.

For funding over the past three years I would like to thank the HRC Māori Masters Research Scholarship, the University of Waikato Māori Excellence Awards and my Iwi Ngati Ranginui for the Ngati Ranginui Iwi Grant and the Turirangi Te Kani Memorial Scholarship.

To mum and dad thank you for proofreading my thesis and for all of your support through "22 bloody years of education". To my little sister Kelly thank you for helping me find time to write and for putting up with my procrastination calls and pretending you're interested in the "dead mice ears" stuff.

To my partner Kevin thank you for your unwavering support and patience throughout Uni and especially during the writing of this thesis, it's been a fun and interesting ride and I couldn't imagine doing it with anyone else. And yes, it's finished. Finally.

Last but not least, my baby girl Sierra who has been right there with me for all of the writing and for most of my research. Mummy loves you.

# ETHICS STATEMENT

Animal ethics approval for this study was received from the University of Waikato (UoW) Animal Ethics Committee in May 2012 (Protocol number: 853, Appendix 4) and all provisions outlined by the approval were adhered to. Training was received for the humane euthanasia of mice which were euthanised with CO<sub>2</sub> and then decapitated according to Standard Operating Procedure number 9 (SOP#9, UoW Appendix 6). Wild type C57/B16/129SV mice were dissected in the animal house at the UoW and further processed in the Molecular Genetics laboratory (C.2.03, UoW). In total, 14 adult mice (two male, 12 female) over postnatal 28 days old (P28+) and four P5 mice pups were used for this thesis. Eleven of the adult mice were acquired from another study, in which the ears were donated from a deceased mouse and thus, did not require ethics approval.

# TABLE OF CONTENTS

<b>ABSTRACT .....</b>	<b>II</b>
<b>ACKNOWLEDGEMENTS .....</b>	<b>IV</b>
<b>ETHICS STATEMENT .....</b>	<b>V</b>
<b>TABLE OF CONTENTS.....</b>	<b>VI</b>
<b>LIST OF FIGURES .....</b>	<b>XII</b>
<b>LIST OF TABLES AND EQUATIONS .....</b>	<b>XV</b>
<b>ABBREVIATIONS .....</b>	<b>XVI</b>
<b>CHAPTER ONE LITERATURE REVIEW AND INTRODUCTION .....</b>	<b>1-1</b>
<b>1.1 Hearing Loss .....</b>	<b>1-1</b>
1.1.1 Classification of Hearing Loss.....	1-4
<b>1.2 Biology of the Mammalian Ear .....</b>	<b>1-6</b>
1.2.1 Use of the Mouse as an Animal Model for Human Hearing Loss.....	1-7
1.2.2 Outer and Middle Ear .....	1-8
1.2.3 Inner Ear .....	1-9
1.2.3.1 Cochlea .....	1-10
1.2.3.2 Organ of Corti.....	1-11
1.2.3.3 Tectorial Membrane.....	1-14
1.2.3.4 Reissner’s Membrane .....	1-15
<b>1.3 Vitelline Membrane Outer Layer 1 Protein.....</b>	<b>1-15</b>
1.3.1 VM01 in the Vitelline Membrane of the Chicken Egg .....	1-15
1.3.2 <i>Vmo1</i> in Reissner’s Membrane of the Mouse Inner Ear .....	1-16
<b>1.4 Hypothesis, Aims and Objectives .....</b>	<b>1-17</b>
1.4.1 Hypothesis.....	1-17
1.4.2 Aim.....	1-18
1.4.3 Objectives .....	1-18

<b>CHAPTER TWO COMPARATIVE GENOMICS .....</b>	<b>2-19</b>
<b>2.1 Nucleotide Comparison of <i>VMO1</i> in Different Species.....</b>	<b>2-19</b>
2.1.1 Prediction of Open Reading Frames .....	2-25
2.1.2 Nucleotide Sequence Comparison of the Mouse, Human and Chicken <i>VMO1</i> .....	2-27
2.1.2.1 Genomic Structure of Mouse <i>Vmo1</i> .....	2-27
2.1.2.2 Genomic Structure of Human <i>VMO1</i> .....	2-28
2.1.2.3 Genomic Structure of Chicken <i>VMO1</i> .....	2-31
2.1.3 Summary of <i>VMO1</i> Genomic Structure .....	2-31
<b>2.2 Characterisation of the Chicken <i>VMO1</i> Protein .....</b>	<b>2-34</b>
2.2.1 Chemical Characteristics and Amino Acid Sequence .....	2-34
2.2.2 Greek Key Motif.....	2-36
2.2.3 3D Crystal Structure of <i>VMO1</i> .....	2-36
2.2.3.1 Internal Three-Fold Symmetry of <i>VMO1</i> .....	2-37
2.2.3.2 Triangular Prism Structure .....	2-39
2.2.3.3 Structure Stabilisation.....	2-40
2.2.3.4 Active Site Cleft.....	2-41
<b>2.3 Analysis of <i>VMO1</i> Protein Homology across 36 Species .....</b>	<b>2-43</b>
2.3.1 Analysis of Homology between the Mouse, Human and Chicken <i>VMO1</i> Protein .....	2-47
2.3.2 Summary of <i>VMO1</i> Protein Structure .....	2-48
<b>CHAPTER THREE METHODS AND MATERIALS .....</b>	<b>3-51</b>
<b>3.1 Agarose Gel Electrophoresis.....</b>	<b>3-51</b>
<b>3.2 Purification and Isolation of Nucleotide Products .....</b>	<b>3-52</b>
3.2.1 PEG Precipitation .....	3-52
3.2.2 Phenol/Chloroform Method.....	3-52
3.2.3 rAPid Alkaline Phosphatase Method .....	3-53
3.2.4 Gel Purification.....	3-53
<b>3.3 Nucleotide Product Quantification and Quality Assessment.....</b>	<b>3-54</b>
3.3.1 Agarose Gel Electrophoresis .....	3-54
3.3.2 Nanodrop Reading.....	3-54
<b>3.4 PCR Reactions.....</b>	<b>3-55</b>
3.4.1 Nested PCR.....	3-55
3.4.2 Colony PCR.....	3-56

<b>3.5</b>	<b>SDS-PAGE .....</b>	<b>3-56</b>
3.5.1	Protein Sample Preparation .....	3-57
3.5.2	Gel Electrophoresis .....	3-57
3.5.3	Visualisation of SDS PAGE Gel .....	3-58
<b>3.6</b>	<b>Cloning and Expression of <i>Vmo1</i> .....</b>	<b>3-58</b>
3.6.1	Preparation of Electrocompetent Cells .....	3-58
3.6.2	Transformation of Vector into DH5 $\alpha$ <i>E. coli</i> .....	3-59
3.6.3	Cloning <i>Vmo1</i> into TA TOPO Cloning Vector .....	3-60
3.6.4	Ligation of the <i>Vmo1</i> Transcript into the pProEX HTb Vector .....	3-60
3.6.4.1	Preparation of pProEX HTb Vector and <i>Vmo1</i> PCR Amplicon .....	3-60
3.6.4.2	Restriction Enzyme Digestion .....	3-61
3.6.4.3	T-Tailing Reaction .....	3-61
3.6.4.4	Ligation .....	3-61
3.6.5	Screening and Sub-cloning of Transformed Colonies using Colony PCR .....	3-62
<b>3.7</b>	<b>Preparation of RNA and Protein from Mouse Tissues.....</b>	<b>3-62</b>
3.7.1	Extraction of mRNA for cDNA Production .....	3-62
3.7.1.1	Preparation of Ear Tissue .....	3-63
3.7.1.2	RNA Extraction from Mouse Ears.....	3-63
3.7.2	Protein Sampling for Western Blot and Bradford Assay .....	3-64
3.7.2.1	Protein Extraction from Soft Tissues.....	3-64
3.7.2.2	Protein Extraction from Temporal Bone .....	3-64
<b>3.8</b>	<b>Determination of the <i>Mus musculus Vmo1</i> Gene Sequence .....</b>	<b>3-65</b>
3.8.1	Oligonucleotide Primer Design for PCR .....	3-65
3.8.1.1	Oligo-dT Primers .....	3-65
3.8.1.2	BFG1F and BFG2R .....	3-65
3.8.1.3	BFG7F and BFG8R .....	3-65
3.8.1.4	BFG27F and BFG28R.....	3-66
3.8.1.5	<i>Mus GAPDH</i> Primers .....	3-66
3.8.1.6	M13 Puc Reverse and BFG28R .....	3-66
3.8.2	Preparation of Total cDNA.....	3-69
3.8.3	Amplification of cDNA using PCR.....	3-69
3.8.4	DNA Sequencing .....	3-70
<b>3.9</b>	<b>VM01 Protein Expression in Mouse Tissue.....</b>	<b>3-70</b>
3.9.1	Protein Concentration Estimation using Bradford Assay .....	3-70
3.9.2	Western Blot Analysis.....	3-71
3.9.2.1	Membrane Preparation.....	3-71
3.9.2.2	Antibody Binding to Protein Target in Tissue Lysates .....	3-72

3.9.2.3	Immunodetection .....	3-72
3.9.2.4	Removal of Antibody from the Membrane.....	3-73
3.9.2.5	Ponceau Staining.....	3-73
3.9.2.6	Protein Transfer.....	3-73
<b>3.10</b>	<b>VM01 Protein Expression in the Inner Ear of the Mouse .....</b>	<b>3-75</b>
3.10.1	Fixation, Embedding and Sectioning of Mouse Ears.....	3-75
3.10.2	Slide Preparation.....	3-76
3.10.3	Sectioning.....	3-76
3.10.4	Section Staining.....	3-78
3.10.4.1	Haemotoxylin and Eosin Anatomy Stain .....	3-78
3.10.4.2	IHC Staining.....	3-79
3.10.4.3	Nuclei staining and slide mounting .....	3-80
3.10.5	Microscopy.....	3-80
<b>CHAPTER FOUR RESULTS.....</b>		<b>4-81</b>
<b>4.1</b>	<b>Isolation of Total RNA from Mouse Inner Ears .....</b>	<b>4-81</b>
<b>4.2</b>	<b>cDNA Synthesis Using Inner Ear Mouse RNA as a Template .....</b>	<b>4-82</b>
<b>4.3</b>	<b>Optimisation of <i>Vmo1</i> Amplification from cDNA.....</b>	<b>4-83</b>
4.3.1	HOT FIREPol® Buffer Optimisation .....	4-84
4.3.2	Magnesium Concentration Optimisation.....	4-84
4.3.3	Temperature Optimisation .....	4-85
<b>4.4</b>	<b>DNA Sequencing Results.....</b>	<b>4-88</b>
<b>4.5</b>	<b>Cloning and Expression of the Mouse <i>Vmo1</i> Amplicon .....</b>	<b>4-90</b>
<b>4.6</b>	<b>Protein Extraction from Whole Cell Lysates of Mouse Tissues .....</b>	<b>4-91</b>
4.6.1	Bradford Assay.....	4-91
4.6.2	SDS-PAGE.....	4-94
<b>4.7</b>	<b>Western Blotting .....</b>	<b>4-97</b>
4.7.1	Protein Transfer .....	4-97
4.7.1.1	Prestained Ladder Transfer.....	4-98
4.7.1.2	Coomassie Blue Staining of Transferred SDS-PAGE .....	4-98
4.7.1.3	Ponceau Staining.....	4-99
4.7.1.4	$\beta$ -actin Antibody Binding.....	4-99
4.7.2	Expression of the VM01 Protein in Mouse Tissue Lysates.....	4-100
4.7.2.1	ProteinTech Antibody .....	4-100

4.7.2.2	GeneTex antibody.....	4-104
<b>4.8</b>	<b>Immunohistochemistry .....</b>	<b>4-106</b>
4.8.1	Mouse Section Integrity .....	4-106
4.8.2	Antibody Binding .....	4-107
<b>CHAPTER FIVE DISCUSSION .....</b>		<b>5-113</b>
<b>5.1</b>	<b>Comparative Genomics and a Suitable Animal Model for Studying <i>VMO1</i></b>	<b>5-113</b>
<b>5.2</b>	<b>Amplification and Sequencing of the <i>Vmo1</i> Gene .....</b>	<b>5-114</b>
5.2.1	RNA Isolation .....	5-115
5.2.2	cDNA Synthesis .....	5-116
5.2.3	Optimisation of <i>Vmo1</i> DNA Amplification from cDNA Template.....	5-117
5.2.3.1	Primer Design.....	5-117
5.2.3.2	Buffer .....	5-118
5.2.3.3	Magnesium Concentration .....	5-118
5.2.3.4	Annealing Temperature.....	5-118
5.2.4	DNA Sequencing of <i>Vmo1</i> PCR Product.....	5-119
<b>5.3</b>	<b>Validation of the VM01 Antibody for IHC .....</b>	<b>5-120</b>
5.3.1	Preservation of Tissue Lysate Proteins.....	5-120
5.3.2	Confirmation of Protein Transfer from SDS-PAGE to PVDF Membrane.....	5-121
5.3.3	Analysis of ProteinTech VM01 Antibody .....	5-123
5.3.4	Analysis of GeneTex VM01 Antibody .....	5-125
<b>5.4</b>	<b>Cloning and Expression of the VM01 Recombinant Protein.....</b>	<b>5-126</b>
5.4.1	Ligation of the <i>Vmo1</i> Transcript into a Vector .....	5-126
5.4.1.1	Restriction Enzyme Digestion.....	5-126
5.4.1.2	Ligation .....	5-127
5.4.2	Screening and Sub-cloning of Transformed Colonies .....	5-128
<b>5.5</b>	<b>Localisation of the VM01 Protein within the Inner Ear using VM01 Antibody</b>	
<b>(GeneTex).....</b>		<b>5-129</b>
5.5.1	Integrity of the Mouse Cochlea.....	5-129
5.5.1.1	Paraffin Embedding and Microtome Sectioning .....	5-130
5.5.1.2	OCT Embedding and Cryostat Sectioning .....	5-131
5.5.2	Haemotoxylin Staining.....	5-131
5.5.3	Immunohistochemistry .....	5-131
<b>5.6</b>	<b>Comparison of the Tectorial Membrane vs. the Vitelline Membrane.....</b>	<b>5-132</b>

<b>CHAPTER SIX CONCLUSION .....</b>	<b>6-134</b>
<b>CHAPTER SEVEN FUTURE RECOMMENDATIONS .....</b>	<b>7-135</b>
<b>7.1 Comparative Genomics.....</b>	<b>7-135</b>
<b>7.2 Complete DNA Sequencing of <i>Vmo1</i> Gene .....</b>	<b>7-136</b>
<b>7.3 Validation of the VMO1 Antibody .....</b>	<b>7-137</b>
<b>7.4 Histology .....</b>	<b>7-142</b>
<b>7.5 Conclusion .....</b>	<b>7-145</b>
<b>REFERENCES .....</b>	<b>8-146</b>
<b>APPENDIX ONE BUFFERS AND SOLUTIONS .....</b>	<b>9-159</b>
<b>APPENDIX TWO VECTOR MAPS .....</b>	<b>10-163</b>
<b>APPENDIX THREE DNA SEQUENCING RESULTS.....</b>	<b>11-168</b>
<b>APPENDIX FOUR ANIMAL ETHICS APPROVAL .....</b>	<b>12-170</b>
<b>APPENDIX FIVE SPECIMEN AND TISSUES TYPE .....</b>	<b>13-174</b>
<b>APPENDIX SIX STANDARD OPERATING PROCEDURE NINE.....</b>	<b>14-175</b>
<b>APPENDIX SEVEN GENETICALLY MODIFIED ORGANISMS.....</b>	<b>15-178</b>
<b>APPENDIX EIGHT COMPARATIVE GENOMICS ANALYSIS .....</b>	<b>16-179</b>



# LIST OF FIGURES

Figure 1: Cause of HL in the HI population of NZ	1-2
Figure 2: % of the total hearing HI population grouped by age/gender	1-2
Figure 3: Prevalence of HL in NZ households grouped by ethnicity/age	1-3
Figure 4: Racial % distribution of reported HL in children under 19	1-3
Figure 5: Mode of inheritance for deafness loci for non-syndromic HL	1-6
Figure 6: Gross anatomy of the mammalian ear	1-6
Figure 7: Movement of sound through the mammalian ear	1-8
Figure 8: Structure of the inner ear	1-9
Figure 9: H&E staining of inner ear	
(A) Cross section of the whole cochlea	
(B) Cross section of a single turn of the cochlea	1-11
Figure 10: Anatomy of the OoC	
(A) P5 mouse inner ear stained with H&E	
(B) Schematic diagram depicting the position of the TM	
(C) SEM image of the apical surface of the OoC	1-13
Figure 11: Structure of the chicken egg	1-16
Figure 12: 35S <i>In situ</i> hybridisation of <i>Vmo1</i> in P5 mouse cochlea	
(A) <i>Vmo1</i> antisense probe bound to <i>Vmo1</i> mRNA in RM	
(B) Negative control	1-17
Figure 13: Gene alignment of <i>VMO1</i> for 8 mammalian species.	2-22
Figure 14: Gene alignment of <i>VMO1</i> for 6 mammalian species	2-23
Figure 15: Gene alignment for avian species	2-23
Figure 16: ORF prediction for all species	2-26
Figure 17: Nucleotide position of <i>Vmo1</i> coding exons in mouse	2-27
Figure 18: Alternative transcripts of Human <i>VMO1</i> gene	2-28
Figure 19: Translated protein for human mRNA splice variants	2-29
Figure 20: Nucleotide structure of the Chicken <i>VMO1</i> gene	2-31
Figure 21: Pairwise alignment of the mouse and human mRNA	2-33
Figure 22: ORF alignment for the mouse, human and chicken	2-33
Figure 23: Amino acid sequence of the chicken <i>VMO1</i> protein	2-35
Figure 24: The Greek key Motif	

(A) The ornamental Greek key design	
(B) The Beta hairpin	
(C) Basic Greek key protein structure	2-36
Figure 25: Alignment of Greek key motifs in the chicken VMO1	2-38
Figure 26: Vase-like structure of the VMO1 protein	
(A) Shows the 3D vase like structure	
(B) Simplified 3D structure	2-39
Figure 27: 2D representation of the 3D structure of chicken VMO1	2-40
Figure 28: Protein alignment of all VMO1 from 36 species	2-46
Figure 29: Annotation of the translated mouse VMO1 protein	2-49
Figure 30: Annotation of the translated human VMO1 protein	2-49
Figure 31: Multiple alignment of chicken, mouse and human VMO1	2-50
Figure 32: DNA Sequence of the Mouse <i>Vmo1</i> gene	3-67
Figure 33: Layout of SDS-PAGE gel on membrane	3-74
Figure 34: Arrangement of WB components	3-74
Figure 35: Position of hemidissected mouse head in the cryomold	3-76
Figure 36: Layout of mouse sections on a microscope slide	3-77
Figure 37: cDNA synthesised by reverse transcription	4-82
Figure 38: cDNA controls using mouse specific primers	4-83
Figure 39: Amplification of cDNA using mouse specific primers	4-84
Figure 40: MgCl <sub>2</sub> optimisation of PCR	4-85
Figure 41: PCR validation of cDNA produced from mRNA	4-86
Figure 42: Annealing temperature optimisation of PCR	4-87
Figure 43: Multiple alignment of the mouse <i>Vmo1</i> mRNA RefSeq	4-89
Figure 44: Agarose gel electrophoresis of ligation reagents	4-90
Figure 45: Bradford assay showing relative concentrations of proteins	4-92
Figure 46: 12% SDS-PAGE gel of 8 undiluted protein lysates	4-94
Figure 47: 10% precast SDS-PAGE gel of mouse protein lysates	4-95
Figure 48: 10% precast SDS-PAGE gel of mouse protein lysates	4-97
Figure 49: Coomassie blue stained SDS-PAGE gel after blotting	4-98
Figure 50: Ponceau stained PVDF membrane after blotting	4-99
Figure 51: WB using the $\beta$ -actin antibody and SPA antibody	
(A) $\beta$ -actin antibody	
(B) SPA antibody	4-100

Figure 52: WB carried out using 2 different antibodies	
(A) VMO1 antibody	
(B) $\beta$ -actin antibody	4-101
Figure 53: WB carried out to duplicate results from Figure 53	4-102
Figure 54: WB of 3 P28+ mouse tissues and chicken VM	4-103
Figure 55: WB showing non-specific binding of VMO1 antibody	4-104
Figure 56: VMO1 antibody WB using ear and tear mouse proteins	4-105
Figure 57: WB of 4 P28+ mouse tissues	4-105
Figure 58: H&E staining of the inner ear of P5	
(A) Whole cochlea	
(B) Cochlear duct	4-106
Figure 59: Results from 3 duplicated IHC reactions	
(A,C,F) Negative controls	
(B,D,G) 1:1000 VMO1 antibody dilution	
(E,H) 1:100 VMO1 antibody dilution	
(I) $\beta$ -actin primary antibody control	4-108
Figure 60: Comparison between 1:100 $\mu$ l antibody and no antibody.	
(A) DAPI fluorescence overlaying the VMO1 antibody	
(B) Negative control	4-109
Figure 61: Whole cochlea IHC under different wavelengths	4-110
Figure 62: 20X zoom of the OoC	
(A) Anchoring of the TM between the interdental cells and the RM	
(B) VMO1 present in the TM	
(C) Fluorescence of the inner pillar cell.	4-111
Figure 63: 1:100 VMO1 antibody with 0:1000 antibody merge	4-112
Figure 64: pET-41a(+) vector map	10-163
Figure 65: pET-42a(+) vector map	10-164
Figure 66: pProEX HTb (Invitrogen) vector map	10-165
Figure 67: pBluescript II SK(+) vector map	10-166
Figure 68: pCR <sup>®</sup> 4-TOPO <sup>®</sup> cloning vector map	10-167
Figure 69: Forward sequencing result chromatogram	11-168
Figure 70: Reverse sequencing result chromatogram	11-169

# LIST OF TABLES AND EQUATIONS

Table 1: Gene data for <i>VMOI</i> for all 17 species available on NCBI	2-21
Table 2: mRNA for all species available on NCBI	2-24
Table 3: Human <i>VMOI</i> variant table	2-30
Table 4: EST data available for human <i>VMOI</i>	2-31
Table 5: Chicken variant table showing one synonymous SNP	2-31
Table 6: All protein data available on NCBI	2-42
Table 7: Type and weight of agarose used	3-52
Table 8: PCR machine settings	3-55
Table 9: Composition of the separating and stacking SDS-PAGE gels	3-57
Table 10: Forward and reverse primer sequences	3-68
Table 11: Procedure for immunoblotting	3-72
Table 12: Protocol for IHC	3-79
Table 13: RNA sample Nanodrop results	4-81
Table 14: Recommended annealing temperatures for primer sets	4-87
Table 15: Nanodrop readings for isolated plasmids	4-91
Table 16: Bradford assay results	4-93
Table 17: Expected protein fragments resulting from Trypsin digestion	7-141
Table 18: Mice used during the course of this research	13-177
Equation 1: Vector to insert ratio equation	5-128

# ABBREVIATIONS

3'	Three prime DNA end
5'	Five prime DNA end
Å	Angstrom(s)
α	Alpha
β	Beta
°C	Degrees Celsius
µg	Microgram
µl	Microlitre
µM	Micromolar
A	Adenine nucleotide
aa	Amino acid(s)
AHL	Acquired hearing loss
APS	Ammonium persulfate
BFG	Blaise Forrester-Gauntlett
BIS	N, N'-methylenebisacrylamide
BLAST	Basic local alignment search tool
BM	Basilar membrane
bp	Base pair(s)
C	Cytosine
C-terminus	Carboxyl terminus
C57/B16/129SV	Wild type mouse strain
cDNA	Complementary DNA
CN	Cochlear nerve
COSMIC	Catalogue of somatic mutations in cancer
Da	Dalton(s)
dB	Decibel(s)
dbSNP	Single nucleotide polymorphism database
dH <sub>2</sub> O	Distilled water
DEPC	Diethyl dicarbonate
DFN	Deafness loci
DFNA	Dominant deafness loci

DFNB	Recessive deafness loci
DFNX	X chromosome deafness loci
DFNY	Y chromosome deafness loci
DH5 $\alpha$	DH5 alpha <i>E. coli</i> strain
DNA	Deoxyribonucleic acid
dNTP	Deoxyribonucleotide
DTT	Dithiothreitol
<i>E. coli</i>	<i>Escherichia coli</i>
EDTA	Ethylenediaminetetraacetic acid
ESTs	Expressed sequence tags
et al	And others
FASTA	File format for nucleotide and protein sequences
G	Guanine nucleotide
GHL	Genetic hearing loss
GITC	Guanidinium isothiocyanate
GJB(2 or 6)	Gap junction protein, beta
<i>GJB2</i> -R75W	Transgenic mouse strain with mutation in <i>GJB2</i> gene
GP	Glycoprotein
HCl	Hydrochloric acid
HI	Hearing impaired
HL	Hearing loss
hr	Hour(s)
Hz	Hertz
IHC	Immunohistochemistry
indels	Insert deletion mutation
inner HC	Inner hair cell
IPC	Inner pillar cell
IPTG	Isopropyl $\beta$ -D-1-thiogalactopyranoside
K	Potassium
kb	Kilobase
kDa	Kilodalton(s)
L	Litre(s)
LB	Luria base
M	Molar

mA	Milliampere(s)
mg	Milligram(s)
MIDD	Maternally inherited diabetes and deafness
min	Minute(s)
mL	Millilitre(s)
mM	Millimolar
MPSS	Massively parallel signature sequencing
mQH <sub>2</sub> O	milliQ water
mRNA	Messenger RNA
MTT	Mitochondrial mutation deafness loci
mV	Millivolt(s)
Na	Sodium
NaOH	Sodium hydroxide
NCBI	National centre for biotechnology information
NEB	New England biolabs
ng	Nanogram(s)
NHLBI	National Heart, Lung, and Blood Institute
OHC	Outer hair cell
OoC	Organ of Corti
OPC	Outer pillar cell
ORF	Open reading frame
P28+	Postnatal 28 or older
P5	Postnatal day 5
PAGE	Polyacrylamide gel electrophoresis
PBS	Phosphate buffered saline
PCR	Polymerase chain reaction
PEG	Polyethalene glycol
ppm	Parts per million
PVDF	Polyvinylidene fluoride
rcf	Relative centrifugal force
RefSeq	Reference sequence database
RM	Reissner's membrane
RNA	Ribonucleic acid
rpm	Revolutions per minute

RT	Room temperature
RT-PCR	Real-time PCR
SDS	Sodium dodecyl sulfate
sec	Second(s)
SNP	Single nucleotide polymorphism
SNV	Single nucleotide variation
T	Thymine nucleotide
TBS	Tris buffered saline
TBS-T	Tris buffered saline with Tween 20
TEMED	Tetramethylethylenediamine
TM	Tectorial membrane
T <sub>M</sub>	Primer melting temperature
TPA	Third party annotation database
U	Uridine nucleotide
U	Enzyme units
uFD	Micro fluorescein isothiocyanate-labelled dextran
US	United states
UTR	Untranslated region
UV	Ultra violet
V	Volt(s)
<i>VMO1</i>	Human and chicken vitelline membrane outer layer 1 gene
VMO1	Human, mouse and chicken vitelline membrane outer layer 1 protein and antibody
<i>Vmo1</i>	Mouse vitelline membrane outer layer 1 gene
Xgal	5-bromo-4-chloro-3-indolyl- $\beta$ -D-galactopyranoside
ZP	Zona pellucida protein



# CHAPTER ONE

## LITERATURE REVIEW AND INTRODUCTION

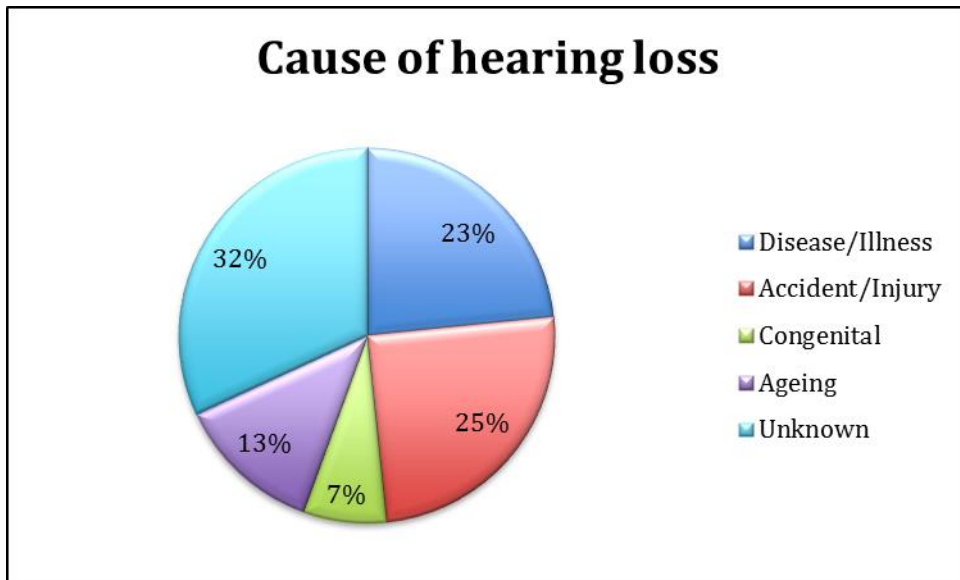
### 1.1 Hearing Loss

Hearing loss (HL) is said to be the most common sensory disability in the world and is defined as the partial or complete loss of the ability to perceive sound in one or both ears. Over 250 million people worldwide suffer from HL which can greatly affect quality of life and has social, psychological, cognitive, financial and health effects on sufferers both directly and indirectly. HL itself, when acquired pre-lingually, can have severe affects on language acquisition, learning and literacy. Every year, one in every 500 children are born with a significant hearing impairment. By the age of five years, this number rises to 5.4 and by adolescence to seven (Hilgert et al., 2009).

In the New Zealand population, the prevalence of people experiencing HL ranges from 10.3% (~400,000), for people reporting HL to 0.05% (~2,100), for people who can't hear one person talking to them. This data resulted from surveys compiled by Greville, 2005 from the New Zealand census data for 1991/92, 1996/97 and 2001/02. However, it excludes individuals with "corrected" HL such as those who use hearing aids. Interestingly, this data is 2% higher than the results from a census in the United States (US) asking similar questions.

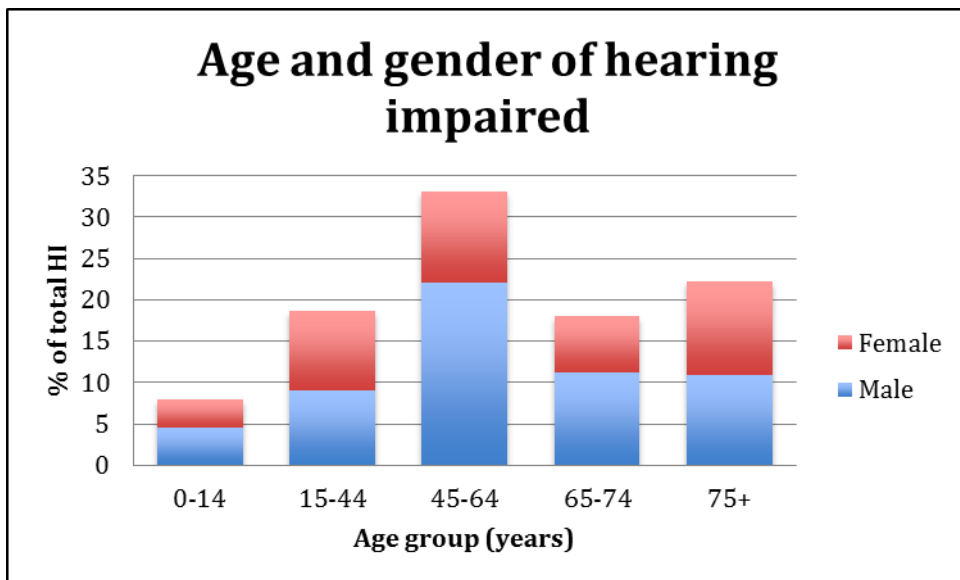
HL can be caused many different factors.

Figure 1 shows the causes of HL in the hearing impaired (HI) New Zealand population; 43% is at birth (congenital) or caused by age, illness or disease, 25% is caused by accident or injury and 32% of cases have an unknown cause (Greville, 2005).



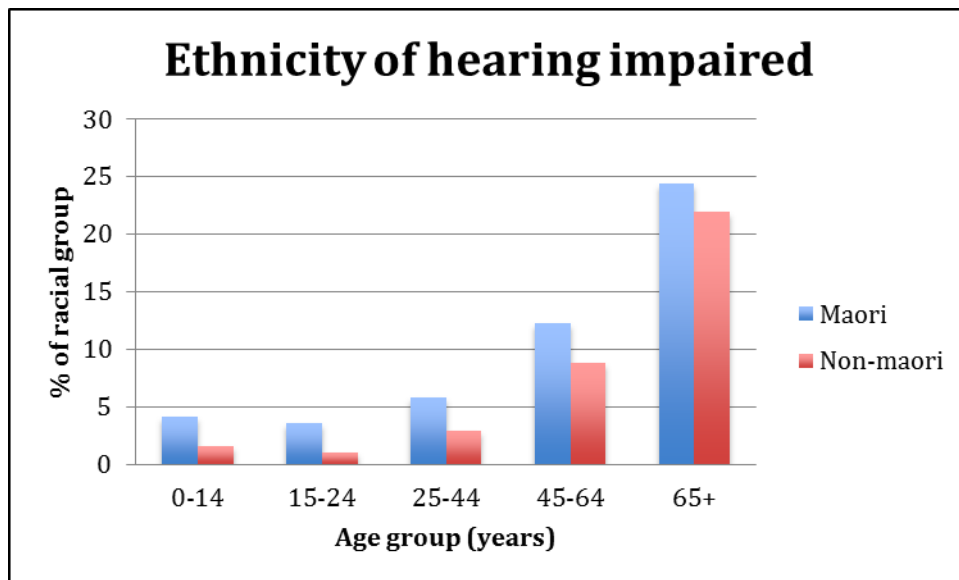
**Figure 1: Cause of hearing loss in the hearing impaired population of New Zealand (Greville, 2005)**

HL rates are shown to be ever-increase with age, due to age related hearing loss, accident/injury and disease/illness. The prevalence of HL in people over 65 is three times higher than that of people aged 15-64 years with 2.2% occurring in children under the age of 14. The study also showed a marked increase in HL in men than in women at all ages (Figure 2). In the age group 0-24 years, this can be attributed to genetics and in the 25+ age group, to noise exposure.



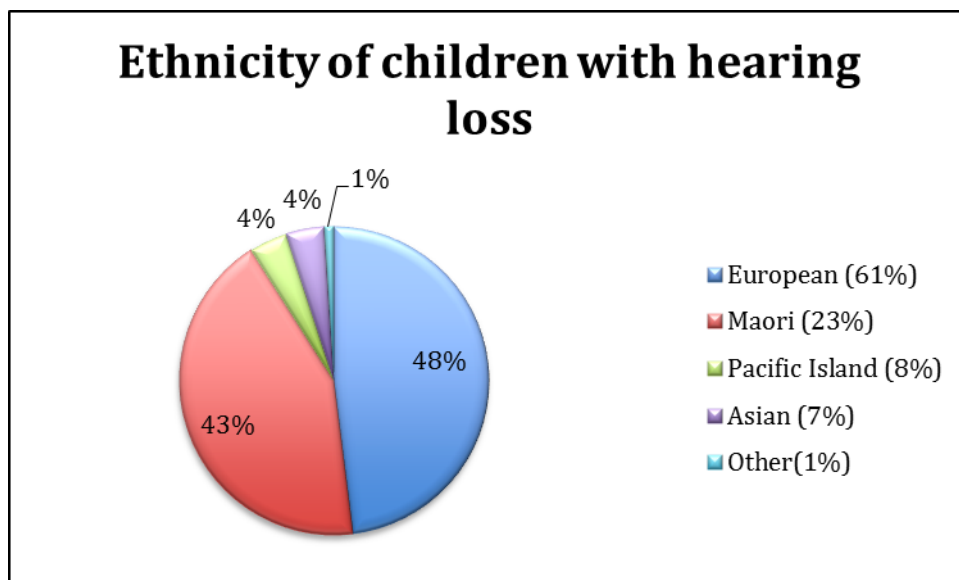
**Figure 2: Percentage of the total hearing impaired population grouped by age and gender (Greville, 2005)**

Figure 3 shows the prevalence of HL in the population compared to the non-Māori population grouped by age. A total of 12.1% of the Māori population experienced HL compared to 9.6% for non-Māori when the low life expectancy of Māori was taken into account (Greville, 2005).



**Figure 3: Prevalence of hearing loss in New Zealand households grouped by ethnicity and age (Greville, 2005)**

The onset of HL can be defined in two ways; prelingual or postlingual. Prelingual HL occurs before the development of normal speech whereas, postlingual HL occurs after normal speech has been acquired (Smith et al., 2012; Hilgert et al., 2009). Review of the New Zealand Deafness Detection Database in 2005 showed that 43% of the HL reported for children with pre-lingual HL was accounted for by Māori, who make up only 23% of the New Zealand population (Figure 4). Of this, 43% had a family history of pre-lingual HL compared to just 25% for non-Māori children (Greville, 2007; Digby, 2012).



**Figure 4: Racial percentage distribution of reported hearing loss in children under 19 in 2005 (Greville, 2007; Digby 2012). The legend also shows the percentage makeup of the total New Zealand population.**

### 1.1.1 Classification of Hearing Loss

Sound is measured in two ways; (1) loudness or intensity which is measured in decibels (dB), and (2) frequency or pitch which is measured in Hertz (Hz). HL can range from mild impairment, where the degree of HL ranges between 26-40dB, to profound deafness where HL is greater than 90dB (Hilgert et al., 2009). It can also be frequency based where the affected person is limited to a range of frequencies at which they can hear (low <500Hz, middle 500-2000Hz or high >2000Hz). Humans, on average can hear best at 1000-3000 Hz and within the range of 20-20,000 Hz. Normal conversations are held at around 60 dB and a rock concert at around 120dB. Hearing damage can be caused at 80 dB or more (Silverthorn, 2004).

The type of HL an individual has can be classified according to the abnormalities in the mammalian ear anatomy. For example, conductive HL is where there are malformations or abnormalities in the outer ear and/or the ossicles in the middle ear. Sensorineural HL is where there is a problem with the inner ear or vestibulocochlear nerve. Central auditory dysfunction is when the part of the brain that translates what the ear delivers does not function properly i.e., in the eighth cranial nerve, cerebral cortex or auditory brain stem. Mixed HL is where you have a combination of one or more of these factors. The HL could also be in both ears (bilateral) or in a single ear (unilateral). The most common type of permanent HL is sensorineural which can occur bilaterally or unilaterally.

HL can be classified as genetic (GHL) or acquired (AHL). GHL is hereditary and is responsible for 50-60% of HL. In comparison, AHL appears after birth and is responsible for 40-50% of HL cases. However, studies have shown that the increasing prevalence of HL with age in the general population is indicative of the impacts of genetics and the environment, and the effect of the environment on an individual's genetic predisposition (Stegman and Carey, 2002). AHL is where hearing loss has been induced by an external or environmental factor. For example, AHL can occur prenatally due to maternal infections in the form of the Herpes virus, Syphilis bacteria, or *Taxoplasmosis gondii* parasite; postnatally from noise exposure or cranial or acoustic trauma; ototoxic drugs such as the antibiotic Gentomicin; infections such as bacterial meningitis caused by

*Neisseria meningitides*, *Haemophilus influenza* or *Streptococcus pneumoniae* or otitis media that results in the inflammation of the inner ear (Petit et al., 2001).

GHL results from the inheritance of a germline mutation in the nuclear or mitochondrial DNA, and is much more variable and complex than AHL.

GHL can be classified by whether it is syndromic or non syndromic. Syndromic HL is where there are a range of symptoms or defects including HL such as individuals with Maternally inherited diabetes and deafness (MIDD), Trisomy 21 (e.g. developmental delay, a flattened face and nose, HL) and Usher's syndrome (e.g. HL and visual impairment) (Karkos et al., 2005, Keats, 2002).

Syndromic HL accounts for 30% of prelingual HL. To date, there are over 400 genetic syndromes that include HL (Burton et al., 2006). Non-syndromic HL is where there are no other medical characteristics and no abnormalities of the external ear or other organs and accounts for 60-70% of prelingual HL. Currently, there are 105 known and 52 unknown genes implicated with hereditary non-syndromic HL and 154 different loci identified (Van Camp and Smith, 2013). The gene loci are named DFN, for DeaFNess, followed by the mode of inheritance and then a number representing the order of gene mapping or discovery. GHL can be inherited as a Mendelian trait; autosomal dominant (DFNA), autosomal recessive (DFNB), X-chromosome linked (DFNX), Y-chromosome linked (DFNY) and through mitochondrial mutations (MTT).

Figure 5 shows a graphical representation of the types of non-syndromic HL occurring prelingually worldwide. DFNB represents the highest proportion of non syndromic HL cases with 75-80%. Consanguineous marriages in countries such as India and the Middle East are responsible for contributing to a higher incidence of DFNB (Zakzouk, 2006; Meyer, 2007). For example, in large families, an unaffected cousin who is a carrier of one copy of the abnormal gene marries their cousin who is also a carrier. Therefore, the resulting offspring born with two copies of the abnormal gene have a deaf phenotype. Half of this (26%) is DFNB1 which is caused by a mutation in the Gap Junction Beta-2 protein (*GJB2*) and/or the *GJB6* gene (Smith and Hildebrand, 2008). In the US, United Kingdom, France, Australia and New Zealand approximately one in 33 people carry the mutation for DFNB1, and 14 in 100,000 people have HL caused by it (Smith and Hildebrand, 2008).

The amount of HL inherited through MMT is more varied, ranging from 0 to 20% due to differences in maternal inheritance and heteroplasmy (Burton et al., 2006).

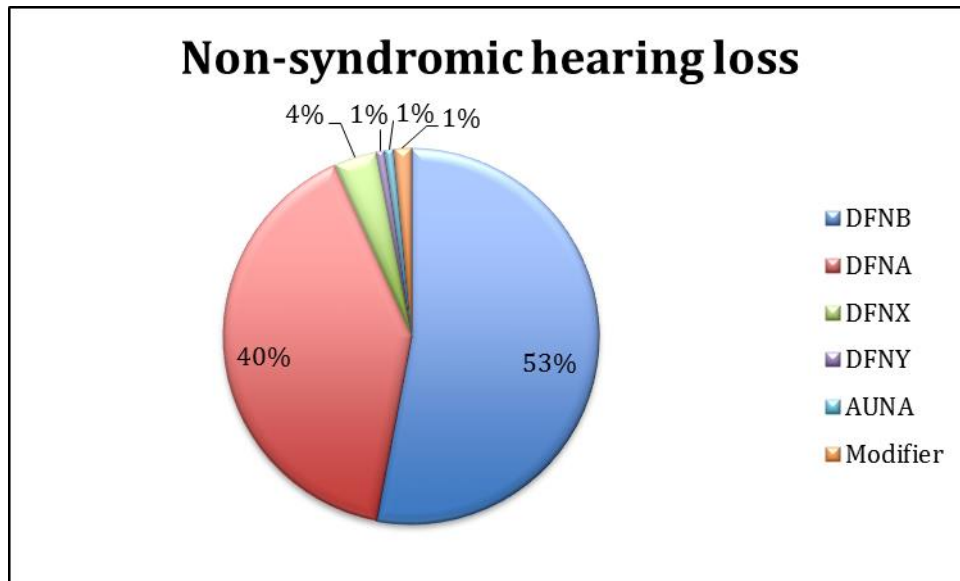


Figure 5: Mode of inheritance for deafness loci for non-syndromic hearing loss worldwide such as autosomal recessive (DFNB), autosomal dominant (DFNA), X-chromosome linked (DFNX), Y-chromosome linked (DFNY), auditory neuropathy (AUNA) and modifier gene linked (Data sourced from Burton et al., 2006 and Van Camp and Smith 2013)

## 1.2 Biology of the Mammalian Ear

The mammalian ear acts as the organ for hearing and balance in both mice and humans. It is composed of three compartments; the outer, middle and inner ear (Figure 6) which are highly conserved in the mouse and human.

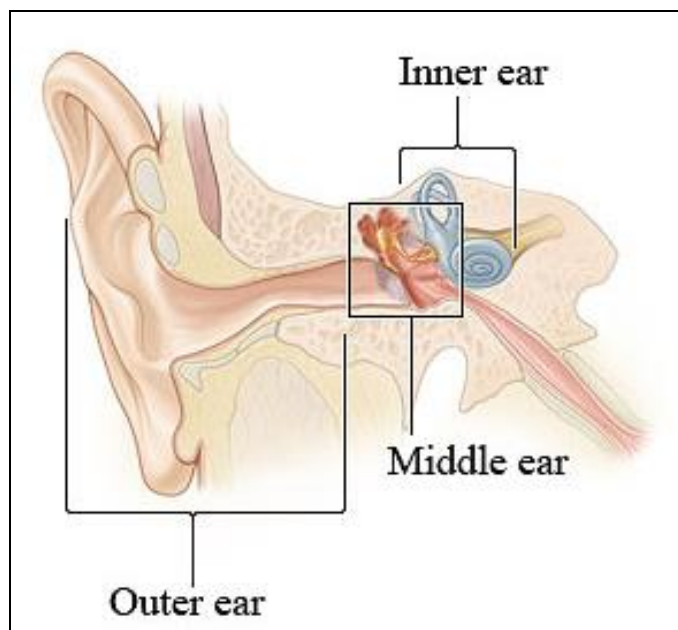


Figure 6: Gross anatomy of the mammalian ear. This diagram shows the three basic compartments for the ear; the outer, middle and inner ear (adapted from <http://www.webmd.com/cold-and-flu/ear-infection/middle-ear>).

## **1.2.1 Use of the Mouse as an Animal Model for Human Hearing Loss**

Studying the development and mechanism of HL in humans is difficult and is usually only possible post-mortem usually within a narrow time interval of 2-4 hours after death to obtain good specimens (Kanonier et al., 1996). For example, the mammalian ear is located within the temporal bone of the skull and therefore, access is restricted to surgery (Figure 6). There are also limitations on the availability of well preserved human ear tissues of different ages and developmental time points (Nadol, 1996). In addition, the ear is relatively small in size, being only 5mm from base to apex and 9mm across at the base (Greys anatomy) in humans and the size of a match head in mice (Personal communication from Linda Peters). Also there is a limited number of messenger RNA (mRNA) transcripts which make up less than 5% of total RNA (Lodish et al., 2000). These mRNA transcripts also have relatively short lifespans ranging from minutes to days) when compared to DNA (Kraeva et al., 2007).

The study of hereditary HL in humans is also made difficult because of the frequency at which HI people, and the children of HI people intermarry. This results in families carrying more than one mutation that can be linked to deafness (Friedman et al., 2007; Zakzouk, 2006).

Most of these limitations can be overcome by using mouse models. The inner ear of mice and humans are very similar; structurally, functionally and at the genetic and proteomic level (Petit, 2001; Dror, 2009). In addition, mice are available at any stage of development (embryonic and postnatal) and can be processed quickly in a clean environment to prevent mRNA transcripts and proteins from degrading and to preserve tissue integrity. The finely dissected ear tissues can also be pooled to increase the chances of finding rare mRNA transcripts and proteins. Also, mice can be manipulated genetically using gene-targeted mutagenesis to produce mutants with HL. The resulting inner ear defects can then be used to study the pathology of HL (Dror, 2009). Currently, there are several mouse mutants available that have isolated inner ear and/or vestibular defects. One of these, the *GJB2-R75W* transgenic mouse, is deaf and has the same mutation in the *GJB2* gene that causes congenital, bilateral, non-syndromic, sensorineural HL in humans (Minekawa et al., 2009).

The study of vestibular dysfunction in mice is also made easier as mice are completely dependent on the sensory information from the inner ear. Dysfunction of the system will cause affected mice to display characteristic behaviours such as the inability to swim, head tossing and circling. Equilibrium and balance in humans is not as dependant on the inner ears sensory information as there is a strong sense of body position from proprioceptors and visual information (Petit, 2001). However, despite this difference in response to vestibular dysfunction the mouse is a good model for balance disorders as the results of a dysfunction are easily identified.

## 1.2.2 Outer and Middle Ear

The outer and middle ear act together to transmit sound waves from the external environment to the inner ear. The pinna of the outer ear directs sound waves into the auditory canal and towards the middle ear and the tympanic membrane (ear drum) where the sound waves are converted to vibrations. Figure 7 depicts the movement of sound from the auditory canal through the middle ear to the cochlea. The middle ear consists of an air-filled cavity connected to the nasopharynx through the eustachian tube and contains three bones or ossicles; the malleus, incus and stapes.

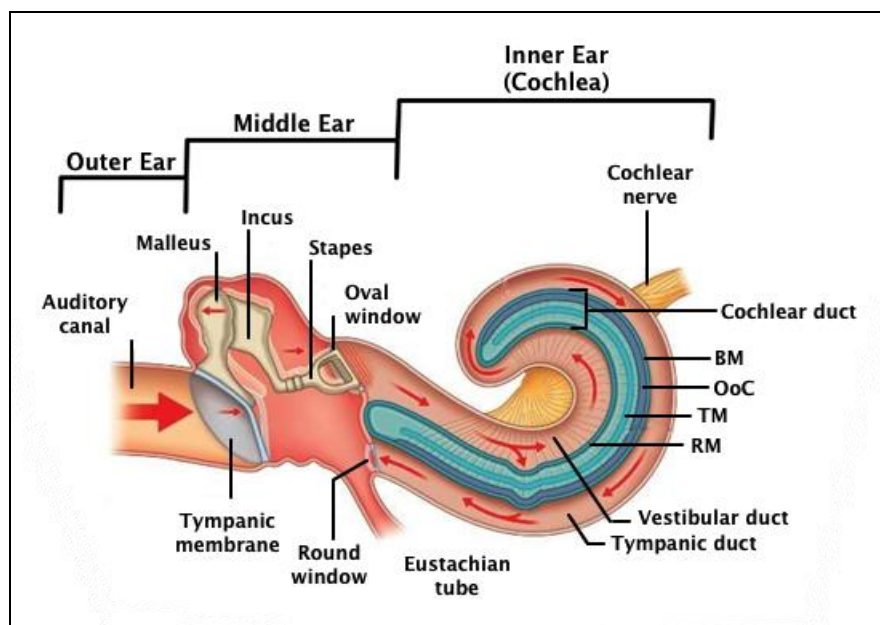


**Figure 7: Movement of sound through the mammalian ear. The red arrows depict the movement of sound through the auditory canal to the tympanic membrane which converts sound waves to vibrations which are further transmitted by the malleus, incus and stapes to the oval window. From the oval window, sound waves are carried through the perilymph filled vestibular duct, across the Reissner's membrane (RM) to the cochlear duct filled with endolymph. The sound waves are then detected by sensory hair cells on the Organ of Corti (OoC) residing on the basilar membrane (BM) (adapted from Drake et al., 2009)**



### 1.2.3 Inner Ear

The inner ear is responsible for two major senses; hearing and balance. Figure 8 shows the inner ear composed of a bony labyrinth that surrounds a fluid filled membranous labyrinth. The membranous labyrinth consists of the snail shaped cochlea for hearing and the vestibular apparatus for balance.

For hearing function, our brains interpret energy in the form of sound waves from the external environment. As seen in Figure 7, sound waves are captured by the pinna and travel down the auditory canal towards the ear drum. The ossicles within the middle ear carry the vibrations from the tympanic membrane to the oval window membrane. The vibrations are converted to pressure waves and travel through fluid in the vestibular duct across the Reissner's membrane (RM) to the cochlear duct and from there to the basilar membrane (BM) where they are detected by hair cells and converted to electrochemical signals that are transmitted to the brain via the auditory nerve. The remaining pressure waves then move into the tympanic duct and out of the round window to be dissipated in the middle ear.

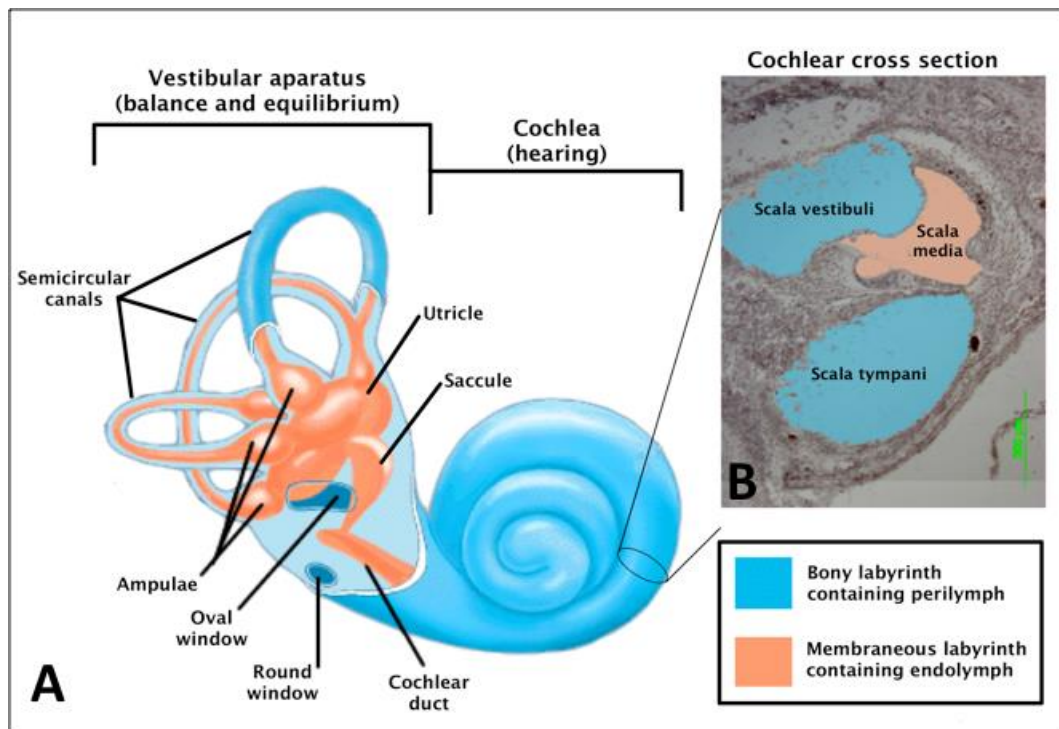


**Figure 8: Structure of the inner ear showing the vestibular apparatus and cochlea. (A) Structure of the bony (orange) and membranous (blue) labyrinths of the inner ear (adapted from Wikipedia [http://en.wikipedia.org/wiki/Inner\\_ear](http://en.wikipedia.org/wiki/Inner_ear)). (B) Cross section of the cochlea with Haematoxylin and Eosin (H&E) stain and showing three compartments; scala vestibuli, scala media and scala tympani. The membranous labyrinth (orange) contains endolymph which is high in potassium ( $K^+$ ) and low in sodium ( $Na^+$ ) whereas the bony labyrinth (blue) contains perilymph which is high in  $Na^+$  and low in  $K^+$ .**

Balance and equilibrium is determined by hair cells that line the vestibular apparatus (Figure 8). The hair cells respond to gravity and acceleration in the

same way hair cells in the cochlea respond to sound waves travelling through the endolymph. The vestibular apparatus consists of the saccule, utricle, membranous ampullae, semicircular ducts and the semicircular canals. As can be seen in Figure 8 the interior of the vestibular apparatus is continuous with the cochlear duct.

### **1.2.3.1 Cochlea**

Specialised sensory epithelium in the cochlea detect and transmit sound waves to the brain via the auditory nerve. The cochlea is a snail shaped organ that when unwound from its coiled shape, consists of three parallel fluid filled chambers separated by two thin membranes; Reissner's membrane (RM) and the basilar membrane (BM) (Figure 9). These two membranes surround the cochlear duct with the RM between the vestibular duct and the BM between the tympanic duct (Silverthorn, 2004) and are thought to control the movement of fluids and electrolytes between the perilymph and endolymph. The vestibular and tympanic ducts contain a fluid called perilymph (Figure 8) that is similar in chemical and ionic composition to that seen in blood plasma with a high concentration (140mM) of sodium ( $\text{Na}^+$ ) and a low concentration (4mM) of potassium ( $\text{K}^+$ ) (Ferrary and Sterkers, 1998).

These two ducts are continuous, with the tympanic duct starting at the round window and connecting to the vestibular duct at the tip of the cochlea at a small opening called the helicotrema. The vestibular duct then leads to the oval window. The cochlear duct differs from the vestibular duct in that it contains endolymph, has a small opening at the beginning to the vestibular apparatus and is closed at the apex of the cochlea. In addition, the fluid is not compressible and sound waves travel straight across the cochlear duct to the basilar membrane.

Endolymph is more similar in ionic and chemical composition to intracellular fluid and has high concentrations of  $\text{K}^+$  (150mM) and low concentrations of  $\text{Na}^+$  (1mM) (Ferrary and Sterkers, 1998). The composition of the endolymph and perilymph is essential for hearing function and is maintained by epithelial cells within the inner ear and allows for the generation of a resting electrochemical potential of +80 to +100 mV relative to the interior of the hair cells in the cochlear duct (Békésy, 1952). The shape of the cochlea allows us to detect changes in pitch and frequency as the different wavelengths are detected at different points along the duct as seen in Figure 7. As the BM extends from the round window towards the helicotrema, it changes in rigidity, width and mass, becoming less stiff and

more flexible. These changes allow for differentiation of frequency with high frequencies resonating at the more rigid end and low frequencies at the more flexible end.

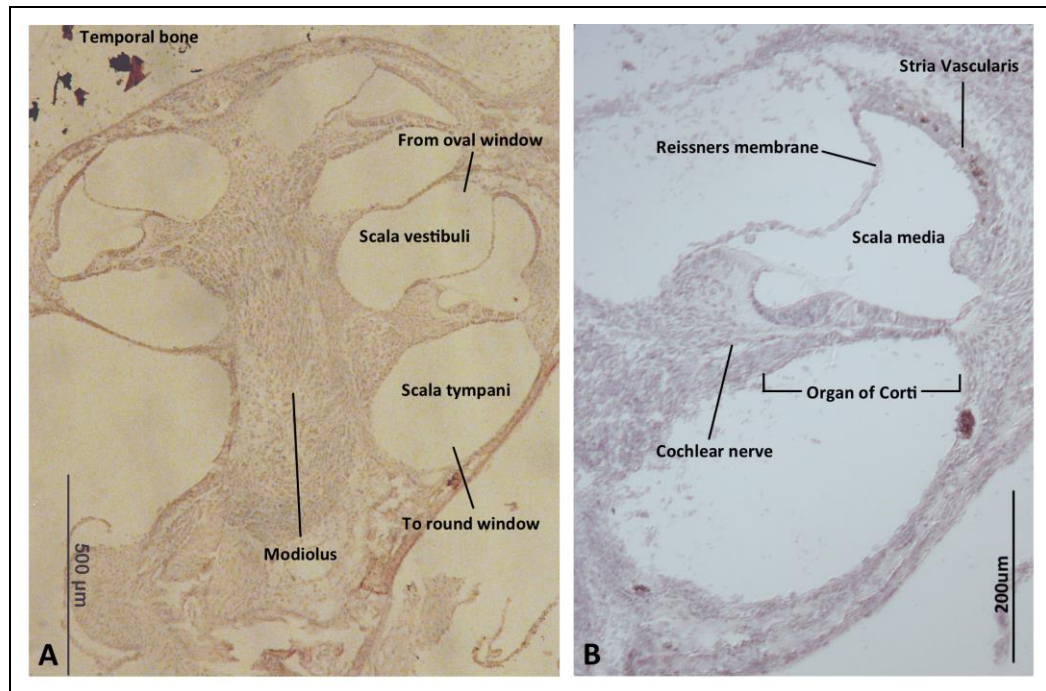


**Figure 9: Haematoxylin and Eosin (H&E) staining of a cross sections from the P5 mouse cochlea. (A) shows a cross section of the whole cochlea within the temporal bone depicted in this are the vestibular duct (scala vestibuli) leading from the oval window and the tympanic duct (scala tympani) leading to the round window. The cochlea spirals around the modiolus. (B) shows a close up cross section of a single turn of the cochlea showing the cochlear duct (scala media) bordered by the Reissner’s membrane, stria vascularis and the organ of Corti. Also shown is the cochlear nerve originating at the organ of Corti.**

### 1.2.3.2 Organ of Corti

The specialised sensory epithelium responsible for hearing resides in the organ of Corti (OoC) of the cochlea (Figure 10). The OoC is located on the BM and is covered by the tectorial membrane (TM). Both membranes move in response to sound waves moving through the vestibular duct. The OoC is made up of two types of auditory hair cells; three rows of very sensitive outer hair cells (OHC) that are directly connected to the TM, and a single row of less sensitive and less vulnerable inner hair cells (inner HC) which are indirectly connected to the TM via sub-tectorial fluid (Zimatore et al., 2011). Both types of hair cells have bundles of stiff slender protuberances (cilia) called “stereocilia” on their apical surface that project towards the TM. The stereocilia are arranged together in rows of decreasing height with the rows connected by protein bridges that act as springs to open and close ion channels in the cilia’s membrane. Movement of the TM and BM causes flexing of the cilia and a corresponding opening or closing of ion channels. Hair cells have a resting potential between -45mV and -70mV compared

to the +80-100mV potential in the cochlear duct (Békésy, 1952, Merchant and Nadol, 2010). The stiffness of the hair bundles decreases from the base towards the apex along with the number of stereocilia in each hair bundle. Inversely, the length of hair bundles increases. The shorter stiffer more numerous hair bundles are more sensitive and have greater angular rotation than the longer ones at the apex. This process of converting mechanical wavelengths to electrical signals is known as mechano-electrical transduction. The hair cells of the inner ear are the final destination of mechanical sound waves that are captured by the outer ear.

In the mouse, the cochlear structures are present at birth and are said to be fully matured by postnatal day 10 (P10) when hearing function is said to begin (Mikaelian and Ruben, 1965). The adult cochlear length is reached at P7 with hair cell numbers matching those of an adult at P3. The mechano-electrical transduction can be detected as early as P1 (Peters et al., 2007). Another paper defines the cochlear organs and TM as fully mature after P14 (Rueda et al., 1996).

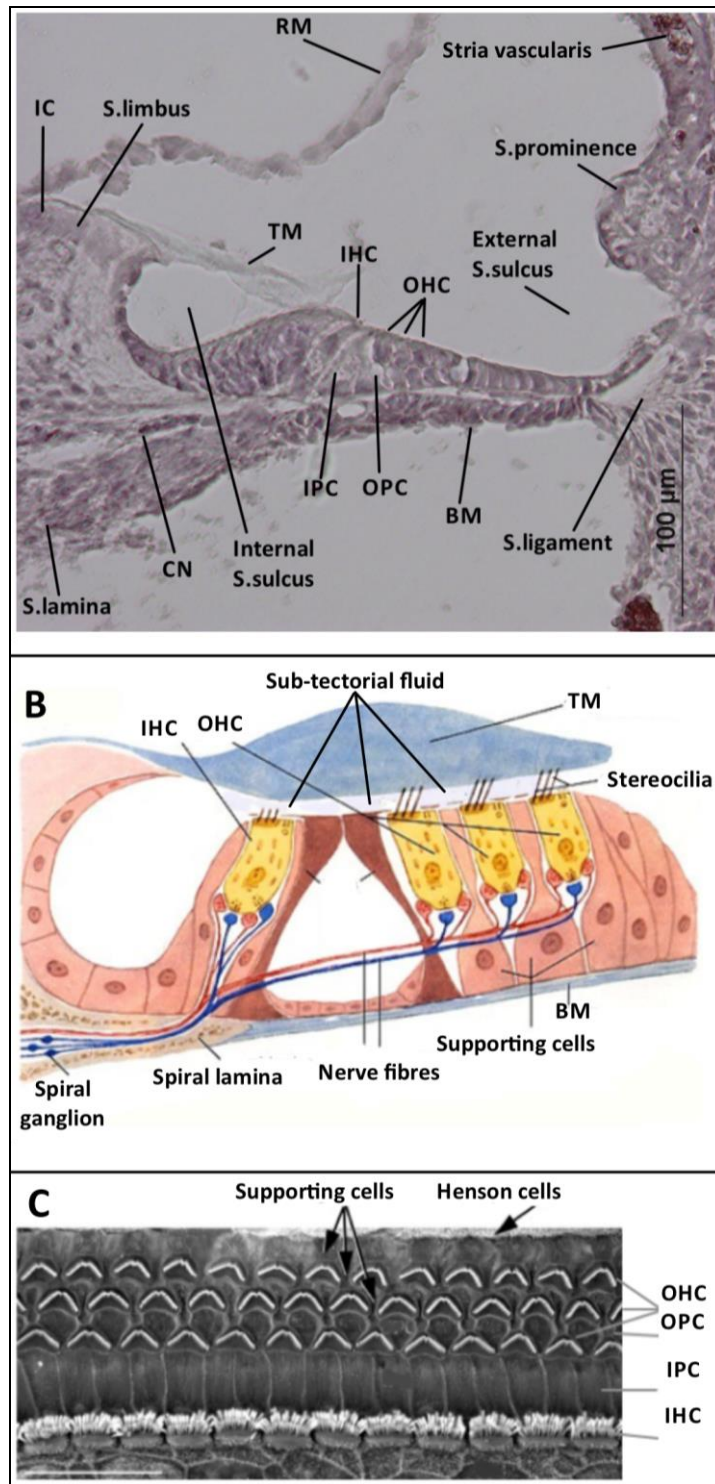


**Figure 10: Anatomy of the OoC.** (A) shows a P5 mouse inner ear stained with H&E. Refer to section 3.10.4.1 for a description of the methods. Depicted are the fine structures of the OoC and spiral structures (spiral ligament (S.ligament), spiral prominence, spiral lamina, spiral limbus, internal spiral sulcus, external spiral sulcus, basement membrane (BM), cochlear nerve (CN), inner pillar cells (IPC), outer pillar cells (OPC), outer hair cells (OHC), inner hair cells (IHC), tectorial membrane (TM), interstitial cells (IC), Reissner's membrane (RM) and stria vascularis. (B) Shows a Schematic diagram depicting the position of the TM relative to the hair cells. OHC are directly connected to the TM via stereocilia. IHC are indirectly connected to the TM via the sub-tectorial fluid (adapted from DeWitt 2005). (C) depicts an electron microscopy image of the apical surface of the organ of Corti showing the position of outer hair cells and inner hair cells (adapted from Quint and Steel)

### 1.2.3.3 Tectorial Membrane

The TM is a collagen-rich extracellular matrix that lies over the OoC running parallel to the BM and is directly connected to the stereocilia of outer hair cells and indirectly connected to the stereocilia of inner hair cells via subreticular fluid. The TM is composed of 97% water with a protein weight consisting of 50% collagen fibres, 25% proteoglycans and 25% non-collagenous glycoproteins (Gueta et al., 2011). It is a polyelectrolyte gel with a structure similar to connective tissue and is the most complex, structurally, of all the acellular gels found in the inner ear. The collagen fibres are what provides the stiffness, integrity and structure to the TM (Gueta et al., 2011).

Glycoproteins (GP) are proteins that contain oligosaccharide chains (glycans) covalently attached to polypeptide side-chains and they are expressed exclusively in the inner ear. This feature makes the TM unique to other mammalian polyelectrolyte gels (Gueta et al., 2011). Genes encoding for GP found in the TM, *alpha*( $\alpha$ )-*tectorin* and *beta*( $\beta$ )-*tectorin*, were identified as being responsible for sensorineural hearing loss, DFNA8 and DFNB21 (Verhoeven et al., 1998). In 2010 Xia et al., at the Baylor college of Medicine, made a *Tecta*<sup>C1509G</sup> knock-in mouse with a point mutation (cysteine to guanine) in the *TECTA* gene, which corresponds to the mutation found in the same gene responsible for DFNA8. Interestingly, the resulting mice displayed near identical pathology as observed in human DFNA8. In a study by Kammerer et al., 2012, a secreted GP, CEACAM16, was localised exclusively in the inner ear and deposited in the TM between P12-P15. Inactivation of this GP produced HL in young mice that progressed with age. This finding correlates with the human DFNA4 phenotype and genetics. For example, a missense mutation was identified in the *CEACAM16* gene (Van Camp G, Smith RJH. Hereditary Hearing Loss Homepage)

The connection of the TM to the stereocilia of the OHC indicates the TM plays a strong role in hair cell stimulation. Movement of the BM and subsequent movement of the hair cells relative to the TM causes the deflection of the stereocilia bundles and fluctuations in membrane potentials for the transduction of sound to electrochemical signals making the TM essential for hearing function (Verhoeven et al., 1998, Xia et al., 2010). The exact composition of the TM and how it functions remain unclear (Ghaffari et al., 2007).



### **1.2.3.4 Reissner's Membrane**

The RM is a double-layered membrane within the inner ear that separates the perilymph in the vestibular duct from the endolymph in the cochlear duct (Valk et al., 2006). The primary function of this membrane is to act as a diffusion barrier and to mediate the composition of these two fluids by facilitating the movement of fluids and electrolytes from one fluid to the other.

In the next section, I will introduce the gene of interest for this MSc thesis, *vitelline membrane outer layer 1 (Vmo1)* and discuss the discovery of this protein in the vitelline membrane of the chicken egg and the mRNA in RM of the mouse inner ear.

## **1.3 Vitelline Membrane Outer Layer 1 Protein**

The vitelline membrane outer layer one protein homolog (chicken) (VMO1) was named for its homology with a protein found in the outer layer of the vitelline membrane (VM) of the chicken egg. It is important to note that the standard nomenclature (HUGO) for abbreviating a gene name is to use italics and sentence case for the mouse gene (e.g. *Vmo1*), and upper case letters for the human and chicken gene (e.g. *VMO1*) and the use of all uppercase for the protein (e.g. VMO1). For the purposes of this thesis where more than one species gene is referred to uppercase italics will be used (e.g. *VMO1*).

### **1.3.1 VMO1 in the Vitelline Membrane of the Chicken Egg**

*VMO1* was found to be expressed exclusively in a restricted area in the hen's oviducts where the infundibulum, a funnel-shaped cavity (the place of fertilisation) joins the magnum (place of egg-white protein production) (Kido et al., 1995). The VM in the chicken egg is a three-layered proteinaceous extracellular matrix that acts as a barrier between the egg yolk and the egg white (albumen) (Kido and Doi, 1988). Figure 11 shows the layout of the three layers in the VM with the thin continuous layer lying between the inner (lamina perivitellina) and outer (lamina extravitellina) fibrous layers. The inner layer is equivalent to the zona pellucida (ZP) in the mammalian oocyte and is formed in the ovary before ovulation. It is made up of a three dimensional network of thick fibres of several kinds of GP (for example GPI, GPII, GPIII and GPIV) and ZP proteins (such as ZPC/ZX3, ZPI and ZPD) (Kido et al., 1995). The outer layer of the VM is a network of fine fibrils that are formed after ovulation in the upper oviduct. This network consists mainly

of the macromolecule ovomucin (43%) (Mann, 2008), which has soluble proteins such as 32% lysozyme (an antimicrobial enzyme) and VMO proteins I (20%) and II (5%) tightly bound to it. The VMO proteins were among the most abundant in the VM next to ovomucin and lysozyme C.

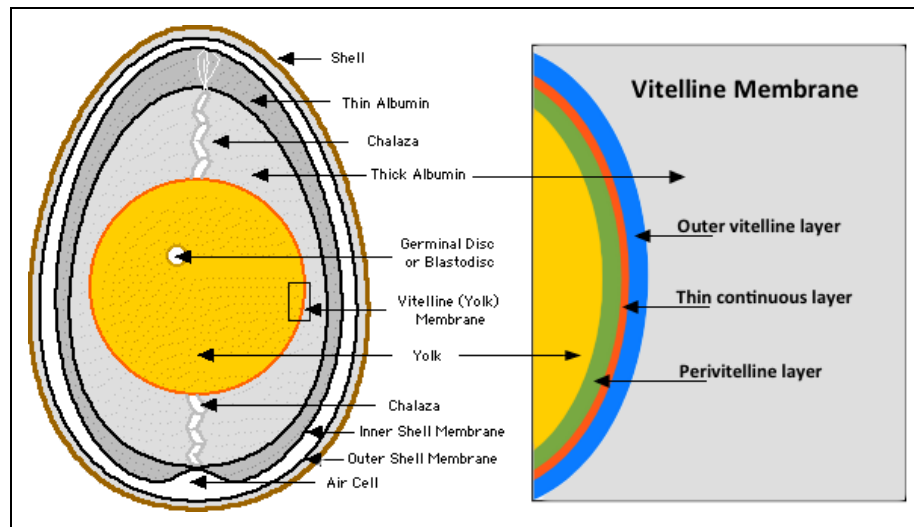


**Figure 11: Structure of the chicken egg.** This figure shows the structure of the chicken egg and the vitelline membrane with its three layers; the outer vitelline layer, thin continuous layer and perivitelline layer abutting the egg yolk (adapted from <http://www.enchantedlearning.com/egifs/eggcrosssection.GIF>)

### 1.3.2 *Vmo1* in Reissner's Membrane of the Mouse Inner Ear

The *Vmo1* gene was discovered to be localised in the Reissner's membrane of the mouse inner ear by using *in situ* hybridisation (Peters et al., 2007). Real-time PCR experiments confirmed expression of *Vmo1* transcripts in the inner ear but absence from adult mouse liver, kidney, pancreas, retina, brain, testes (Peters et al., 2007) using massively parallel signature sequencing (MPSS) libraries. *Vmo1* was not detected within 87 other mouse tissues (MRT project). In addition, the *Vmo1* signature was highly abundant in the inner ear. The authors concluded that they had found the first example of a transcript expressed exclusively in Reissner's membrane. MPSS is method used to identify as well as quantify mRNA transcripts within a sample by tagging PCR products produced from complementary DNA (cDNA) and amplifying them. These tagged sequences are attached to microbeads using ligation and then sequenced and quantified on a flow cell. The sequence signatures are then analysed for gene identification (Peters et al., 2007).

Due to its unique and restricted location, *Vmo1* is of interest as a candidate for being involved in human hearing loss and balance disorders such as Ménière's



disease. This disease is thought to be a build up of excess fluid in the inner ear and is associated with the distension or disruption of the RM and can cause disabling attacks of vertigo, progressive hearing loss and tinnitus, a ringing or roaring sound in the ear (Valk et al., 2006).

Figure 12 shows the expression of *Vmo1* in the mouse auditory system using *in situ* hybridisation. However, this result is unable to resolve which layer(s) *Vmo1* mRNA is expressed in. Using a non-radioactive probe, Digoxigenin labelled antisense *Vmo1* hybridised to the inner layer of RM (Peters, personal communication, 2013). To date, the localisation of VMO1 protein in the auditory system has not yet been determined or published. The presence of *Vmo1* mRNA in the RM indicates that the protein could remain exclusively in the RM or be secreted and transported to cells within the mouse ear.

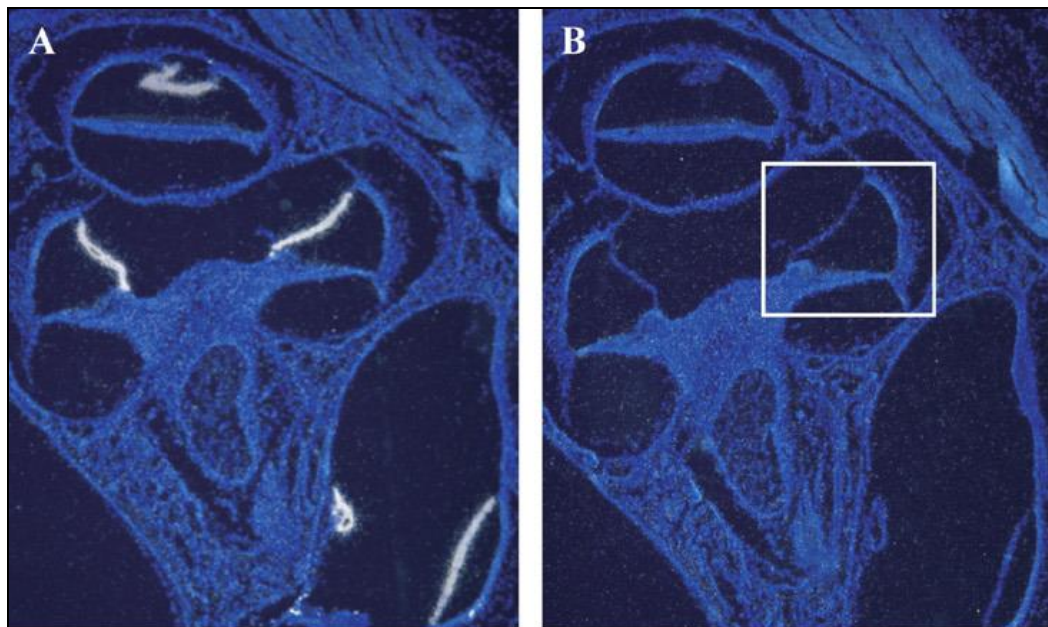


**Figure 12:** <sup>35</sup>S *In situ* hybridisation of *Vmo1* in cross sections of a P5 mouse cochlea. (A) *Vmo1* antisense probe labelled radioactive (silver grains) binds to *Vmo1* mRNA in RM. (B) Negative control - *Vmo1* sense labelled radioactive probe (Peters et al., 2007)

## 1.4 Hypothesis, Aims and Objectives

### 1.4.1 Hypothesis

Movement of fluid and electrolytes is controlled by proteins in the RM and changes to these proteins could influence hearing and/or balance. Our hypothesis is that the VMO1 protein is expressed in RM and plays an important role in the mechanism and/or maintenance of hearing and/or balance.

### 1.4.2 Aim

The main aims of the research undertaken in this thesis was to 1) characterise the possible function of *Vmo1* gene using comparative genomics and 2) investigate the protein expression of VMO1 at different developmental time points in the mouse auditory system using immunohistochemistry (IHC).

### 1.4.3 Objectives

To determine the possible function of VMO1 protein, a bioinformatics approach was used and will be discussed in depth in Chapter 2. Briefly, bioinformatics was carried out to achieve

- a) Nucleotide sequence comparison of *VMO1* in 17 species;
- b) Nucleotide sequence comparison of *VMO1* in the mouse, human and chicken;
- c) Characterisation of the chicken VMO1 protein;
- d) Protein sequence comparison of VMO1 in 36 species;
- e) Protein sequence comparison of VMO1 in the mouse, human and chicken;

To determine the protein localisation of VMO1 in the mouse ear, molecular methods were used to

- a) amplify and sequence *Vmo1* mRNA;
- b) clone and express recombinant VMO1 protein;
- c) validate VMO1 antibodies using whole protein tissue lysates and recombinant protein via western blotting;
- d) test the VMO1 antibody on OCT sections of the mouse inner ear using IHC;
- e) analyse VMO1 binding using a fluorescent microscope.

This data will address the question of whether *VMO1* mRNA transcript and the predicted protein is conserved among birds and mammals, and if the translated VMO1 protein remains within RM or is secreted and transported to cells within the mouse mammalian ear.

## CHAPTER TWO

# COMPARATIVE GENOMICS

Comparative genomics is the study of genome sequence data across different species to identify regions of difference and similarity. The information from these comparisons leads to a better understanding of the function and structure of genes and is an especially important tool for the study of human disease.

*VMOI* nucleic acid and protein sequences were sourced from the National Center for Biotechnology Information (NCBI). The sequences were downloaded and then analysed using a variety of molecular websites (see Appendix 8).

mRNA sequences were generated from transcript and genomic sequence data such as complementary DNA (cDNA) and expressed sequence tags (ESTs) from several sources such as GenBank, RefSeq and third party annotation (TPA).

Predicted sequences were generated by automated computational analysis using the Gnomon (NCBI) gene prediction method and derived from genomic sequences and ESTs.

### 2.1 Nucleotide Comparison of *VMOI* in Different Species

*VMOI* nucleotide sequences were compared for all the species currently annotated on NCBI as of June 2013 to give a general indication of the gene sequence using a wide range of species such as birds and mammals. This included 17 annotated gene sequences and 72 mRNA sequences. The annotated mRNA sequences were limited to Reference Sequences (RefSeq). RefSeq were chosen as they are well supported and represent the more prevalent allele where variations have been found and included 52 sequences for 34 different species. High homology between nucleotide and protein sequence would be indicative of an important function for the *VMOI* gene.

The *VMOI* gene structure and genome location varies greatly between the 17 ortholog species compared (Table 1). For example, the nucleotide length of *VMOI* ranges from 1004 to 3991 base pairs (bp) in length. The genes can be loosely grouped based on taxonomy (avian and mammalian) and then by the DNA strand either sense (5' to 3' coding strand) or the antisense (3' to 5')

complementary strand) on which they are found.

**Table 1: Gene data for *VMOI* for all 17 species available on NCBI. In alphabetical order, the organism species are listed for which *VMOI* gene data was available with the gene ID number, orientation, chromosome location and size of the mRNA transcript (bp).**

Species Name		Accession number	5' to 3' Direction	Chromosome Location	Size (bp)
Common	Scientific				
Baboon (olive)	<i>Papio anubis</i>	101020527	Antisense	16:4475345-4476403	1059
Cat	<i>Felis catus</i>	101092652	Sense	E1:1761741-1762744	1004
Cattle	<i>Bos taurus</i>	526730	Sense	19:27208472-27209491	1020
Chicken	<i>Gallus gallus</i>	418974	Sense	1:179979236-179983226	3991
Chimpanzee	<i>Pan troglodytes</i>	748359	Antisense	17:4802630-4803881	1252
Dog	<i>Canis lupus familiaris</i>	489457	Sense	5:31786057-31787068	1012
Gibbon	<i>Nomascus leucogenys</i>	100603388	Sense	19:76931339-76932591	1253
Gorilla	<i>Gorilla gorilla gorilla</i>	101134564	Antisense	17:4889625-4890877	1253
Human	<i>Homo sapiens</i>	284013	Antisense	17:4688580-4689729	1150
Mouse	<i>Mus musculus</i>	327956	Antisense	11:70513516-70514616	1101
Orangutan	<i>Pongo abelii</i>	100456789	Antisense	17:4709430-4710681	1252
Pig	<i>Sus scrofa</i>	100512921	Sense	12:54329836-54330890	1055
Rat	<i>Rattus norvegicus</i>	360553	Antisense	10:56878079-56879164	1086
Rhesus monkey	<i>Macaca mulatta</i>	709950	Antisense	16:4575276-4576341	1066
Sheep	<i>Ovis aries</i>	101116070	Sense	11:26193505-26194621	1117
Turkey	<i>Meleagris gallopavo</i>	100541696	Sense	1:188369141-188371020	1880
Zebra finch	<i>Taeniopygia guttata</i>	100220541	Sense	1:75113231-75114940	1710

Figure 13 shows a multiple alignment of the antisense *VMOI* gene for 8 mammalian species. All species have mRNA consisting of three coding exons with the exception of the human and western lowland gorilla which both have four variants due to alternative splicing, one of which is lacking exon two.

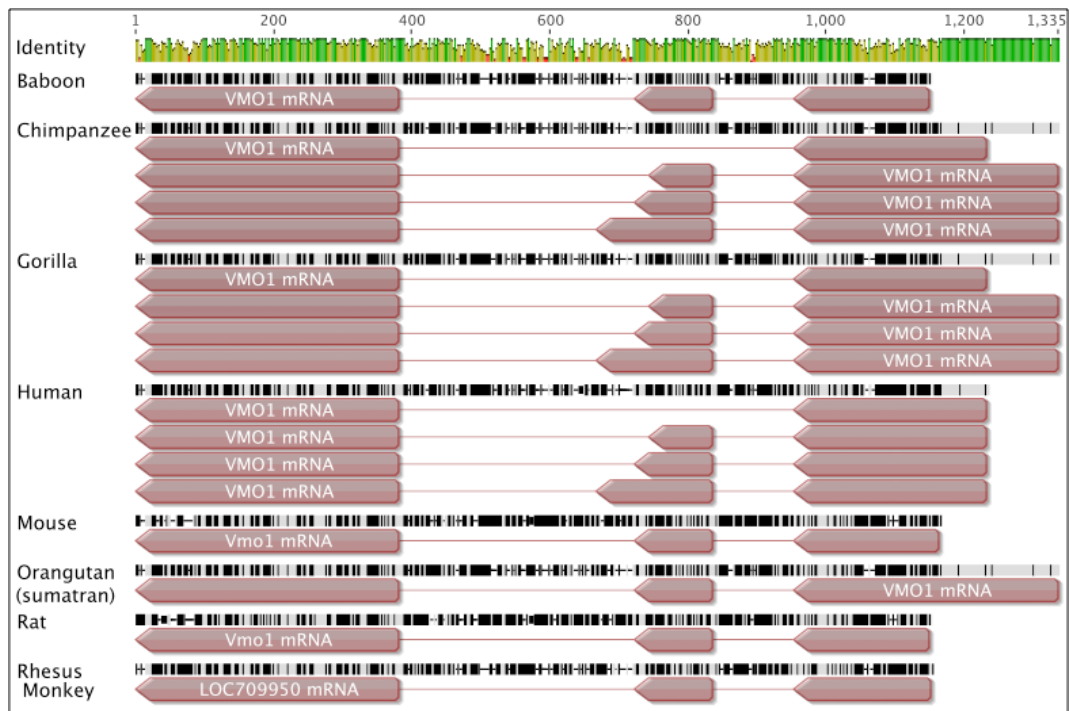


**Figure 13: Gene alignment of *VMO1* for 8 mammalian species. The top identity line represents genomic DNA sequence numbered from nucleotide position 1 to 1335. This line indicated the level of identity shared between eight species with bright green indicating 100% nucleotide identity, dark green representing a change in at least one of the sequences and red which indicates more than one possible nucleotide variation. Depicted below are the *VMO1* mRNA sequences from 8 mammalian species (Table 1) in alphabetical order. The black and white bars represent the consensus genomic DNA sequence of *VMO1* with black showing 100% nucleotide identity. The red arrows show the three coding exons of *VMO1* mRNA in the antisense direction. Exon two is absent from the one each of the human and chimpanzee variants due to alternative transcripts (Geneious® R6).**

Figure 14 shows a multiple alignment of the mammalian species for which the *VMO1* gene is found on the sense strand. All species have mRNA consisting of three coding exons with the exception of the gibbon which has four variants, one of which is lacking exon two.

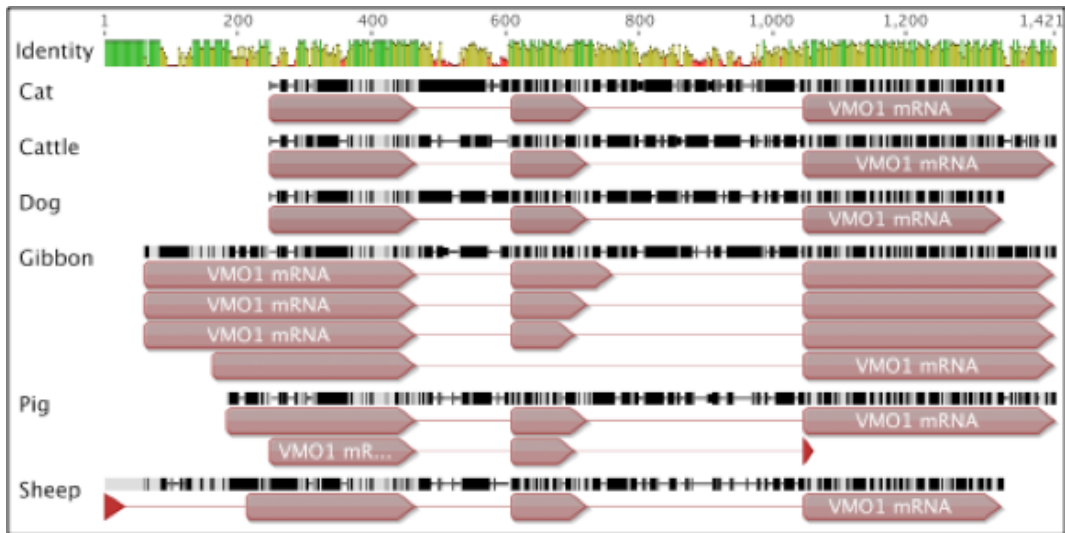


Figure 14: Gene alignment of *VMO1* for six mammalian species with the gene found on the sense strand. The top identity line represents genomic DNA sequence numbered from nucleotide position 1 to 1421. This line indicated the level of identity shared between six species with bright green indicating 100% nucleotide identity, dark green representing a change in at least one of the sequences and red which indicates more than one possible nucleotide variation. Depicted below are the *VMO1* mRNA sequences from six mammalian species (Table 1) in alphabetical order. The black and white bars represent the consensus genomic DNA sequence of *VMO1* with black showing 100% nucleotide identity. The red arrows show the three coding exons of *VMO1* mRNA in the antisense direction. Exon two is absent from northern white checked gibbon due to alternative transcripts (Geneious® R6).

Figure 15 shows a multiple alignment of avian species for which the *VMO1* gene is found on the sense strand. All species have mRNA consisting of three coding exons.

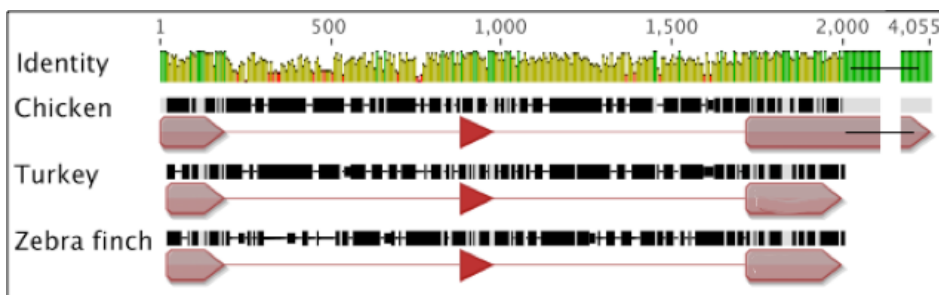


Figure 15: Gene alignment for avian species with *VMO1* gene found on forward/sense strand. The top shows a graph of the identity shared between species with bright green indicating 100% identity, dark green representing a change in at least one of the sequences and red which indicates more than one possible nucleotide variation. The black and white bars represent the consensus genomic DNA sequence of *VMO1* with black showing 100% nucleotide identity. Depicted below are the *VMO1* mRNA sequences from three avian species (Table 1) in alphabetical order. The red arrows show the three coding exons of *VMO1* mRNA in the sense direction. Nucleotide 2000-4055 of the chicken is completely unique to the chicken and does not share any homology with the turkey or zebra finch (Geneious® R6).

The *VMO1* mRNA sequences were compared for 34 different species (Table 2) including predicted sequences from 28 species which are indicated in the table by an asterix (\*) to give a better indication of homology within the coding regions of the gene.

The mRNA of all species except the chicken, nine-banded armadillo, cattle, bottlenose dolphin, ferret, small madagascar hedgehog, southern white rhino and pacific walrus had very similar lengths between 552-906 nucleotides.

**Table 2: mRNA for all species available on NCBI including predicted sequences (\*). Listed are common and scientific names, accession numbers for their sequences and the bp lengths.**

Species		Accession number	Size (bp)
Common name	Scientific name		
Chicken	<i>Gallus gallus</i>	NM_001167761	2626
Human	<i>Homo sapiens</i>	NM_182566	785
	<i>Homo sapiens</i>	NM_001144939	821
	<i>Homo sapiens</i>	NM_001144940	765
	<i>Homo sapiens</i>	NM_001144941	669
Mouse	<i>Mus musculus</i>	NM_001013607	672
Pig	<i>Sus scrofa</i>	NM_001244728	729
Rat (Norway)	<i>Rattus norvegicus</i>	NM_001191823	662
Rhesus monkey	<i>Macaca mulatta</i>	NM_001194053	692
*Armadillo (nine banded)	<i>Dasybus novemcinctus</i>	XM_004447256	1532
	<i>Dasybus novemcinctus</i>	XM_004447257	1457
	<i>Dasybus novemcinctus</i>	XM_004447258	607
*Baboon (olive)	<i>Papio anubis</i>	XM_003912150	689
*Cat	<i>Felis catus</i>	XM_003996152	606
*Cattle	<i>Bos taurus</i>	XM_002695774	667
*Cattle (truncated)	<i>Bos taurus</i>	XM_605104	465
*Chimpanzee (pygmy)	<i>Pan paniscus</i>	XM_003810200	870
*Chimpanzee	<i>Pan troglodytes</i>	XM_001161578	870
	<i>Pan troglodytes</i>	XM_003315319	850
	<i>Pan troglodytes</i>	XM_003315320	906
	<i>Pan troglodytes</i>	XM_003315321	652
*Degu	<i>Octodon degus</i>	XM_004638351	591
*Dog	<i>Canis lupus familiaris</i>	XM_546575	606
*Dolphin	<i>Tursiops truncatus</i>	XM_004330265	300
	<i>Tursiops truncatus</i>	XM_004330264	686
*Ferret	<i>Mustela putorius furo</i>	XM_004804243	1421
*Galago (small-eared)	<i>Otolemur garnettii</i>	XM_003791201	600
*Gibbon (northern white-cheeked)	<i>Nomascus leucogenys</i>	XM_003277870	870
	<i>Nomascus leucogenys</i>	XM_003277871	850
	<i>Nomascus leucogenys</i>	XM_003277872	906
	<i>Nomascus leucogenys</i>	XM_003277873	652
*Gorilla (western lowland)	<i>Gorilla gorilla gorilla</i>	XM_004058334	870
	<i>Gorilla gorilla gorilla</i>	XM_004058335	850
	<i>Gorilla gorilla gorilla</i>	XM_004058336	906
	<i>Gorilla gorilla gorilla</i>	XM_004058337	652
*Hedgehog (small madagascar)	<i>Echinops telfairi</i>	XM_004716125	609
	<i>Echinops telfairi</i>	XM_004716126	213
*Jerboa (lesser egyptian)	<i>Jaculus jaculus</i>	XM_004666874	600
*Manatee (florida)	<i>Trichechus manatus latirostris</i>	XM_004376078	606
*Mole (star-nosed)	<i>Condylura cristata</i>	XM_004685108	597
*Mole-rat (naked)	<i>Heterocephalus glaber</i>	XM_004857279	677
*Orangutan (sumatran)	<i>Pongo abelii</i>	XM_002826874	870
*Orca	<i>Orcinus orca</i>	XM_004266988	686
*Pika (american)	<i>Ochotona princeps</i>	XM_004594844	612
*Rhino (southern white)	<i>Ceratotherium simum simum</i>	XM_004433193	600
	<i>Ceratotherium simum simum</i>	XM_004433194	300
*Sheep	<i>Ovis aries</i>	XM_004013281	690
*Shrew (european)	<i>Sorex araneus</i>	XM_004604921	603
*Squirrel monkey (bolivian)	<i>Saimiri boliviensis boliviensis</i>	XM_003931388	874
*Tasmanian devil	<i>Sarcophilus harrisii</i>	XM_003770628	636
*Walrus (pacific)	<i>Odobenus rosmarus divergens</i>	XM_004398570	300
*Zebra finch	<i>Taeniopygia guttata</i>	XM_002197848	552



### 2.1.1 Prediction of Open Reading Frames

The open reading frame (ORF) within a mRNA sequence can be read in six possible reading frames; three in the forward direction (e.g. +2) and three in the reverse direction (e.g. -2) and begins with a start codon (nucleotides AUG) and ends with one of three stop codons (nucleotides UAA, UAG or UGA) with no stop codons in between, and can potentially be translated into a polypeptide. ORFs were predicted using ORFinder function on the bioinformatics software programme Geneious® R6. This programme identified ORFs by searching for sections of DNA which begin with a start codon, end with a stop codon and contain no stop codons in between. The choice of ORF was verified individually by analysing the resulting peptide produced and comparing it to the protein (or predicted protein) found on NCBI. Sequences were considered full length if they contained the three-fold symmetry observed in the chicken VMO1 protein and the highly conserved amino acid (aa) sequence consisting of an aspartic acid (Asp), threonine (Thr), and asparagine (Asn) with three variable amino acids (X) in the order Asp, X, Thr, X, X, Asn repeated three times.

The ORF of all species excluding the chicken and olive baboon are of similar length of around 600bp. Figure 16 shows a multiple alignment of the ORF for all species found on NCBI and highlights how conserved the *VMO1* gene is.

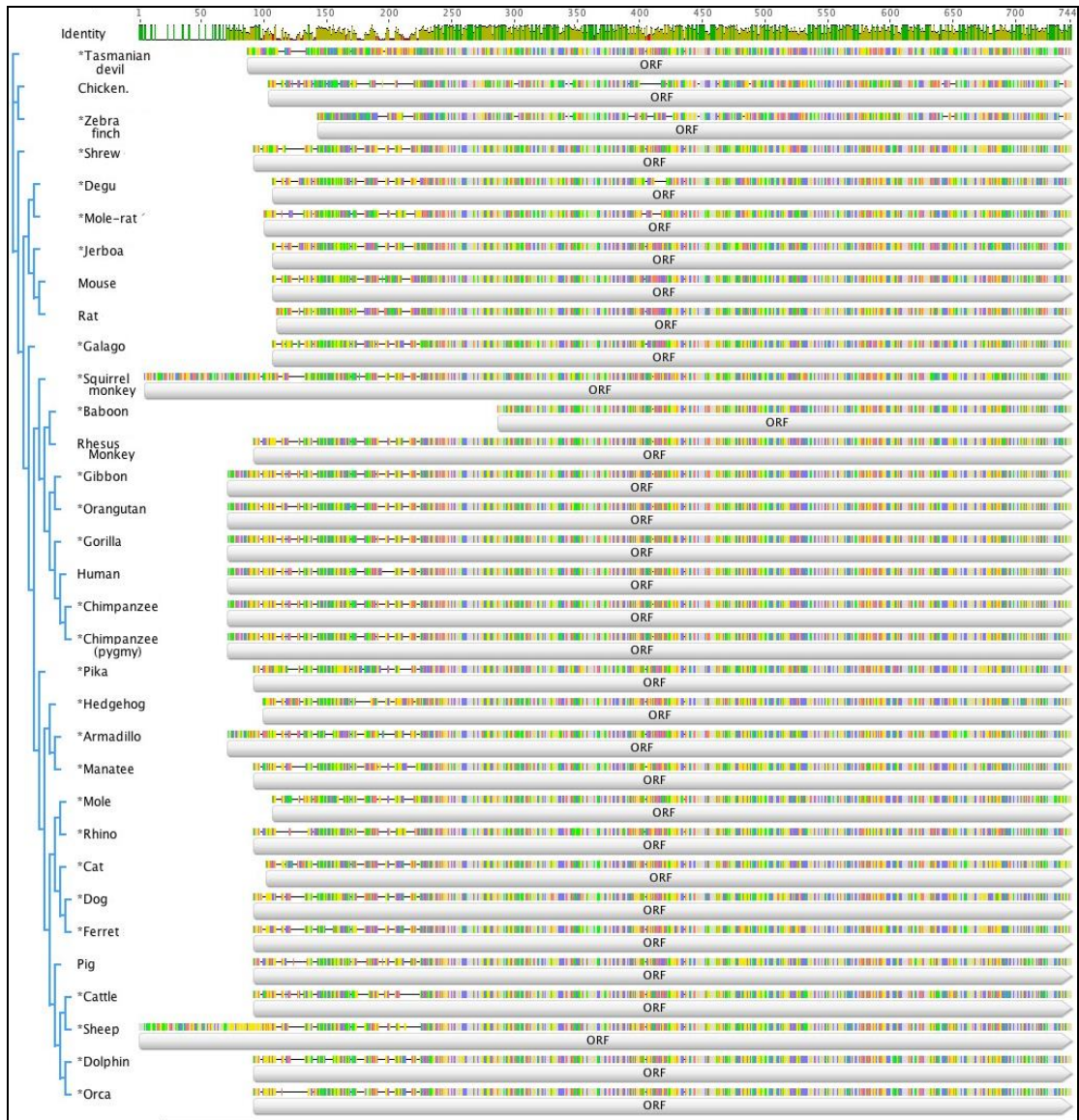


**Figure 16: ORF prediction for all species showing phylogenetic relationship based on sequence homology. The top shows a graph of the identity shared between species with bright green indicating 100% identity and dark green representing a change in at least one of the sequences and red indicating a change to more than one possible nucleotide change. The coloured bar is coloured for each individual amino acid with the gaps representing areas of low identity between species. To the left of the species names is a phylogenetic tree showing the taxonomic relationship between species based on nucleotide sequence similarity (Geneious® R6).**

## 2.1.2 Nucleotide Sequence Comparison of the Mouse, Human and Chicken *VMO1*

An in-depth analysis of the *VMO1* sequences for the *Mus musculus* (mouse), *Homo sapiens* (human) and *Gallus gallus* (chicken) species was carried out to provide a greater understanding of the suitability of the mouse and chicken as animal models for *VMO1*.

### 2.1.2.1 Genomic Structure of Mouse *Vmo1*

The mouse *Vmo1* is 1101bp long and located on chromosome 11 at position 70,513,516 to 70,514,616 on the antisense strand (Figure 17). *Vmo1* was formally known under the alias of GM741 or RP23-122P1.11. The *Vmo1* mRNA transcript (Accession number: NM\_001013607) is 672 bp long and consists of three exons; 206, 116 and 350bp long, respectively. The open reading frame is 606 bps in length with a +3 frame shift.

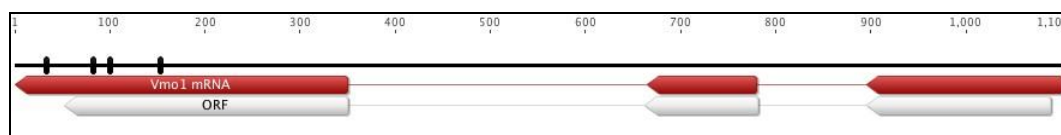


**Figure 17: Nucleotide position of *Vmo1* coding exons on mouse chromosome 11. The schematic diagram shows a black line that represents genomic DNA on chromosome 11 from nucleotide position 1 to 1,010. The four non-synonymous variants are indicated by black bars on this line. Depicted below is the alignment of *Vmo1* mRNA (red) showing three exons in the antisense direction. Exon 1 is 206 bp (nucleotides 1,101 to 896), exon 2 is 116bp (nt 781 to 666) and exon 3 is 350bp (nt 350 to 1). The white arrow represents the ORF of *Vmo1* which is 606 bp (Geneious® 6.1.6).**

The mouse *Vmo1* has four non-synonymous single nucleotide variants (SNV) within its protein-coding region (Table 3). An SNV is a change to a single nucleotide in a sequence that has not been well characterised or is only seen in one individual as opposed to a single nucleotide polymorphism (SNP) that occurs in a well characterised allele at a higher frequency. These non-synonymous SNV do not change the amino acid sequence of the protein. For example, rs251432110 is a SNV on chromosome 11 at nucleotide position 70513712, where there is a nucleotide change of an adenine (A) to a guanine (G). The amino acid encoded by the codon remains a proline (Pro) at position 154 of the VMO1 protein.

**Table 3: Non-synonymous SNVs in the mouse *Vmo1* coding region showing the base pair change that occurs**

([http://www.ensembl.org/Mus\\_musculus/Gene/Variation\\_Gene/Table?g=ENSMUSG00000020830;r=11:70513516-70514616;t=ENSMUST00000021179](http://www.ensembl.org/Mus_musculus/Gene/Variation_Gene/Table?g=ENSMUSG00000020830;r=11:70513516-70514616;t=ENSMUST00000021179))

Ensembl ID	Genome Position	Alleles	AA	AA co-ordinates
rs251432110	11:70513712	A/G	P	154
rs246511382	11:70514186	G/A	S	101
rs217069436	11:70514240	T/C	L	83
rs238425283	11:70514501	G/A	I	34

### 2.1.2.2 Genomic Structure of Human *VMO1*

*VMO1* is the approved gene symbol for vitelline outer layer membrane 1 by the Human Gene Nomenclature Committee. Previously, it was known as ERGA6350 or PRO21055. This gene is located on the antisense strand of chromosome 17p13.2 from nucleotide position 4688580 to 4689728. It is 1149 bps long and contains numerous mutations (Figure 18); three of which result in three additional splice variants. The human *VMO1* transcript is represented by 37 ESTs from 22 cDNA libraries that correspond to four different isoforms.

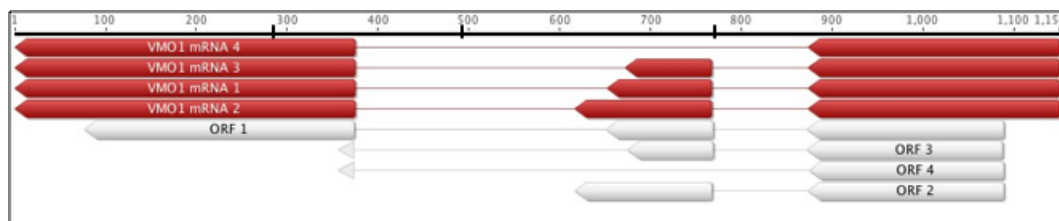


**Figure 18: Alternative transcripts of Human *VMO1* gene. The schematic diagram shows a black line at the top which represents genomic DNA on chromosome 17p13.2:4688580-4689728 from 1-1150. Along this line are 3 black lines that represent the three nucleotide variations that result in the splice variants. The alignment of the four *VMO1* mRNA variants (red) is shown below in the antisense direction. Depicted below are the ORF for the four transcripts as indicated by white arrows (Geneious® 6.1.6).**

*VMO1* transcript variant 1 (NM\_182566.2) is 785bp long, composed of three exons and predicted to translate to a 202aa *VMO1* protein (NP\_872372) of molecular weight 22kDa. *VMO1* transcript variant 2 (NM\_001144939.1) is 821bp long, composed of three exons and is the result of a SNP in a splice region (dbSNP ref no: rs13847834) at chromosome position 17:4688962 and results in a truncated protein 114aa long (NP\_001138411). *VMO1* transcript variant 3 (NM\_001144940.1) is 765bp long, composed of three exons and is the result of two SNPs, one in the splice region (dbSNP ref no: rs13847834) at chromosome position 17:4688962 and the other (dbSNP ref no: rs149577678), which results in a stop codon, at position 17:4689448 which results in a truncated protein 103aa long (NP\_001138412.1). In contrast, the *VMO1* transcript variant 4 (NM\_001144941) is 669bp long, composed of two exons and is the result of a

somatic substitution (COSMIC ref no: COSM1141184) at chromosome position 17:4689448 and results in a truncated protein 70aa long (NP\_001138413). Figure 19 shows a multiple alignment of the four human VMO1 proteins.

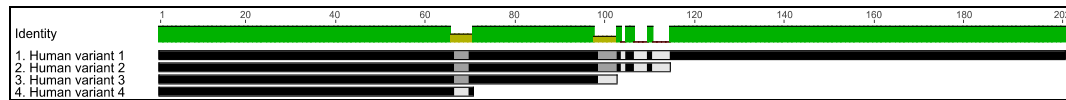


**Figure 19: Translated protein for mRNA splice variants for human *VMO1*. The green graph shows the similarity between the four mRNA transcripts with bright green representing 100% identity. Olive green indicates a difference in one of the mRNA variants. The black lines represent the mRNA variants and are interrupted by grey to show where identity is not conserved between the variants (Geneious® 6.1.6)**

Numerous variants were identified within the human *VMO1* gene using Ensembl. Ensembl is a publicly accessible database of sequence data that has a compilation of variations, including SNPs, somatic mutations and insert/deletions (indels) from databases such as the National Heart, Lung and Blood Institute (NHLBI) exome sequencing project, the short genetic variations database (dbSNP), and the catalogue of somatic mutations in cancer (COSMIC).

**Table 3: Human *VMOI* variant table showing the variants resulting in splice variants and non-synonymous variants occurring in the translated regions (COSMIC project, dbSNP database NCBI, NHLBI Exome Sequencing Project).**

Ensemble ID	Chromosome:bp	mRNA coord	Alleles	Class	Type	AA	AA coord	Transcript Variant
COSM131196	17: 4688658	1070	C/A	somatic_SNV	Stop lost	*/L	203	1
TMP_ESP_17_4688664	17: 4688664	1064	C/T	SNP	Missense	R/H	201	1
rs140800596	17: 4688682	1046	G/A	SNP	Missense	A/V	195	1
rs192962559	17: 4688704	1024	C/T	SNP	Missense	D/N	188	1
TMP_ESP_17_4688713	17: 4688713	1015	C/A	SNP	Missense	G/S	185	1
COSM178972	17: 4688713	1015	C/A	somatic_SNV	Missense	G/C	185	1
rs201001569	17: 4688743	985	C/T	SNP	Missense	G/S	175	1
rs145186131	17: 4688747	981	C/T	SNP	Synonymous	A	173	1
rs139005779	17: 4688749	979	C/T	SNP	Missense	A/T	173	1
rs201850470	17: 4688754	974	T/C	SNP	Missense	K/R	171	1
COSM298216	17: 4688755	973	-/GGGG	somatic_insertion	Elongation, Frameshift		171	1
TMP_ESP_17_4688822	17: 4688822	906	G/C	SNP	Missense	D/E	148	1
TMP_ESP_17_4688849	17: 4688849	879	C/A	SNP	Synonymous	A	139	1
rs116521670	17: 4688895	833	G/A	SNP	Missense	S/L	124	1
rs200001295	17: 4688904	824	A/G	SNP	Missense	V/A	121	1
rs150447995	17: 4688944	784	A/G	SNP	Missense	W/R	108	1
rs150447995	17: 4688944	784	A/G	SNP	Missense	M/T	101	3
rs138473834	17: 4688962	766	G/T	SNP	Intron variant, Splice Region	-	-	1,2 and 3
rs199657463	17: 4689190	538	A/T	SNP	Intron variant, Splice Region	-	-	2
rs138226966	17: 4689231	497	C/A	SNP	Missense	R/S	104	2
TMP_ESP_17_4689232	17: 4689232	496	C/G	SNP	Splice Region, Missense	S/T	104	1
TMP_ESP_17_4689232	17: 4689232	496	C/G	SNP	Missense	R/T	104	2
COSM216399	17: 4689233	495	T/G	somatic_SNV	Splice Region, Missense	S/R	104	1
COSM216399	17: 4689233	495	T/G	somatic_SNV	Synonymous	R	104	2
rs149577678	17: 4689235	493	C/A	SNP	Stop gained	G/*	103	1
rs149577678	17: 4689235	493	C/T	SNP	Missense	G/E	103	1 and 2
rs148311119	17: 4689237	491	A/G	SNP	Synonymous	S	102	1 and 2
COSM561170	17: 4689248	480	C/G	somatic_SNV	Missense	E/Q	99	1 and 2
rs142988795	17: 4689254	474	C/T	SNP	Missense	V/M	97	1 and 2
rs142988795	17: 4689254	474	C/T	SNP	Splice Region, Missense	V/M	97	3
TMP_ESP_17_4689259	17: 4689259	469	G/C	SNP	Missense	T/R	95	1, 2 and 3
rs200589085	17: 4689268	460	A/G	SNP	Missense	L/P	92	1, 2 and 3
rs111749791	17: 4689280	448	C/T	SNP	Missense	R/H	88	1, 2 and 3
TMP_ESP_17_4689283	17: 4689283	445	G/A	SNP	Missense	A/V	87	1, 2 and 3
rs149233371	17: 4689289	439	T/C	SNP	Missense	H/R	85	1, 2 and 3
rs201957775	17: 4689309	419	T/A	SNP	Synonymous	A	78	1, 2 and 3
rs2279961	17: 4689313	415	G/C	SNP	Missense	T/S	77	1, 2 and 3
COSM178973	17: 4689332	396	C/A	somatic_SNV	Missense	G/C	71	1, 2 and 3
COSM1141184	17: 4689448	280	CC/AA	somatic_substitution	Intron variant, Splice Region	-	-	All
TMP_ESP_17_4689484	17: 4689484	244	T/A	SNP	Missense	D/V	55	All
rs147226483	17: 4689488	240	G/A	SNP	Missense	P/S	54	All
TMP_ESP_17_4689523	17: 4689523	205	C/T	SNP	Missense	G/D	42	All
rs140581643	17: 4689545	183	C/T	SNP	Missense	V/I	35	All
COSM472960	17: 4689557	171	C/T	somatic_SNV	Missense	G/S	31	All
COSM707039	17: 4689561	167	C/G	somatic_SNV	Synonymous	R	29	All
rs4790706	17: 4689572	156	T/C	SNP	Missense	T/A	26	All
COSM73254	17: 4689599	129	G/A	somatic_SNV	Missense	R/W	17	All
TMP_ESP_17_4689623	17: 4689623	105	G/C	SNP	Missense	L/V	9	All

Table 4 shows the human *VMOI* EST data showing *VMOI* mRNA was found to be expressed in 28 different human tissues ranging over 71 developmental time points using two different methods; RNA sequencing and microarrays (Ensembl). RNA sequencing uses MPSS to quantify the presence of a particular RNA sequence in a tissue at any given moment in time using next-generation sequencing.

Microarrays measure the expression levels of genes simultaneously by using short sections of nucleotides to hybridise cDNA to a biochip followed by DNA sequencing.

**Table 4: EST data available for human *VMO1*. The table outlines the tissue in which the *VMO1* transcript has been found and the method used to identify it ([http://www.ensembl.org/Homo\\_sapiens/Gene/Expression?g=ENSG00000182853;r=17:4688580-4689728](http://www.ensembl.org/Homo_sapiens/Gene/Expression?g=ENSG00000182853;r=17:4688580-4689728)).**

Methodology	Tissues
Microarray	Adipose, blood, breast, bronchus, colon, conjunctiva, frontal lobe, fertilised oocyte, liver, lung, myometrium, nasopharynx, nose, pituitary, prostate, putamen, vagina, trachea, temporal lobe, spleen, skin, skeletal muscle, sinus, retina
RNA Sequencing	Cerebellum, frontal lobe, heart, kidney, liver, testis

### 2.1.2.3 Genomic Structure of Chicken *VMO1*

The *Gallus gallus* (chicken) *VMO1* gene (Gene ID no: 418974) is 3991 bps long and found on the sense strand of chromosome 1:179979236-179983226 (Figure 20). The mRNA (NM\_001167761.1) is 2626 base pairs long and composed of three exons, 189, 95 and 2342bp long, respectively with a single synonymous SNP (guanine to adenine) at chromosome position 1:179981137 (Table 5).

The *VMO1* gene is a protein-coding gene with an ORF 552 bps long, with a frame shift of +1 (Figure 20), which produces a single protein of 183aa in size.

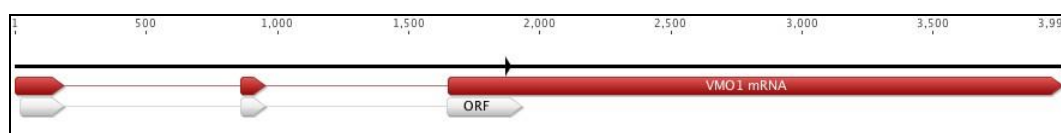


**Figure 20: Nucleotide structure of the Chicken *VMO1* gene. This schematic shows the chicken *VMO1* gene found on chromosome 1 position 179979236 to 179983226 represented from 1-3991 along the top in black with the position of the synonymous SNP represented by a black arrow. Below this is the 2626bp mRNA travelling in the sense direction and showing the position of the three exons 189, 95 and 2342bp depicted in red arrows. Below this is the position of the 552bp ORF with a +1 frame shift in white arrows (Geneious® R6).**

**Table 5: Chicken variant table showing one synonymous SNP**

Ensembl ID	Chromosome position	Base change	Type	AA coordinate
ss538136531	1:179979236-179983226	G/A	Synonymous SNP	Asp173

### 2.1.3 Summary of *VMO1* Genomic Structure

The chicken *VMO1* gene sequence was very different from the mouse and human gene due to the length of the introns and the amount of non-coding sequence. It is



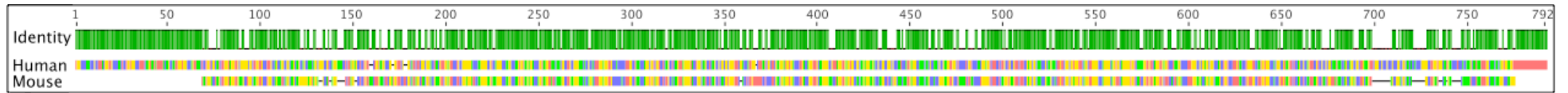
nearly four times larger than the human or mouse gene and is found on the sense DNA strand as opposed to the antisense strand. The mouse and human *VMO1* genes could be aligned to 64% nucleotide identity. Although all three species had mRNA composed of three coding exons, there was still a great difference between the length of the mRNA transcript due to the third exon of chicken *VMO1* being approximately seven times longer than that of the mouse and humans. However, the chicken *VMO1* transcript was identified by RNA sequencing to be expressed in the brain, breast, cerebellum, fibroblasts, embryo, heart, kidney, liver, macrophages, somites and testes. These match the tissues in which *VMO1* was found in humans using RNA sequencing, indicating a good level of conservation.

Figure 21 shows a pairwise alignment of the mouse and human mRNA transcript showing a high level of nucleotide conservation with 72% shared identity. The chicken mRNA transcript could not be accurately aligned with the mouse and human transcript due to its relatively large intron length and the difference in exon sizes.

Figure 22 shows a multiple alignment of the ORF for the mouse, human and chicken *VMO1* showing a very high level of homology despite widely varying gene and mRNA sequences. The predicted ORF of chicken *VMO1* has 54.6% identity with human *VMO1* and 54.3% identity with mouse *Vmo1* gene. The mouse and human gene share 75% identity.

Following analysis of the nucleotide structure, the next section will focus on the *VMO1* protein and take an in depth look at the amino acid sequences in the mouse, human and chicken. Conservation of the *VMO1* protein is especially important for defining protein function.





**Figure 21: Pairwise alignment of the mouse and human mRNA showing shared identity in a green graph above the sequences (Geneious® R6).**

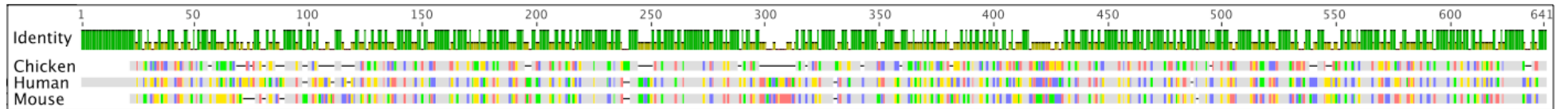


**Figure 22: ORF alignment for the mouse, human and chicken showing the identity shared in green graph above the sequences (Geneious® R6).**

## **2.2 Characterisation of the Chicken VMO1 Protein**

VMO1 protein was first identified in the outer layer of the VM in the chicken egg (Back et al., 1982). In this section, I will review the literature to determine the three dimensional (3D) or quaternary structure of the chicken VMO1 protein and the importance of the secondary structures, such as  $\beta$ -sheets and  $\alpha$ -helices, and tertiary structures, such as the Greek key motif, found within it. The 3D structures of proteins are important for their biological function and are determined by non-covalent interactions that form the secondary and tertiary structures such as van der Waals forces, ionic interactions, hydrogen bonding and hydrophobic packing. The 3D structure of chicken VMO1, isolated from the outer layer of the VM of hen's eggs, was published in 1994 by Dr Morikawa's laboratory at the Protein Engineering Research Institute, Japan.

### **2.2.1 Chemical Characteristics and Amino Acid Sequence**

The chicken VMO1 protein (NP\_001161233.1) was isolated from the VM outer layer of the hen's egg and crystals grown using the hanging drop, vapor diffusion method and then analysed using iso-electrophoresis. The resulting protein was identified as a basic, extracellular enzyme with an isoelectric point of 10 (Kido et al., 1995). This is slightly lower than egg albumen lysozyme (Mann, 2008). The VMO1 amino acid sequence was determined by analysis on a pulsed-liquid-phase sequenator (Model 477A, Applied Biosystems) and amino terminal sequence analysis by Edman degradation and carboxypeptidase Y treatment (Kido et al., 1995). It is 183aa long and rich in glycine (Gly), serine (Ser) and basic amino acids such as arginine (Arg), lysine (Lys) and histidine (His) (NCBI) and has a calculated molecular mass of 18kDa and an estimated mass of 18kDa (Kido et al., 1995). Figure 23 shows the linear layout of the amino acid sequence and the positions of the structures and motifs within it. The protein consists of a 20aa signal peptide and a 163aa mature protein. The signal peptide is usually found on secreted proteins and suggests that VMO1 is secreted. Analysis by Back et al., 1982 showed chicken VMO1 did not contain methionine (Met) suggesting it is a secreted protein with post translational modifications to the N-terminal end of the polypeptide chain.

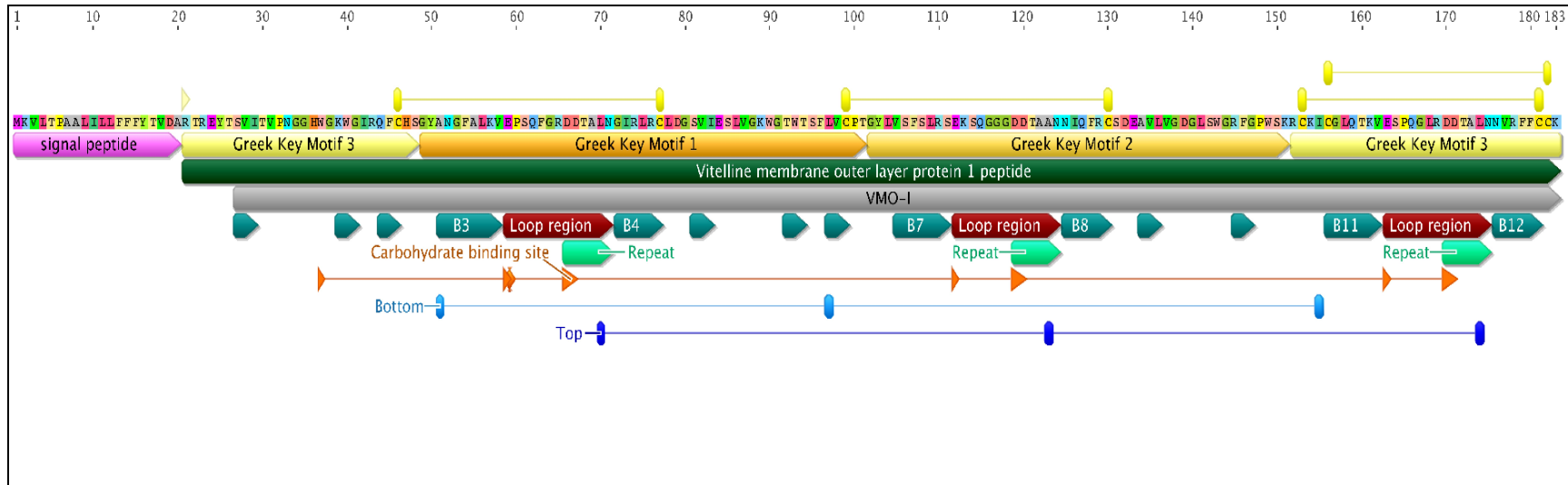


**Figure 23: Amino acid sequence of the chicken VMO1 protein. The numbering of amino acids is shown at the top of the diagram from position 1 to 183 and underneath, the actual amino acid sequence of VMO1. This schematic shows the various structures identified in the 3D structure of the chicken VMO1 protein (Shimizu et al., 1994); in yellow are the four disulfide bonds between cysteine (Cys) residues at position Cys 26 and 57, Cys 79 and 110, Cys133 and Cys161, and Cys136 and Cys162. Below the amino acid sequence are the annotated protein motifs, the signal peptide (pink arrow) the three Greek key motifs (yellow arrows) and the mature peptide in green. Below this is the VMO1 domain (grey) within the mature peptide. Depicted below by blue/green arrows are the 12 beta sheets and the three loop regions (red arrow). Depicted by the connected orange arrows is the proposed carbohydrate binding sites found in the active site cleft at the top of the 3D protein structure. At the top and bottom of this 3D structure is the bottom hydrogen bonding network (light blue) and top hydrogen bonding network (dark blue) that stabilise the structure (Geneious® R6).**

## 2.2.2 Greek Key Motif

The crystal structure of chicken VMO1 protein has the formation of three Greek key motifs, named after the ornamental Greek fret or key design found in decorative elements such as jewellery and pottery (Figure 24a, Wikipedia). This motif is a simple structure involving three antiparallel  $\beta$ -sheets connected by short loops of two to five amino acid (usually containing Gly or Pro) to make  $\beta$ -hairpins (Figure 24b) with a fourth  $\beta$ -sheet looping back to lie antiparallel to the first sheet (Figure 24c).

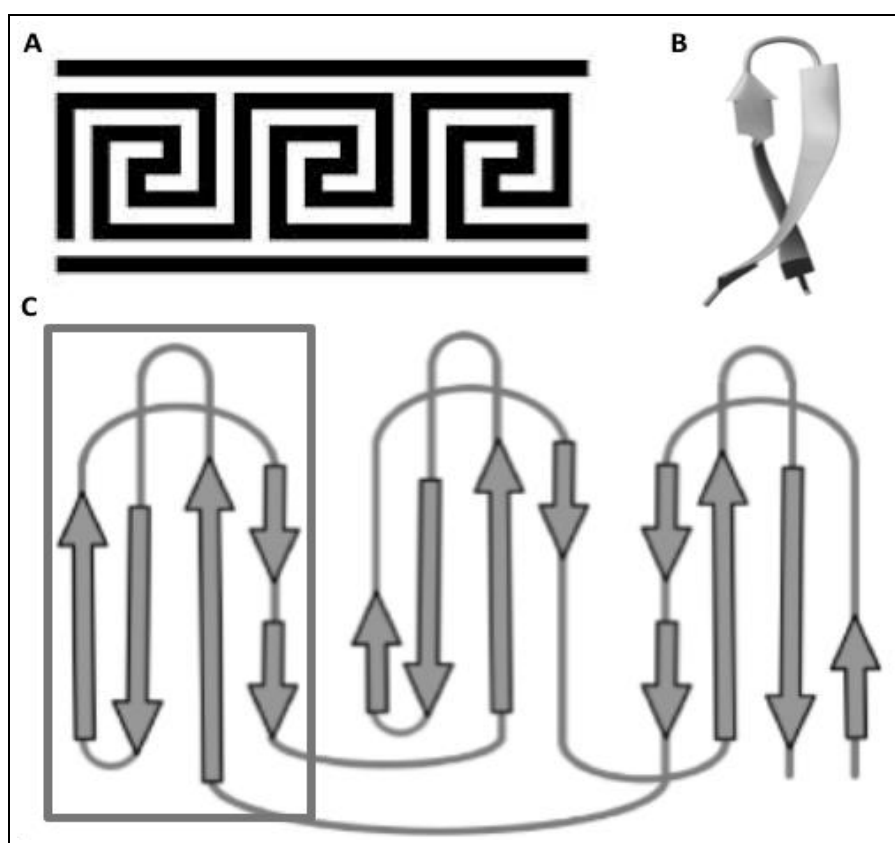


**Figure 24: The Greek key Motif. (A) The ornamental Greek key design which the motif was named after (adapted from wikipedia.org). (B) the Beta hairpin; the basic unit of the Greek key motif (Daidone, 2011) (C) Basic Greek key structure of the chicken VMO1 protein showing the protein structure of the Greek key motif showing the beta sheets (arrows) lying parallel to each other and connected together by amino acid loops and the internal three-fold symmetry with a single Greek key motif outlined in grey.**

## 2.2.3 3D Crystal Structure of VMO1

The 3D structure of chicken VMO1 isolated from the VM outer layer of hen's eggs was published in 1994 by Dr Morikawa's laboratory at the Protein Engineering Research Institute, Japan (Shimuzu et al., 1994).

The 3D structure of the chicken VMO1 was determined by multiple isomorphous replacement (MIR) that is a variation of X-ray crystallography that involves the comparison of normal crystals with crystals that have been co-crystalised with heavy atoms. This gave a resolution of 3.0 angstroms (Å), which was then refined to 2.2Å and an R-factor of 18.8% by Shimizu et al., 1994. The crystal model consisted of a two-chain monomer with 144 water molecules. The crystal structure was determined to be a collection of three  $\beta$ -sheets arranged into a prism shape (termed the “ $\beta$ -prism”) with internal pseudo three-fold symmetry (Figure 25c) and therefore classified as an all  $\beta$ -protein (Kido et al., 1995; Shimizu et al., 1994). All  $\beta$ -proteins are a class of proteins in which the secondary structure is almost completely made of  $\beta$ -sheets and includes the  $\beta$ -barrel found in the human retinol binding protein, the  $\beta$ -propeller protein found in the viral envelope of the influenza virus and the immunoglobulin fold, which also has Greek key topology, found in antibodies (Murzin et al., 1995; Gromiha, 2004).

#### **2.2.3.1 Internal Three-Fold Symmetry of VMO1**

The crystal structure of chicken VMO1 protein has the formation of three Greek key motifs (Figure 24a, Wikipedia). This motif is a simple structure involving three antiparallel  $\beta$ -sheets connected by short loops of two to five amino acids (usually containing Gly or Pro) to make  $\beta$ -hairpins (Figure 24b, Daidone, 2011) with a fourth  $\beta$ -sheet looping back to lie antiparallel to the first sheet (Figure 24c).

The VMO1 protein displays an internal three-fold symmetry that is important for the formation of the 3D vase-like structure. The three internal repeats make up the three sides of the overall triangular prism shape and allow for the positioning of the loop regions thought to be important for VMO1 function at the top of the structure. Each repeat is a standalone Greek key motif and were aligned using an amino acid multiple alignment to show how highly conserved the sequences are between the repeats.

Figure 25 shows the VMO1 amino acid sequence structure aligned to show the internal symmetry of a repeated unit of approximately 53aa. The alignment shows that this repeat shows a very high degree of similarity and identity especially in the sequence highlighted by a green arrow (Asp, X, Thr, X, X, Asn), which is found at the C-terminus end of the three loop regions. Greek key motif 1 is made of three short and two long  $\beta$ -strands lying antiparallel to each other. The second

Greek key motif has almost the same structure only lacking one short  $\beta$ -strand that is replaced by hydrogen bonding between Ser side residues (Ser86, Ser88 and Ser130) interacting with main chain atoms. The formations of these three Greek key motifs form the sides of the vase-like shape of the 3D structure.

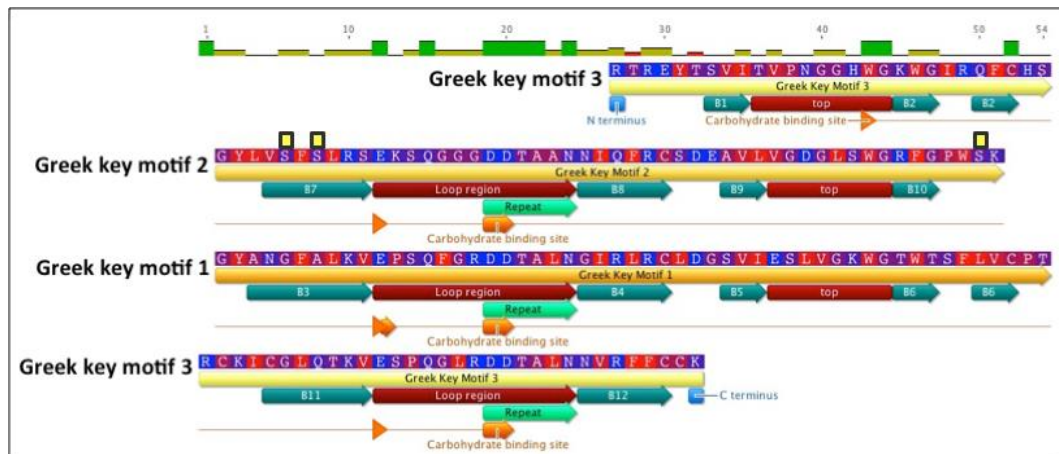


**Figure 25: Alignment of Greek key motifs in the chicken VMO1 protein.** The graph at the top shows the identity shared between the amino acid sequence with bright green being identical across all three motifs and dark green identical across two of the motifs. The numbers represent the number of amino acids. Below this graph is the amino acid sequence which is shaded to show hydrophobicity; hydrophobic (red), hydrophilic (blue). In addition, this highlights the similarity between the side chains groups of the amino acids. Beneath the amino acid sequence are the Greek key motifs (yellow arrows) in the order they appear within the sequence. The schematic shows 100% identity in the carbohydrate binding sites (connected orange arrows) and a high level of similarity in the loop regions (red arrow) and the beta sheets (blue/green arrow). The beta strands are indicated by dark green arrows with the missing third beta strand in motif 2 being replaced by 3 H bonds between serine residues and main chain atoms indicated by black lined yellow squares (Geneious® R6).

### 2.2.3.2 Triangular Prism Structure

The three Greek key motifs of the VMO1 protein are arranged together to form a vase-like triangular prism structure (30x30x45Å) held together by stabilising interactions (Figure 26). The 3D arrangement forms an active site cleft at the top of the structure where carbohydrate binding is thought to occur. This carbohydrate-binding site is a chemical binding site thought to play a role in sugar hydrolysis or recognition and contains two Asp residues frequently involved in hydrogen binding between proteins and sugar (Kido et al., 1994).

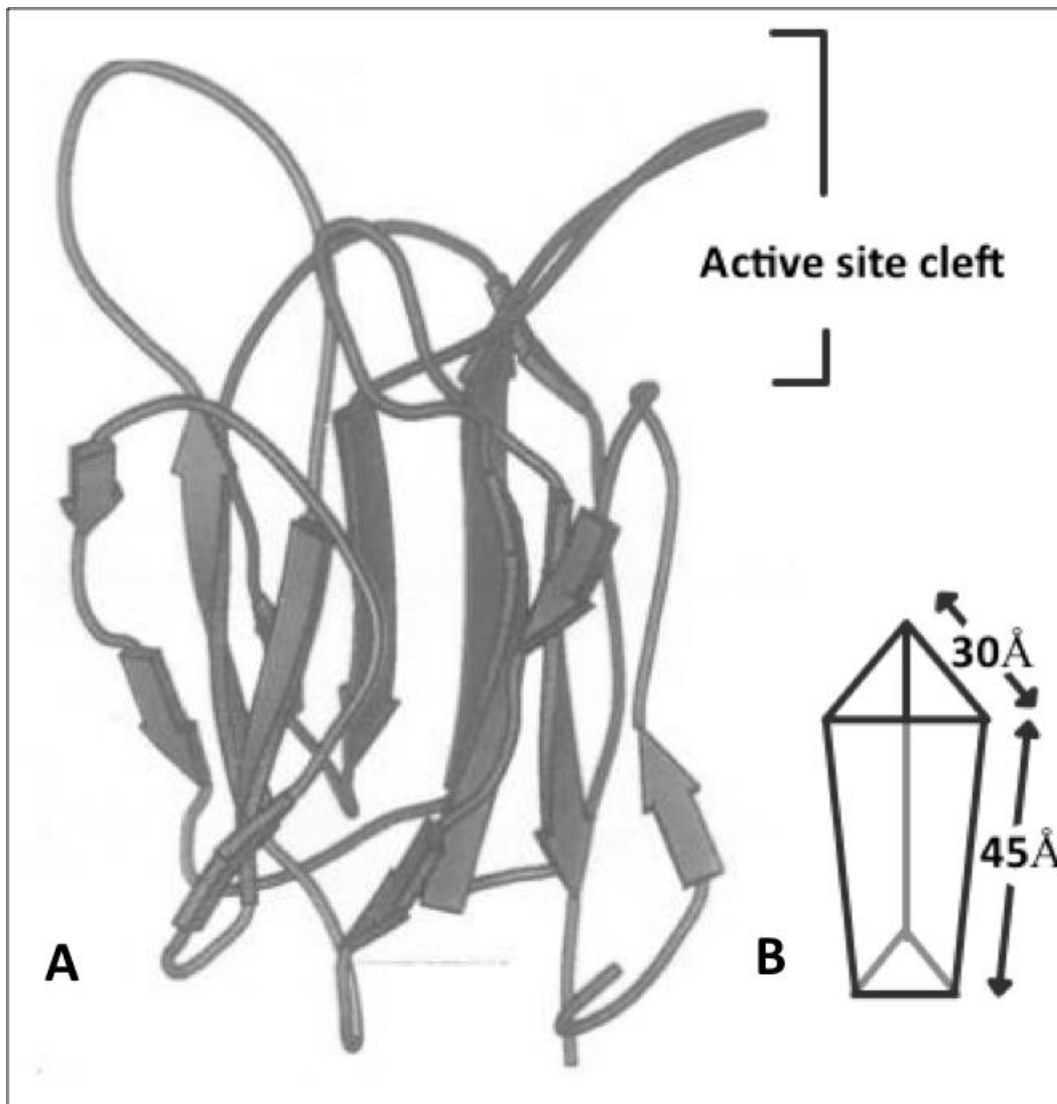


**Figure 26: Vase-like structure of the VMO1 protein as described by Shimuzu et al., (adapted from Shimuzu et al., 1995). (A) Shows the 3D vase like structure formed by the three Greek key motifs with the long variable loops projecting out from the top edges of the vase. (B) Shows a simplified 3D structure with the dimensions of the protein in angstroms (Å)**

Figure 27 shows a two dimensional (2D) representation of the 3D structure of the VMO1 protein highlighting the threefold symmetry of the Greek key motifs and the position of the flexible loops found at the top of the protein structure which

form the active site cleft. Carbohydrate binding is specifically thought to occur at the amino acid highlighted in orange.

The formation of these sites and the Greek key motifs is dependent on stabilising forces between amino acids that hold the structure together.

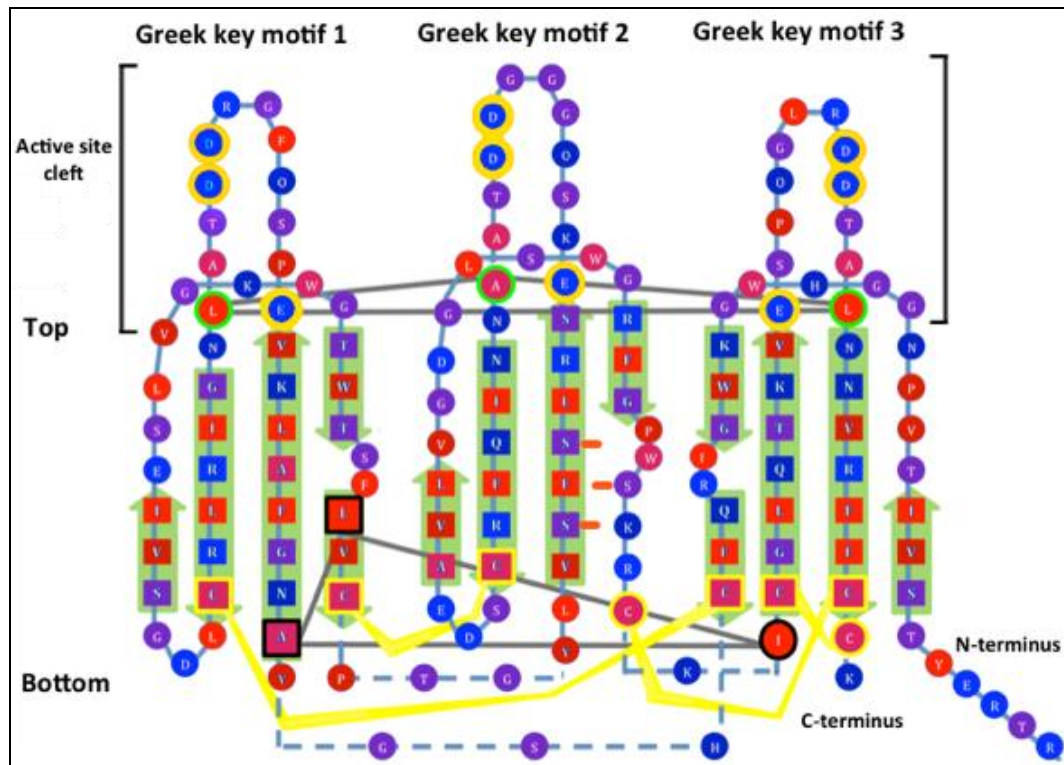


**Figure 27:** 2D representation of the 3D structure of chicken VMO1 protein. Depicted is a representation of the layout of the three Greek key motifs found in the chicken VMO1 protein adapted from Shimizu et al., 1995. The top of the schematic diagram shows the long loop regions that form the surrounding of the active site cleft in the 3D model. The amino acid highlighted in orange show where carbohydrate binding is thought to occur. The amino acid highlighted in green and connected by grey lines show the top hydrogen-bonding network and the bottom hydrogen-bonding network is outline in black and connected by grey lines. The yellow lines are the disulfide bonds between Cys residues. In pink lines are the hydrogen bonds between Ser residues and main chain atoms in place of a beta sheet. Individual amino acids are colour coded to show hydrophobicity: red hydrophobic, blue hydrophilic.

### 2.2.3.3 Structure Stabilisation

Structure stabilisation is achieved by weak non-covalent interactions between side chains of amino acids that add together to give a stable 3D structure. These interactions include hydrogen bonding, disulfide bonds and non-polar hydrophobic interactions.

Two hydrogen-bonding networks occur; one at the top of the protein structure between the amino acids alanine (Ala) 31, leucine (Leu) 84 and isoleucine (Ile) 135, and one at the bottom that connects Leu50, Ala103 and Leu174. The disulfide bonds occur between all of the Cys residues in the amino acid sequence; Cys26 and Cys57, Cys79 and Cys110, Cys133 and Cys161, and Cys136 and



Cys162. The first three disulfide bonds are especially important as they tie the  $\beta$ -sheets to each other. The internal region of the protein is filled with side chains of hydrophobic amino acid residues such as phenylalanine (Phe), Ile, Leu and valine (Val) that act together to stabilise the protein in hydrophilic conditions by mutually repelling water and attracting one another. The hydrophobicity of the individual amino acids is especially important for the overall stability of the 3D structure. The side and bottom regions are covered with positive charges. These positively charged regions and basic residues are where binding to ovomucin is thought to occur. The top region of the protein is clustered with negative charges and forms the base of the active site cleft. This active site is where the enzymatic action of VMO1 is thought to occur.

#### **2.2.3.4 Active Site Cleft**

The cleft or cavity at the top of the structure is the location of the active site of the VMO1 protein and is similar in size ( $25 \times 10 \times 5 \text{ \AA}$ ) and shape to the one found in the lysozyme where polysaccharide hydrolysis occurs. Conservation of the shape and size of this site would be indicative of similar function between species. It contains 9 amino acid (six Asp residues, two glutamic acid (Glu) residues and one Leu residue) thought to play a role in carbohydrate binding. Surrounding the cavity are the three long flexible loops each attached to a single  $\beta$ -sheet. Unlike the side and bottom regions of the structure, which are covered in positive charges, the active site cleft has a cluster of negative charges generated by amino acid residues at the base of the three loops (Asp46, Asp47, Asp99, Asp100, Asp150 and Asp151, and Glu39, Glu92 and Glu143), which are highly conserved in the three Greek key motifs (Figure 25). The size of the cavity and its negative charge makes it suitable for binding ligands such as oligosaccharides. The actual function of the VMO1 protein could possibly be attributed to the flexible loops, which are known to contribute to functional variability in other proteins with Greek key structure.

Kido et al., 1995, was the first to report enzymatic properties for VMO1, similar to the transferase activity of lysozyme. They showed, using bacterial cells, that VMO1 was unable to lyse bacterial cell walls unlike lysozyme but could carry out the transferase activity and synthesise N-acetylchitooligosaccharides from a monosaccharide derivative of glucose (N-acetylglucosamine) four times faster. They also showed it to have an inhibitory affect on hemagglutination (the

clumping of red blood cells) and possibly have carbohydrate binding activity due to a putative carbohydrate-binding site within the active cleft. In addition, Shimizu et al., 1995 have demonstrated that preparations of VM extracts are capable of several enzymatic activities including the transfer of phosphate groups from one molecule to another such as pyruvate kinase, and nucleotidase. To date, the enzyme activity of VMO1 has not been validated and published in a peer-reviewed journal.

Following the review of the chicken VMO1 protein, the next section will focus on comparing VMO1 protein sequences between species, in particular between the mouse, human and chicken species, to give an indication of the homology shared between them as an indication of functional and structural homology.

### **2.3 Analysis of VMO1 Protein Homology across 36 Species**

Table 6 shows a total of 57 protein sequences from 39 species available for the comparative genomics analysis. Four of the species; human, chimpanzee, northern white cheeked gibbon and the gorilla, have four alternative mRNA transcripts resulting from similar variants in the nucleotide sequence. The chimpanzee, gibbon and gorilla sequences are predicted based on EST data and share the greatest homology with human VMO1 protein. The cattle, bottlenose dolphin, small madagascar hedgehog and the southern white rhino have two transcript variants, a full length VMO1 protein of between 199-202aa long and a truncated protein between 70-154aa long. The nine banded armadillo has three variants; a truncated 154aa protein, a full length 200aa protein and an extended 225aa protein.

**Table 6: All protein data available on NCBI including variants and predicted proteins (\*). Listed are the species with their common and scientific names, and their respective accession numbers and the amino acid size.**

Species Name		Protein Accession number	Length (aa)
Common	Scientific		
Bullfrog	<i>Rana catesbeiana</i>	ACO51858	188
Catfish (blue)	<i>Ictalurus furcatus</i>	ADO28351	205
Catfish (channel)	<i>Ictalurus punctatus</i>	ADO28775	210
Chicken	<i>Gallus gallus</i>	NP_001161233	183
Ferret	<i>Mustela putorius furo</i>	AES09520	196
Human	<i>Homo sapiens</i>	NP_872372	202
		NP_001138411	114
		NP_001138412	102
		NP_001138413	70
Mouse	<i>Mus musculus</i>	NP_001013625	201
Pig	<i>Sus scrofa</i>	NP_001231657	200
Rainbow smelt	<i>Osmerus mordax</i>	ACO10125	213
Rat (norway)	<i>Rattus norvegicus</i>	NP_001178752	201
Rhesus monkey	<i>Macaca mulatta</i>	NP_001180982	202
Salmon (atlantic)	<i>Salmo salar</i>	NP_001134967	216
*Armadillo (nine banded)	<i>Dasypus novemcinctus</i>	XP_004447313	225
		XP_004447314	200
		XP_004447315	154
*Baboon (olive)	<i>Papio anubis</i>	XP_003912199	202
*Cat	<i>Felis catus</i>	XP_003996201	201
*Cattle	<i>Bos taurus</i>	XP_002695820	199
		XP_605104	154
*Chimpanzee	<i>Pan troglodytes</i>	XP_001161578	202
		XP_003315367	102
		XP_003315368	114
		XP_003315369	70
*Chimpanzee (pygmy)	<i>Pan paniscus</i>	XP_003810248	202
*Degu	<i>Octodon degus</i>	XP_004638408	196
*Dog	<i>Canis lupus familiaris</i>	XP_546575	201
*Dolphin (bottlenose)	<i>Tursiops truncatus</i>	XP_004330312	199
		XP_004330313	99
*Galago (small eared)	<i>Otolemur garnettii</i>	XP_003791249	199
*Gibbon (northern white cheeked)	<i>Nomascus leucogenys</i>	XP_003277918	202
		XP_003277919	102
		XP_003277920	114
		XP_003277921	70
*Gorilla (western lowland)	<i>Gorilla gorilla gorilla</i>	XP_004058382	202
		XP_004058383	102
		XP_004058384	114
		XP_004058385	70
*Hedgehog (small madagascar)	<i>Echinops telfairi</i>	XP_004716182	202
		XP_004716183	70
*Jerboa (lesser egyptian)	<i>Jaculus jaculus</i>	XP_004666931	199
*Manatee (florida)	<i>Trichechus manatus latirostris</i>	XP_004376135	201
*Mole (star nosed)	<i>Condylura cristata</i>	XP_004685165	198
*Mole-rat (naked)	<i>Heterocephalus glaber</i>	XP_004857336	196
*Orangutan (sumatran)	<i>Pongo abelii</i>	XP_002826920	202
*Orca	<i>Orcinus orca</i>	XP_004267036	199
*Pika (american)	<i>Ochotona princeps</i>	XP_004594901	203
*Rhino (southern white)	<i>Ceratotherium simum simum</i>	XP_004433250	199
		XP_004433251	99
*Sheep	<i>Ovis aries</i>	XP_004013330	229

*Shrew (european)	<i>Sorex araneus</i>	XP_004604978	200
*Squirrel monkey (bolivian)	<i>Saimiri boliviensis boliviensis</i>	XP_003931437	202
*Tasmanian devil	<i>Sarcophilus harrisii</i>	XP_003770676	211
*Walrus (pacific)	<i>Odobenus rosmarus divergens</i>	XP_004398627	99
*Zebra finch	<i>Taeniopygia guttata</i>	XP_002197884	183

A multiple alignment of the protein available for all species shows a very high level of conservation of both identity and similarity of amino acids despite very distant taxonomic relationships. This indicates that VMO1 serves an essential role within these species and could have wider applications than originally thought.

The next step was to align the amino acid sequence of the VMO1 protein from the 39 species listed in Table 6. Figure 28 shows a multiple alignment of VMO1 proteins from different species (not including truncated variants) and their phylogenetic relationship based on amino acid sequence variations. The individual amino acids are colour coded to show amino acid hydrophobicity. This is important for the formation of the tertiary structure of VMO1 (hydrophobic red, hydrophilic blue). Within the protein there is a high level conservation of both amino acid similarity and identity especially across the 3D structural features found in the chicken. There is also a very high level of conservation in the loop region where the six amino acid repeat Asp, X, Thr, X, X, Asn is found. This highly conserved sequence is found in triplicate in all but one species (walrus). In addition, all Cys amino acids responsible for the formation of the four disulphide bonding sites are identical in all but one species (chimpanzee 1). The six amino acid repeat is also found in the antibiotic biosynthesis monooxygenase found in *Runella slithyformis strain 19549* (YP\_004659013), the ABC transporter ATP-binding protein in *Arcanobacterium haemolyticum* (YP\_003697806.1) and deoxycytidine triphosphate deaminase in *Clostridium thermocellum* (YP\_005688722.1).



**Figure 28: Protein alignment of all VMO1 from 36 species. To the left of the species names is a phylogenetic tree showing the relationship of species based on VMO1 amino acid sequences. Each amino acid for each species sequence is colour coded to show hydrophobicity: hydrophobic red, hydrophilic blue. This also gives an indication of amino acid side chain similarity. Along the top is a scale showing the number of amino acids. Below this shows a graph of the identity shared between species with bright green indicating 100% amino acid identity, dark green representing amino acid similarity and red representing changes to dissimilar amino acids. The phylogenetic tree on the left shows the taxonomic relationship between species based on amino acid sequence similarity which is the same as that shown in Figure 16 except for the addition of some species.**

### 2.3.1 Analysis of Homology between the Mouse, Human and Chicken VMO1 Protein

The mouse VMO1 protein (Figure 29) is predicted to be a secreted protein 201aa long consisting of a 20aa signal peptide and a 180aa mature peptide. Within this peptide are four disulfide bonds, an overall three-fold symmetry, the highly conserved sequence of six amino acid (Asp, X, Thr, X, X, Asn) and a putative carbohydrate binding site. The protein has a predicted molecular weight of 21,956.73g/mol (22kDa), with a charge of -4.0 and an isoelectric point of 4.9644 (NCBI).

There are four human *VMO1* mRNA transcripts described in the database (Table 3) and can be translated into VMO1 protein. Transcript 1 results in a full-length 202aa polypeptide. Transcript variant 2 is the result of a SNP in a splice region (dbSNP ref no: rs13847834) at chromosome position 17:4688962 and results in a truncated protein 114aa long (NP\_001138411). Transcript variant 3 is the result of two SNPs, one in the splice region (dbSNP ref no: rs13847834) at chromosome position 17:4688962 and the other (dbSNP ref no: rs149577678), which results in a stop amino acid, at position 17:4689448 which results in a truncated protein 103aa long (NP\_001138412.1). Transcript variant 4 is the result of a somatic substitution (COSMIC ref no: COSM1141184) at chromosome position 17:4689448 and results in a truncated protein 70aa long (NP\_001138413).

For the purposes of this thesis, variant 1 (NM\_182566.2) will be discussed in further detail. The human *VMO1* variant 1 codes for a VMO1 protein (Figure 30) consisting of a 24aa signal peptide and 178aa mature peptide and containing the characteristic four disulfide bonds, three repeat units and the putative carbohydrate binding site. It has a predicted charge of -5.5, an isoelectric point of 4.6752 and a calculated molecular weight of 21534.09g/mol (21.5kDa). Within this protein there is one stop signal variant, three synonymous variants and 26 missense variants.

Figure 31 shows a multiple alignment of the VMO1 proteins within the mouse, human and chicken. The mouse and human share 71.8% identity and 80.2% amino acid similarity. Similarity is where the amino acid side residues share the

same chemical properties such as, hydrophobicity, acidity, and polarity and whether they are aliphatic, carry a charge or are aromatic. A comparison of the mouse and chicken VMO1 protein showed a 47.1% identity and a 60.3% similarity. The structural motifs identified in the crystal protein structure (the super-secondary structure) have been annotated in this diagram (Shimuzu et al., 1994). The conservation of amino acid sequences in the areas where structural motifs are found is much greater than in those without a structural or catalytic role.

### **2.3.2 Summary of VMO1 Protein Structure**

Conservation of the VMO1 protein is especially important for defining protein function. Comparative genomics analysis showed the VMO1 protein to be highly conserved in both identity and similarity across all species despite distant taxonomic relationships. Comparison of the mouse, human and chicken VMO1 proteins show a 80.2% similarity between the mouse and human and 60.3% similarity between the mouse and chicken. Most of the conservation was seen in amino acids shown to have a structural or catalytic role such as the hydrophobic core, the Cys residue disulfide bonds and the  $\beta$  sheets that fold into the Greek key motif.



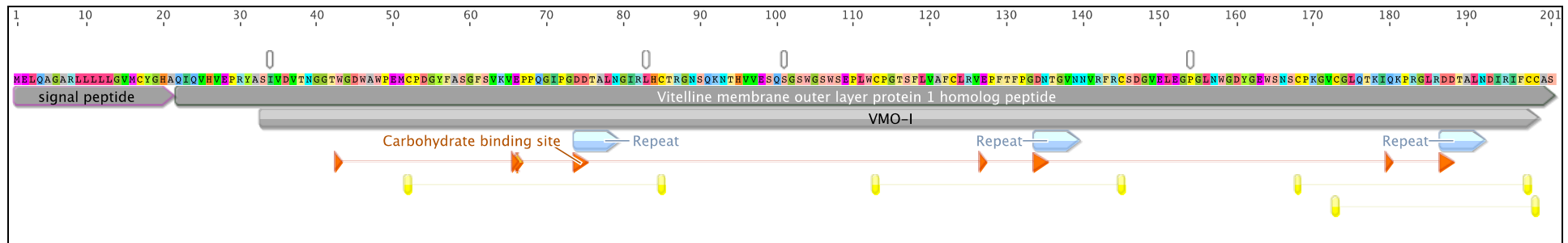


**Figure 29: Annotation of the translated mouse VMO1 protein.** Figure shows a VMO1 protein sequence along the top in multi colours from 1 to 201 with the 20aa signal peptide (pink arrow) and 180aa mature peptide (green arrow) depicted below it. Below this is the VMO1 domain in grey and the positions of the Asp, X, Thr, X, X, Asn repeat in blue/grey arrows. Four disulfide bonds are shown with connected yellow lines and the putative carbohydrate-binding site by orange connected arrows. Also shown are the synonymous variants (black lines) (Geneious® R6).

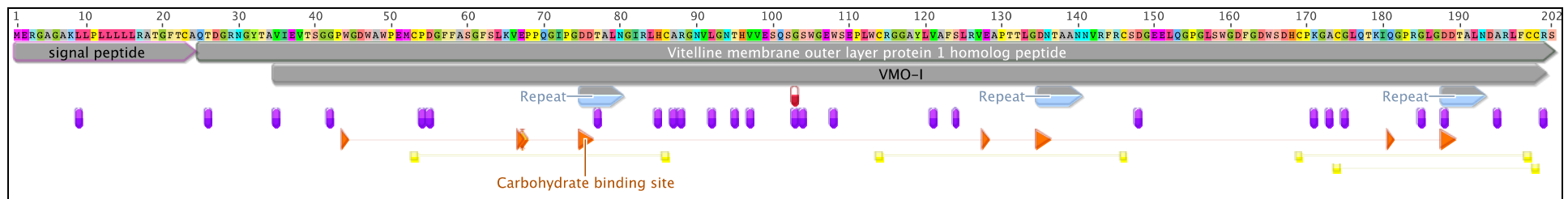


**Figure 30: Annotation of the translated human VMO1 protein.** The top scale bar shows the amino acid position from 1 to 202 and the amino acid sequence of VMO1. The 24aa signal peptide is highlighted with a pink arrow with the 178aa mature peptide (green arrow) depicted beside it. Below this is the VMO1 domain in grey and the positions of the Asp, X, Thr, X, X, Asn repeat in blue/grey arrows. Four disulfide bonds are shown with connected yellow lines and the putative carbohydrate-binding site by orange connected arrows. Also shown is one stop signal variant (red line) and 26 missense variants (purple lines) (Geneious® R6).

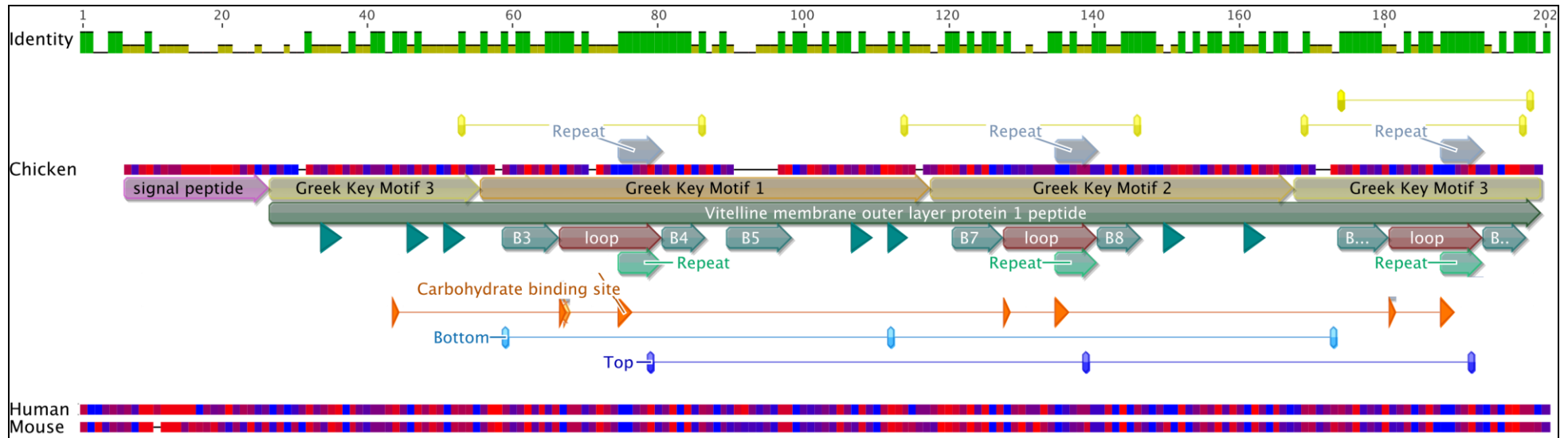


**Figure 31: Multiple alignment of chicken, mouse and human VMO1 protein. Depicted at the top of the diagram is the identity scale bar. This represents the VMO1 amino acid homology from position 1 to 202; bright green indicates 100% amino acid identity and dark green representing a change in at least one of the amino acid sequences. Absence of a bar indicates differences between all three species. This alignment shows the individual amino acids coloured to show hydrophobicity and general similarity in residue side chain properties; hydrophobic red, hydrophilic blue. Below the identity scale is the chicken VMO1 protein sequence with annotations highlighting the various structures found in the 3D crystal structure (Shimizu et al., 1994); disulfide bonds between Cys26 and Cys57, Cys79 and Cys110, Cys133 and Cys161, and Cys136 and Cys62 (yellow), signal peptide (pink arrow), three Greek key motifs (grey/yellow colours), 12  $\beta$  sheets (green arrows), the three loop regions (red arrow), carbohydrate-binding sites (orange arrows), bottom H-bonding network (light blue connected lines) and the top H-bonding network (dark blue connected lines) (Geneious® R6).**

# CHAPTER THREE

## METHODS AND MATERIALS

All processes were carried out in the C.2.03 Molecular Genetics Lab at the University of Waikato unless otherwise stated. Autoclaved 15-18 megohm-cm double distilled deionised water (mQH<sub>2</sub>O) was used to prepare all solutions (Barnstead double distilled/deionisation system). However, for RNA work, mQH<sub>2</sub>O was further treated with 0.1% Diethylpyrocarbonate (DEPC). Unless otherwise stated, all chemicals and solvents (salts, buffers, organic solvents,) were obtained from Sigma-Aldrich and all molecular biology reagents (enzymes and buffers) were obtained from Invitrogen. All glassware was washed in the dishwasher and then autoclaved before use and all experiments were carried out using aseptic techniques on a bench cleaned with 70% ethanol. All solution and buffer recipes can be found in Appendix 1. All Centrifugation was carried out in an Eppendorf Benchtop Centrifuge at room temperature (RT) between 18-24°C, unless otherwise stated.

### 3.1 Agarose Gel Electrophoresis

An Owl gel electrophoresis system dedicated to use with RedSafe™ stain was used to visualise and analyse RNA and DNA for reasons of purification, quantification and identification. Agarose gel electrophoresis was carried out in a dedicated gel room at RT, using 1X TAE buffer stained with RedSafe™ dye (Intron Biotechnology). The weight per volume concentration (*w/v*) of agarose used was determined by the products being electrophoresed and downstream applications they would be used in. Agarose solution was made up by weighing out dry agarose powder (Table 7) and adding to 100mL of 1X TAE buffer in a flask and heating in a microwave with intermittent stirring until no crystals could be seen. The liquid gel was allowed to cool to less than 50°C before 5µl of RedSafe stain was added and then poured into the levelled gel caster. Two combs were inserted into the liquid gel which was then left to cool and set completely before use. The set gel was placed in an electrophoresis tank and covered with 1X TAE buffer. Into the first and/or last well of the gel, 5µl of ladder (500 ng, Genscript) was loaded to serve as a measuring scale for quantity and estimated size of the nucleotide products. Five to twenty microlitres of nucleotide product

was mixed with 2µl of 6X loading dye before being loaded into individual wells. The gel was electrophoresed with a set 90V for 30 minutes (min) and then visualised on a Safe Imager (Invitrogen) and photographed using a COHU High Performance CCD camera and Scion Image software (Release Beta 4.0.2).

**Table 7: Type and weight of agarose used for a 100mL gel and the application for which it was used as well as the ladder used.**

Application	Percentage (w/v) gel	Agarose	Ladder used 100bp (Solis Biodyne) or 1000bp (Gibco)
Gel purification	4%	0.4g SeaKem®	100 and 1000bp
cDNA and PCR analysis	2%	0.2g SeaKem®	100bp
Vector analysis	1%	0.1g SeaKem®	1000bp
RE digestions	0.8%	0.08g LMP	100bp

## 3.2 Purification and Isolation of Nucleotide Products

Three methods were used for nucleotide isolation and clean-up depending on the size of the nucleotide product and the downstream applications applied to it.

These were the PEG precipitation method, phenol/chloroform method, rAPid Alkaline Phosphatase method and gel purification method.

### 3.2.1 PEG Precipitation

Polyethelene Glycol (PEG) precipitation was used to purify nucleotide products for use in cloning, ligation, PCR and RE digestion.

An equal volume of PEG was added to liquid to precipitate DNA and vortexed to mix then left to stand at RT for 10min. The sample was then centrifuged with a balance at 1600 relative centrifugal force (rcf) for 10min to pellet. The supernatant was removed and the pellet washed in 100% ethanol, pelleted and washed again in 70% ethanol. The ethanol was removed and the pellet allowed to dry at RT before being resuspended in 10µl of TE buffer.

### 3.2.2 Phenol/Chloroform Method

This method was used to isolate plasmid DNA from bacterial *Escherichia coli* (*E. coli*) cells. A transformed culture was incubated at 37°C and allowed to grow overnight before a 1.5mL sample was removed for plasmid isolation. 1.5mL was pelleted by centrifuging for 10min at 16100rcf. The supernatant was removed and the pellet was resuspended in 50µl TE buffer followed by the addition of 300µl TENS to chelate positively charged ions and disrupt the cell membrane under alkaline conditions. This was mixed well by inverting the tube six times before

150µl of 3M sodium acetate (NaOAc) was added to neutralise the charge on the sugar-phosphate backbone of DNA to facilitate DNA recovery. The tube was mixed well by inversion and then spun for 2min at 16100rcf to pellet cellular debris. The pellet was removed using a sterile toothpick and 300µl of phenol/chloroform was added to the supernatant to denature proteins and left at RT on a rotator for 10min. The tube was centrifuged for 5min at 16100rcf to separate the aqueous layer from the organic layer. This top aqueous layer was collected with care taken to avoid the protein interface and mixed with an equal volume of isopropanol to precipitate the plasmid DNA. The tube was centrifuged for 10min at 16100rcf to pellet the precipitated DNA. The isopropanol was removed and the pellet washed in 70% ethanol to remove residual salts. Ethanol was removed and the pellet allowed to air dry before being resuspended in 40µl TE buffer and left at RT for 30min.

### **3.2.3 rAPid Alkaline Phosphatase Method**

rAPid Alkaline Phosphatase (Roche) method was used to purify PCR products to be sequenced where only a single amplicon was produced. Briefly, 10µl of PCR product was run on a 1% agarose gel to check for expected band size and to estimate quantity. To the remaining 10µl of PCR sample, 0.5µl of Exonuclease I (10U) and 0.5µl of Alkaline Phosphatase (1U) was added and heated at 37°C for 30min. Exonuclease degrades excess single-stranded primer oligonucleotides and any extraneous single-stranded DNA produced in the PCR. Alkaline Phosphatase degrades unincorporated dNTPs. The reaction was then deactivated by heating at 85°C for 15min before being checked for quantity and quality on a NanoDrop™ 8000 Spectrophotometer (Nanodrop).

### **3.2.4 Gel Purification**

Gel punching was used to remove specific bands resolved in an agarose gel when restriction enzyme (RE) digestion was carried out or when more than one PCR product was observed on the gel. A 600µl tube was prepared by punching a hole in the base with a flamed 18 gauge needle (Becton Dickinson) and the addition of a 3mm sterile glass bead (Ajax Chemicals). This tube was then placed into a 1.7mL tube and set aside ready for use. The entire nucleotide sample was loaded into a single well in a 2% 1X TAE agarose gel and electrophoresed at 91V for 30min. The gel was visualised on a blue safe imager and the bands extracted using

the hub of a pipette tip. The punched gel band was placed in the prepared centrifugation tube and frozen at  $-80^{\circ}\text{C}$  for 30min then centrifuged at 16100rcf for 15min. The 600 $\mu\text{l}$  tube was discarded and the centrifuged solution in the 1.7mL tube retained.

### **3.3 Nucleotide Product Quantification and Quality Assessment**

DNA was quantified and assessed for quality using two methods; 2% agarose gel electrophoresis with a 100 base pair (bp) ladder (Solis Biodyne) and Nanodrop reading. Vector quality and quantity was assessed using a 1% agarose gel with a 1kb ladder (Gibco). RE digests of PCR products and vectors were assessed together on 2% agarose gel with both a 1kb ladder and a 100bp ladder.

#### **3.3.1 Agarose Gel Electrophoresis**

This method relied on the comparison of the brightness of the bands in the ladders with known DNA concentrations and the brightness of the unknown products band. The comparison would give an approximate estimation of DNA concentration in the unknowns. This method also gave information on the banding patterns produced for RE digestion and specificity of the primers. Products that underwent RE digestion or that contained more than one band were extracted from the gel and gel purified before being quantified and assessed for quality on the Nanodrop.

#### **3.3.2 Nanodrop Reading**

Nucleotide concentration and purity was measured using a Nanodrop. This method relied on a spectrophotometer reading comparison between a “blank” and a purified product resuspended in a known solution. Nucleic acid concentration was determined by the absorbance reading at 260nm and sample purity determined by the 260/280nm ratio. One microlitre of sample was measured against either mQH<sub>2</sub>O or TE buffer depending on what it was resuspend in during the final purification step. Samples with 260/280nm ratios less than 1.80 greater than 2.0 or an excessive peak at 230nM were deemed as low quality and underwent another purification step in order to improve purity.

### 3.4 PCR Reactions

Polymerase chain reaction (PCR) was carried out using cDNA extracted from the mouse inner ear (protocol 3.7.1) to amplify the *Vmo1* mRNA to determine its gene sequence and for the preparation of a recombinant protein expression construct. PCR reactions were carried out in a BIORAD T100 Thermal Cycler in single 200µl PCR tubes (Axygen). Solutions were defrosted on ice while in use. Master mixes were prepared and aliquoted into individual PCR tubes in a PCR dedicated UV hood. The primers and template were added to the individual tubes on a dedicated PCR bench, which was kept free of contaminants and wiped before use with 70% ethanol solution. Sterile DNase and RNase free filtered pipette tips and dedicated PCR pipettes were also used.

PCR reactions were performed with final concentrations of 1X HOT FIREPol® 10X Buffer B2 PCR buffer (Solis Biodyne), 0.2mM dNTPs (Solis Biodyne), 2.5mM magnesium chloride (MgCl<sub>2</sub>), 1U HOT FIREPol® DNA polymerase (Solis Biodyne), and 0.25mM of each forward and reverse primer (Table 10). In addition, all PCR reactions were carried out with controls to provide proof of possible contamination and to verify that mouse *Vmo1* is present and amplifiable. The positive PCR control used primer set BFG1/2 with 1µl template and had an expected band size of 495bp. The negative PCR control contained primer set BFG1/2 and no template DNA.

All PCR reactions were carried out with the following settings unless otherwise stated.

**Table 8: PCR machine settings showing the temperatures and times for each step**

Step		Temperature	Time
<i>Taq</i> activation		95°C	15min
Cycling Steps (X35)	Denaturation	95°C	30secs
	Annealing	See Table 10	30secs
	Extension	72°C	1min
Final Extension		72°C	5min

#### 3.4.1 Nested PCR

Nested PCR involved the amplification of a mouse inner ear cDNA sample followed by a second amplification of *Vmo1* PCR products produced in the primary reaction. This technique was used to yield optimal concentrations of *Vmo1* amplicon for the purposes of cloning and sequencing. PCR parameters were the same as outlined in protocol 3.4 using 1µl of PCR product as a template.

### 3.4.2 Colony PCR

Colony PCR was used to screen for the orientation of inserts ligated into a vector and transformed into DH5 $\alpha$  *E. coli*. The primers M13puc reverse and BFG28R (Table 10) were used to selectively amplify the *Vmol* insert produced from primer set BFG27/28 and oriented in the 5'-3' direction to produce an amplicon 893bp long. For the template a single colony was picked with a clean sterile toothpick and briefly dipped into PCR mix before being streaked onto an LB<sup>+</sup> agar plate or used to inoculate LB<sup>+</sup> broth. Alternatively a sterile toothpick was dipped into LB<sup>+</sup> broth containing the transformed *E. coli* and then briefly dipped into the PCR mix. PCR parameters were the same as outlined in protocol 3.4.

### 3.5 SDS-PAGE

Denaturing sodium dodecyl sulfate polyacrylamide gel electrophoresis (SDS-PAGE) was used to separate whole tissue protein lysates between 10-150kDa in size for the purposes of western blotting and visualisation of proteins in the mouse tissues. Two types of gels were used, the 10% Mini-PROTEAN® TGX Stain-Free™ Gel (BIORAD) and 12% hand-cast gels. SDS-PAGE consisted of gel preparation, sample preparation and electrophoresis. 37:1 Acrylamide:N,N'-methylenebisacrylamide (BIS) solution was weighed out while wearing a face mask, gloves and lab coat and liquid mixed with powders in the fume hood.

Hand-cast gels were made according to the method described below and the protocol described by Towbin et al., 1979, with a 5% stacking gel to focus the protein band and 12% separating gel to separate the proteins out by molecular weight. To cast gels, a Hoefer mighty small SE250/SE260 gel rig was used and the glass plates, spacers (0.75mm) and combs were cleaned with detergent, rinsed with dH<sub>2</sub>O and dried with paper towels. They were then cleaned again with 70% ethanol and assembled. The corresponding volumes (Table 9) of mQH<sub>2</sub>O, SDS, Tris buffer and Acrylamide:BIS were added to a flask and mixed together. To prevent polymerisation occurring rapidly, the ammonium persulphate (APS) and tetramethylethylenediamine (TEMED) were added just before gels were cast, mixed quickly and then taken up in a 1mL transfer pipette (Raylab) and poured between the assembled glass plates. To prevent drying, a layer of 2-butanol was added to the top of the gel and left to set. Once set, the butanol was carefully



removed from the top of the gel using filter paper and the stacking gel prepared and added. A gel comb (10 tooth) was carefully inserted into the stacking gel, which was then left to polymerise with a damp paper towel covering the top to prevent drying. If not being used the gel was wrapped in a damp paper towel and plastic gladwrap and stored at 4°C for no more than one week. To use, the comb was removed from the stacking gel and the wells rinsed with dH<sub>2</sub>O to remove any unpolymerised acrylamide and debris.

**Table 9: Composition of the separating and stacking SDS-PAGE gels showing the solutions/reagents and the volume used**

Reagent	Volumes (sufficient for 2 gels)	
	Stacking gel	Resolving gel
10% SDS	125.0ul	150ul
1M Tris	1.6mL	-
3M Tris pH8.8	-	2.0mL
37:1 Acrylamide:BIS	1.6mL	8.2mL
dH <sub>2</sub> O	9.0mL	4.5mL
10% APS	65.0ul	150.0ul
TEMED	12.5ul	15.0ul

### 3.5.1 Protein Sample Preparation

Protein samples and a bovine serum albumin (BSA) control sample (10mg/mL) were defrosted on ice and then mixed in a 50:50 ratio with 2X SDS loading dye followed by heating at 99°C for 3min to denature and linearise the proteins. Samples were briefly centrifuged before being loaded into wells in the stacking gel.

### 3.5.2 Gel Electrophoresis

SDS-PAGE of the pre-cast gels was carried out in a Mini-PROTEAN® Tetra Cell (BIORAD) and hand-cast gels were electrophoresed in a Hoefer ‘Mighty Small II’ gel electrophoresis unit. The set gel and plates were put into the electrophoresis tank and SDS running buffer added. The protein products and BSA control were mixed with SDS loading dye and denatured for 3min at 99°C. Twenty microlitres was then taken up in a pipette and loaded into individual wells of the gel along with a molecular weight ladder. The protein products and were run into the stacking gel at 15mA for 15min. The current was then increased to 30mA and left to run until the dye front reached 1cm above the bottom of the gel. The gel was then used for either western blotting (protocol 3.9.2) or visualised for analysis of protein quality and concentration (protocol 3.5.3).

### 3.5.3 Visualisation of SDS PAGE Gel

Pre-cast SDS-PAGE gels were visualised on a Gel Doc™ EZ System (BIORAD) on a stain free plate (BIORAD). The gel was carefully removed from between the plastic plates and placed on the stain free plate and then placed into the Gel Doc™ and imaged using Image Lab software (BIORAD). Hand-cast SDS-PAGE gels were visualised by staining with Coomassie Blue R-250. Briefly, the SDS-PAGE gel was carefully removed from between the glass plates and placed in a glass container with 100mL of Coomassie blue stain. This was then microwaved at 800W on high until just boiling then allowed to cool to RT while shaking. The Coomassie stain was discarded and the gel rinsed with distilled water (dH<sub>2</sub>O), and then destained overnight shaking at RT in dH<sub>2</sub>O. The gel was transferred onto Whatmans no.1 paper and analysed.

### 3.6 Cloning and Expression of *Vmo1*

Five vectors were used in this research to clone the mouse *Vmo1* into an expression vector for the expression of recombinant VMO1 protein (Appendix 9); pCR™4-TOPO® TA Vector (Invitrogen, TOPO® TA cloning Kit), pBluescript II SK(+) (Molecular Genetics Laboratory, UoW) and the expression vectors pPro EX HTb (Life Technologies USA), pET41a(+) (Linda Peters, UoW) and pET42a(+) (Microbiology Laboratory, UoW). Briefly, mouse cDNA was amplified using PCR and primer set BFG27/28. A double RE digestion was carried out on both the PCR amplicon and plasmid vector to enable ligation of the PCR amplicon into the vector. This ligated vector was transformed into electrocompetent bacterial cells, grown overnight at 37°C and screened for correctly oriented inserts using colony PCR.

#### 3.6.1 Preparation of Electrocompetent Cells

*E. coli* strain DH5α (Hanahan, 1985) were sourced from glycerol stock stored at -20°C (Molecular Genetics Laboratory, UoW), streaked onto a Luria Base (LB) agar plate and incubated upside down in a 37°C oven overnight. A single colony from this plate was used to inoculate 10mL of LB broth (Invitrogen) and grown overnight at 37°C, shaking at 200rpm. A 5mL aliquot of this culture was then used to inoculate 1L of LB broth which was grown to Log Phase of growth with an OD<sub>600nm</sub> of 0.69 (BIORAD SmartSpec™ 3000). The 2L flask was chilled on

ice for 30min before being pelleted in a centrifuge (Heraeus Multifuge 1 S-R Centrifuge) at 4000rcf for 15min at 4°C.

The cells were then pelleted and resuspended through sterile ice-cold glycerol at the following volumes:

1L fresh 10% glycerol;

500mL fresh 10% glycerol;

20mL fresh 10% glycerol;

This final pellet was resuspended in 3mL fresh 10% glycerol, aliquoted into 50µl volumes into sterile 1.7mL tubes, and stored at -80°C.

### **3.6.2 Transformation of Vector into DH5α *E. coli***

Transformation of DH5α was carried out in the University of Waikato Transitional/Containment Facility (Appendix 7) using a BIORAD Gene Pulser™ and a BIORAD pulse controller set to 25 µFD capacitance with 200ohms resistance and 2.5V for 3sec. Prior to the transformation, 50µl aliquots of electrocompetent bacterial cells (protocol 3.6.1) were defrosted on ice, LB<sup>+</sup> agar plates containing 100µg/mL ampicillin were spread with 40µl 5-bromo-4-chloro-3-indolyl-β-D-galactopyranoside (Xgal 20mg/mL) and 4µl Isopropyl β-D-1-thiogalactopyranoside (IPTG 200mg/mL) and LB broth was prewarmed to 37°C. Ampicillin was used to select for transformed *E. coli* which contained the plasmid and Xgal and IPTG were used to screen colonies containing an insert with blue and white colony selection.

A 2µl sample of ligation reaction or undigested vector was added to the electrocompetent bacterial cells and mixed together on ice before being transferred to a chilled 0.2cm cuvette (Gene Pulser® Cuvette BIORAD). The exterior of the cuvette was dried using a power towel, placed into the electroporator and an electrical pulse applied. Immediately after electroporation, 1mL of prewarmed LB broth was added to the cuvette and the contents of cuvette transferred to a 1.7mL tube. These tubes were then incubated shaking at 37°C for 1 hour (hr) to induce expression of antibiotic resistant gene. This culture was then spread using a glass rod very gently onto three LB<sup>+</sup>/Xgal/IPTG agar plates in 600µl, 300µl and 100µl volumes to make a serial dilution of *E. coli*. The agar plates were then incubated upside down at 37°C overnight. The following day, the agar plates were inspected for blue and white colonies and stored at 4°C. White colonies were selected for colony PCR or inoculation into LB broth.

### **3.6.3 Cloning *Vmo1* into TA TOPO Cloning Vector**

*Vmo1* PCR products were directly ligated into the TOPO® TA cloning vector (Invitrogen) for sequencing. Following the protocol recommended by the supplier 1µl of PCR mix containing amplicons produced by primer set BFG27/28 was added to 1µl of vector and incubated at RT for 5min. The transformation was then carried out as outlined in protocol 3.6.2.

### **3.6.4 Ligation of the *Vmo1* Transcript into the pProEX HTb Vector**

*Vmo1* PCR product produced by primer set BFG27/28 (protocol 3.4) was ligated into the expression vector pProEX HTb for the purposes of expression of the VMO1 recombinant protein. Briefly, the vector was amplified by transformation into *E. coli* DH5α electrocompetent cells, isolated and purified. Both the PCR amplicon and vector were RE digested, electrophoresed and then gel purified. The purified products were then ligated together to make a circular recombinant vector containing the PCR amplicon oriented in either the 5prime (5') to 3prime (3') or 3'-5' direction. This ligated product was then transformed into DH5α and grown overnight and screened for insertion of the PCR amplicon in the 5'-3' direction.

#### **3.6.4.1 Preparation of pProEX HTb Vector and *Vmo1* PCR Amplicon**

The vector was transformed into *E. coli* DH5α electrocompetent cells described in section 3.6.2 and a single white colony was selected to inoculate a 10mL LB<sup>+</sup> broth with a final concentration of 10ug/mL ampicillin antibiotic. The plasmid was isolated by using the phenol/chloroform method (protocol 3.2.2) and the size and concentration confirmed by visualisation on a 1% agarose gel (protocol 3.1). RE digestion was carried out using the HindIII enzyme as described below on the remaining plasmid and the linearised product run on a 2% agarose gel containing gel safe stain. Resulting bands were visualised on a SafeImager and gel purification carried out as per protocol 3.2.4.

*Vmo1* PCR product was produced using the protocol outlined in 3.4 with primer set BFG27/28 and then digested with RE HindIII (NEB).

#### **3.6.4.2 Restriction Enzyme Digestion**

RE digestion was carried out on the PCR product and vector to make compatible sticky ends for the insertion of a correctly oriented digested PCR product into the vector. HindIII (NEB) was used to linearise the pPro Ex HTb vector and to digest the PCR product at the 5' and 3' ends. The insert PCR RE digest was carried out with 20µl of *Vmo1* PCR product produced by protocol outlined in 3.4, 2U HindIII, 2.5µl 10X NEB2 buffer (NEB) made up to a final volume of 27µl with mQH<sub>2</sub>O. The vector RE digest was carried out in a 20µl volume containing 1µl vector (5.5µg/mL), 1U HindIII, 2.5µl 10X NEB2 buffer and 15.5µl mQH<sub>2</sub>O. Digestion was carried out at 37°C overnight, and stopped by heating at 65°C for 20min. Products were then electrophoresed as outlined in 3.1 using both a 1kb ladder and a 100bp ladder to estimate band sizes. Bands of expected sizes were excised from gels and underwent gel purification for future ligation reactions.

#### **3.6.4.3 T-Tailing Reaction**

Phenol/chloroform purified linear plasmid was repelleted following protocol 3.2.2 and resuspended in 50µl mQH<sub>2</sub>O. T-tailing reaction mix was made with 1X HOT FIREPol® 10X Buffer B1 (Solis Biodyne), 2.5mM MgCl<sub>2</sub>, 200µM dTTP (Invitrogen) and 1U HOT FIREPol® DNA polymerase (Solis Biodyne) and made up to a volume of 100µl with mQH<sub>2</sub>O. This was heated at 95°C for 3min to activate the *Taq* DNA polymerase. Fifty microlitres of the purified plasmid was added to the T-tailing reaction mix and incubated at 72°C for 2hr to add a thymine nucleotide to the 5' ends of the linearised plasmid.

#### **3.6.4.4 Ligation**

Ligation reaction was carried out with a Vector:Insert ratio of 1:3 to produce circular recombinant molecules. Each ligation mix contained mQH<sub>2</sub>O, 5X T4 DNA Ligase Buffer (Invitrogen), 1U T4 DNA Ligase (Invitrogen), purified digested vector (5.3µg/µl) and purified digested PCR product (1.5µg/µl) made up to a final volume of 10µl. The ligation reaction was mixed, briefly centrifuged to bring contents to bottom of tube, and then incubated at 37°C for 10min then overnight at RT. In addition controls were carried out simultaneously to test the efficiency of the T4 DNA ligase, the efficiency of the RE digestion of both the vector and insert and the efficiency of the transformation of the plasmid into *E. coli*.

### **3.6.5 Screening and Sub-cloning of Transformed Colonies using Colony PCR**

Single white colonies produced from protocol 3.6.4 were picked using a sterile pipette tip and dipped briefly in a PCR master mix (3.4) containing forward primer (M13puc) and reverse primer (BFG2R) (Table 10) to check for the correct orientation of the insert. The pipette tip was then used to streak an LB<sup>+</sup> plate which was incubated overnight at 37°C (Precision). The following day single colonies were used to inoculate 1mL of LB<sup>+</sup> broth and incubated for 1hr shaking at 37°C. One hundred microlitres of this culture was then used to inoculate 10mL fresh LB<sup>+</sup> broth, and streaked onto an LB<sup>+</sup> plate for storage. The rest was processed to extract the vector DNA and then used for RE digests, sequencing and PCR.

## **3.7 Preparation of RNA and Protein from Mouse Tissues**

Wild type C57/B16/129SV *Mus musculus* (house mouse) were sourced from AgResearch, euthanised using University of Waikato Animal Ethics Committee SOP9, and tissue dissected in the animal house (BL1.G.02, UoW). Tissues were covered with RNA extraction buffer or protein lysis buffer to prevent degradation of the RNA and protein in the samples and stored at -80°C for future use.

### **3.7.1 Extraction of mRNA for cDNA Production**

Six temporal bones from three P28+ female mice were pooled before being processed for RNA extraction. Animals were dissected as quickly as possible to avoid RNase activity and contamination. To avoid exogenous DNA, RNA and nuclease contamination, all RNA work was carried out on a bench dedicated to RNA work. This workspace was regularly cleaned with RNase AWAY™ (Life Technologies) and all RNA work was carried out using sterile DNase and RNase free disposable tubes (Axygen), filtered pipette tips (Sorenson BioScience) and containers. Glassware was washed in the dishwasher then autoclaved and baked in a 250°C oven for 2hr (Thermophile Research Laboratory, UoW). All equipment used was wiped with RNase AWAY™ and only used for RNA work. Dissection tools were washed, autoclaved and baked at 80°C and in between uses were wiped with RNase AWAY™ and heated briefly in a Germinator 500 Glass Bead Steriliser. The Heidolph DIAX 600 homogeniser was disassembled and the

individual pieces washed with detergent, rinsed with mQH<sub>2</sub>O, 70% ethanol and then wiped with RNase AWAY™ before reassembly and use.

#### **3.7.1.1 Preparation of Ear Tissue**

Single mice were dissected one at a time to reduce the amount of time ears were stored on ice. The temporal bones were removed using a sterile number 21 scalpel blade and sterile dissection scissors and rinsed in ice cold sterile 1X PBS which was changed twice during dissection to minimise cross-contamination. They were then placed in ice-cold RNA extraction buffer (Quiagen, USA) for storage. In instances where protein from additional tissues was extracted from the same mouse the ears were done first and stored on ice to prevent contamination from other tissues. Ears were stored on ice for no longer than 20min then frozen at -80°C until further processed.

#### **3.7.1.2 RNA Extraction from Mouse Ears**

RNA was extracted and purified using RNeasy Fibrous Tissue Mini Kit (Quiagen, USA) according to the manufacturer's protocol. Briefly, six temporal bones were removed from the -80°C freezer and allowed to defrost to -20°C overnight then to 4°C the following day. Ears were then pooled into a 15mL falcon tube (CELLSTAR®) and covered with RLT buffer (Quiagen, USA). Bones were homogenised with a Heidolph DIAX 600 homogeniser for 15sec intervals in between which they were stored on ice for 1min to cool and prevent overheating of sample. Homogenisation was repeated 10 times until most of the bone fragments had been liquefied and then stored on ice for 5min. The sample was transferred to three 1.7mL tubes to which 590µl of RNase-free water and 10µl Proteinase K (Quiagen, USA) was added and incubated in a Thermomixer (Eppendorf) at 55°C for 10min to digest proteins. Samples were centrifuged at 10,000rcf for 3min to pellet bone fragments and the supernatant transferred to new 1.7mL tubes. A 0.5 volume of 100% ethanol was added to each sample to precipitate DNA and RNA, before being transferred to RNeasy column in a 2mL tube. The samples were centrifuged for 15secs at 8000rcf and the flow-through discarded. The column was washed again with 350µl RW1 buffer, centrifuged and then the flow-through discarded. Ten microlitres of DNase stock solution with 70µl RDD buffer was added to column and incubated at 22°C for 15min to remove DNA. Column was washed with 350µl RW1 buffer with flow-through discarded and then again with RPE buffer. A final wash included the addition of

500µl RPE buffer, and centrifugation at 8,000rcf for 2min. Thirty microlitres of RNase free water was added to the column, incubated at 22°C for 2min before being centrifuged at 8,000rcf for 1min into a clean collection tube. Elution was repeated with eluent and then stored at -80°C.

The quality and quantity of isolated RNA was examined in two ways; spectrophotometry using the Nanodrop and PCR of the cDNA produced by reverse transcription.

### **3.7.2 Protein Sampling for Western Blot and Bradford Assay**

#### **3.7.2.1 Protein Extraction from Soft Tissues**

Non-bony tissues from six mice, male and female P28+, was dissected out and transferred to a 2mL tube (Axygen) containing sterile glass beads (BioSpec Products) and protein lysis buffer. The tissue was disrupted by bead beating in a FastPrep® FP120 at a speed of 6 for 25sec intervals in between which they were chilled on ice for 1min. The tubes were centrifuged to the pellet glass beads, nuclei and cell debris at 300rcf for 5min at 4°C. The supernatant was removed to new tubes in 100µl aliquots and stored at -20°C.

#### **3.7.2.2 Protein Extraction from Temporal Bone**

Seven temporal bones from four P28+ mice (3 female, 4 male) were removed from the -80°C freezer and allowed to defrost to -20°C overnight then to 4°C the following day. They were then pooled into a 15mL falcon tube and 600µl lysis buffer added. Bones were homogenised with a Heidolph DIAX 600 homogeniser for 30sec intervals and in between, they were stored on ice for 1min to cool and prevent overheating of the sample. Homogenisation was repeated three times until most of the bone fragments had been liquefied. The sample was left to cool for 5min and the supernatant decanted into a new 1.7mL tube (Ear sample 1). The homogeniser was partially disassembled and bone fragments removed from the teeth of the homogenising wand then rinsed with no more than 300µl of fresh protein lysis buffer which was collected in the 15mL falcon tube. The sample was homogenised again as described above and the supernatant was decanted into a new 1.7mL tube (Ear sample 2). The homogeniser was again disassembled and bone fragments removed from the teeth of the wand and scraped then rinsed with 100µl of fresh protein lysis buffer which was collected in the 15mL falcon tube. A final homogenisation step was carried out 10 times to liquefy all of the remaining



bone fragments and the entire sample transferred to a new 1.7mL tube (Ear sample 3). The three samples were centrifuged for 10secs to pellet any large fragments of bone then aliquoted into 100µl samples and stored at -20°C.

### **3.8 Determination of the *Mus musculus Vmo1* Gene Sequence**

In this section, the design of PCR primers, the reverse transcription of total RNA isolated from the inner ear of P28+ mice, amplification of cDNA using *Vmo1* specific primers, and DNA sequencing methodology will be described.

#### **3.8.1 Oligonucleotide Primer Design for PCR**

Unless otherwise stated forward and reverse primers were designed using Primer-BLAST software (<http://www.ncbi.nlm.nih.gov/tools/primer-blast/>) and were synthesised by Integrated DNA Technologies Ltd (IDT) (Table 10). Primers were resuspended in TE buffer (pH 8) to a final concentration of 200pmol/µl. Working stock of primer solutions were diluted to a final concentration of 20pmol/µl. Primers were analysed using IDT OligoAnalyzer 3.1 and stored at -20°C. Mouse specific *Vmo1* primers were designed using the reference sequence NM\_001013607.1.

##### **3.8.1.1 Oligo-dT Primers**

Oligo-dT primers (Life Technologies) were used to synthesise cDNAs from the total RNA sample. Oligo-dT primers bind specifically to the poly-adenine tail junction of the mRNA template and are specific to eukaryotic mRNA.

##### **3.8.1.2 BFG1F and BFG2R**

This primer pair was generated using primers published by Peters et al., 2007 and serves as a positive control. These primers are specific to the mouse *Vmo1* gene and binds to the 3' end of the transcript to produce an amplicon 495bp long at an optimal annealing temperature of 55°C.

##### **3.8.1.3 BFG7F and BFG8R**

This primer pair was designed to be specific to *Vmo1* cDNA produced from the mRNA transcript only. BFG7F was designed to cover the first exon-exon boundary for the *Vmo1* cDNA and BFG8R was designed to cover the second exon-exon boundary. A single amplicon of 193bp in length was produced at an optimal annealing temperature of 50°C.

#### **3.8.1.4 BFG27F and BFG28R**

This primer pair was designed to encompass the entire *Vmo1* ORF for ligation into a cloning or expression vector. Incorporated into both the forward and reverse primer was the HindIII restriction sites so the whole sequence could be easily removed or inserted into cloning and expression vectors. The restriction site in the forward primer was placed specifically to produce a digested amplicon that was in frame with the expression vector pPRO Ex HTB to produce a recombinant protein identical to the VMO1 protein reference sequence on NCBI (NP\_001013625.1). A single amplicon of 671bp length was produced at an optimal annealing temperature of 50°C.

#### **3.8.1.5 *Mus GAPDH* Primers**

This primer pair was sourced from the molecular genetics lab primer stocks (Greg Jacobson, UoW) and are specific to mouse Glyceraldehyde-3- phosphate dehydrogenase (*GAPDH*) gene. This gene is a housekeeping gene and is required for the maintenance of basic cellular function, and is expressed in all cells of an organism under normal and patho-physiological conditions (NCBI; Barber et al., 2005). Primers were used as a positive control for the initial PCR reaction carried out on mouse cDNA to confirm the presence of mouse cDNA and absence of mouse genomic DNA and that the PCR were successful. An amplicon estimated at 150bp long was produced at an optimal annealing temperature of 60°C.

#### **3.8.1.6 M13 Puc Reverse and BFG28R**

This primer pair was used to confirm the presence of *Vmo1* in the expression vector in the correct orientation to produce the VMO1 recombinant protein. An amplicon of 843bp in length was produced at an optimal annealing temperature of 50°C.

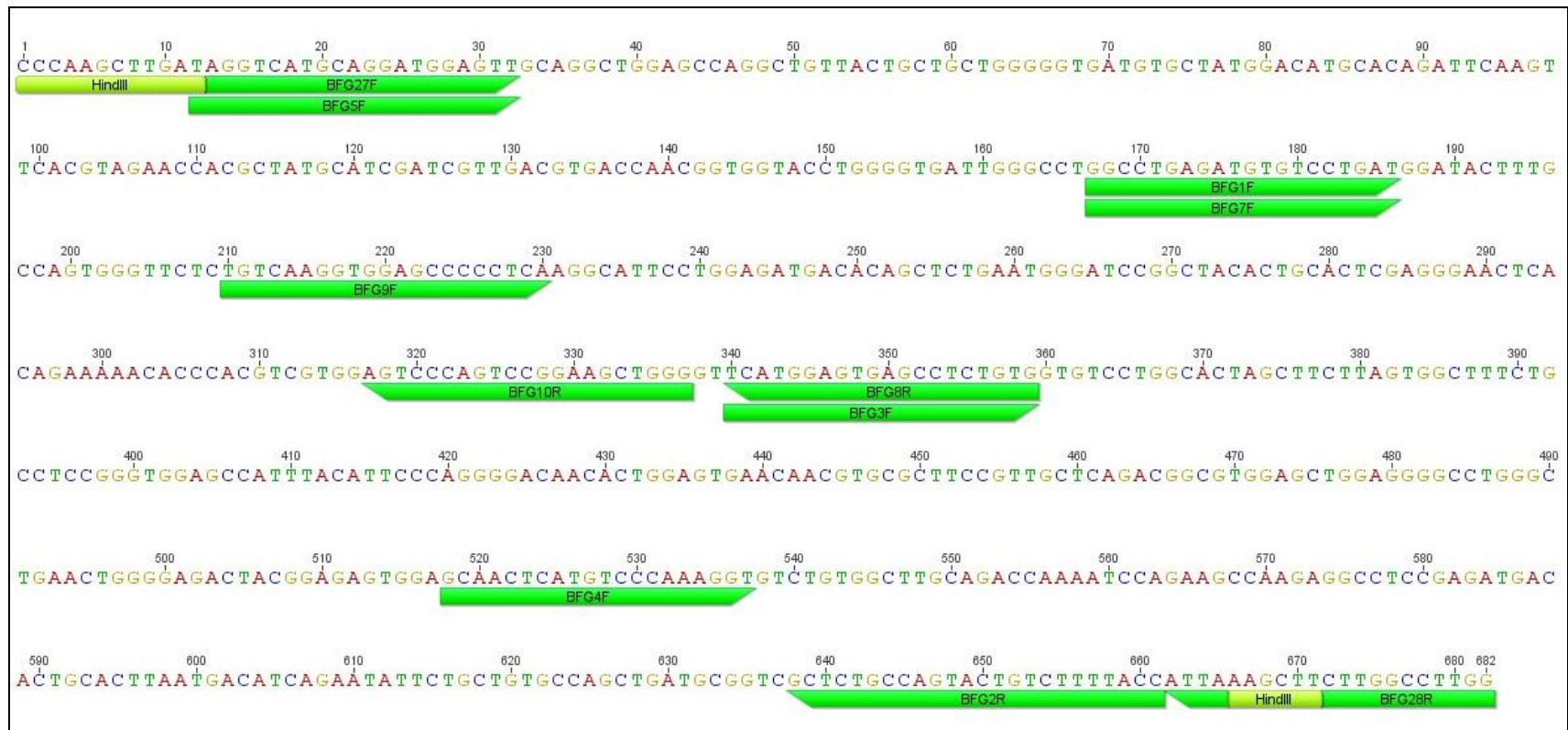


Figure 32: DNA Sequence of the Mouse *Vmo1* gene from nucleotide position 1 to 892. This diagram shows the position and direction of the PCR primer binding sites (green) and HindIII restriction enzyme sites (yellow).

**Table 10: Forward and reverse primer sequences used throughout this thesis. Primers were named according to BFG (Blaise Forrester Gauntlett) the order in which they were ordered and the strand on which they bind either reverse complement or forward (R or F). Underlined nucleotide bases illustrate the position of the restriction enzyme site.**

Primer name	Sequence	Species and gene target	Primer sequence source	IDT melting temperature	Thesis recommended annealing temperature	Product length
BFG1F	GGCCTGAGATGTGTCCTGAT	Mouse <i>Vmo1</i> gene (NM_001013607.1)	Peters et al., 2007	56.7	55	495bp
BFG2R	GGTAAAAGACAGTACTGGCAGAGC			57.5		
BFG7F	GGCCTGAGATGTGTCCTGAT	Mouse <i>Vmo1</i> cDNA (NM_001013607.1)	Primer-BLAST	56.7	50	193bp
BFG8R	CACAGAGGCTCACTCCATGA			56.5		
BFG9F	TGTCAAGGTGGAGCCCCCTCA	Mouse <i>Vmo1</i> cDNA (NM_001013607.1)	Primer-BLAST	63.0	55	128
BFG10R	CCCAGCTTCCGGACTGGGACT			63.6		
BFG27F	CCCAAGCTTGGGAGGTCATGCAGGATGGAGTT	Mouse <i>Vmo1</i> gene (NM_001013607.1)	Primer-BLAST	62.8	50	671
BFG28R	CCAAGGCCAAGAAGCTTTAAT			53.5		
M13puc rev	CACACAGGAAACAGACCATGTC	pPRO EX HTb		56		
mus <i>GAPDH</i> primers	Unknown	Mouse <i>GAPDH</i> gene (NM_001013607.1)			60	~150

### **3.8.2 Preparation of Total cDNA**

RNA extracted from temporal bones as described in 3.7.1.2 was used to produce cDNA. The reverse transcriptase reaction was carried out in 20µl volumes in PCR tubes. An initial reaction mix containing 5µl RNA sample, 4µl of DEPC treated mQH<sub>2</sub>O and 2µl of Oligo-dT primers was incubated at 70°C for 5min to anneal primers to the polyadenylated tail found on the 3' end of mammalian mRNA transcripts, then stored on ice for 2min. To this, 10µl of Reverse transcriptase solution mix (Invitrogen USA) was added which contained SuperscriptIII reverse transcriptase (1U), 0.1M dTT and 1X first strand buffer, this final reaction mix was incubated at 50°C for 60min to carry out reverse transcription and then 85°C for 5min to deactivate the enzyme. cDNA was then stored at -80°C. Two types of negative controls were carried out simultaneously and expected to produce no cDNA; a negative, no template control to test for exogenous contamination of the reverse transcriptase reaction, and a negative no reverse transcriptase control to test for genomic contamination of the total RNA samples.

### **3.8.3 Amplification of cDNA using PCR**

To obtain full length *Vmo-1* specific cDNA (696bp NM\_001013607.1), total cDNA was amplified using primer set BFG27/28 (Table 10), at an annealing temperature of 50°C (protocol 3.4) to yield an amplicon 671bp long.

PCR reactions were carried out in 20µl volumes using 1µl cDNA obtained as outlined in 3.8.3, 1X HOT FIREPol® DNA Polymerase (Solis Biodyne), 1X HOT FIREPol® 10X Buffer B2 (Solis Biodyne), 2.5mM MgCl<sub>2</sub> (Invitrogen), 200µM dNTPs (Invitrogen), 0.25mM each of primers BFG27F and BFG28R and mQH<sub>2</sub>O.

After the reaction was completed the PCR products were electrophoresed on a 2% agarose gel with a 100bp ladder (Solis Biodyne) as per protocol outlined in 3.1.

Using primer set BFG1/2 (Table 9) at an annealing temperature of 55°C a negative, no template control and a positive *Vmo1* control were used to test for exogenous contamination and verify successful PCR.

For PCR products to be sequenced, they were then purified using the rAPid Alkaline Phosphatase method as outlined in 3.2.3 and sent for DNA sequencing to

determine if the correct sequence had been amplified and ensure complete coverage of the gene for the purposes of cloning and protein expression.

### **3.8.4 DNA Sequencing**

DNA sequence data was obtained from the University of Waikato DNA Sequencing Facility (Hamilton, New Zealand) using an Applied Biosystems 3130xl Genetic Sequence Analyzer. Forward and reverse reactions were carried out using BFG27F and BFG28R primers (Table 9) and the sequences analysed by Applied Biosystems Software, BLAST online tools and Geneious software (Appendix 8).

## **3.9 VMO1 Protein Expression in Mouse Tissue**

The expression of the VMO1 protein in mice was assessed in two ways; immunohistochemistry (IHC) of the mouse inner ear, and immunoblotting of various tissues and organs from the mouse on a western blot. For immunoblotting, protein was extracted and the concentration measured using Bradford assay. Further assessment was made using SDS-PAGE gel electrophoresis for both concentration and quality.

### **3.9.1 Protein Concentration Estimation using Bradford Assay**

The Bradford assay was used to estimate protein concentrations from dissected mouse tissues. BSA standards were prepared in a serial dilution and 1µl of each placed into individual wells in a 96 well microtitre plate (CELLSTAR®). One microlitre of each undiluted samples was placed in individual wells. One hundred microlitres of diluted dye reagent (BIORAD) was added to each well using a multipipette and mixed thoroughly by pipetting up and down. Reactions were incubated and left at RT for 5min before protein concentrations were estimated on a fluorescent plate reader (BMG Labtech FLUOstar Optima). Estimated protein concentrations were used as a guide for diluting protein samples for use on SDS-Page gel for the estimation of protein quality.

### **3.9.2 Western Blot Analysis**

Western blotting was used to detect the presence of VMO1 in a range of mouse tissue protein lysates that were separated by size on an SDS-PAGE gel and to validate the specificity of the VMO1 antibody used for IHC. The membrane and Whatmans paper (No.1) was cut slightly larger than the SDS-PAGE gel to ensure complete coverage and effective transfer of proteins then prepared as outlined in protocol 3.9.2.1 and shown in Figure 33. A Precision Plus Protein™ Dual Color Standards ladder (Biorad) was used as a positive control for protein transfer and to estimate protein molecular weight size.

Immunoblotting was used to detect, analyse and identify the VMO1 protein within crude preparations of homogenised mouse tissue proteins. Analysis was carried out using the proteins extracted from the mouse and BSA (NEB) at a concentration of 10mg/mL as a negative protein control. Proteins were labelled by incubating with a primary antibody which was then incubated with a secondary antibody conjugated to Horseradish Peroxidase (HRP). Binding of the secondary antibody to the primary antibody was detected using Thermo Scientific™ SuperSignal™ West Femto Chemiluminescent Substrate (ECL) and then imaged in a FujiFilm Intelligent DarkBox II (AlphaTech) and analysed using FujiFilm LAS 1000 lite V1.5 software. Following imaging of the membrane it was stripped of antibodies and reprobed using mouse Beta actin ( $\beta$ -actin) as the primary antibody for a positive antibody control to show successful blotting and the presence of proteins at detectable concentrations.

#### **3.9.2.1 Membrane Preparation**

Polyvinylidene fluoride (PVDF) membrane (Amersham Life Science) was handled minimally with clean tweezers to prevent contamination with exogenous proteins. The membrane was prepared by cutting to appropriate size with a notch placed in the upper right corner and marked lightly with pencil to orient protein samples. The membrane was covered with methanol for 10secs which was rinsed away and replaced with mQH<sub>2</sub>O for 5min followed by incubation in transfer buffer for 1min.

### 3.9.2.2 Antibody Binding to Protein Target in Tissue Lysates

The membrane was rinsed for 1min in dH<sub>2</sub>O to wash and then placed in a plastic container protein side up and the antibody binding carried out following the procedure outlined in Table 11.

Blocking was carried out using 10% w/v low-fat milk (Anchor) to prevent non-specific binding of the primary and secondary antibodies. Antibody incubation was carried out in a humidity chamber to prevent drying of the membrane and evaporation of the antibody solution using 1.5mL of primary antibody diluted to 1:1000. The membrane was rinsed vigorously in TBS to remove the antibody solution and then washed in TBS and TBS-T to remove non-specifically bound antibodies to increase sensitivity and reduce background noise. HRP-Goat Anti-rabbit secondary antibody (GeneTex) binding was carried out in a 2mL volume with a dilution factor of 1:5000.

**Table 11: Procedure for immunoblotting outlining the order and times for incubation in various solutions.**

Step	Solution	Duration
Block (shaking)	10% w/v low-fat milk in 1X TBS-T buffer	Overnight at 4°C
Primary antibody	Diluted rabbit anti goat antibody in Blocking solution	Overnight at 4°C in a humidity chamber
Rinse	1X TBS-T buffer	x3
Wash (shaking)	1X TBS-T buffer	15min x3
Secondary antibody	Diluted rabbit anti goat antibody in Blocking solution	1hr at RT in a humidity chamber
Rinse	1X TBS-T buffer	x3
Wash (shaking)	1X TBS-T buffer	15min x1 5min x2
	1X TBS buffer	5min

### 3.9.2.3 Immunodetection

Binding of the secondary antibody (GeneTex) was detected using ECL development according to the manufacturer's recommendations (Thermo Scientific). A 600µl aliquot of each developing solution were mixed together and poured over the membrane to completely cover it then left to develop for 2min at RT in a light proof drawer. Care was taken to expose developing solution to as



little light as possible to prevent photo-bleaching of the developing reagents. The membrane was drained of the excess solution and placed in a developing film and exposed for an appropriate amount of time in a FUJIFILM Intelligent Dark Box II LAS-1000.

ECL development caused a chemical reaction resulting in the oxidation of luminol by the HRP to emit light for the detection of the protein of interest at a level of 1-10pg.

#### **3.9.2.4 Removal of Antibody from the Membrane**

Following imaging, the membrane was stripped of antibodies using a protocol adapted from Abcam® and reprobed as outlined in 3.9.2.2 using  $\beta$ -actin antibody at a concentration of 1:1000. Following immunodetection, the membrane was rinsed twice for 5min each in 1X TBS. Stripping buffer was heated in a water bath to 50°C and then poured over the membrane and incubated at RT for 5min shaking. The stripping buffer was replaced with fresh buffer and then left shaking at RT for a further 10min. Stripping buffer was discarded and the membrane washed twice in 1X PBS shaking at RT for 10min followed by two washes in 1X TBS-T for 5min.

#### **3.9.2.5 Ponceau Staining**

Following immunodetection, the membrane was placed in Ponceau stain to act as a positive control to check for the presence of proteins at detectable levels. The membrane was placed in a glass dish and covered with Ponceau stain and left rocking at RT for 5min. Ponceau stain was discarded and the membrane rinsed in tap water to remove excess stain.

#### **3.9.2.6 Protein Transfer**

Proteins were transferred from an SDS-PAGE gel (protocol 3.5) onto a PVDF membrane using an SE300 miniVE Integrated Vertical Electrophoresis and Blotting Unit (Hoefer) with the membrane and gel laid as illustrated in Figure 33

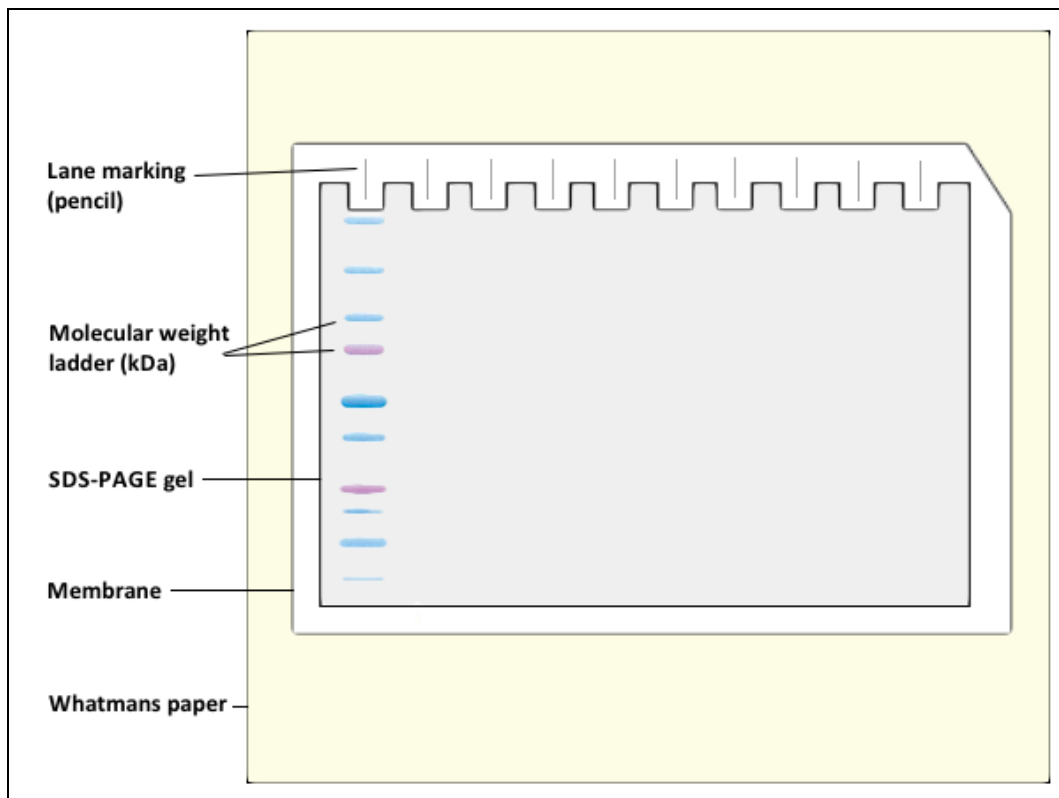


**Figure 33: Layout of SDS-PAGE gel on membrane ready for protein transfer. The position of the molecular weight ladder (BIORAD) and pencil marking in lane position are shown.**

The membrane and gel were assembled with Whatmans paper and sponges in the blotting case as outlined in **Figure 34** and then covered with transfer buffer so the membrane and Whatmans paper were fully submerged.

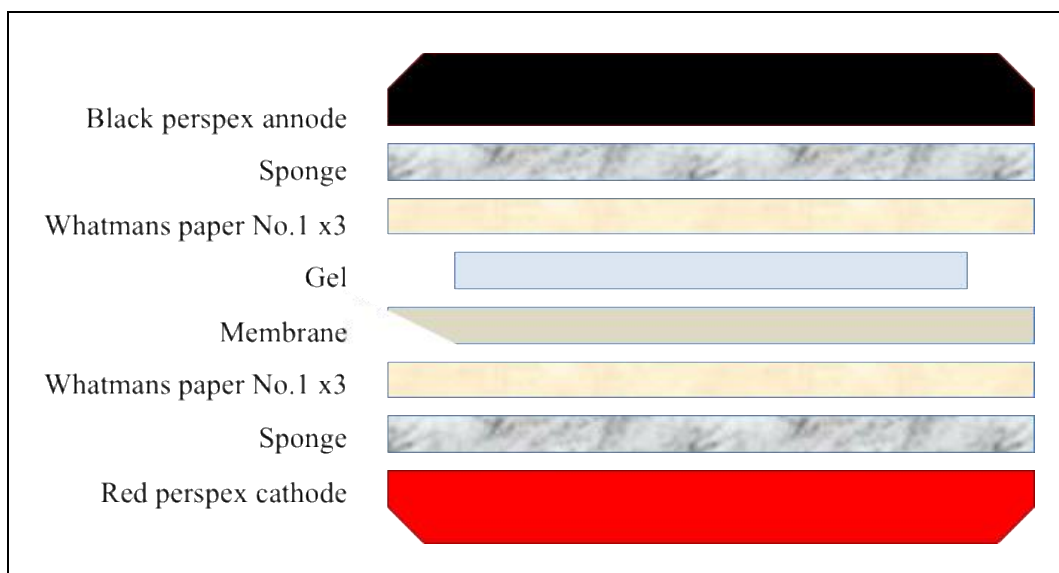


**Figure 34: Arrangement of western blotting components for protein transfer**

The assembled blotting case was then placed into the blotting unit filled with chilled water and electrophoresed for 2hr at 25-50 volts.

### **3.10 VMO1 Protein Expression in the Inner Ear of the Mouse**

To maintain cell morphology and integrity of the tissue sample, 4% paraformaldehyde (PFA) was used to fix the sample. This prevents protein degradation and preserves the antigenicity of the target proteins by protein cross linking and antimicrobial action of PFA. Optimal cutting temperature (OCT) freezing medium was used to embed the specimens which were then sectioned (10µm) on a Leica CM1850 UV cryostat (Leica Biosystems) and collected onto 75x25mm gelatin coated single frosted pre-cleaned Corning microscope slides (Corning Inc). The slides were then processed for either IHC or H&E staining. Stained slides were visualised on a Leica fluorescent microscope.

#### **3.10.1 Fixation, Embedding and Sectioning of Mouse Ears**

Six P5 mice (wild type C57/B16/129SV) were euthanised with CO<sub>2</sub> according to SOP9 (UoW) and then decapitated. The skin of the head was removed then hemidissected and the brain removed. Tissue was dipped in 1X PBS and then placed in 50mL Falcon tube and covered in 4% PFA to fix overnight rocking gently at 4°C. The following day, the PFA was replaced with fresh 4% PFA and again left overnight rocking gently at 4°C. The following day, the specimens were removed from PFA and rinsed with 1X PBS, washed three times for 10min each in fresh 1X PBS and finally rinsed with 30% sucrose for cryopreservation. Sucrose wash was repeated twice for 10min each and a final wash of 30% sucrose was left overnight, rocking gently at 4°C to dehydrate tissue. The following day, half of the sucrose was removed and replaced with OCT embedding media (Tissue-Tek 4583, 118mL VWR, Sakura) and left at 4°C rocking gently for 1hr.

A cryomold was filled with OCT and a single specimen was removed from the OCT/sucrose solution with sterile tweezers and allowed to drip drain before being placed carefully (avoid air bubbles) in the cryomold. Using a dissection microscope, the tissue was oriented with the head towards the top of the mould with the back facing left and sitting as flat as possible to maintain even sectioning.

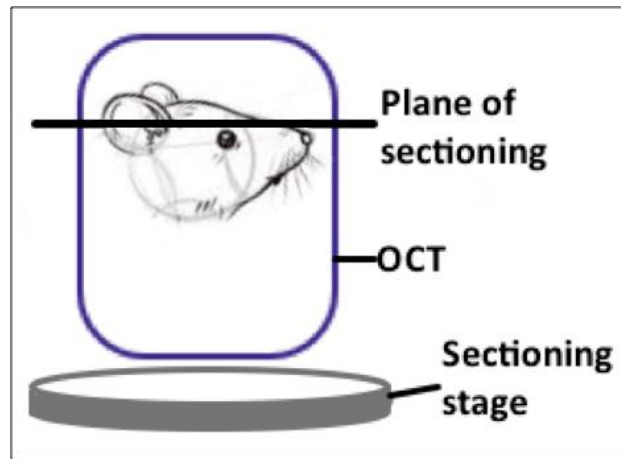


**Figure 35: Position of hemidissected mouse head in the cryomold. The plane of sectioning is also shown.**

Once oriented correctly the cryomold was placed in the dry ice/methylbutane slurry to set OCT rapidly. Moulds were individually wrapped in tin foil, labelled and stored at  $-80^{\circ}\text{C}$ .

### **3.10.2 Slide Preparation**

Corning frosted slides were coated in gelatin in preparation for sectioning and to ensure sections remained on the slides during IHC and staining procedures. Fifty slides were placed in four glass racks and soaked in hot tap water with Virkon® detergent for 1hr and then rinsed under hot running tap water for 1hr followed by rinsing in  $\text{dH}_2\text{O}$  three times. They were then air dried in a  $37^{\circ}\text{C}$  oven for 1 hour. To gelatin coat the slides, 1L of RNase free DEPC treated  $\text{mQH}_2\text{O}$  was brought to boil in a 2L beaker and then slowly allowed to cool while being stirred using a magnetic flea. At  $60^{\circ}\text{C}$ , 2g of Gelatin Type A (300 Bloom, Sigma category number G-2500) was added. At  $50^{\circ}\text{C}$ , 0.1g of Potassium Chrome III Sulfate ( $\text{KCr(III)SO}_4$ ) was added and the solution allowed to cool to  $35^{\circ}\text{C}$ . Each rack was dipped in the solution for 1min and allowed to dry on its side with the frosted portion down for 5min. Dipping was repeated once and the slides allowed to dry overnight at  $35^{\circ}\text{C}$ . Slides were stored in the original boxes at RT prior to use.

### **3.10.3 Sectioning**

The cryostat temperature was set to  $-25^{\circ}\text{C}$ , 30min prior to sectioning. OCT embedded mouse heads were transported on ice from the  $-80^{\circ}\text{C}$  freezer to the cryostat as quickly as possible to prevent defrosting of the OCT, and immediately

placed into the sectioning chamber along with the round metallic stage, razor blades and brushes. The cryostat was left for 30min to allow the machine to reach the set operating temperature. The embedded tissue was then removed from the cryomold in preparation for mounting onto the stage. Enough OCT was placed onto the stage to support the tissue sample and the tissue placed on the stage as shown in Figure 35 and the base covered in OCT and frozen in place using cryospray. Once completely set, the stage was clamped into place in the stage clamp and retracted as far from the blade holder as possible ready for sectioning. The blade was inserted into the blade holder, and the angle adjusted to 10° and secured in place. The stage was moved to just in front of the blade and the thickness of the sections set to 50µm. The roll bar was lifted away from the blade and sections made to expose the embedded tissue. The thickness of the sections was adjusted to 20µm and sectioned until the eye was visible. The thickness was again adjusted to 10µm and the roll bar lowered over the blade. Sections were taken by rotating the handle in a smooth steady motion and the tissue trimmed using a razor blade to ensure flat even sectioning. Every fifth section was collected on a slide at RT and checked for inner ear anatomy on a dissection microscope. Once the inner ear was reached, sections were collected in series of four or five slides with 9 sections per slide by lifting the roll bar to expose the section and the slide gently placed on top of it to collect it. The slides were allowed to dry at RT for 1hr and then stored in glass slide racks wrapped in foil at -20°C.

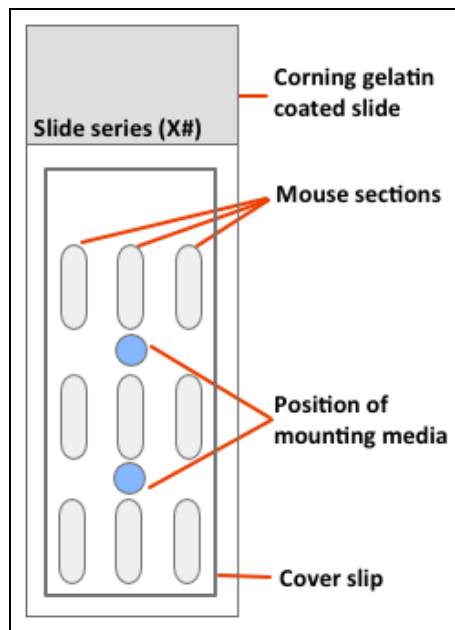


**Figure 36: Layout of mouse sections on a microscope slide showing the positions of the coverslip and where mounting media was placed.**

### **3.10.4 Section Staining**

Three types of staining methods were used on serial sections collected from the OCT embedded mouse specimens. They were used to visualise the anatomy of sectioned tissue to check for tissue integrity, to identify individual cells and structures within the inner ear, and to localise the VMO1 and/or  $\beta$ -actin protein.

#### **3.10.4.1 Haematoxylin and Eosin Anatomy Stain**

Haematoxylin and Eosin stain (H&E) is a histological stain used to determine the integrity of tissue after sectioning and to visualise cells in a tissue section. It consists of two dyes haematoxylin and eosin. Haematoxylin stains the DNA in the nuclei, RNA in the ribosomes and rough endoplasmic reticulum as well as keratohyalin granules and calcified material and carbohydrates in the cartilage a purple blue colour. Following haematoxylin staining, eosin is used to stain the cytoplasm of cells, cytoplasmic filaments in muscle cells, intracellular membranes, and extracellular fibres shades of red, pink and orange (Anderson, 2011).

To prepare for H&E staining, slides were brought to RT by leaving on the bench covered in tinfoil for 3hr and rinsed in 1X PBS for 5min. Slides were removed from the liquid and the excess wiped away from the underside of the slide and around the tissue using a paper towel but was not allowed to dry out. Using a pipette tip, 1mL of haematoxylin solution was slowly dropped onto slide and

tilted to cover the tissues then left at RT for 5min. The reverse of the slide was then placed under gently running tap water to rinse then placed in 1X PBS for 5min. Slides were removed from the PBS and the excess liquid wiped away from the underside of the slide. One millilitre of eosin was carefully dropped onto the tissue and left for 5min then rinsed in running tap water. The slide was then mounted directly under a 22x60mm coverslip (MenzelGlaser) in Fluoroshield™ with DAPI (Sigma-Aldrich). Fluoroshield™ was used to preserve the fluorescence of the antibodies and Dapi to visualise cell nuclei.

#### **3.10.4.2 IHC Staining**

IHC was carried out using the indirect method in which an unlabeled primary antibody was incubated on tissue sections followed by a second reaction in which secondary antibody conjugated to the fluorophore Fluorescein was reacted with the primary antibody to localise the VMO1 protein within the inner ear with the VMO1 antibody (GeneTex). Slides were incubated in the solutions listed in Table 12 for the appropriate times. The detergent Triton X-100 was used to reduce surface tension of the tissue to give better coverage of the tissue sections.

Hydrogen peroxide (H<sub>2</sub>O<sub>2</sub>) was used to eliminate endogenous peroxidase activity which results in high levels of non-specific background noise. Blocking and antibody incubation was carried out in a humidity chamber with a light proof lid. Tissue was blocked in 5% goat serum (Sigma) at 4°C overnight to reduce non-specific hydrophobic binding of the primary and secondary antibodies. Primary antibody was pipetted directly onto the tissue to preserve volume and diluted in 10% blocking solution at a dilution of either 1:100 or 1:1000. Secondary antibody was diluted in 10% blocking solution at a dilution of 1:5000 and pipetted over the slides to cover the tissue. A negative antibody control was carried out to ascertain the amount of background noise by substituting primary antibody for 1X PBS. A positive control using the β-actin antibody, which is known to be ubiquitous in mouse tissue and present in the mouse inner ear, was used as a primary antibody to validate the IHC protocol.

**Table 12: Protocol for IHC using a primary and secondary antibody showing the solutions/reagents used the incubation times and the amount of times each procedure was repeated**

<b>Solution</b>	<b>Incubation time</b>
1X PBS	5min x2
0.5% TRITON X-100 (in 1X PBS)	30min
1X PBS	5min x2
0.9% H <sub>2</sub> O <sub>2</sub> (in 1X PBS)	30min
1X PBS	5min x3
100µl 5% goat serum	Overnight at 4°C
100µl Primary antibody in 10% blocking solution (1:100 or 1:1000)	Overnight at 4°C
1X PBS	10min x3 shaking
1X PBS	Overnight at 4°C
500µl Rabbit IgG H+L antibody FITC in 10% blocking solution (1:5000)	1hr
1X PBS	10min x3 shaking
Mount	

### **3.10.4.3 Nuclei staining and slide mounting**

Hoescht (Sigma) and 4,6-diamidino-2-phenylindole (DAPI) stains were used alternately as blue fluorescent dyes to stain DNA in cell nuclei. Both are excited by UV light (350nm) and emit blue fluorescent light around 460nm and are commonly used in fluorescence microscopy and IHC.

The Fluoroshield™ with DAPI mounting media was used to mount all of the IHC slides except where otherwise stated. Alternatively, after IHC was carried out the slide was stained with 200µl of Hoescht solution (0.5µg/mL) for 30min then mounted in glycerol mounting fluid. To mount, two drops of mounting media were placed in the centre of the slides as shown in Figure 36 and a clean dry coverslip was gently placed on top of the slide with care taken to avoid air bubbles. The slides were left to dry in a light proof slide container overnight at RT.

### **3.10.5 Microscopy**

IHC and H&E stained slides were visualised on a Leica DMR Microscope with a Nikon Digital Camera attached. FITC secondary antibody was conjugated to the VMO1 and β-actin primary antibodies and was visualised with UV light and a 460-490nm cube filter. Hoescht and DAPI staining were visualised using UV light with a 352-402nm filter block. H&E stain was visualised using light microscopy with no filter.



# CHAPTER FOUR

## RESULTS

This section outlines the results from the molecular methodologies used to amplify and sequence *Vmo1* mRNA, clone and express recombinant VMO1 protein, validate antibodies using whole protein tissue lysates and recombinant protein via western blotting, and finally, determine the protein localisation of VMO1 in the mouse inner ear via IHC.

### 4.1 Isolation of Total RNA from Mouse Inner Ears

Thirty microlitres of total RNA was extracted and isolated from six inner ears dissected from three adult P28+ female mouse specimens which were pooled together to optimise RNA yield using the method outlined in protocol 3.8.2 which was adapted from the supplier recommended procedure. Three aliquots were collected from the homogenised tissue sample: aliquot 1, 2 and 3, respectively.

Extracted RNA samples (Aliquot 1, 2 and 3) were quantified using the Nanodrop. Table 13 shows the Nanodrop results for the three aliquots of total RNA collected using protocol 3.8.2. As expected, the ratio of absorbance at 260 nm and 280 nm, which measures the purity of the samples, were within acceptable limits (1.8 – 2.0) with DNA expected at 1.8 and RNA at 2.0. The chromatogram produced was also analysed for contamination by reagents used in the isolation of the total RNA such as Trizol, phenol and guanidinium thiocyanate, which produce large peaks around the 230nm range.

Therefore, the results suggest the RNA can be used as a template for cDNA synthesis.

**Table 13: RNA sample Nanodrop results showing the concentration, purity and contamination with extraction and purification reagents such as Trizol, guanidinium thiocyanate (GITC) and phenol.**

Sample	260/280 ratio	Contamination with extraction reagents (Trizol, GITC, Phenol)	Concentration (ng/μl)
Aliquot 1	2.03	Negligible	2461.5
Aliquot 2	2.07	Negligible	1209.7
Aliquot 3	2.05	Negligible	3633.3

## 4.2 cDNA Synthesis Using Inner Ear Mouse RNA as a Template

RNA extracted from the inner ear of the mouse was used to produce double stranded cDNA for the purposes of amplification by PCR for cloning and sequencing.

Figure 37 shows three aliquots of cDNA: RNA1, 2 and 3 respectively, electrophoresed on a 2% TAE agarose gel stained with RedSafe™. A 5µl sample of each of the three aliquots were electrophoresed to check for purity and concentration and show a characteristic smear of cDNA between 100-700bp long.

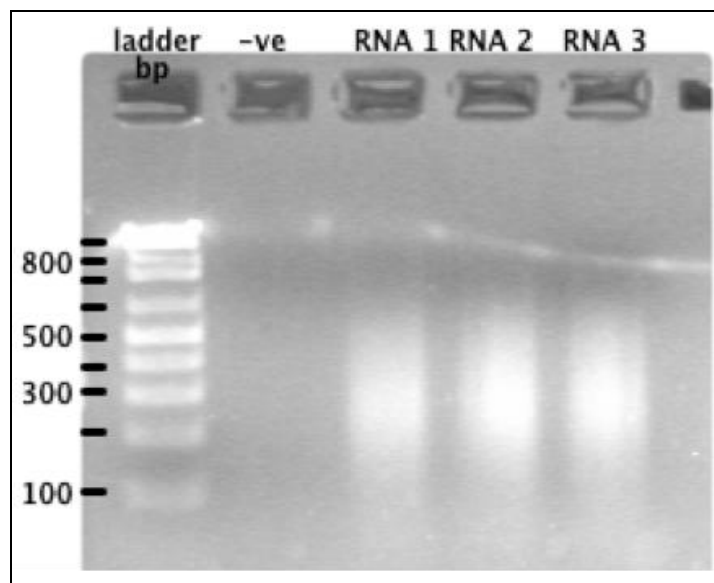


**Figure 37: cDNA synthesised by reverse transcription of three RNA samples extracted from P28 mouse inner ears using the oligo-dT primers. 5µl of each sample were electrophoresed on a 2% TAE agarose gel stained with RedSafe™ to check for purity and concentration and show a characteristic smear of cDNA between 100-700bp long compared against a 100bp ladder (Solis Biodyne).**

In addition to cDNA synthesis negative controls were prepared in order to assess genomic DNA contamination (cDNA-). This control included no reverse transcriptase enzyme. With PCR amplification the negative cDNA control should not produce any amplicons and therefore no visible bands. Figure 38 shows amplification of two cDNA templates using *GAPDH* mouse specific primers (*GAPDH1/2*) and *Taq* DNA Polymerase. The negative control (-ve) has no cDNA template and therefore, measures PCR contamination. The cDNA- negative controls were produced during cDNA reverse transcription reaction and contain no reverse transcription enzyme to test for the presence of genomic DNA in the RNA template.

PCR produced single bands of expected size (150bp). Band intensity is indicative of PCR product concentration with cDNA1 containing greater concentrations.

This fits with the Nanodrop results that show the concentration of RNA in sample 1 is twice that of sample 2. Contamination of cDNA1- (black arrow) is the result of genomic DNA contamination and indicates that the high Nanodrop concentration of aliquot 1 is partly due to genomic DNA contamination.

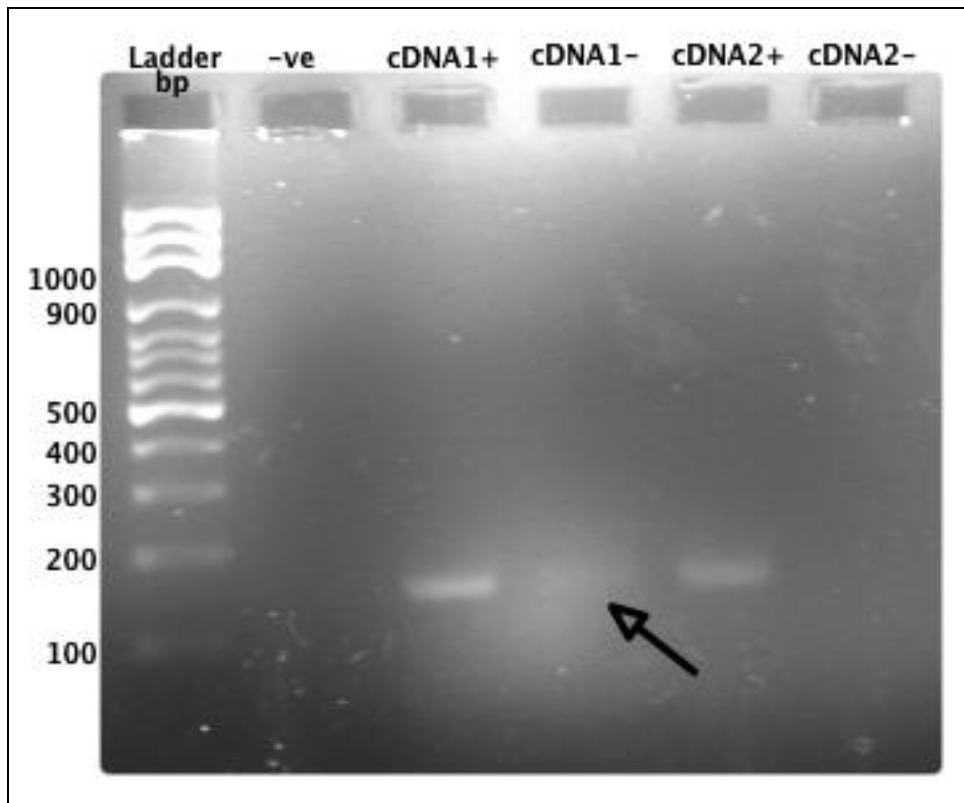


**Figure 38: cDNA controls using mouse specific primers (*GAPDH1/2*) electrophoresed at 91V for 30min on a 2% TAE agarose gel stained with RedSafe™ dye with bands of expected size (150bp). Possible genomic DNA contamination indicated with black arrow. Electrophoresed for 30min at 90V on a 1% 1X TAE, agarose gel stained with RedSafe™ and compared to the 100 bp molecular weight ladder (Solis Biodyne). Bands lower than 100 bp are primer dimers.**

This electrophoresis result and the Nanodrop readings indicate high purity and high concentration of the RNA2 template. The RNA1 sample contains genomic DNA contamination but is otherwise pure of contaminants. The next step is to use the cDNA2+ as a template for PCR amplification.

### **4.3 Optimisation of *Vmo1* Amplification from cDNA**

PCR was carried out with cDNA2 samples to check for amplifiable *Vmo1* cDNA. Optimal results from PCR were achieved using protocol 3.4 with the annealing temperatures listed in Table 9.

PCR reactions were carried out using different concentrations of PCR reagents and annealing temperatures to maximise amplification of template cDNA for DNA cloning and DNA sequencing. Optimal results, where there were bright,

sharp, single bands of expected sizes were achieved using higher  $MgCl_2$  concentrations (2.5mM) and HOT FIREPol® 10X Buffer B2 (Solis Biodyne) which contains Tris-HCl,  $(NH_4)_2SO_4$  and detergent. The best results for primer set BFG1/2 (495bp) were achieved with an annealing temperature of 55°C and primer set BFG27/28 (671bp) with an annealing temperature of 50°C.

#### 4.3.1 HOT FIREPol® Buffer Optimisation

Figure 39 shows the amplification of cDNA2 and cDNA2- at 60°C using mouse specific primers and HOT FIREPol® DNA polymerase and the HOT FIREPol® B1 buffer. --ve is a negative genomic DNA control using cDNA2- and BFG1/2 primer set, -ve is a negative PCR control with no template cDNA. Lanes 1, 2 and 4 show no amplification of the *Vmo1* cDNA for primer sets BFG27/28, BFG7/8 and BFG9/10. Lane 3 shows amplification of the *Vmo1* cDNA using primer set BFG1/2. Subsequent PCR reactions were adjusted to include the HOT FIREPol® 10X Buffer B2.

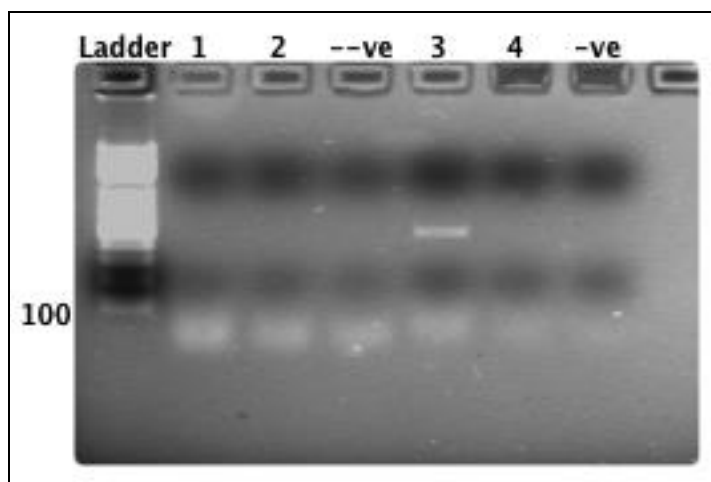


**Figure 39: Amplification of cDNA2 and cDNA2- at 60°C using mouse specific primers and HOT FIREPol® *Taq* DNA polymerase with a  $MgCl_2$  concentration of 1.5mM and HOT FIREPol® B2 buffer and then electrophoresed at 90V for 30min on a 1% TAE agarose gel. Lane 1:unsuccessful PCR using primers BFG27/28, lane 2: unsuccessful PCR using primers BFG7/8, lane 3: successful PCR using primer set BFG1/2 of an expected 493bp, lane 4: unsuccessful PCR using primers BFG9/10, --ve is a negative genomic DNA control using cDNA2- and BFG1/2 primer set, -ve is a negative PCR control with no template cDNA. Electrophoresed for 30min at 90V on a 1% 1X TAE, agarose gel stained with RedSafe™ and compared to the 100 bp molecular weight ladder (Solis Biodyne). Bands lower than 100 bp are primer dimers.**

#### 4.3.2 Magnesium Concentration Optimisation

Figure 40 shows a gel electrophoresis of PCR products produced at 60°C by cDNA2 and cDNA2- samples using mouse specific primers, HOT FIREPol® DNA polymerase and HOT FIREPol® 10X Buffer B2. Lane one is a negative

control for the PCR reaction and contains no cDNA template. Lane 2 is a positive control using cDNA2 and *GAPDH* primer set. Lane 3 contains cDNA2- amplified with *GAPDH* primer set to test for genomic DNA contamination. Lane 4 shows an amplicon produced by the primer set BFG27/28 with 1.5mM MgCl<sub>2</sub>. Lane 5 shows an amplicon produced by the primer set BFG27/28 with 2.5mM MgCl<sub>2</sub>. Subsequent PCR reactions were adjusted to include 2.5mM MgCl<sub>2</sub>.

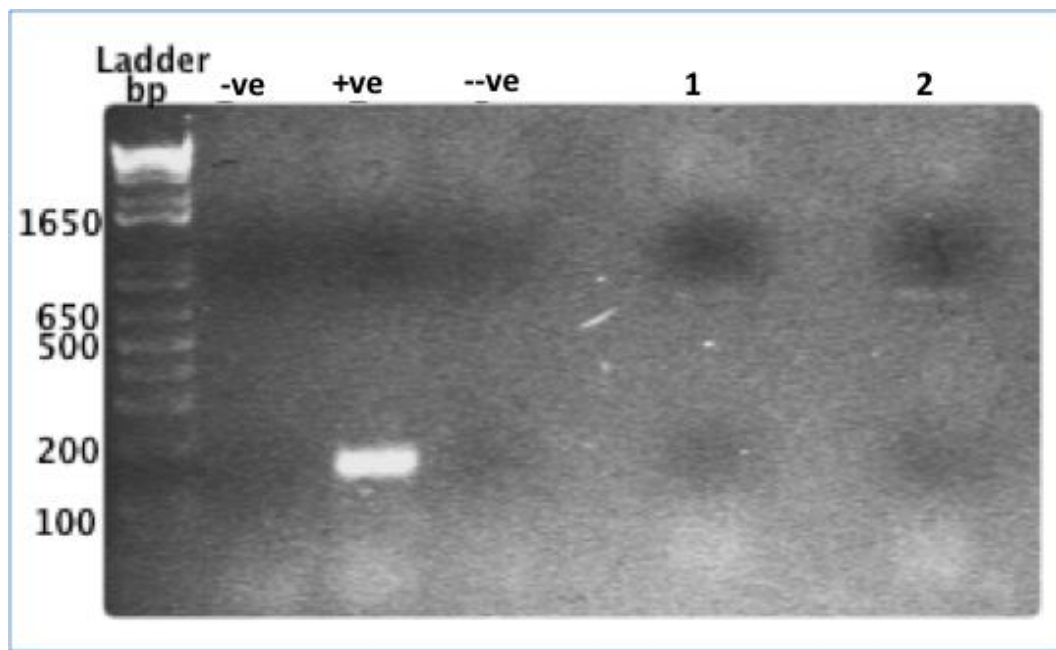


**Figure 40:** 1% TAE agarose gel of PCR products using cDNA2 and two different MgCl<sub>2</sub> concentrations on the primer set BFG27/28 at 60°C. -ve is a negative control using no cDNA, +ve is a positive control using *GAPDH* primers, --ve is a negative genomic DNA control using *GAPDH* specific primers, lane 1 is MgCl<sub>2</sub> at 1.5mM, lane 5 shows greater intensity band with MgCl<sub>2</sub> at a concentration of 2.5mM. Electrophoresed for 30min at 90V on a 1% 1X TAE, agarose gel stained with RedSafe™ and compared to the 100 bp molecular weight ladder (Solis Biotec). Bands lower than 100 bp are primer dimers.

### 4.3.3 Temperature Optimisation

Figure 41 shows a gel electrophoresis of PCR products produced at 55°C by cDNA2 and cDNA2- samples using *Vmo1* specific primers, 2.5mM MgCl<sub>2</sub> HOT FIREPol® DNA polymerase and HOT FIREPol® 10X Buffer B2. Lane one is a negative control for the PCR reaction and contains no cDNA template. Lane 2 contains cDNA2- amplified with primer set BFG1/2 to test for genomic DNA contamination. Lane 3 is a positive control using cDNA2 and primer set BFG1/2 (495bp) to show the amplification of *Vmo1* cDNA. Lane 4 shows an amplicon produced by the primer set BFG27/28 which is a full length *Vmo1* mRNA and includes two RE sites for HindIII to produce a digested amplicon containing the full ORF for translation of the VMO1 protein for use in cloning and sequencing

reactions. Lane 5 is a second positive control for *Vmo1* cDNA and is specific to *Vmo1* cDNA only by including the two exon junctions found in the mRNA (193bp). The optimal annealing temperature for the primer set BFG1/2 and BFG7/8 was determined to be 55°C and used for these primer sets in subsequent PCR reactions.

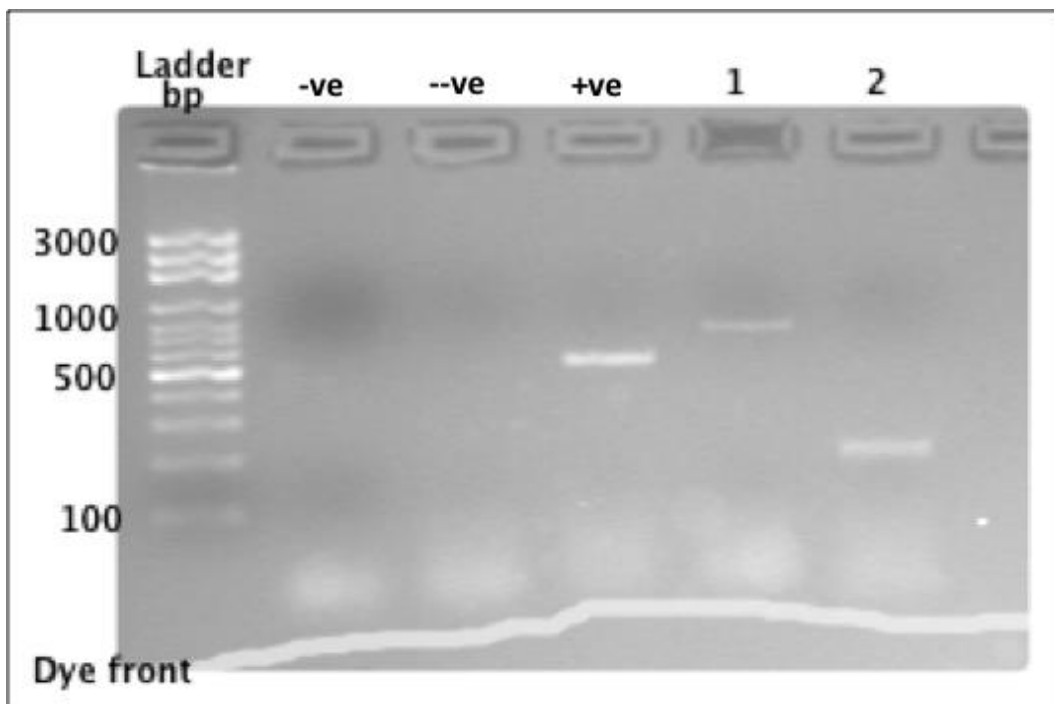


**Figure 41: Amplification of cDNA2 and cDNA2- at 55°C using mouse specific primers and HOT FIREPol® *Taq* DNA polymerase with a MgCl<sub>2</sub> concentration of 2.5mM and then electrophoresed at 90V for 30min on a 1% TAE agarose gel. -ve is a negative PCR control with no template cDNA, --ve is a negative genomic DNA control using cDNA2- and BFG1/BFG2 primer set, +ve is a positive control using primer set BFG1/2, lane 1 uses primer set BFG27/28, lane 2 uses primer set BFG7/8. Electrophoresed for 30min at 90V on a 1% 1X TAE, agarose gel stained with RedSafe™ and compared to the 100 bp molecular weight ladder (Solis Biodyne). Bands lower than 100 bp are primer dimers.**

Figure 42 shows a gel electrophoresis of PCR products produced at two different annealing temperatures used with primer set BFG27/28 and 2.5mM MgCl<sub>2</sub>, HOT FIREPol® DNA polymerase and HOT FIREPol® 10X Buffer B2. Lane one is a negative control for the PCR reaction and contains no cDNA template. Lane 2 contains cDNA2- amplified with primer set BFG1/2 to test for genomic DNA contamination. Lane 50°C shows results for PCR carried out at 50°C and is much more intense than those shown in lane 55°C where the PCR was carried out at 55°C. Lane +ve and -ve are positive and negative PCR controls respectively and were carried out using primer set BFG1/2 at an annealing temperature of 55°C. Along the bottom of the gel at less than 100bp are primer dimers for all of the

reactions. The optimal annealing temperature for the primer set BFG27/28 was determined to be 50°C and used for these primer sets in subsequent PCR reactions.

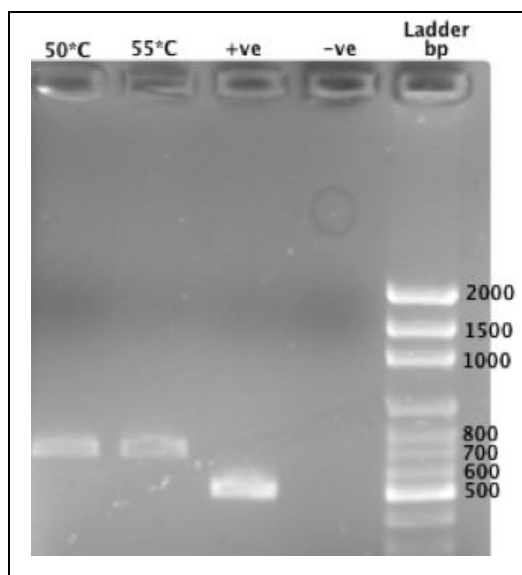


**Figure 42: Effect of annealing temperature on band intensity for primer set BFG27/28**  
 Amplification of mouse inner ear cDNA using *Vmo1* specific primers (BFG27/28) and HOT FIREPol(R) *Taq* DNA polymerase at different annealing temperatures (55°C and 50°C). The PCR products are electrophoresed for 30min at 90V on a 1% 1X TAE, agarose gel stained with RedSafe™ and compared to the 100 bp molecular weight ladder (Solis Biodyne). Bands lower than 100 bp are primer dimers. -ve is a negative PCR control and +ve is a positive *Vmo1* control using primer set BFG1/2 at 55°C.

Table 9 shows the recommended annealing temperatures (5°C below lowest  $T_m$  in primer pair) for *Vmo1* primers based on melting temperatures ( $T_m$ ) recommended by oligonucleotide supplier (IDT) and the recommended annealing temperatures found through experimentation.

**Table 14: Recommended annealing temperatures for primer sets used in standard PCR with 2.5mM MgCl<sub>2</sub>, HOT FIREPol® DNA polymerase and HOT FIREPol® 10X Buffer B2.**

Primer set	Calculated IDT recommended annealing temperature	Thesis recommended annealing temperature
BFG1/2	51.7°C	55°C
BFG7/8	51.5°C	55°C
BFG27/28	58.5°C	50°C
musGAPDH	-	60°C

#### **4.4 DNA Sequencing Results**

Applied Biosystems Software, BLAST online tools and Geneious software were used to analyse DNA sequencing results (Appendix 8) obtained from the UoW DNA sequencing facility to determine if the correct sequence had been amplified and ensure complete coverage of the gene for the purposes of protein expression in an expression vector. The forward and reverse complement sequences (Figure 43) were compared to each other and checked against the mouse mRNA reference sequence (NM\_001013607.1).



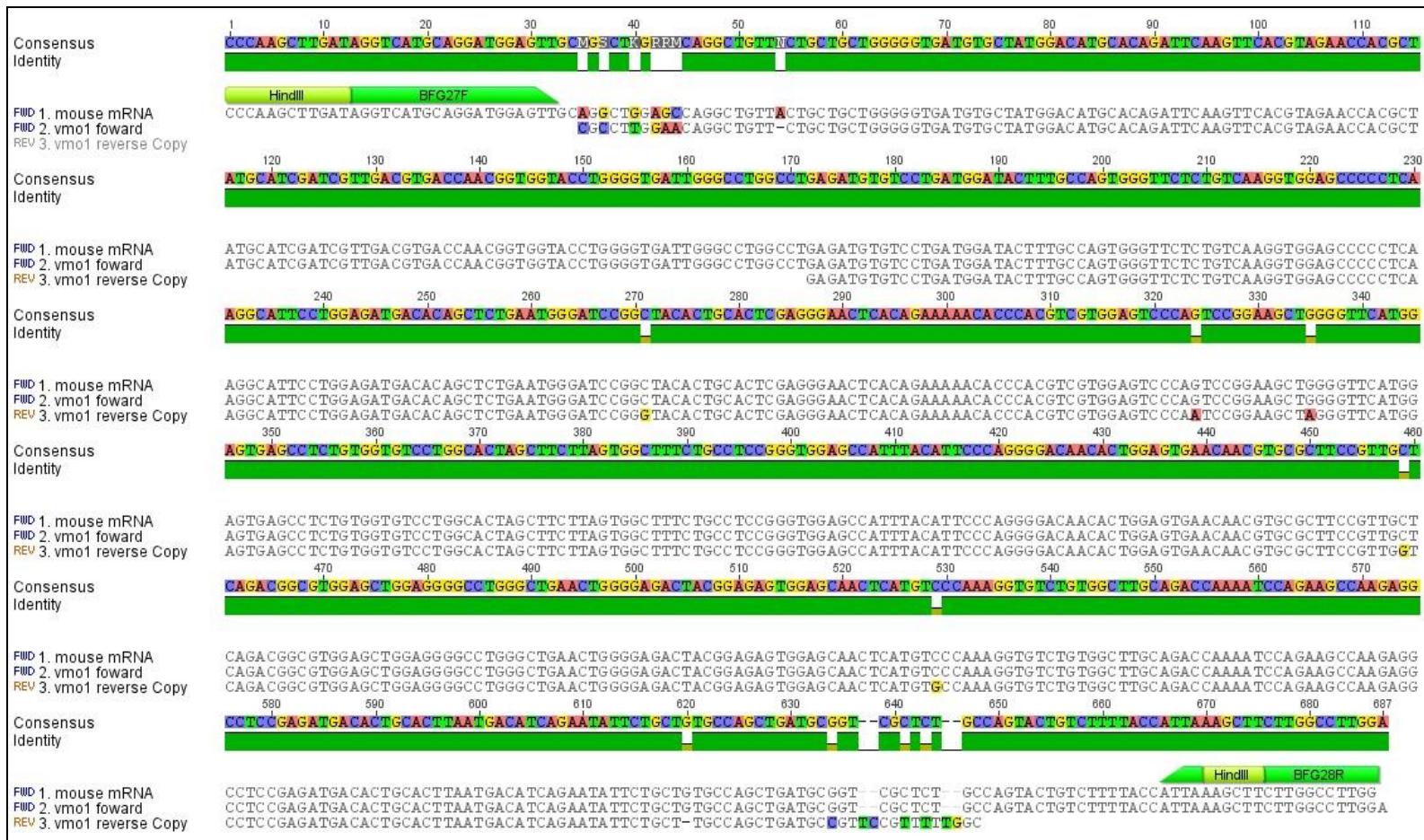
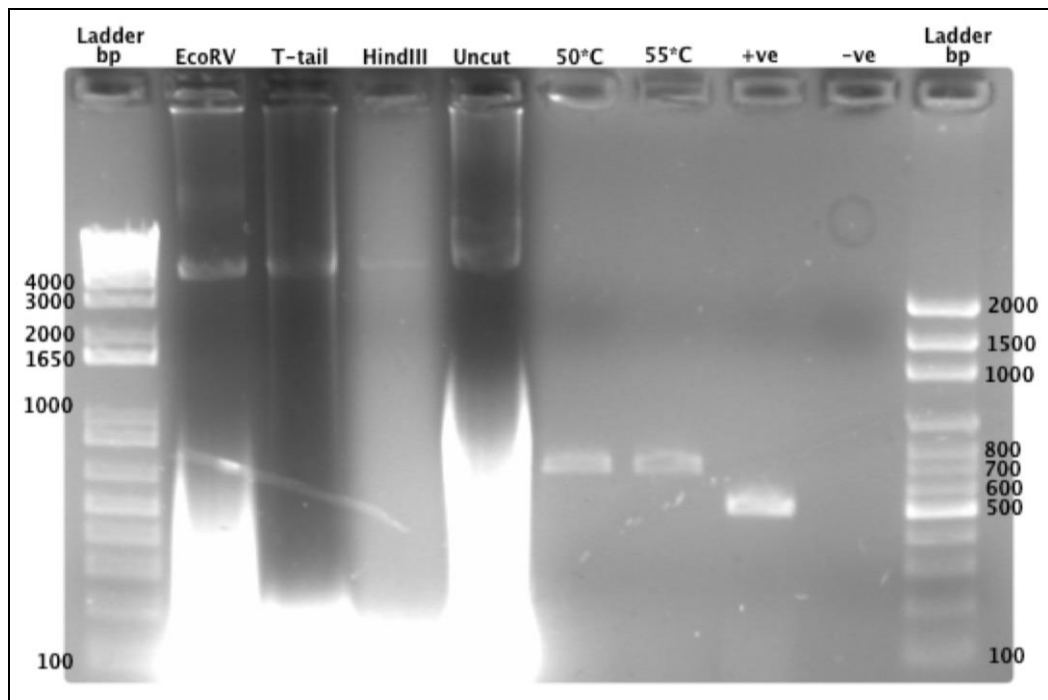


Figure 43: Multiple alignment of the mouse *Vmo1* mRNA reference sequence (NM\_001013607.1) with the forward sequence and reverse complement of the reverse sequence obtained from the UoW DNA sequencing facility.

## 4.5 Cloning and Expression of the Mouse *Vmo1* Amplicon

*Vmo1* was successfully PCR amplified using primer set BFG27/28 following protocol 3.4 with an annealing temperature of 50°C.

Electrocompetent *E. coli* DH5 $\alpha$  cells were shown to be competent and allowed the incorporation of the frozen stocks of the pProEX HTb and pBluescript vector into *E. coli* cells with a high efficiency with over 50 colonies seen on plates containing 100 $\mu$ l of transformed culture. Single colonies of transformed DH5 $\alpha$  were successfully isolated and grown overnight for amplification of the plasmid which was then isolated using the phenol/chloroform methods and quantified on a 1% agarose gel and on the Nanodrop. Ligation of the *Vmo1* transcript into the isolated vectors was unsuccessful and is discussed in 5.4.1. Figure 44 shows the presence of the pProEX HTb vector at high concentrations throughout the digestion and T-tailing procedure. Also shown are the PCR amplicons produced by primer set BFG27/28 at two different temperatures 50°C and 55°C. A positive *Vmo1* control using primer set BFG1/2 and a negative control with no template cDNA.



**Figure 44:** Agarose gel electrophoresis of products processed for ligation into vectors which included digestion with the EcoRV RE, T-tailing, HindIII RE digestion and the uncut plasmid at an estimated 4000-5000bp size. Also shown are PCR amplicons produced by primer set BFG27/28 at 50 and 55°C and a positive and negative control produced using primer set BFG1/2.

**Table 15: Nanodrop readings for isolated vectors showing the type of vector, the bp length of the plasmid and the concentration in ng/μ**

DNA Sample	Classification	Size (bp)	Concentration (ng/μl)
pET41a(+)	Circular Plasmid	5933	-
pET42a(+)	Circular plasmid	5930	11659
pBluescript II SK (+)	Circular Plasmid	3000	970 and 1158
pProEX HTb	Circular plasmid	4779	5457, 4562, 5339 and 6615
pCR®4-TOPO	Linear Plasmid	3956	Not stated by supplier

## 4.6 Protein Extraction from Whole Cell Lysates of Mouse

### Tissues

Protein was extracted from 20 different tissues (Table 16) dissected from P28+ mice for the purposes of validating the VMO1 antibody.

Inner ears were extracted from four P28+ mouse specimens and pooled together for extraction to optimise protein yield using the method outlined in protocol 3.7.2.2 and then aliquoted into 100μl samples. Other organ and tissue samples were dissected from six mice and the protein extracted following protocol 3.7.2.1. In all protein experiments purified BSA of a known concentration (10mg/mL) was used as a control to compare unknown protein concentrations and sizes. In all antibody experiments β-actin antibody (GeneTex) was used to validate the immunodetection protocol and validate protein presence at detectable concentration. Protein quality and concentration was measured in two ways, Bradford assay which was analysed visually and with a fluorescence plate reader, and by SDS-PAGE.

#### 4.6.1 Bradford Assay

Bradford assay was used to estimate the concentration of tissue lysate proteins extracted from the mouse following protocol 3.7.

Table 16 shows the estimated protein concentrations of some of the proteins extracted from the mouse using the Bradford assay using a quick visual display. For a more accurate determination, a fluorescence plate reader (BMG LABTECH FLUOstar OPTIMA) was used (Table 16). The standards did not produce reliable readings on the fluorescent plate reader nor did they agree with the duplicate standards carried out. A visual reading of the fluorescent plate (not shown) was

used to roughly group proteins into high, medium and low concentrations and nothing where no visible colour change was seen.

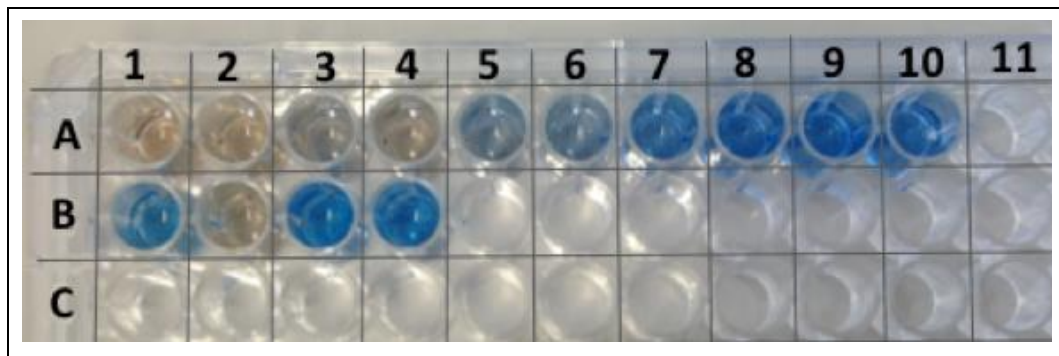


**Figure 45: Bradford assay showing relative concentrations of proteins. Row A (1-10) shows BSA standards of concentrations 0, 0, 0.1, 0.25, 0.5, 1, 2, 4, 6 and 10mg/mL respectively. Row B shows four samples adrenal gland, gall bladder, liver and kidney respectively.**

**Table 16: Bradford assay results.** Table shows the results for three Bradford assays carried out on tissue lysates from P28+ female mouse. all three assays were assessed visually. Assay 3 was also analysed on a fluorescent plate reader (BMG LABTECH FLUOstar OPTIMA). Table shows relative concentrations of proteins from each sample compared to the BSA controls.

	Sample	Bradford Assay 1	Bradford Assay 2	Bradford Assay 3		
		Visual display	Visual display	Fluorescent plate reader		Visual display
<b>BSA standards (mg/ml)</b>	0.00	Nothing	Nothing	0.000	0.000	Nothing
	0.10	Nothing	Nothing	0.045	-0.001	Nothing
	0.25	Low	Low	-0.003	0.058	Low
	0.50	Low	Low	-0.020	0.000	Low
	1.00	Medium	Medium	0.001	0.003	Medium
	2.00	Medium	Medium	0.008	0.027	Medium
	4.00	High	High	0.044	0.067	High
	6.00	High	High	0.077	0.168	High
	10.00	High	High	-	-	-
<b>Mouse tissue lysates</b>	Adrenal gland	Low	Medium	0.017		Low
	Bladder		High			
	Brain	High	High	-		-
	Ear 1	Medium		0.016		Medium
	Ear 2	Medium		0.025		Medium
	Ear 3	Medium		0.004		Medium
	Eye	High		0.185		High
	Gall bladder	Low	Low	0.000		Nothing
	Heart	High	High	0.128		High
	Kidney	High	High	-		-
	Liver	High		0.192		High
	Lung	High	High	0.044		High
	Lymph node	Low		0.010		Low
	Ovaries		High			
	Pancreas	Medium		0.256		Medium
	Reproductive system (female)	High		0.051		High
	Spleen	High		0.088		High
	Stomach		High			
	Tear	Medium		0.044		Medium
Thymus	Low		0.085		Low	
Tongue	Low	Medium	0.090		Nothing	
Uterus		Medium				

## 4.6.2 SDS-PAGE

SDS-PAGE was used to visually assess the concentration and quality of protein samples for subsequent western blotting procedures.

All SDS-PAGE gels were carried out with 5µl of Precision plus Protein™ Dual Color Standards (BIORAD) to estimate the size of the proteins and a 10mg/mL BSA standard mixed with SDS loading dye at a ratio of 1:10. Electrophoresis was initially carried out at 10mA for 15min then followed by 30mA until the dye front reached 1cm above the bottom of the gel as per protocol 3.5.

Due to the highly variable results shown with the Bradford assay the proteins were left undiluted prior to being mixed with loading dye and analysed on an SDS-PAGE gel (Figure 46). The results from this gel and the rough groups allocated by the visual Bradford assay were used to dilute the proteins for the subsequent SDS-PAGE gels.

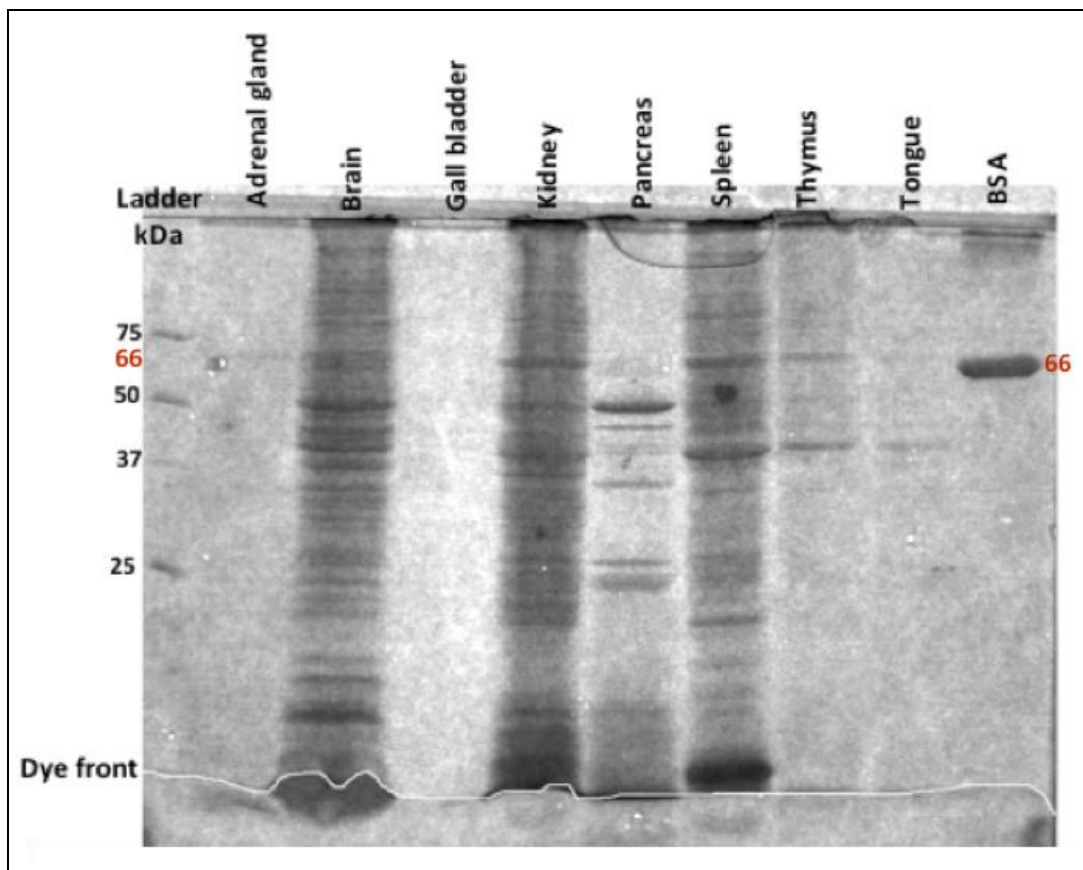


**Figure 46:** 12% 0.75mm thick hand-cast SDS-PAGE gel with a 5% stacking gel showing electrophoresis of 8 undiluted protein lysates. Gel was electrophoresed in 1X SDS running buffer for 15min at 10mA stacking and at 30mA resolving until dye front was 1cm from the bottom of the gel. All samples were loaded with equal volumes of SDS loading dye excluding Tongue and Gall bladder which were loaded at a 4:1 ratio.

Proteins assessed as being high in concentration were diluted in equal volumes of protein lysis buffer before being mixed with loading buffer. Medium and low



concentration proteins were left undiluted. Protein lysates and SDS loading dye were mixed together according to the ratios outlined in Figure 47 and Figure 48 (loading dye:protein lysate) and 20µl loaded onto two 10% Mini-PROTEAN® TGX™ Precast gels (BIORAD). Gels were electrophoresed together in a Mini-PROTEAN® Tetra Vertical Electrophoresis Cell (BIORAD) and then visualised in the Gel Doc™ EZ System on a stain free sample tray using Image Lab™ Software (BIORAD).

Figure 47 shows protein lysates from the pancreas, heart, eye, liver, thymus, tongue and spleen with good separation of proteins between 15-25kDa. All tissues except the liver are of approximately equal concentrations and of good quality with visible bands of varying sizes. BSA standards show very low levels of contamination around 150kDa and below 15kDa in size. The most intense band in the BSA lane occurs between 75-50kDa, which fits with the expected band size of 66kDa for the BSA protein.

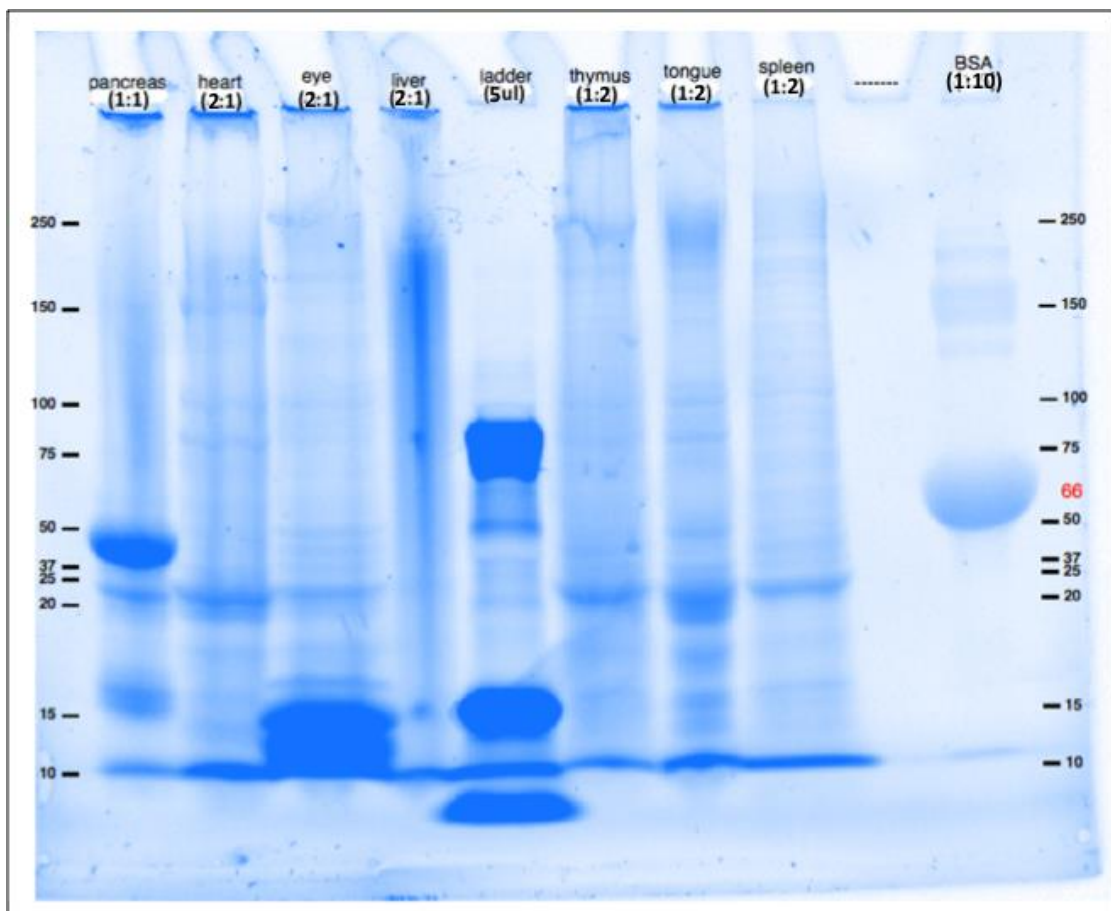


**Figure 47: 10% 1mm thick precast SDS-PAGE gel (BIORAD) showing electrophoresis of mouse protein lysate sample and the ratios at which they were loaded with SDS loading dye. Proteins were denatured at 99°C for 3min prior to loading. Red labelled BSA loaded at a concentration of 10mg/mL produce a band of expected size (66kDa).**

The SDS-PAGE gel in Figure 48 contained the three aliquots of ear proteins extracted from 8 ear samples from four mice that were pooled together. The first collected aliquot (ear1) was collected by homogenising all of the bony inner ears collected in less than 3mL of protein lysis buffer. The supernatant and fine bone fragments from this were collected and set aside on ice. The second aliquot (ear2) was collected by removing bone fragments from the teeth of the homogenising wand and rinsing with 1mL of protein lysis buffer before repeating homogenisation of the larger bony fragments left from the first sample. The supernatant and fine bone fragments were again collected and set aside on ice. The third sample (ear3) was a 700µl final rinse of the wand. Bone fragments were removed from teeth of the wand and homogenised a final time before the wand was disassembled and all bone fragments and supernatant scraped carefully together and collected. The three samples were centrifuged for 10sec at maximum speed to pellet the larger fragments before being aliquoted in 100µl samples. The SDS-PAGE results reflect the relative concentrations of these three aliquots with the first (ear1) being the most concentrated and the second and third samples less concentrated. The other lanes contain tissue lysate from the lymph node and gall bladder mixed together, the adrenal gland, lung, tear gland, and the reproductive system of female mouse. The BSA standard again shows very low levels of contamination around 150kDa and below 15kDa in size. The most intense band in the BSA lane occurs between 75 and 50kDa, which fits with the expected band size of 66kDa for the BSA protein. The tear sample shows contamination from the reproductive tissue sample and the gall bladder and lymph node mix sample. Aside from this, samples show roughly even loading samples of good quality proteins ranging in size from 15-250kDa.



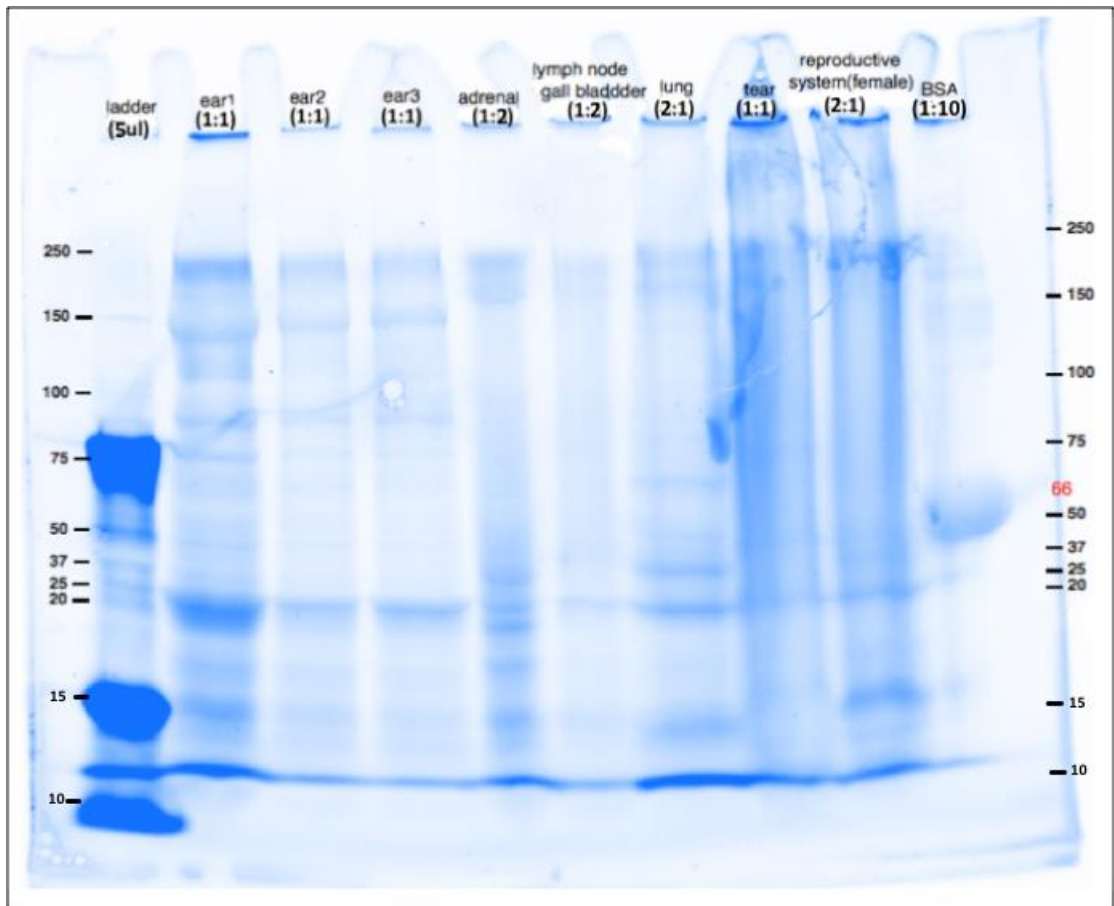


**Figure 48:** 10% 1mm thick precast SDS-PAGE gel (BIORAD) showing electrophoresis of mouse protein lysate sample and the ratios at which they were loaded with SDS loading dye. Proteins were denatured at 99°C for 3min prior to loading. Red labelled BSA loaded at a concentration of 10mg/mL produce a band of expected size (66kDa).

## 4.7 Western Blotting

Western blotting was used to detect the VMO1 protein within tissue lysates and to validate the two VMO1 antibodies sourced from GeneTex and ProteinTech.

Denatured tissue protein lysates were separated by SDS-PAGE and then transferred to a PVDF membrane which was then probed using the VMO1 antibody. Following immunodetection the membrane was stripped of primary and secondary antibodies and reprobbed with the  $\beta$ -actin antibody as a control for protein loading and transfer.

### 4.7.1 Protein Transfer

Protein transfer from the SDS-PAGE gel to the PVDF membrane was assessed in four ways: (1) by using a prestained molecular weight ladder, (2) Ponceau staining of the PVDF membrane; (3) Coomassie blue staining of the SDS-PAGE gel after transfer; (4)  $\beta$ -actin immunodetection following immunodetection and stripping of the VMO1 antibody.

#### 4.7.1.1 Prestained Ladder Transfer

The prestained molecular weight ladder (Precision Plus Protein™ Dual Color Standards) was used to estimate molecular weight of proteins and as a primary indicator of successful transfer of the proteins to the PVDF membrane. Transfer of the ladder onto the membrane and away from the SDS-PAGE gel indicated successful movement of at least some of the proteins. In some cases the ladder was also shown in the Whatmans paper used in the blotting reaction indicating excessive transfer possibly past the PVDF membrane.

#### 4.7.1.2 Coomassie Blue Staining of Transferred SDS-PAGE

After horizontal electrophoresis of the SDS-PAGE to transfer the proteins to the PVDF membrane the SDS-PAGE gel was stained with Coomassie blue stain following protocol 3.5.3. Figure 49 shows the Coomassie blue staining of a SDS-PAGE gel after the proteins have been successfully transferred away from the gel. Blue banding shows the presence of large molecular weight proteins that were not transferred from the gel but good transfer of proteins in the resolving portion of the gel. The ladder has been completely transferred and is not present in the gel.

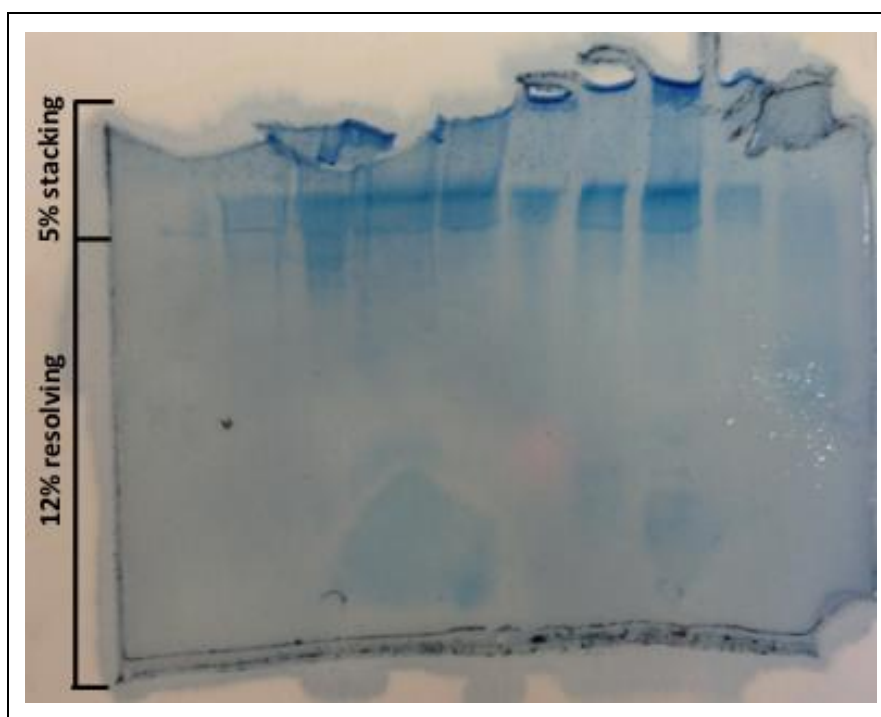


**Figure 49: Coomassie blue stained SDS-PAGE gel after blotting to PVDF membrane showing good transfer of the smaller molecular weight proteins between 10-150kDa in size and traces of large molecular weight proteins still remaining in the gel.**

#### 4.7.1.3 Ponceau Staining

Ponceau stain was used to assess the transfer of proteins from the SDS-PAGE gel to the PVDF membrane. Figure 50 shows a PVDF membrane stained with Ponceau stain with clear banding patterns indicating the successful transfers of proteins onto the PVDF membrane.

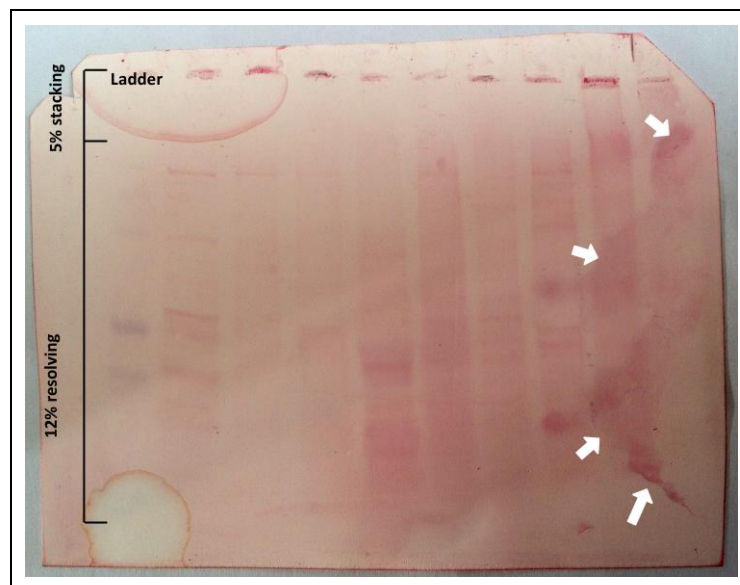


**Figure 50: PVDF membrane western blot stained with Ponceau stain showing good transfer of proteins from within the resolving gel. Stain was carried out after immunodetection and washing in TBS-T buffer which caused fading of the molecular weight ladder (labelled) which is only slightly visible in the Ponceau stain. Staining also shows possible exogenous contamination with proteins indicated with white arrows.**

#### 4.7.1.4 $\beta$ -actin Antibody Binding

$\beta$ -actin was used as a positive control for the western blotting method to determine if protein transfer to the PVDF membrane was successful and if proteins were present in high enough concentrations to be detected using antibody probing and chemiluminescence. Figure 51 shows the successful western blotting using protocol 3.9.2 of 8 mouse tissues, BSA and molecular weight ladder using two different antibodies (GeneTex), the  $\beta$ -actin antibody of expected size 42kDa and the surfactant protein A (SPA) antibody of expected 30-60kDa in size. This blot also showed the successful stripping of the  $\beta$ - actin antibody to reprobe with the SPA antibody.

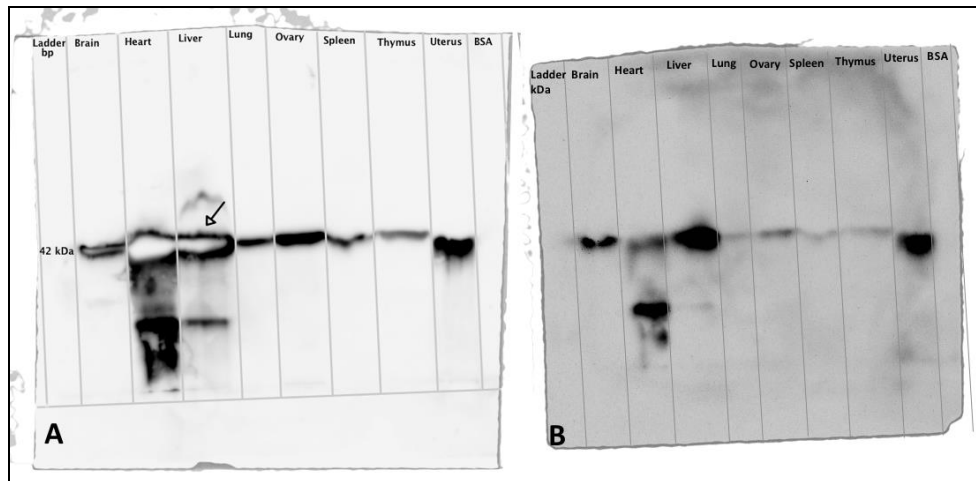


**Figure 51:** Western blot using the  $\beta$ -actin antibody and SPA antibody on 8 mouse tissues and BSA negative control at a concentration of 10mg/mL. (A) Shows the immunodetection of the control bands seen in all tissues at concentrations representative of the  $\beta$ -actin antibody showing expression in all tissues as expected with no binding occurring in the BSA control lane. The black arrow indicates a bubble in the gel which interfered with the running of the gel. (B) shows the same membrane which had been stripped using protocol 3.9.2.4 of  $\beta$ -actin antibody and re-probed with SPA antibody again showing expression in all tissues and no expression in BSA control of a slightly larger molecular weight.

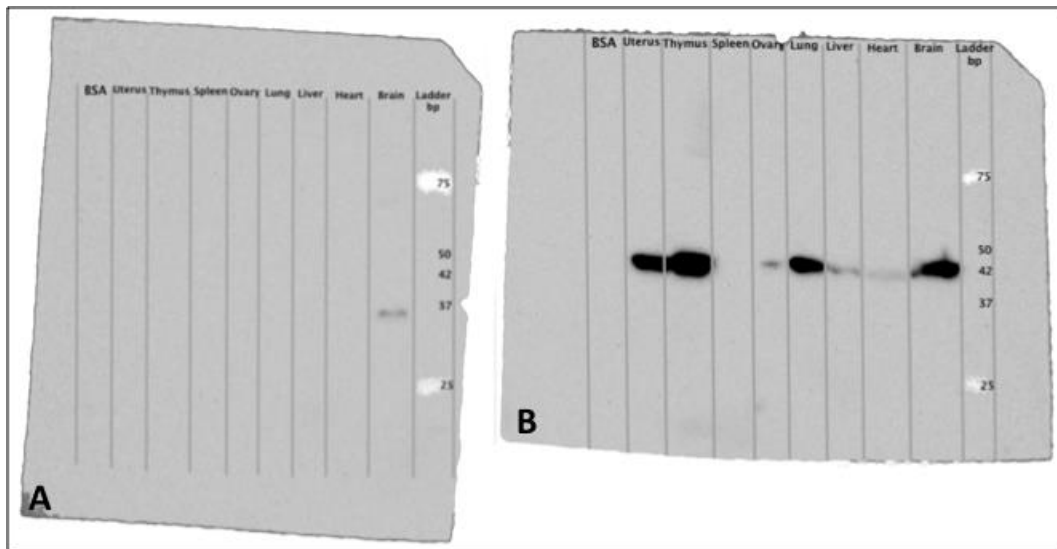
#### 4.7.2 Expression of the VMO1 Protein in Mouse Tissue Lysates

Antibody probing was carried out using two VMO1 antibodies, sourced from GeneTex and ProteinTech, to test for the presence of the VMO1 protein and with a  $\beta$ -actin antibody (GeneTex) as a positive control.

VMO1 antibody binding was carried out on western blot containing the three ear tissue samples and tear gland sample as well as the BSA control to show expression of the VMO1 protein and to validate the VMO1 antibody.

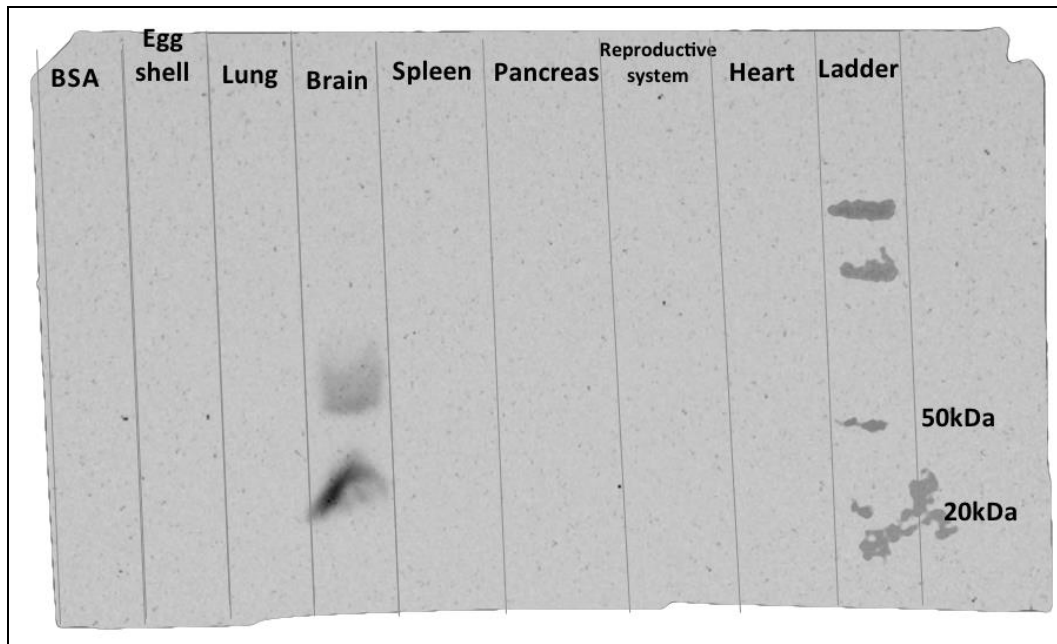
##### 4.7.2.1 ProteinTech Antibody

Figure 52 shows two 10% SDS-PAGE gel carried out simultaneously using 8 mouse tissue samples and successfully transferred to PVDF membranes. The membranes were then blocked and incubated with 1:1000 VMO1 antibody or 1:5000 of  $\beta$ -actin antibody. Figure 52a shows that the VMO1 antibody recognised a protein in the brain lysate between 25-37kDa with no binding to the negative control. Figure 52b shows recognition of the  $\beta$ -actin protein by the  $\beta$ -actin antibody at high concentrations in the uterus, thymus, lung and brain with low concentrations in the heart and ovaries and no binding occurring in the spleen or BSA control and demonstrates that protein transfer was successful and of detectable concentrations. The ear samples were not analysed due to the limited sample volumen and to test other tissues for VMO1 protein.



**Figure 52: Two western blots carried out simultaneously using protein from eight tissues from a P28+ mouse tissues, BSA control, and two different antibodies. Proteins were loaded onto a 10% hand-cast SDS-PAGE gel, transferred for 2 hours at 25V to a PVDF membrane in transfer buffer. Membranes were developed for 2min using ECL developing solution (Thermo Scientific). (A) VMO1 antibody binding in the brain tissue with no binding occurring for any other tissues or the BSA control. (B) positive control using the  $\beta$ -actin antibody with binding occurring at high concentrations in the uterus, thymus, lung and brain and at low concentrations in the heart liver and ovary with no binding occurring with the spleen and BSA control.**

Attempts were made to duplicate the results seen in Figure 53 with very little success. Figure 53 shows the presence of two bands between 20 and 50kDa in the brain and non-specific binding of the antibody to the molecular weight ladder. With no binding observed in the BSA control, chicken egg shell, mouse lung, spleen, pancreas, reproductive system or heart. The chicken egg shell was added as a negative control with no binding of the VMO1 antibody expected. A 12% SDS-PAGE gel and PVDF membrane were used and western blotting carried out as per protocol 3.9.2.



**Figure 53: Western blot carried out to duplicate results from Figure 53 using protein from eight tissues from a P28+ mouse and a BSA control. Protein samples were loaded onto a 10% hand-cast SDS-PAGE gel electrophoresed, at 15mA for 10 min followed by 30mA to separate and transferred for 2 hours at 25V to a PVDF membrane in transfer buffer. Membranes were developed for 2min using ECL developing solution (Thermo Scientific) showing VMO1 expression in brain tissue lysate indicated by bands of two different sizes**

Following these results, a fresh mouse was dissected and a western blot carried out using chicken egg vitelline membrane, mouse brain, kidney and lung tissue as well as a BSA control. Figure 54 shows the results of this blot with non-specific binding seen in the molecular weight ladder and VMO1 antibody binding to the chicken vitelline membrane as expected between 15-50kD A very faint signal in the brain was detected between 15-250kDa and 15-50kDa. The lung also shows binding at two different molecular weight sizes between 50-150kDa and 150-25kDa. This gel was stripped and reprobred with  $\beta$ -actin to yield good results (not shown) indicating even loading and transfer of proteins to the PVDF membrane with no binding occurring to the BSA control.

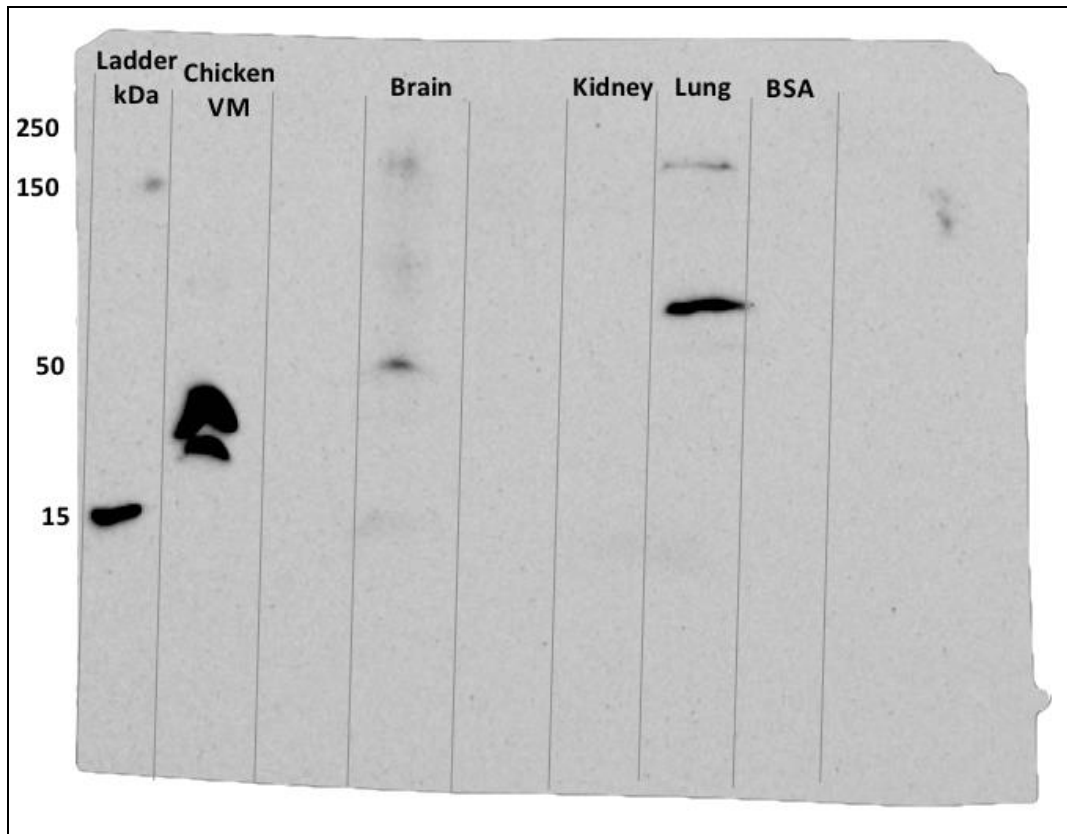


**Figure 54: Western blot using protein from three P28+ mouse tissues, BSA control and chicken vitelline membrane. Protein samples were loaded onto a 10% hand-cast SDS-PAGE gel, electrophoresed at 15mA for 10 min followed by 30mA to separate and transferred for 2 hours at 25V to a PVDF membrane in transfer buffer. The blot was incubated with VMO1. Membranes were developed for 2min using ECL developing solution (Thermo Scientific). The figure shows VMO1 antibody binding in the brain tissue at around 50kDa and the lung at 2 different sizes 50-150kDa and 150-250kDa. Vmo1 binding is also shown in the vitelline membrane of the chicken at two sizes between 10-50kDa with no binding occurring in the BSA control.**

The next experiment was designed to immunodetect VMO1 protein under the same western blot conditions as Figure 54 except using the female reproductive system, spleen, lung, tears, eyes and three ear samples with BSA as a control. Figure 55 shows this western blot with binding of the VMO1 antibody occurring on all of the tissue samples at multiple sizes and to the molecular weight ladder between 50-100kDa and at 15kDa. Most of the binding occurred between 50-250kDa with some binding occurring in the spleen and lung between 10-25kDa.

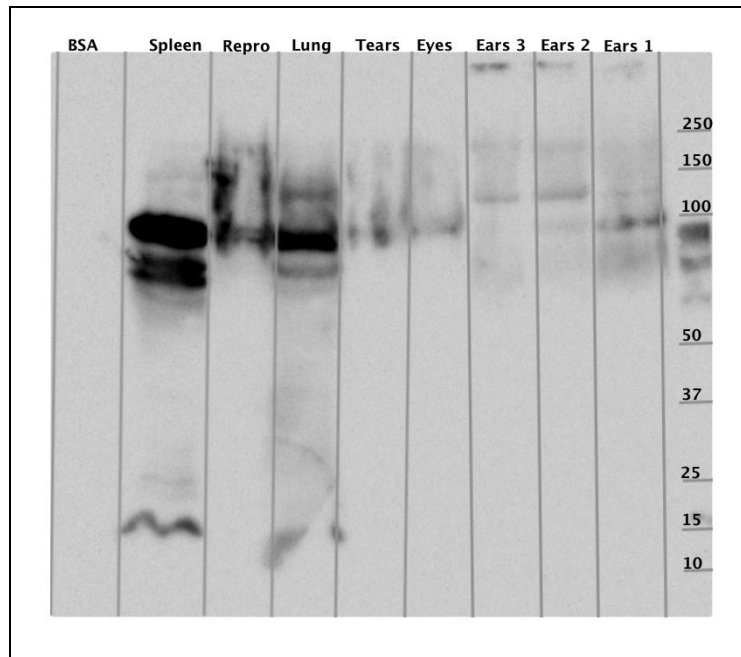


**Figure 55: Western Blot showing non-specific binding of VMO1 antibody to proteins from the mouse. Protein from six P28+ mouse tissues, BSA control including three inner ear samples of different concentrations were loaded onto 10% hand-cast SDS-PAGE gel, electrophoresed at 15mA for 10 min followed by 30mA to separate and transferred for 2 hours at 25V to a PVDF membrane in transfer buffer and probed with VMO1 antibody. Membranes were developed for 2min using ECL developing solution (Thermo Scientific). The figure shows VMO1 antibody binding in all tissues multiple times between 50-250kDa and binding to the spleen and lung between 10-25kDa no VMO1 binding is shown in the BSA control.**

#### **4.7.2.2 GeneTex antibody**

Figure 56 shows a western blot carried out with three ear tissue samples at two different concentrations showing bands of the expected 20-37kDa size. Intensity of bands suggests ear sample 1 is of higher concentration than ear sample 2 and 3. The band intensity also suggests the VMO1 protein is found in higher concentrations in the inner ear than in the tear glands. The duplicates of the ear samples and tear gland samples were diluted by half and have a corresponding decrease in band intensity indicating that the VMO1 antibody is binding specifically to the VMO1 protein and can be roughly quantified to show loading concentration. No binding of the VMO1 protein has occurred with the BSA standard or to the recombinant protein ladder.  $\beta$ -actin antibody control was not performed on this blot as it was damaged while washing and not retrievable.



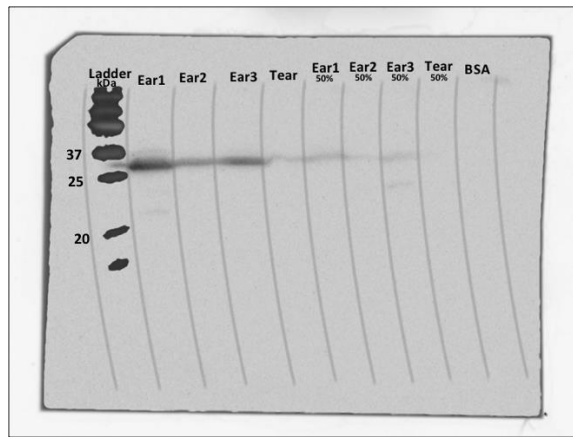


**Figure 56: VMO1 antibody western blot using ear and tear mouse proteins. Lanes 1 shows prestained precision plus ladder (BIORAD). Lane 3-5 contains 8 $\mu$ l of proteins loaded with 2 $\mu$ l of loading dye. Lanes 6-9 contain 4 $\mu$ l of protein with 5 $\mu$ l of loading dye. Relative intensity of chemiluminescence indicates that the signal is a real one. Ear samples 1-3 are each subsequently more dilute due to the way the homogenised protein was collected.**

Western blotting was carried out to duplicate results seen in Figure 56. Figure 57 shows a western blot carried out using protocol 3.9.2 and showing antibody binding to the inner ear samples at greater than 150kDa and single bands shown in the eye, tear gland and ear tissue samples around 37kDa 50-250kDa and no VMO1 binding is shown in the BSA control, adrenal gland or thymus.

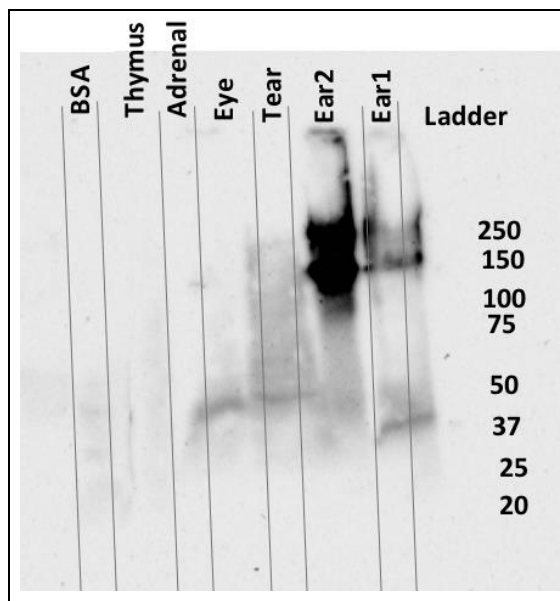


**Figure 57: Western blot carried out using protein from 4 P28+ mouse tissues BSA control including two inner ear samples of different concentrations indicated by the VMO1 antibody using a 10% hand-cast SDS-PAGE gel transferred for 2hr at 25V to a PVDF membrane in transfer buffer. Membranes were developed for 2min using ECL developing solution (Thermo Scientific). The figure shows VMO1 antibody binding in the inner ear samples at greater than 150kDa and a single band shown in the eye, tear gland and ear tissue samples between 37-50kDa and no VMO1 binding is shown in the BSA control adrenal gland or thymus.**

## 4.8 Immunohistochemistry

IHC is a process by which the principle of antibody to antigen binding is used to detect specific antigens (proteins) in a biological tissue sample. The secondary antibody in this thesis was conjugated with a fluorophore called Fluorescein which will emit a green light under wavelength of 490nm. IHC was carried out on P5 mouse heads embedded in OCT and sectioned on a cryostat (Leica) to localise the VMO1 protein within the inner ear with the VMO1 antibody supplied by GeneTex.

### 4.8.1 Mouse Section Integrity

P5 mice heads were dissected out and cryoembedded in preparation for sectioning on a cryostat as outlined in protocol 3.10.1. Sections were collected from the inner ear at a width of 10 $\mu$ m on slides coated in gelatin as outlined in 3.10.2. Slides were kept at -20°C prior to IHC staining to preserve the mouse tissue. H&E staining was carried out to determine the integrity of the sectioning and as a histological control to compare the structural anatomy of the mouse inner ear between sections with different IHC stains. Figure 58 shows a cochlea section from P5 mouse stained with H&E and shows good histology and preservation of the structural integrity of the cochlea and the membranes within it.

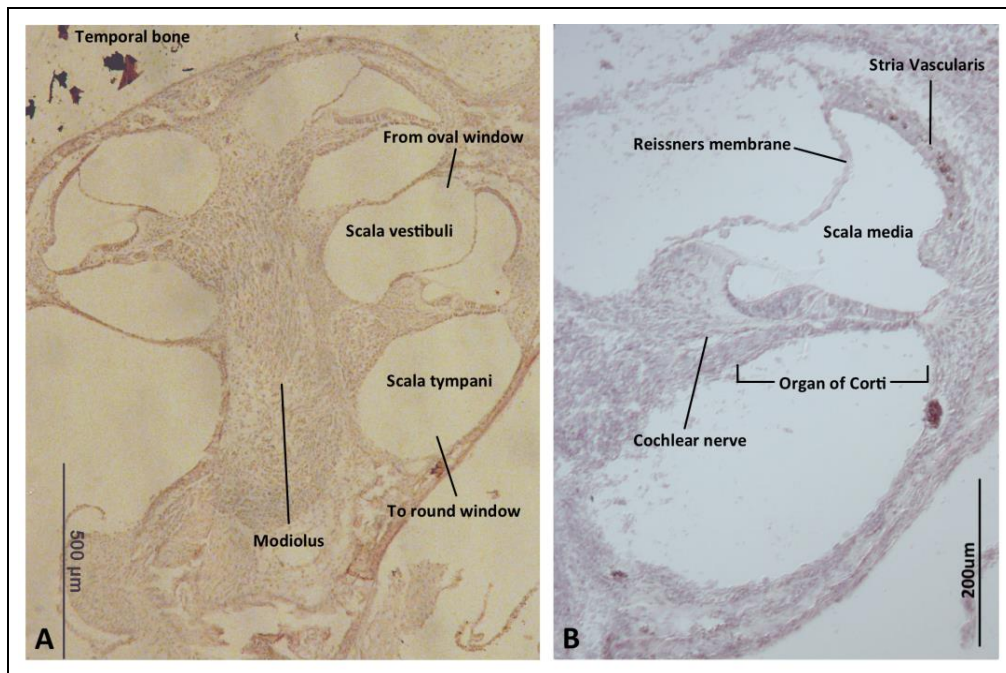


**Figure 58: H&E staining of the inner ear of P5 mice showing good structural integrity of the temporal bone, Reissner's membrane and tectorial membrane and an intact organ of Corti. (A) Shows the whole cochlea of the mouse with intact membranes and no shearing of bony tissue. (B) Shows a close up view of the cochlear duct showing an intact organ of Corti with easily definable cells and structures.**

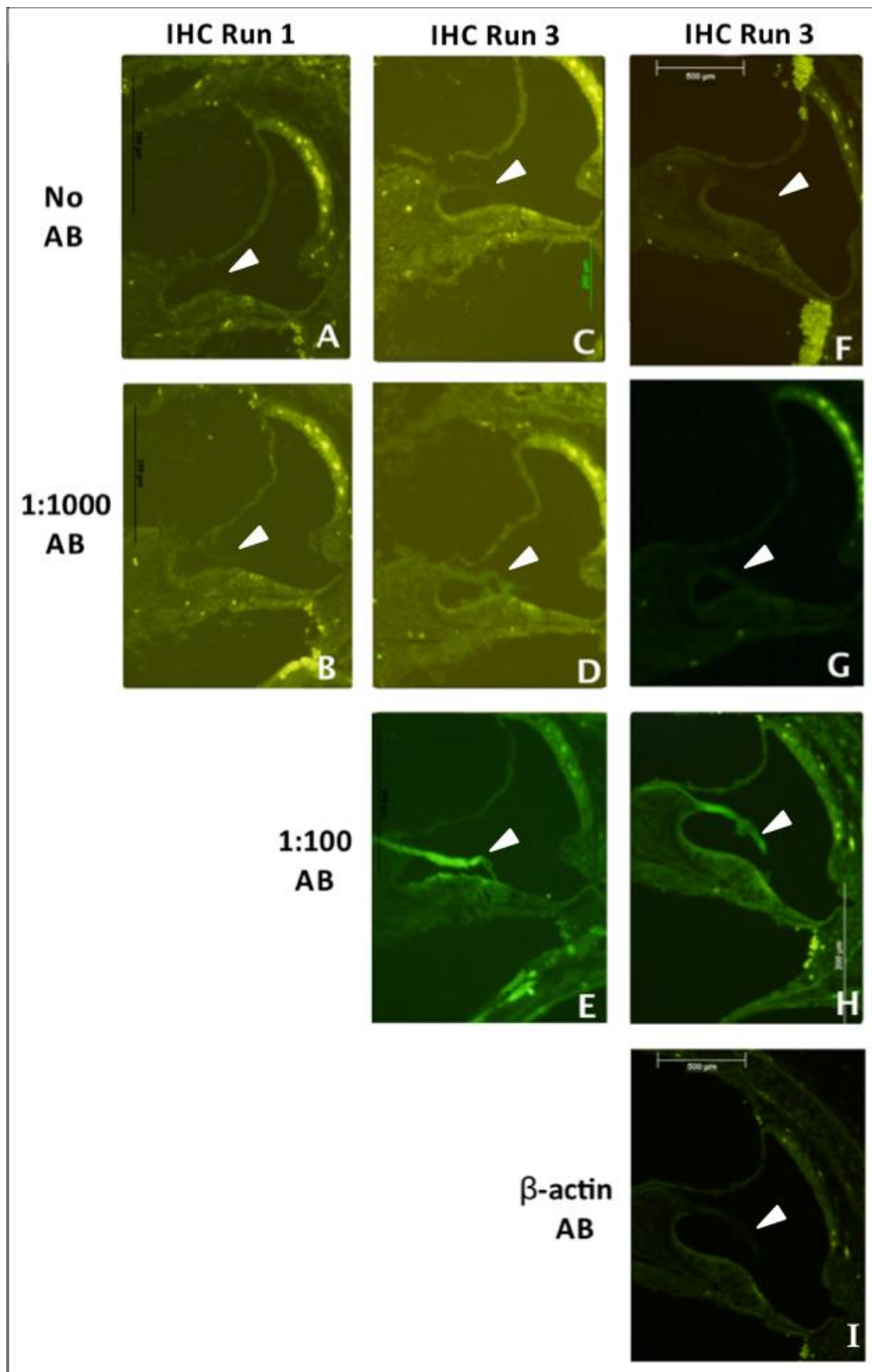
## 4.8.2 Antibody Binding

Immunohistochemistry (IHC) was carried out to determine the protein localisation of VMO1 in the cochlea of P5 mice.

Figure 59 shows a comparison between triplicate IHC carried out on sections of the cochlea. For all IHC carried out a negative control was included to be able to quantify background noise and eliminate the possibility of reading false positives. To do this the primary antibody was substituted with 1000 $\mu$ l of 1X PBS and IHC carried out as per protocol 3.10.4.2. Any fluorescence detected in a negative control can be attributed to non-specific binding of the primary and/or secondary antibody. For each subsequent run of IHC an extra washing step was added and blocking and washing times were increased. The effect of extra washing and blocking can be seen with the decrease in background noise and auto fluorescence for each subsequent run (Figure 59a, c and f). All three runs were also carried out using VMO1 primary antibody (AB) at a concentration of 1:1000 $\mu$ l (Figure 59a, d and g). The 1:1000 $\mu$ l antibody dilutions (Figure 59b, d and g) show very slight differences in fluorescence in the tectorial membrane when compared to the negative controls but do not give a conclusive result.

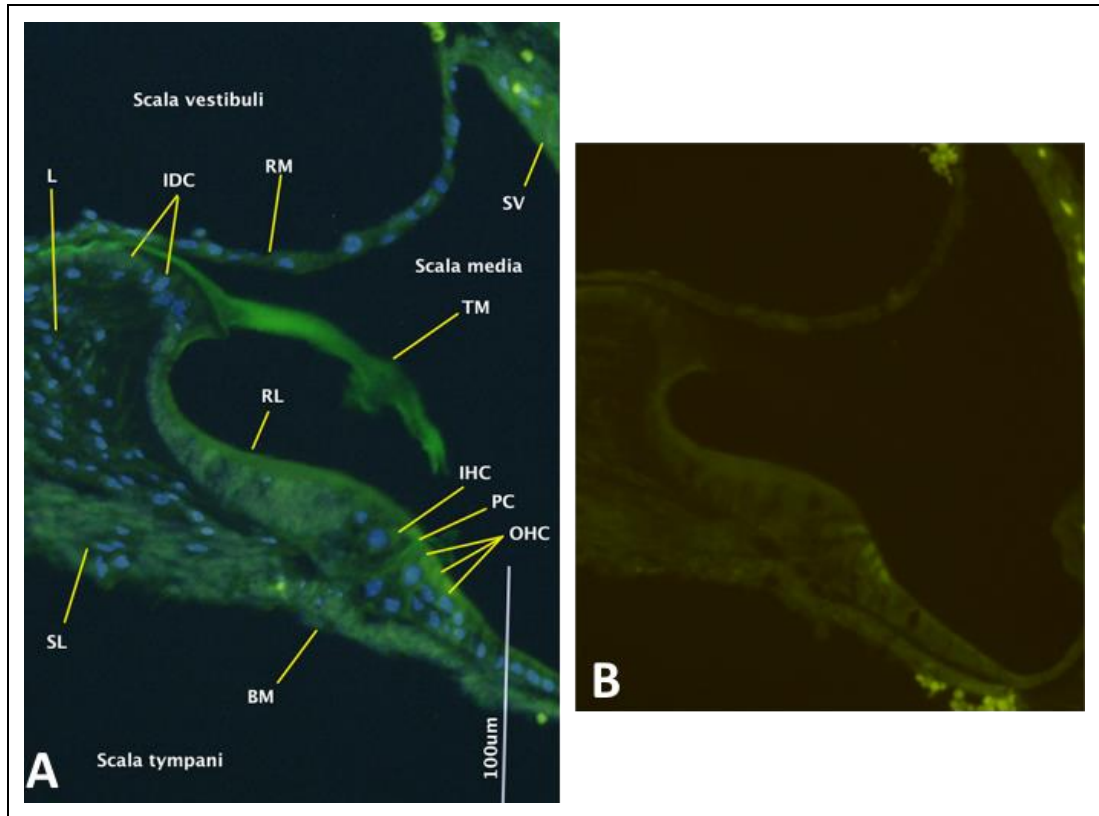
The second run of IHC was expanded to include a 1:100 $\mu$ l dilution (Figure 59e and h) of the VMO1 primary antibody. Both 1:100 $\mu$ l AB dilutions clearly show very brightly fluorescing tectorial membranes.

The third IHC run was expanded again to include a  $\beta$ -actin primary antibody at a concentration of 1:100 $\mu$ l to act as a positive control (Figure 59i) and shows ubiquitous expression of the  $\beta$ -actin protein within the inner ear with a very slight increase in fluorescence in the stria vascularis.



**Figure 59:** Results from three duplicated IHC reactions carried out on sections of P5 mouse inner ears. Each subsequent run was performed with additional washing steps and increased washing times. Blocking time was increased to reduce non-specific binding. White arrows show the position of the tectorial membrane (TM). (A,C,F) show negative controls with no primary antibody and show a decrease in background noise due to the extra washing steps introduced with each subsequent run. (B, D, G) show results from incubation in VMO1 primary antibody showing very slight fluorescence in the TM. (E,H) shows the addition of a 1:100 concentration of the VMO1 antibody and shows a corresponding increase in observed fluorescence in the TM indicating the VMO1 is located at high concentration in the TM. (I) shows the addition of the  $\beta$ -actin primary antibody control

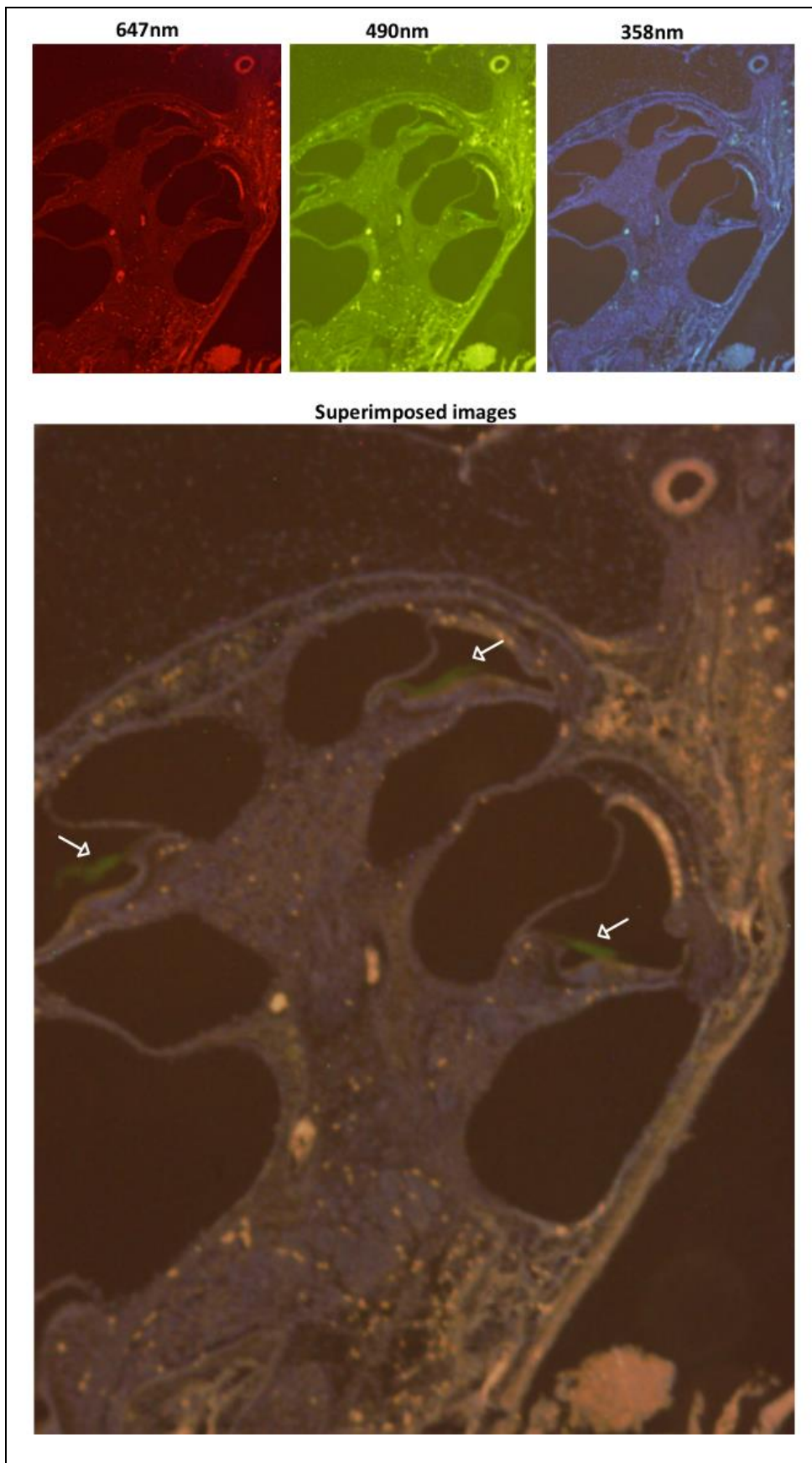
Figure 60A shows a superimposed image of the excitation of the DAPI nuclei stain at 358nm and the VMO1 antibody at 490nm. This indicates the VMO1 protein is a secreted protein found in high concentrations in the TM. Figure 60B is a negative control with no VMO1 primary antibody and indicates the fluorescence seen in the TM is real.



**Figure 60: comparison between 1:100µl antibody and no antibody. (A) depicts DAPI fluorescence overlaying the VMO1 antibody at 1:100µl dilution. DAPI fluorescence was used to show the position of individual cell nuclei. Depicted are the inner hair cells (IHC) the pillar cells (PC) outer hair cells (OHC) basilar membrane (BM) spiral lamina (SL) reticular lamina (RL) tectorial membrane (TM) interdental cells (IDC) stria vascularis (SV) Reissner's membrane (RM) spiral limbus (L). In green is the excitation of the VMO1 antibody at 490nm showing high concentration in the TM. (B) depicts negative control with no primary antibody.**

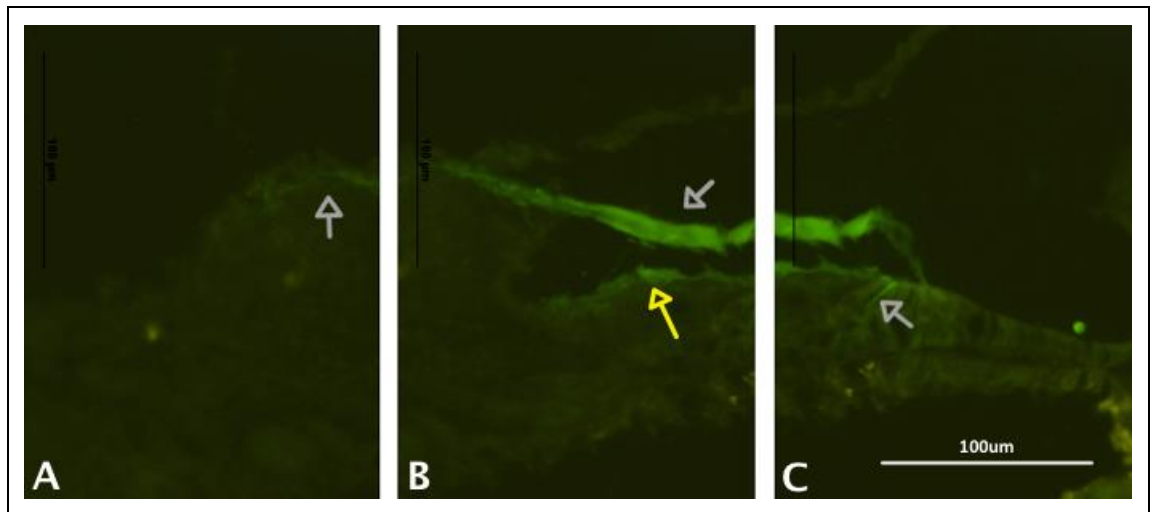
Figure 61 shows the whole cochlea viewed under three different wavelengths of light to show background (647nm), the excitation of the VMO1 antibody (490nm) and the excitation of the DAPI stain (358nm). Depicted below this is a superimposed image of the three different views showing high levels of excitation in the TM indicated by the white arrows.





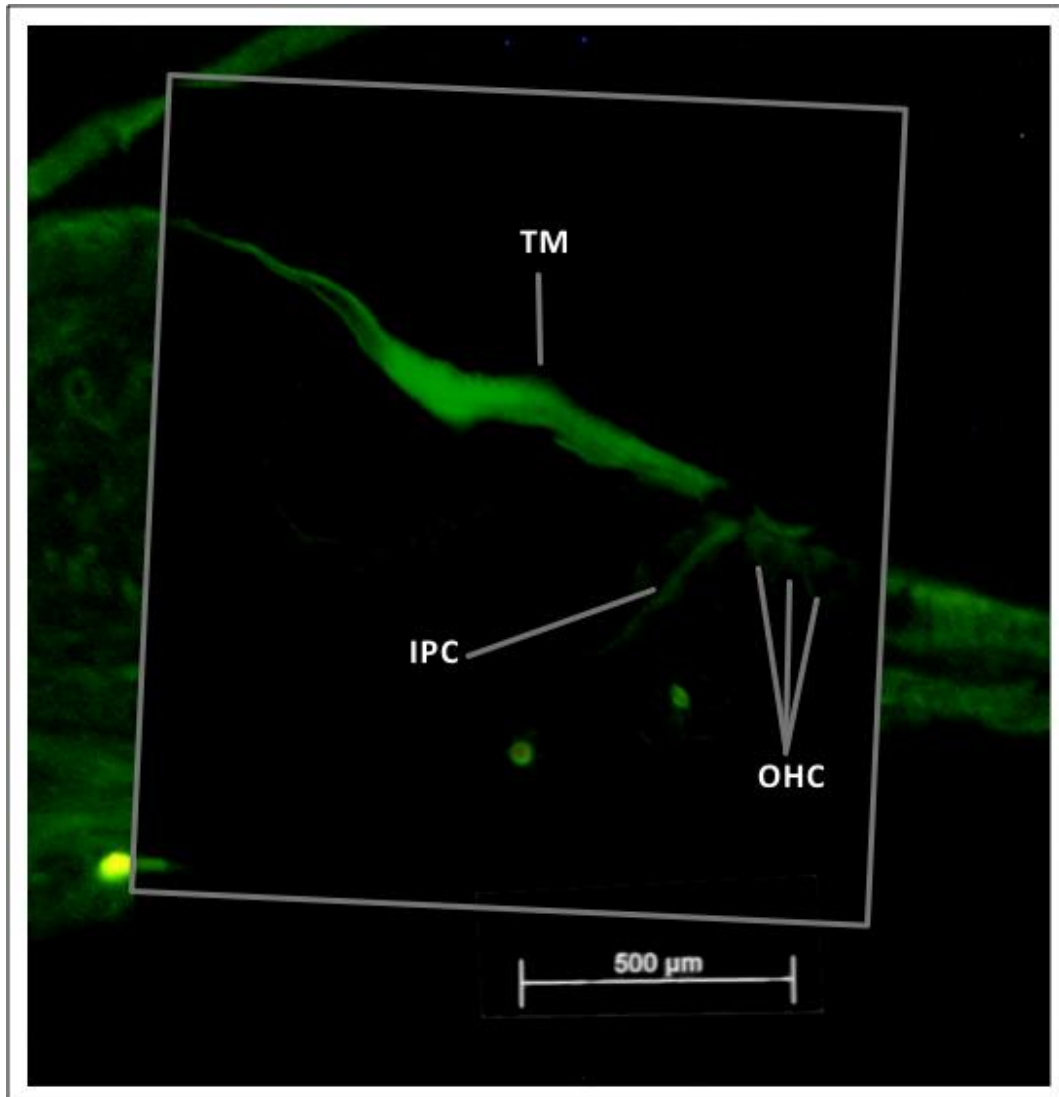
**Figure 61:** the whole cochlea viewed under different wavelengths of light and then superimposed upon each other to show expression of the VMO1 antibody at high concentrations in the TM as indicated by white arrows.

Figure 62 shows the organ of Corti with a 1:100 VMO1 primary antibody concentration. Figure 62a shows where the tectorial membrane is anchored in the vestibular lip of the spiral limbus below the RM where it is made by the interdental cells. Figure 62b shows the tectorial membrane stretching over the organ of Corti indicated by a white arrow. The yellow arrow shows fluorescence which is either specific to the reticular lamina or an artefact caused by tectorial membrane shearing during sectioning. Figure 62c shows fluorescence of the inner pillar cells, which lie between the outer hair cells and the inner hair cells indicated by the white arrow.



**Figure 62: 20X zoom of the organ of Corti showing scale bar of 100µm. White arrows show fluorescence detected where binding of the VMO1 antibody has occurred (A) shows the anchoring of the TM between the interdental cells and the Reissner's membrane. (B) Shows the high concentration of VMO1 present in the TM with possible VMO1 expression seen on the reticular lamina indicated by yellow arrow. (C) shows fluorescence of the inner pillar cell.**

Figure 63 shows the negative superimposition of the negative control (no antibody) over the 1:100µl VMO1 antibody to show the expression of the VMO1 antibody exclusively in the TM and the pillar cells of the organ of Corti.



**Figure 63:** 1:100 VMO1 antibody with 0:1000 antibody control fluorescence removed (within grey box) with Pixelmator™ programme. This figure shows the localisation of the VMO1 protein throughout the entire tectorial membrane and in the pillar cells of the organ of Corti. Fluorescence is also seen in the apical surface of the outer hair cells which could be real or due to the embedding of the outer hair cells in the tectorial membrane.



# CHAPTER FIVE

## DISCUSSION

The aim of this project was to characterise the possible function of the *Vmo1* gene and investigate the protein expression of VMO1 at different developmental time points in the mouse auditory system. To investigate possible functions of *Vmo1*, comparative genomics analysis was conducted. To determine protein expression IHC was used.

### 5.1 Comparative Genomics and a Suitable Animal Model for Studying *VMO1*

RefSeq sequences were downloaded from NCBI and used for comparative genomics analysis. Results showed that *VMO1* gene has three exons that are conserved across the 17 species analysed. The mouse (*Mus musculus*) was shown to have one 672bp transcript that translated to a protein 201aa long with a predicted molecular weight of 22kDa. The human (*Homo sapiens*) was shown to have four transcript variants produced by alternative splicing. Variant one produced a characteristic 202aa VMO1 protein, which also had a predicted molecular weight of 22kDa.

The general structure of the inner ear in all vertebrates is comparable with slight variations seen between avian and mammalian species (Magariños et al., 2012). The chicken inner ear has been shown to have a straight cochlear and to be capable of regeneration of hair cells in the ear, unlike the mouse and human which have a coiled spiral shaped cochlea and are unable to regenerate hair cells once they are damaged or lost (Bissonnette and Fekete, 1996).

Comparative genomics analysis demonstrated a distant taxonomic relationship between the chicken and mammalian species. The mouse and human *VMO1* genes showed a high level of nucleotide sequence identity with increased homology seen in the protein sequences with 71.8% identity and 80.2% amino acid similarity. In comparison, the mouse and chicken *VMO1* protein showed 47.1% identity and 60.3% similarity. However, analysis of the *VMO1* protein for the mouse, human and chicken showed a high level of identity shared in the amino

acids responsible for the formation and stabilisation of the chicken VMO1 3D structure. All eight Cys residues that form the disulfide bonds found in the chicken were found in identical positions in the mouse and human (Figure 31). In addition the overall threefold symmetry was preserved with a high level of similarity, if not identity, observed across the amino acids deemed to be involved in structure stabilisation or enzymatic function in the chicken protein such as the  $\beta$ -sheets forming the Greek key motif and the putative carbohydrate-binding sites (Figure 24).

Comparisons showed a high level of homology between the human, chimpanzee (*Pan troglodytes*) and western lowland gorilla (*Gorilla gorilla gorilla*). Both the gorilla and chimpanzee were predicted to produce the same four splice variants as seen in the human, with the chimpanzee and gorilla sharing 96.6% and 95.6% protein identity respectively. The presence of the four alternate splice variants indicates a very high level of homology and therefore a conservation of function and structure making either of these species the most suitable animal models to study the role of human VMO1 in the auditory system. However, the ethics, cost and availability of using these animals in New Zealand makes the use of them as models inhibitive.

The homology seen in the VMO1 amino acid sequence and the H&E staining of the mouse ear demonstrated high similarity with the human ear indicating the mouse is an appropriate model for the role of human VMO1 in the auditory system. Another option would be the rat (*Rattus norvegicus*) which shares nearly complete gene identity and structural anatomy with the mouse. Furthermore, the size of the ear is larger for easier manipulation. This would also yield higher concentrations of proteins and mRNA transcripts.

## **5.2 Amplification and Sequencing of the *Vmo1* Gene**

In order to characterise the mouse *Vmo1* gene and validate the VMO1 antibody, the *Vmo1* mRNA transcript was isolated, amplified, DNA sequenced and cloned to produce recombinant protein. To achieve this, a variety of molecular biology techniques were used and the results will be discussed in this chapter. Firstly, RNA was extracted from mouse inner ears.

### 5.2.1 RNA Isolation

Efficient isolation of high yield and intact RNA from mammalian tissue is essential for full-length, high-quality cDNA synthesis. However, total RNA extraction from the inner ear of the mouse is recognised as problematic due to the short half-life of RNA transcripts (minutes to days), the small size of the inner ear and the scarcity of the targeted mRNA transcripts (Invitrogen). Ribonuclease (RNase) is a nuclease enzyme that acts to degrade RNA into smaller fragments and is found in large quantities in all organisms and is responsible for the relatively short half-life of RNA (Campbell and Reece, 2005)

To address these three issues, six inner ear samples from three P28+ mice were pooled together to increase the likelihood of target mRNA being present and to increase the RNA concentration. In general, mRNA only makes up 1-2% of total RNA (Campbell and Reece, 2005). P28+ mice were chosen because development of the inner ear is complete, the availability of mice of this age and the ease of dissection due to its size. Studies have shown that the structure of the ear is constant from P3 throughout adulthood (Zine and Romand, 1996).

When working with RNA it is important to maintain an RNase-free environment to prevent contamination of the RNA samples with exogenous RNase enzyme. Firstly, this was attained by wearing gloves and a laboratory coat, and working in dedicated RNA workspace in the Laboratory of Molecular Genetics. Secondly, workspaces and equipment were cleaned and wiped using RNase Away™. Also, glassware was cleaned and sterilised by soaking in detergent and baked at 200°C before use. Solutions were made with sterile DEPC mQH<sub>2</sub>O and autoclaved at 121°C for 20min before use. Disposable sterile RNase-free tubes, pipette tips and containers were used where possible. Finally, mice were euthanised and the ears removed quickly by dissection and stored in RNase-free extraction buffer at -80°C until homogenisation.

Homogenisation was used to disrupt the bony ear tissue and releases the cell's RNA from its intracellular compartment. A minimal amount of RNase extraction buffer was used in order to increase the RNA concentration. To reduce damage caused by heating, the sample was homogenised for 10 second intervals in between which it was stored on ice. While the sample was cooling, bony

fragments were removed from the teeth of the wand and added to the sample. The sample was homogenised until all bones had been broken up to a thin slurry. This sample was aliquoted into three samples and RNA isolation carried out according to protocol 3.7.1.2. The three RNA samples were analysed on a Nanodrop and the  $A_{260/280}$  reading suggested they were free of chemical contaminants such as GITC, phenol and Trizol, and were of high nucleic acid concentration and purity. A total of 21,912µg of total RNA was isolated from six inner ears dissected from three mouse specimens.

To preserve the volume of the total RNA required for cDNA synthesis, samples were not analysed on an agarose gel. If they were analysed on a denaturing agarose gel, we could conclude that the RNA was intact if two ribosomal bands (28S and 18S) were observed with no evidence of a smear.

### **5.2.2 cDNA Synthesis**

To synthesis cDNA, inner ear total RNA from pooled mice was reverse transcribed using the enzyme reverse transcriptase Oligo-dT primers which annealed to 3' poly-A tail of mRNA transcripts. Oligo-dT primer was chosen over random hexamer primers to increase the percentage of *Vmo1* mRNA within the cDNA. The random hexamer primers would have bound to all RNA samples to produce cDNA for all RNA of which only 1-2% would be mRNA with *Vmo1* only a small fraction of this (Invitrogen).

The integrity of the cDNA synthesised was examined by running a small aliquot onto an agarose gel, and as a PCR template for amplification using primers that were designed to target and anneal to *Vmo1*. The first-strand cDNA synthesis was analysed on a 2% agarose gel and showed a high concentration of cDNA indicated by a bright characteristic smear between 100-700bp in length. The manufacturer states that RNA targets ranging from 100 bp to greater than 12 kb can be detected using this enzyme (Invitrogen).

Two samples of cDNA (cDNA1 and cDNA2, respectively) were amplified by PCR using mouse specific *GAPDH* primers to confirm the synthesis of cDNA. As expected, a transcript of 150bp in size was amplified. However, amplification of

the negative control that contained no reverse transcriptase amplified a product (150bp) as a result of cDNA synthesis from using RNA aliquot 1 as a template. This band is a result of amplification from genomic DNA and indicated contamination of RNA aliquot 1 with genomic DNA. cDNA2 produced from RNA aliquot 2 was shown to be free of genomic contamination due to the observation of a single band at the expected size with no band seen in the negative control (Figure 39).

To overcome genomic DNA contamination, the RNA aliquot 1 sample could have been incubated with DNase to degrade DNA or alternatively, PCR primers could have been designed to anneal to the exon-exon boundary of the gene of interest. For the purposes of this thesis a full length *Vmo1* transcript amplicon was needed for cloning and expression so RNA aliquot 1 was stored at -80°C and RNA aliquot 2 was used instead.

### **5.2.3 Optimisation of *Vmo1* DNA Amplification from cDNA Template**

Since only a few copies of DNA are required for amplification, all PCR reactions were setup in a dedicated PCR workspace with a UV light, to degrade potentially contaminating DNA, and that had equipment available such as PCR-dedicated pipettors and sterile pipette tips. Wearing gloves and using sterile consumables prevented contamination with genomic DNA and enzymes.

The PCR conditions were based on the recommendations by the manufacturer of the *Taq* DNA Polymerase (Solis Biodyne) and the melting temperatures recommended by the oligonucleotide supplier IDT. Optimisation of PCR using *Vmo1* primers and mouse ear cDNA involves a number of parameter such as primer design, constituents of the PCR buffer, magnesium concentration and annealing temperature of primers. In the next section, these will be discussed in more detail.

#### **5.2.3.1 Primer Design**

Two primers sets were designed for the purposes of this thesis. Primer set BFG27/28 was designed to cover the entire 606bp of the ORF of the *Vmo1* mouse transcript and to incorporate the HindIII restriction enzyme sites outside of the

ORF for the purposes of insertion into a vector for the purposes of cloning and expression. Because this primer set was not specific to cDNA and would amplify genomic DNA, primer set BFG7/8 was designed to be specific to *Vmo1* cDNA only and spanned the two exon junctions to produce an amplicon 193bp in length (Figure 41).

#### **5.2.3.2 Buffer**

PCR buffer was used at a final concentration of 1X and acts to mediate the reaction by keeping pH within optimal ranges for *Taq* DNA Polymerase. Initial PCR used a magnesium free and detergent free buffer (HOT FIREPol® 10x Buffer B1). For subsequent reactions, the B1 buffer was replaced with 1X HOT FIREPol® 10X Buffer B2 which was free of magnesium but contained Tris-HCl, ammonium sulphate and detergent. This reaction produced a clear single band of expected size (495bp) for *Vmo1* using primer set BFG1/2 (Figure 41).

#### **5.2.3.3 Magnesium Concentration**

Magnesium ( $Mg^{2+}$ ) is required for PCR due to the  $Mg^{2+}$  dependent nature of *Taq* DNA polymerase. The amount of free  $Mg^{2+}$  available in the reaction can be affected by template concentration, dNTPs, proteins and chelating agents such as EDTA. Low  $Mg^{2+}$  concentrations will affect the enzymatic activity of the *Taq* DNA polymerase and reduce amplicon yield. Excessive  $Mg^{2+}$  can result in non specific binding of primers and inhibit denaturation of the double stranded DNA and therefore reduce amplicon yield (Peterson, 1988). With PCR reactions carried out using B2 buffer and primer sets BFG1/2 and BFG27/28,  $Mg^{2+}$  concentrations were increased from 1.5mM to 2.5mM. This resulted in the observation of increased band intensity for the amplicons produced on the agarose gel (Figure 40).

#### **5.2.3.4 Annealing Temperature**

The annealing temperature required for optimal amplification depends on the length and composition of the primers used. In general, the annealing temperature is 5°C below the lowest melting temperature of the primer set (table 13). With decreased annealing temperatures, the primer specificity is decreased which increases the chances of non-specific amplification but potentially increasing the yield of targeted amplicon. PCR was carried out with increasingly lower

annealing temperatures in an attempt to increase the yield of *Vmo1* amplicon using the primer set BFG27/28.

In conclusion, PCR reactions were carried out with 2.5mM MgCl<sub>2</sub> and 1X B2 buffer. Optimal annealing temperatures were obtained for primer sets BFG27/28 (50°C) and BFG1/2 (55°C). cDNA was amplified with primer set BFG27/28 to produce a 671bp *Vmo1* transcript that spanned the ORF of the VMO1 protein using nested PCR. Agarose gel electrophoresis showed a single sharp band which resembled the expected size. The remaining PCR sample was cleaned up using rAPid method as outlined in 3.2.3 and sent to the Waikato DNA Sequencing Facility at the University of Waikato.

#### **5.2.4 DNA Sequencing of *Vmo1* PCR Product**

Two DNA Sequencing reactions were carried out in both the forward and reverse direction to ensure complete coverage of both ends of the *Vmo1* amplicon. The forward and reverse sequencing chromatograms were manually checked for miscall and noise, and a pairwise alignment was carried out between each sequence and the NCBI reference mouse *Vmo1* mRNA (NM\_001013607.1) (Figure 43)

The forward sequence was 648bp long and covered the reference sequence from nucleotide 25 to 672 with 100% identity from base pair 45 to 672. The chromatogram showed good quality sequencing from 125 to 519 with very little baseline noise and evenly spaced peaks of single colours (Appendix 3, Figure 69). Nucleotides 45 to 125 were discarded as being of too poor quality with high levels of baseline noise and poor resolution. Nucleotides 25 to 45 contained 7 miscalls due to high baseline noise, heterozygous peaks and poor resolution. After nucleotide 519, the sample quality gradually became poorer due to increasing baseline noise and decreasing resolution. Therefore, sequencing data past nucleotide position 634 was discarded.

The reverse compliment of the reverse sequence was aligned with the reference sequence to check for sequence similarity and the chromatogram checked for quality. The chromatogram immediately showed low quality sequencing with uneven peak widths and sizes throughout the sequence and variable levels of

baseline noise (Appendix 3, Figure 70). Thirteen miscalls were detected by sequencing analysis software three of which were able to be manually recalled. The reverse sequence was 476bp long and covered the reference sequence from nucleotide 39 to 516 which made it inappropriate for use in resolving the 5' end of the forward sequence.

For the purposes of this thesis, the sequencing data was used to confirm the identity of the amplicon produced with primer set BFG27/28 and confirm complete coverage of the *Vmo1* ORF. In conclusion, the sequencing results show that the sequence of *Vmo1* was amplified and 100% identical to the reference sequence.

The next step was then to digest this amplicon using HindIII RE and clone into a vector for the induction of protein. The resulting expressed protein would be purified to be used as a sample to validate the VMO1 antibody.

### **5.3 Validation of the VMO1 Antibody for IHC**

Immunohistochemistry (IHC) was performed to localise VMO1 protein expression in the mouse inner ear. Firstly, the VMO1 antibody was validated to ensure specific binding of the antibody to the VMO1 protein. This would give us confidence that the IHC results were real and not due to nonspecific binding of the antibody. To test the specificity of VMO1 antibody, protein lysates from a range of mouse tissues were used for western blot analysis. Western blotting involves the transfer of proteins that have been separated by gel electrophoresis onto a membrane, followed by immunological detection with the VMO1 specific primary antibodies and a secondary antibody, and finally, membrane development and imaging. Following visualisation of antibody binding, the membrane was stripped of antibody using the protocol outlined in 3.9.2.4 and reprobed with a  $\beta$ -actin antibody. The theoretical protein molecular weight size for VMO1 based on amino acid sequence data is approximately 22kDA.

#### **5.3.1 Preservation of Tissue Lysate Proteins**

Tissues were dissected from the mouse using clean, sterile equipment to prevent contamination with exogenous proteases. Following dissection, the tissue was quickly transferred to a tube containing ice-cold lysis buffer. The lysis buffer



contained phosphatase and protease inhibitors to prevent proteolytic digestion of the protein in the tissue. To further prevent proteolysis, samples were stored on ice after homogenisation and stored at -80C until required for SDS-PAGE. Prior to SDS-PAGE the samples were defrosted on ice before being denatured by heat and loaded onto the SDS-PAGE.

### **5.3.2 Confirmation of Protein Transfer from SDS-PAGE to PVDF Membrane**

For western blot analysis it is important that all the separated proteins from the SDS-PAGE gel have been completely transferred (blotted) onto the Polyvinylidene fluoride (PVDF) membrane. Four methods were used to confirm the complete transfer of proteins from the SDS-PAGE gel and onto the PVDF membrane. The first method involved using the Precision plus protein™ dual color standard available from BIORAD. This standard is a prestained ladder used to estimate protein sizes ranging from 10–250kDa. The ladder was transferred along with the proteins to the PVDF membrane and due to the colours incorporated into the standards was easily visible during electrophoresis without additional stains being required. This ladder was also used as a marker to orient the position of the bands seen with immunodetection. However, the use of TBS-T buffer in the antibody probing protocol caused the colour staining of the ladder to diminish so the volume of ladder used was increased from 5ul to 7ul and the membrane marked with pencil or notched when first removed from blotting apparatus to orient the position of the samples loaded.

The second method involved Coomassie blue staining of the SDS-PAGE gel after western blotting with successful transfers resulting in clear gels with no visible bands in the resolving part of the gel. Staining of the gel was carried out as the membrane was washed in preparation for antibody probing and results dictated whether antibody incubation was carried out.

The third method involved using  $\beta$ -actin antibody as a positive loading control to show successful transfer of the all mouse proteins from the SDS-PAGE gel to the PVDF membrane and to serve as an internal positive control to verify that all of the reagents were functioning as they should. Mouse  $\beta$ -actin protein has been confirmed to be present in most mouse tissue types (BioGPS) and was therefore,

an appropriate control for assessing transfer of proteins to the PVDF membrane with successful transfer resulting in clear sharp bands of the expected 42kDa size being visible with immunodetection.

Finally, the fourth method involved the Ponceau stain. Ponceau staining was carried out after immunodetection of antibodies was complete, or before if the Coomassie stain indicated no transfer, to check for protein transfer and concentration. Ponceau stain binds to all proteins and also showed any possible exogenous contamination of the membrane that could have occurred during or after the blotting protocol.

In conclusion, western blot results indicate the transfer of proteins from the 12% hand-cast 0.75mm thick SDS-PAGE gels to the PVDF membranes was complete with the ladder only visible on the membrane and no ladder present on the gel. Very little banding was seen on the Coomassie stained gel and where visible the bands were of very large molecular weight (>150kDa). Bright, sharp bands were detected for the  $\beta$ -actin antibody and clear, sharp banding patterns seen on the Ponceau stained membrane. A 12% hand-cast gel of 1.0mm thickness underwent western blotting but no immunodetection was carried out as the ladder was visible on both the gel and membrane and the Coomassie and Ponceau controls showed incomplete transfer of proteins from the gel to the PVDF membrane.

A second type of SDS-PAGE gel 10% Mini-PROTEAN® TGX Stain-Free™ Gel (BIORAD) was trialled for western blotting. Using this gel resulted in an even straight separation of tissue lysates that could be visualised on the Gel Doc™ EZ System on a stain free sample tray using Image Lab™ Software (BIORAD). The advantage of using this system is that you do not require for additional staining such as Coomassie blue or preparing of SDS-PAGE gels. Therefore, it saves time.

Results for the transfer of proteins from the 10% pre-cast 1.0mm thick SDS-PAGE gels to the PVDF membrane were not very successful. The ladder was only slightly visible on the membrane and imaging of the gel showed incomplete transfer of proteins with visible banding patterns clearly seen. Probing with the  $\beta$ -actin antibody of the PVDF membrane confirmed the transfer of some of the proteins but the bands were very faint. Ponceau staining of the PVDF membrane

confirmed the poor transfer of proteins with very faint banding patterns visible despite prolonged incubation in Ponceau stain. Probing of the membrane with the VMO1 antibody was unsuccessful. This could be due to the thickness of the precast gel or to the tri-halo compounds incorporated into it that react with the tryptophan amino acid residues to produce chemiluminescence. However, the poor results obtained with the pre-cast gels meant western blotting was only carried out using hand cast gels of 0.75mm thickness.

### **5.3.3 Analysis of ProteinTech VMO1 Antibody**

The first antibody for VMO1 was sourced from Proteintech due to availability, cost and evidence of validation by the company as well as the ability to recognise both human and mouse VMO1. The VMO1 ProteinTech antibody was validated by western blotting of protein lysates from human cervical cancer cell line (Hela), and Human Embryonic Kidney 293 cell line (HEK-293) and confirmed to be compatible with ELISA and western blotting analysis. It was also stated to be specific to the human, mouse and rat although how they determined this was not stated nor was the site of recognition defined. In addition the supplier did not allow access to the peptide used to induce VMO1 antibody production in the rabbit. This along with a peptide fragment known not to have the VMO1 antibody epitope could have been run alongside other tissues in the gel to act as a positive and negative control for antibody binding could have been used. Therefore a future recommendation would be to source an antibody with a known binding epitope or that comes with its own positive and negative controls.

Western blotting using the VMO1 antibody sourced from ProteinTech shows immunodetection of VMO1 protein at various sizes in 7 of the 13 tissues extracted from the mouse, and the VM extracted from the chicken egg (Figure 52-56); ranging between 10-150kDa. The expected band size of 22kDa (15-37kDa) for VMO1 was observed in the mouse brain (Figure 52, 54 and 55), and spleen (Figure 55), as well as the chicken VM (Figure 54). However, this was not reproducible in duplicate western blots. Non-specific binding to the Precision plus Protein™ Dual Color Standards was also observed at 10, 15 and 75kDa. This was reproduced multiple times with no binding occurring to the BSA standard. Binding of the antibody to the ladder protein standards could be due to the nature of the

recombinant protein sequences used. Conversely, the  $\beta$ -actin antibody consistently reproduced results with no binding occurring with the BSA control.

The variations in protein size detected in the western blots with this antibody could be due to a number of different reasons. For example, protein dimerization, binding of the VMO1 protein to other proteins to form a protein complex, unidentified splice variants or coding exons in the mouse *Vmo1*, or post-translational modification of VMO1 protein such as phosphorylation to increase the protein size.

The western blot results could also be a result of non-specific binding of the VMO1 antibody. This antibody was purchased from a commercial company that had validated the antibody using human cell lines (Hela and HEK-293) although it was not stated how these cells were transfected or the specific sequence used to do so. Also, the antibody was delayed at customs for six weeks under unknown conditions. This may have affected the specificity and performance of the antibody.

Denaturation by heating at 99°C for 3min in a loading dye containing beta-mercaptoethanol prior to loading the PAGE gel is thought to remove dimers. However, there are examples of proteins that are resistant to heat and chemical denaturation such as the Proline Rich Homeodomain proteins PRH/Hhex (Shukla, 2012). Western blotting was carried out nine times in order to reproduce results with no success. Initially, western blotting was carried out using protocol 3.9.2 with additional washing and blocking steps added with each subsequent run. In an attempt to reduce the non-specific binding, the wash step was eventually increased to three 1-hour washes in TBS-T at RT followed by an overnight wash at 4°C in 1X PBS

The blocking buffer used for western blot analysis was supermarket grade milk powder but may not be ideal for the VMO1 antibody, since each antibody-antigen pair has unique binding characteristics. Therefore, a future recommendation would be to optimise the blocking solution and test a variety of commercial blocking solution available on the market such as the Thermo Scientific

SuperBlock Blocking Buffers. However, for the purpose and time constraints of this study, we decided to purchase and validate a second antibody for IHC.

#### **5.3.4 Analysis of GeneTex VMO1 Antibody**

A second VMO1 antibody was sourced after reviewing the research by Shamsi et al., 2011. The authors used an anti human VMO1 antibody sourced from GeneTex and their western blots showed binding of the VMO1 protein at approximately 20kDa in camel and sheep tears. Following review of this study, we purchased the VMO1 antibody from GeneTex. However, it was noted that the authors failed to disclose if they used a peptide or recombinant protein to validate the antibody.

Western blotting using the VMO1 antibody sourced from GeneTex was carried out twice. The first western blot contained three ear tissue samples at two different concentrations and a positive result was achieved. Results showed the molecular weight of VMO1 protein in the inner ear to be between 25-37kDa with a second band of smaller size being detected between 20-25kDa (Figure 56). Band intensity also suggests the VMO1 antibody can be used in a roughly quantitative manner to detect different amounts of VMO1 protein. A tear gland sample was also analysed at two different concentrations with a single band between 25-37kDa of lower intensity than seen in the ear samples indicating a lower concentration of VMO1 present. However,  $\beta$ -actin antibody control was not performed on this blot as it was damaged while washing and not retrievable. This control would have given an indication of the concentrations of tear and ear protein loaded. No binding of the VMO1 protein was observed with the BSA standard or to the recombinant protein ladder.

The second blot was carried out on two separate gels with 16 different tissue samples and the BSA control. Analysis of the transfer of the ladder from the gel to the membrane showed transfer of the ladder through the membrane and blotting paper and into the second gel. Immunodetection of this blot using the VMO1 antibody showed the proteins from the first blot to be present in the second blot and rendered the second blot useless for analysis. The presence of VMO1 was faintly visible in the first blot between 25-37kDa in size and also at more than 150kDa for the inner ear. Antibody binding also occurred in the tear gland

between 25-37kDa only. As discussed previously, this could be due to dimerization, or binding of the VMO1 protein to other proteins, splice variants, post-translational modification or non-specific binding.

VMO1 antibody binding was not detected in five of the 8 tissues sampled with duplicate results seen for the ear and tear glands (Figure 56 and 58), and a single result for the eye (Figure 57). Studies by Shamsi, 2011 and Chen, 2011 have identified a VMO1 homolog in the tears of camels and humans but not in the tears of mice. This could indicate VMO1 is found in the tear gland tissue rather than the tear fluid. However, results presented here show that the VMO1 antibody binds specifically to VMO1 protein in the inner ear tissue lysates. Thus, the VMO1 antibody is suitable for IHC of the mouse inner ear. However, to support this claim, we decided to further validate the antibody by preparing a recombinant VMO1 protein that expresses the antibody epitope.

## **5.4 Cloning and Expression of the VMO1 Recombinant Protein**

To develop VMO1 recombinant protein, a PCR insert containing the amplified *Vmo1* gene using primer set BFG27/28 needed to be ligated into a protein expression vector. The induced and purified protein would serve as a positive control on the western blot for further validation of the VMO1 antibodies.

### **5.4.1 Ligation of the *Vmo1* Transcript into a Vector**

Three digested cloning vectors (pProEx HTb, pET42a, and pBluescript) were ligated with purified RE digested *Vmo1* amplicon and transformed into electrocompetent *E. coli* DH5 $\alpha$  cells. The steps of restriction enzyme digestion and ligation are discussed in more detail below.

#### **5.4.1.1 Restriction Enzyme Digestion**

The amplified *Vmo1* DNA and cloning vector was digested to make compatible sticky ends for the ligations and insertion of a correctly oriented digested PCR product into the vector. Two different RE combinations were used for ligation into the pProEX HTb vector. Firstly, HindIII was used to linearise the vector and create sticky ends on the BFG27/28 PCR amplicon for unoriented insertion of the *Vmo1* amplicon into the vector. Thus, creating a recombinant circular vector.

The second combination used HindIII digestion of a BFG27/2 PCR amplicon to produce a sticky HindIII 5' end and a sticky adenine 3' end. The cloning vector pProEX HTb was digested with EcoRV to create a linear vector. This vector was then T-tailed and digested with HindIII RE to create a linear pProEX HTb vector with a sticky thymine 5' end and a sticky HindIII 3' end.

#### **5.4.1.2 Ligation**

Following purification of the digested PCR insert and linearised cloning vector, ligation reactions were set up to create a circular vector. DNA ligation was confirmed to be unsuccessful by the use of a control testing the efficiency of the transformation reaction. This involved using uncut vector to transform electrocompetent cells. Transformed cells were screened for the presence of the vector by growth on LB<sup>+</sup> plates containing ampicillin and further validated by RE digestion of the isolated plasmid to confirm size.

To optimise DNA ligation, the following methods were implemented using two different stocks of T4 DNA ligase from commercial suppliers to determine if the DNA ligase was working efficiently.

The first control was a positive transformation control that included an uncut vector to check for the viability of competent bacterial cells and uptake of the DNA and to verify the action of antibiotic resistance found in the vector for positive selection. The results of this control showed the electrocompetent DH5 $\alpha$  cells to be viable and antibiotic resistance of the plasmid verified by growth of at least 50 colonies on LB<sup>+</sup> ampicillin plates.

The second DNA ligase control involved re-ligating a 1kb ladder to test the action of the two T4 DNA ligases. A 1 $\mu$ l sample of unstained 1kb ladder of 12 bands (Solis Biodyne) was ligated successfully using 1 $\mu$ l T4 DNA ligase.

Electrophoresis of the un-ligated ladder alongside the ligated ladders from the two samples of T4 DNA ligase showed the production of a new banding pattern with additional bands and a reduction in intensity of 9 of the 12 original bands indicating ligation of the ladder and therefore confirmation of the activity of both ligases.

The third control involved determination of the effect of the different reagents in the ligation reaction on the viability of the competent cells and consisted of three reactions: undigested vector with insert, undigested vector with T4 DNA ligase and undigested vector with insert and T4 DNA ligase. Results shown were similar to those seen with the positive transformation control with more than 50 colonies seen and indicating that the viability of electrocompetent cells was not being affected by the T4DNA ligase or insert.

The fourth controls were negative controls to determine the amount of background noise seen due to ampicillin resistance in the competent cells, the efficiency of the RE digestion and to test for recircularisation of the plasmid and involved three reactions: no vector; digested vector with no DNA ligase and digested vector with DNA ligase. All of the negative controls showed very little background with less than 3 colonies seen on each plate indicating the RE digest was successfully producing a linear vector which was not recircularising and that the competent cells did not contain ampicillin resistance on its own.

The vector and insert samples were analysed on a Nanodrop to determine the DNA concentrations for determination of the insert:vector ratios to used. Molar ratio for ligation is important for efficiency of the ligation reaction. A high vector to insert ratio is will result in excess empty plasmids. If too low, excess linear plasmids or circular homo/heteropolymer plasmids will result. This included a rough 1:3, 3:1, 2:1 and 1:2 ratios based on concentrations and a calculated 1:3 and 1:2 ratio based on concentrations and worked out using Equation 1.

$$\left( \frac{\text{ng concentraion of vector} \times \text{bp size of insert}}{\text{kb size of vector}} \right) \times \left( \text{molar ratio of } \frac{\text{insert}}{\text{vector}} \right)$$

**Equation 1: Equation used to work out insert:vector ratio of reagents based on Nanodrop concentrations (Cursons, 2013)**

#### **5.4.2 Screening and Sub-cloning of Transformed Colonies**

Blue and white screening was used to verify the presence of an insert within the vector. Transformed cells were grown in the presence of ampicillin antibiotic, Xgal and IPTG. The ampicillin was used to select for colonies containing the vector insert and IPTG was used to induce expression of the  $\beta$ -galactosidase protein to allow the use of Xgal as a substrate and therefore resulting in blue



colonies. Ligation of an insert into the vector resulted in interruption of the LacZ gene used to make the  $\beta$ -galactosidase resulting in white colonies.

Single white colonies produced from protocol 3.6.4 were picked using a sterile pipette tip and dipped briefly in a PCR master mix (protocol 3.4) containing forward primer (M13puc) and reverse primer (BFG28R) to check for the insertion of *Vmo1* in the correct orientation. Screening of the colonies via PCR failed to show the *Vmo1* insert within the vectors in the 5' to 3' direction indicating *Vmo1* was favourably inserted in the 3' to 5' direction. RE digestion of isolated plasmid was also used to confirm the size of insert to no effect. It was later discovered that the incorrect primer (BFG28R) was being used to check for the correct orientation. This was due to the excision of the primer binding site with the HindIII enzyme during RE digestion prior to the ligation step.

## **5.5 Localisation of the VMO1 Protein within the Inner Ear using VMO1 Antibody (GeneTex)**

IHC and section staining was used to localise the VMO1 protein within the inner ear of P5 mice. This age was also chosen due to the ease of processing as the temporal bone in mice is not fully calcified until after P12 and therefore does not require a decalcification step to prevent the artefacts commonly seen when sectioning fully calcified tissue such as shearing of the bone or tearing of soft tissues (Cunningham, 2001).

### **5.5.1 Integrity of the Mouse Cochlea**

During the IHC process it is important to maintain the integrity of the mouse auditory system. This structure is rather delicate and during the embedding and IHC process, the tissue is exposed to harsh chemicals, pH and temperatures. With respect to using paraffin sections, OCT embedding and cryostat sections of the mouse inner ear was considered to be easier and more robust for analysis of the mouse cochlea.

In P12 mice and humans, the temporal bone is an extremely hard calcified bone which acts as a shield for the delicate sensory organ, and an acoustic chamber to increase hearing sensitivity and enable detection of low intensity sounds. The calcification of this bone makes it difficult to section and requires decalcification

before embedding and sectioning (Cunningham, 2001). To overcome the sectioning artefacts that result from using P12+ mice, P5 mice were used for IHC analysis. P5 mice do not have fully calcified temporal bones and does not need an additional decalcification step after dissection. In addition, fixation and embedding of mouse tissue was carried out immediately after dissection to reduce the chances of false positive results and prevent breakdown and putrefaction of tissue samples.

#### **5.5.1.1 Paraffin Embedding and Microtome Sectioning**

Seven mouse ears dissected from four P28+ mice were fixed in 4% PFA, decalcified in EDTA and embedded in paraffin wax. Two of the specimens were sectioned on a microtome and processed for IHC and H&E staining. While sectioning, it was noted that there was shearing and breaking of the temporal bone. After inspection of paraffin sections, between 10-20% were discarded as considered too damaged or too difficult to collect due to rolling of the section. Also noted were inconsistencies in the thickness of the paraffin block, with a dip observed in the middle of the paraffin block. This was thought to be caused by the shrinking of paraffin as it cooled and set. The thickness of the sections was also adjusted from 5-10-15-20um to improve the quality and decrease the amount of shearing and breakage. However, no noticeable changes were detected. The collection of individual sections and placement onto slides was also difficult due to the small size of the inner ears and the awkwardness of removing them from the collection plate to the slides, and floating them on 30% ethanol without disturbing the sections already floating. Serial slides were collected and analysed under a light microscope to check orientation and anatomy before staining or IHC was carried out.

H&E staining showed poor general anatomy across all of the sections with shearing of the RM, BM and no discernible TM as well as shearing and breakage of the temporal bone. IHC carried out on paraffin sections required an antigen revival step in which the slides were microwaved in a citrate antigen revival buffer until just boiling twice. This step resulted in more than one section per slide being lost and caused the sections to move around on the slide leading to folded tissue sections and more shearing of the temporal bone and membranes of the inner ear.

The mouse heart and liver tissue were also embedded in paraffin and sectioned on a microtome to act as a sectioning control and for future IHC antibody validation. Both sections were stained with H&E to help visualise anatomy with mixed results. The liver sections were flaky and crumbly during sectioning and did not hold together very well during rehydration and staining. The heart sections were much more robust and were easily sectioned, rehydrated and stained with little loss of morphology or sections. The results are most likely a reflection of the types of tissue used with the liver being a soft glandular tissue and the heart a solid muscular organ. Neither are very good controls for sectioning of the inner ear as they do not contain any calcified bony tissue nor do they contain membranous fluid filled ducts. Following the unsuccessful IHC carried out on the paraffin sections, the embedded inner ears were store in a labelled box and we switched to the cryosectioning method instead.

#### **5.5.1.2 OCT Embedding and Cryostat Sectioning**

For the cryosectioning method P5 mice were used due to the ease of dissection of whole heads and the fact that the temporal bones were not yet fully calcified. Sections obtained using this method were more consistent and easier to collect. In addition, they did not require a deparafinisation or antigen revival step.

#### **5.5.2 Haemotoxylin Staining**

To confirm the integrity and anatomy of the OCT mouse sections, H&E staining was performed. H&E staining showed good preservation of inner ear anatomy with an easily identifiable TM and intact RM, BM and temporal bone with only minimal shearing seen. These results are shown in the literature review (Figure 8, 9 and 10). However one limitation of H&E staining is its incompatibility with immunofluorescence because of the fluorescence of eosin (Fischer, 2008).

#### **5.5.3 Immunohistochemistry**

The *Vmo1* mRNA has been demonstrated to be expressed exclusively in RM of the mouse ear but was not shown to be the location of the VMO1 protein. IHC results suggest the VMO1 protein to be a secreted protein as levels of green fluorescent signal were identified at high levels within the TM of the inner ear.

The IHC protocol was optimised by changing the incubation times, antibody concentration and washing steps. The first IHC experiment was carried out using a 1:1000 dilution of the VMO1 antibody, and showed very faint fluorescence of the TM. This result was deemed inconclusive due to the amount of background noise (Figure 59b). The following IHC was optimised to include an extra antibody dilution of 1:100 (Figure 59e) and increasing the incubation time in blocking solution from 1 hour at RT to overnight at 4°C. One additional washing step was also included after incubation with the primary and secondary antibody. The fluorescence of the TM was shown to be much greater with the 1:100 antibody dilutions as would be expected if the signal was real and background noise was reduced. Following this, IHC was repeated with the addition of a  $\beta$ -actin antibody control to validate the IHC protocol. For the  $\beta$ -actin control fluorescence would be expected to be ubiquitous throughout the mouse tissue. The washing times after antibody incubation were increased from 5 to 10min and following washing after primary antibody incubation, slides were left overnight at 4°C in PBS buffer. Changes to the methodology resulted in the VMO1 antibody binding to the TM and the pillar cells at high concentrations. The reduction in background noise was very slight. Therefore, these changes made no difference to the IHC protocol.

The  $\beta$ -actin control was deemed to be unsuitable due to its ubiquitous expression within mouse tissue. Results for this IHC showed a slight increase in fluorescence in the stria vascularis and the apical surface of the hair cells as expected but results were not easily distinguishable from the background noise of the sections. In addition the non-specific binding of  $\beta$ -actin antibodies to other isoforms of actin such as F-actin and gamma-actin have been documented. (Dittmer and Dittmer, 2006)

To understand the function of the VMO1 protein, the structure and composition of the TM and VM will be examined.

## **5.6 Comparison of the Tectorial Membrane vs. the Vitelline Membrane**

IHC carried out on the mouse inner ear during the course of the thesis identified the VMO1 protein at high concentrations within the TM. Structurally and

chemically the TM is more similar to the VM of the chicken egg than it is to the RM of the mouse in which the *Vmo1* mRNA was found to be exclusively expressed (Peters et al., 2007).

The RM is a double layered membrane composed of two layers of flattened epithelial cells separated by a basal lamina and acting primarily as a diffusion barrier between the scala vestibuli and the scala media (Valk et al., 2006).

In contrast both the TM and VM are acellular proteinaceous matrixes composed primarily of water.

The VM is composed of two layers the outer and inner VM layers separated by a thin continuous fibrous layer. The VMO1 protein was localised within the outer VM layer which is a proteinaceous extracellular matrix composed of a network of fine fibrils formed after ovulation and consisting mainly of the macromolecule ovomucin. This protein was shown to be tightly bound to the VMO1 protein along with other proteins such as lysozyme and VMOII (Mann, 2008). The structural integrity of the outer VM is thought to be attributed to the disulfide bonds in ovomucin (Kido and Doi, 1988).

The TM is a collagen-rich extracellular matrix that lies over the organ of Corti running parallel to the BM and is directly connected to the stereocilia of outer hair cells, and indirectly connected to the stereocilia of inner hair cells via subtektorial fluid. Structurally, the TM is similar to connective tissue with the collagen fibres providing stiffness, integrity and structure to the TM (Gueta et al., 2011).

The TM is unique to other membranes in the inner ear due to the glycoproteins found to be expressed exclusively in the inner ear such as,  *$\alpha$ -tectorin* and  *$\beta$ -tectorin*, which have also been identified as being responsible for sensorineural hearing loss, DFNA8 and DFNB21 (Verhoeven et al., 1998). Thus, highlighting the importance of the TM for hearing function. The exact composition of the TM and how it functions remain unclear but studies have shown it is essential for hearing function (Ghaffari et al., 2007).

# CHAPTER SIX

## CONCLUSION

The original aim was to characterise the possible function of the *Vmo1* gene and investigate protein expression within the mouse inner ear at different developmental time points with the hypothesis that it would be found in the RM and therefore play an important role in the mechanism and/or maintenance of hearing or balance.

In conclusion the data presented within this thesis addressed the question of whether *VMO1* mRNA transcript and the predicted protein is conserved among birds and mammals, and if the translated VMO1 protein remains within RM or is secreted and transported to cells within the mouse mammalian ear.

Based on the comparative genomics analysis and anatomy, the mouse is most suitable for studying the role of human VMO1 in the auditory system with results indicating that the *Vmo1* gene is highly conserved across mammalian species. IHC performed on P5 mice suggests the VMO1 protein is translated and secreted within the mouse inner ear with high concentrations seen in the TM and inner pillar cells. A review of literature identified the TM as being essential for hearing function with the pillar cells also playing an important role in coupling movement of the BM, upon stimulus by sound waves, to the movement of hair cells. The importance of these two tissues and the localisation of the VMO1 protein within them therefore indicates an important role for VMO1 in hearing function.

The next section will address future recommendations for the characterisation and localisation of the VMO1 protein in the inner ear.

# CHAPTER SEVEN

## FUTURE RECOMMENDATIONS

### 7.1 Comparative Genomics

Comparative genomics analysis of VMO1 protein demonstrates that this protein is conserved across different species and therefore, indicates an importance in role or function.

To provide an absolute indicator of protein conservation the amino acid sequence could be determined using Mass spectrometry. Furthermore, the 3D structure of the VMO1 protein from the mouse and human could also be resolved using X-ray crystallography. Comparing the 3D structure of the mouse and human VMO1 would give an indication of how conserved the VMO1 protein are between these two species, and how good the mouse is as a model for studying human VMO1. Mass Spectrometry instrumentation could give an indication of any post-translational modifications occurring in the VMO1 protein and identify any differences between the VMO1 proteins found in the inner ear and the tear glands. In addition to Mass Spectrometry, optical imaging and fluorescent probes could be used to investigate gene expression, active transport and metabolism of *VMO1* in living cells (Xie et al., 2006).

In addition, a knockout mouse should be generated. As yet there are none available but a vector construct is available for purchase from International Knockout Mouse Consortium. The *Vmo1* gene in this construct has been mutated using a combination of gene trapping and gene targeting in C57BL/6 mouse embryonic stem cells.

Generation of a knockout mouse would involve the preparation of a genetically engineered mouse in which the *Vmo1* gene has been inactivated and would give a direct indication of gene function and would serve as a negative control for IHC studies. It would be interesting to observe if these mice have a hearing loss and/or balance phenotype.

## 7.2 Complete DNA Sequencing of *Vmo1* Gene

To sequence the complete coding region of *Vmo1* requires the extraction of RNA, reverse transcription, DNA amplification of cDNA, clean-up and DNA sequencing methodologies. The following recommendations could be implemented in the future to confirm the complete sequence of the *Vmo1* gene in order to prepare a protein expression construct containing the *Vmo1* ORF.

### **Recommendation 1: Remove Genomic DNA from RNA Sample**

The primers designed to amplify the *Vmo1* transcript were not specific to the mRNA. Therefore, genomic DNA had to be eliminated from the RNA template to ensure only cDNA was amplified and not genomic DNA. This was accomplished using DNase but results show that genomic DNA was present. To eliminate genomic DNA contamination, a second DNase treatment could be added to the RNA isolation protocol or carried out after RNA is isolated. Alternatively, gene specific primers for exon-intron boundaries could be designed for amplifying overlapping contigs across the three coding exons.

### **Recommendation 2: Rapid Amplification of cDNA Ends**

In addition to the removal of genomic DNA from the RNA sample rapid amplification of cDNA ends (RACE) should be used. This involves the direct sequencing of the *Vmo1* mRNA template where the RNA is reverse transcribed to cDNA followed by PCR amplification using specific primers (Schaefer, 1995).

### **Recommendation 3: Validate Quantity and Quality of RNA**

To validate the RNA yield, integrity, and purity, a number of methods could be employed based on access to equipment and funding. For example, the automated Agilent 2100 Bioanalyzer machine (Agilent Technologies) or performing an RNA Qubit™ Assay (Life Technologies). The Qubit RNA assay involves using two rRNA standards and a fluorometre and is highly selective for RNA. The Bioanalyzer uses electrophoresis separation of RNA samples and laser induced fluorescence detection coupled with a computer algorithm to interpret sample concentration, integrity and to generate ribosomal ratios.



#### **Recommendation 4: Clone *Vmo1***

The quality of the sequencing results for the 671bp *Vmo1* amplicon varied between the forward and reverse sequencing reaction. The forward sequence had 96% coverage and 99% identity to the reference sequence with miscalls only seen in the first 20 nucleotides of the 5' end which is due to primer binding. The reverse sequence had 70% coverage for the reverse sequence with 98% identity and miscalls found throughout the length of the sequence. With optimal quality DNA the Waikato DNA sequencing facility should produce a 600 nucleotide read, the size and quality of the forward sequence indicates a problem with the reverse sequence only and a repeat of the reverse reaction is recommended.

The low quality of DNA sequencing results could be an indication of poor primer design and non-specific binding. This could be improved by designing primers or by running a touchdown PCR protocol to ascertain the optimal annealing temperature for all primer combinations (Don et al., 1991).

To ensure high copy numbers and complete coverage, the amplified *Vmo1* DNA could be cloned into a cloning vector and then directly sequenced using vector specific primers. In addition, this would allow easier manipulation of the *Vmo1* transcript for insertion into an expression vector (assuming compatible restriction enzyme sites and in frame ORF).

Alternative methodologies to confirm the complete *Vmo1* sequence could include RNA-seq. For example, you could use *Vmo1* targeted RNA sequencing with a customised Ion AmpliSeq™ gene panel (Life Technologies and Toedling, 2012). This would result in the quantitative gene expression of *Vmo1*.

### **7.3 Validation of the VMO1 Antibody**

To conclusively determine the localisation of VMO1 protein in the mouse inner ear, a recombinant VMO1 protein construct needs to be developed or purchased. Electrophoresis of the resulting expressed purified recombinant protein and western blot analysis would ultimately demonstrate the specificity of the VMO1 antibody for recognising the VMO1 epitope.

It should be noted that the ProteinTech VMO1 antibody was validated using HeLa and HEK-293 cells and the GeneTex VMO1 antibody using a recombinant VMO1 protein. HeLa and HEK-293 cells are immortal cell lines derived from human tissue that are easily transfected with the gene of interest to produce expressed protein (Ahlin et al., 2009). Therefore, a future recommendation would include the protein lysate from cultured HeLa cells on a western blot as well as a recombinant VMO1 protein.

The next section discusses the methodology and future recommendations for the preparation of a recombinant VMO1 protein.

### **Recommendation 1: Preparation of Cloning Vector**

RE digestion of the vectors for linearisation and creation of sticky ends for the ligation of a *VmoI* insert was shown to be incomplete with undigested plasmid remaining in the sample. Therefore, this resulted in a decreased concentration of ligated plasmid and lead to inefficient transformation of recombined circular plasmid into the electrocompetent *E. coli* cells. To increase the efficiency of the RE digestion, an additional purification step could be performed after the isolation of the plasmid DNA from transformed *E. coli* cells, and the units of RE increased. In addition, the digested plasmid could be separated on a lower percentage agarose gel to improve the separation of the digested and undigested plasmid bands. The digested band could then be easily identified and if required, could be gel purified in order to increase the concentration of digested vector in the ligation reaction.

Rather than using a plasmid with sticky ends for cloning purposes, you can digest a vector with a blunt RE, T-tail and ligate a PCR product with 3'-A overhangs. The T-tailing reaction is the addition of a thymine amino acid to the 3' ends of a linearised blunt vector and results in a 2bp increase in the size of the vector which is undetectable on a 1% agarose gel. To confirm the T-tailing reaction, T4 DNA ligase could be used. This would involve using T4 DNA ligase to recircularise the un-T-tailed, digested vector and comparing the amount of colonies produced following transformation with a colonies produced following transformation of a digested vector with no T-tailing carried out. Theoretically, when compared to the positive control, successful T-tailing would result in a lower colony count due to

the thymine nucleotides preventing recircularisation of the vector. This would also act as an additional control to test the activity of the T4 DNA ligase. Extra effort must also be made to avoid nuclease contamination, which would remove the A or T overhang on the insert and vector respectively and to use a SafeImager to visualise PCR products and avoid UV light which would cause degradation of the DNA (Promega).

## **Recommendation 2: Ligation and Transformation of the Circular Recombinant Vector**

Following the preparation of digested vector and PCR insert, the ligation reaction was carried out multiple times to generate a circularised vector. Optimisation of the ligation reaction included using a different stock of T4 DNA ligase, changing the amount of T4 DNA ligase and adjusting the ratio of insert:vector. Ligation and Transformation controls were also carried out to test the viability, transformation efficiency, and antibiotic resistance of electrocompetent cells as well as the action and efficiency of the T4 DNA ligase enzyme. Blue and white colonies resulted following transformation but the wrong colony PCR screening method was employed to detect positive inserts.

It was noted that during the writing of the thesis that the incorrect primer was used to check orientation of the inserts.

In future, colonies should be screened using *Vmo1* specific primers that only amplify cDNA produced from *Vmo1* mRNA such as BFG7F or BFG8R combined with a vector specific primer such as M13 Puc Reverse to identify the orientation of the inserts.

In addition, the colony should be cultured to produce high copy numbers for DNA extraction for sequencing and RE digestion. RE digestion would be used to confirm the size and orientation of the insert. Sequencing of the plasmid would give the full length sequence of the insert and allow for the confirmation of the ORF and confirm the size and the orientation of the insert.

## Protein Expression

In the future, upon the identification of a positive clone and a correct ORF, the following steps are recommended for the expression of a VMO1 recombinant protein.

Briefly, you should inoculate a flask filled with 10mL of LB<sup>+</sup> broth with transformed DH5 $\alpha$  containing the *Vmo1* insert in the 5' to 3' direction. Allow, the culture to grow at 37°C to an OD<sub>600nm</sub> of 0.698 (logarithmic phase) and induce by adding 1mM IPTG. You should also include a control – no induced. Following three hours of growth, remove a 4mL culture for protein extraction. Leave the remaining culture shaking overnight for protein extraction.

To extract protein, pellet the cultures by centrifuging at 16100rcf for 2min. Remove the supernatant and resuspend the cells in 100 $\mu$ l of binding buffer and freeze at -80°C for 30min. Heat the samples at 75°C for 30min followed by centrifugation to pellet cell debris and insoluble proteins. The supernatant will contain soluble expressed proteins and should be removed to a new tube. Aliquots of the pellet and supernatant from all of the samples can be analysed on an SDS-PAGE to determine if the recombinant protein had been induced, which induction time produced the highest concentrations of recombinant protein, whether the protein was soluble or insoluble, and finally, whether it is of roughly the expected size for the mouse VMO1 protein (22kDa). The protein can then be purified on a Nickel resin column using the histidine (His) tag expressed on the recombinant protein.

Following the purification of the recombinant protein, the amino acid sequence of the protein can be confirmed using Trypsin digestion and western blotting.

Trypsin digestion is a method that uses the Trypsin enzyme to proteolytically cleave polypeptides at the C-terminal end of Lys and Arg. This would result in cleavage of the VMO1 protein to produce 13 fragments (ExPASy, 2013) as shown in Table 17.

The digested recombinant protein could then be analysed on a 2D SDS-PAGE gel or using mass spectrometry. 2D western blotting of the digested protein using VMO1 antibody would theoretically show binding to a fragment 1.8kDa in size.

**Table 17: Expected protein fragments resulting from Trypsin digestion of the purified mouse VMO1 recombinant protein**

Mass (kDa)	Position	Peptide sequence
3.7	31-64	YASIVDVTNGGTWGDWAWPEMCPDGYFASGFSVK
3.7	93-125	NTHVVESQSGSWGSEPLWCPGTSFLVAFCLR
2.8	145-170	CSDGVELEGPGLNWGDYGEWSNSCPK
2.5	9-30	LLLLLGVMCYGHAAQIQVHVEPR
1.9	126-142	VEPFTFPDNTGVNNVR
1.8	65-82	VEPPQGIPGDDTALNGIR
1.0	187-195	DDTALNDIR
0.9	1-8	MELQAGAR
0.8	171-178	GVCGLQTK
0.6	196-201	IFCCAS
0.6	179-183	IQKPR
0.6	83-87	LHCTR
0.5	88-92	GNSQK

Western blotting would then be used to validate the specificity of the VMO1 antibody with binding expected to occur and produce a band around 22kDa in size.

### **7.3.1 Optimisation of the Western Blotting Method**

The immunodetection of the VMO1 protein in tissue lysates blotted onto a PVDF membrane was carried out with varying degrees of success. While the VMO1 antibody was shown to bind to a protein of expected size (20-37kDa) in the inner ear and tear gland it also showed binding to a high molecular weight (>250kDa) protein in the inner ear. This could be due to the VMO1 protein complexing with a high molecular weight protein such as collagen. To determine if the VMO1 protein is bound to collagen, an antibody or stain such as Fuschin or Safranin, which bind to collagen, could be used. In addition Co-immunoprecipitation (Co-IP) could be used to identify protein-protein interactions and verify binding of VMO1 to a high molecular weight protein such as collagen. Co-IP uses binding of the VMO1 protein to an antibody to form an immune complex that is then precipitated or bound to a beaded support. At the same time VMO1 is precipitated the proteins complexed with it are as well which can then be analysed them to gain a new insight into the function of VMO1 (Sambrook et al., 2005).

Alternatively the two-hybrid screen method could be used. This involves using yeast to incorporate two foreign plasmids containing the genes of interest. Once transcribed the genes of interest produce proteins that are fused to a second protein. If the two proteins of interest interact the attached proteins attached to

protein fragments. If the genes of interest interact the attached proteins induce the expression of a reporter gene that changes the phenotype of the cell (Feilotter, 1994).

The percentage of SDS-PAGE gel used (12%) for the western blot analysis gave good separation of proteins in the 20-100kDa range but did not allow for the resolution of high molecular weight proteins or low molecular weight proteins. To address this issue, a lower percentage gel (7%) could be used to resolve the high molecular weight proteins and to improve the size recording of the larger protein VMO1 antibody is binding to. To improve the detection of the low molecular weight protein size the VMO1 antibody is binding to, an SDS-PAGE gel of higher percentage (15%) could be used. In addition, inner mouse ear proteins could be analysed on a 2D western blot which could then be probed with both the VMO1 antibody and a collagen antibody.

Denaturation of the mouse tissue protein lysates was carried out in a SDS loading buffer containing  $\beta$ -mercaptoethanol and heated for 3min at 99°C. A more robust method could be used to denature the proteins to investigate the removal of the high molecular weight proteins. To achieve this, the SDS loading buffer could be prepared with fresh  $\beta$ -mercaptoethanol and/or the sample heated for an additional 5min (abcam.com/technical - Harlow and Lane, 1999). Alternative reducing agents such as Dithiothreitol (DTT) or Tributylphosphine (TBP) (BIORAD) could also be tried. In addition, the western blot could be carried out using native protein lysates to see if this eliminated the band observed between 20-37kDa.

## **7.4 Histology**

IHC was performed and showed the VMO1 was localised in the mouse inner ear. However, only a single developmental time point was analysed during the course of this thesis. To obtain a better understanding of the expression profile of VMO1, and the development of the TM, IHC should be investigated using mouse ear sections from gestational day 18, when the major TM is first observed to P14, when the cochlea is fully developed morphologically (Rueda et al., 1996). Mouse hearing is said to be fully developed by P10 but mechano-electrical transduction can be detected as early as P1 (Peters et al., 2007). However, cochlear structures

are present at birth and adult cochlear length is reached at P7 with hair cell numbers matching those of an adult at P3 (Mikaelian and Ruben, 1965).

#### **1.4.1 Embedding and Sectioning of the Mouse Inner Ear**

In the future, if you decided to return to using paraffin embedded sections, the following recommendations should be considered to prevent shearing of the TM, BM, temporal bone, and loss of the sections during the antigen revival step. Firstly, decalcification of the temporal bone in EDTA in the microwave as described by Cunningham et al., 2001. Secondly, using mice younger than P12 since the temporal bone is said to be fully calcified (Cunningham et al., 2001). Thirdly, heating the citrate antigen revival buffer prior to slide incubation instead of boiling the slides in the buffer using a microwave. Finally, embedding whole hemidissected mouse heads instead of inner ears to help with orientation of the inner ear.

For OCT embedding, use of deeper cryomolds would ensure even and complete coverage of the specimen with OCT, and the collection of thinner sections (<10µm) to be able to resolve individual cells more clearly.

#### **H&E and Counter Staining of the Mouse Sections**

H&E staining was carried out to aid in visualisation of cell nuclei and section morphology with good results observed. However, due to the fluorescent nature of eosin it was not compatible with fluorescent IHC and did not stain the TM due to its acellular nature and 97% water composition. Also, although the H&E stain was able to show the general morphology of the tissue, improvements could be made to enhance the resolution of the individual cells within the inner ear. Briefly H&E staining was carried out by first washing in 1X PBS for 1min followed by 5min in haematoxylin stain, a brief rinse of the reverse side of the slide in cold running tap water, 30sec in Eosin followed by another rinse in tap water and 5min washing in 1X PBS.

To improve H&E staining, Rüegg & Meine, 2012, recommend washing slides in warm tap water for 1 minute to remove PFA as opposed to 1min in 1X PBS, 5min haematoxylin staining and blueing of the haematoxylin stain. The addition of blueing involves washing the slides under warm running tap water for 10min to aid in neutralising the acidic haematoxylin and freeing the OH group that results

in a bluer stain. In addition, 10min, instead of 30sec, eosin staining was recommended followed by three 1min washes in dQH<sub>2</sub>O.

Alternatively, you could use a different stain that is visible under light microscopy such as Fuchsin or Safranin, which will both stain collagen; Alcian Blue stain which will stain cartilage (Pirvola et al., 2004); or to use a fluorescent stain such Phalloidin which will bind to filamentous actin but not globular actin conjugated to a different fluorophore than the FITC used with the VMO1 antibody (Thermo-Scientific, 2013).

### **Immunohistochemistry**

IHC results could be improved in multiple ways to increase specificity of antibody binding, and to quantify background noise and autofluorescence of the tissue sections.

The noise observed on the sections could be due to non-specific binding of the primary or secondary antibody, autofluorescence of the tissue itself or from contamination of the polyclonal antibody.

Goat serum was used to block tissue and prevent non specific binding. To increase blocking of non-specific sites, incubation times could be increased or an additional incubation with fresh serum added to the protocol. Another alternative would be to optimise the embedding and fixation protocol to reduce background noise and autofluorescence by trialling other OCT mediums and protocols.

Autofluorescence was not tested for in this thesis and should be tested by viewing a section of tissue under a fluorescent microscope with different wavelength filters.

The endogenous peroxide activity which leads to autofluorescence of sections is prevented by incubation in H<sub>2</sub>O<sub>2</sub>. Peroxidase activity was prevented by incubating section slides in 0.9% H<sub>2</sub>O<sub>2</sub> for 30min. To reduce the level of autofluorescence, the concentration and/or incubation time in H<sub>2</sub>O<sub>2</sub> could be increased, using fresh solutions of H<sub>2</sub>O<sub>2</sub> or preparing in diluted methanol rather than water to accelerate the destruction of heme groups.



To address possible contamination of the polyclonal antibody, a monoclonal antibody, (not yet available) could be used to decrease chances of contamination from other antibodies.

To address antibody specificity and binding efficiency, additional IHC controls should be included. These include the use of a mammalian cell line or tissue known to not express the protein of interest such as a knock-out mutant or the mouse thymus which has consistently shown no antibody binding in western blots; transfection of non-expressing cells with the protein of interest as a positive control; and the use of cell lines biologically proven to not express the protein of interest (Bordeaux et al., 2010).

## 7.5 Conclusion

There are a variety of methodologies available to determine the gene function of *Vmo1*. Firstly, the 3D structure of the mouse and human VMO1 protein need to be resolved using X-ray crystallography and a *Vmo1* knock-out mouse created to determine phenotype(s). Secondly, with Human Ethics approval, recruit human subjects suffering from HL and/or balance disorders to sequence their *VMO1* gene and search for mutations, such as SNPs, and compared against a cohort of normal hearing individuals. To date there have been no human or mouse deafness loci mapped to the *VMO1* chromosomal region 17p13.2:4688580- 4689728 (Van Camp G, Smith RJH. Hereditary Hearing Loss Homepage). Thirdly, analyse mouse mutants with a known hearing or vestibular phenotype to determine if changes to the morphology of the inner ear or the proteins expressed in the inner ear has any affect on the localisation and expression of the VMO1 protein. The *Tecta*<sup>C1509G</sup> knock-in mouse has been shown to have altered development of the TM leading to shortening of the TM in adult mice that is not observed in wild-type mice (Gueta et al., 2011). This would provide a good comparison for the localisation of VMO1 within the TM and inner pillar cell. Finally, VMO1 protein expression was only analysed at two developmental time points (P5 and P28+) for this thesis. Changes in VMO1 protein expression between gestational day 18 and P14 would give an indication of the function and importance of VMO1 and in addition, show how expression in the TM changes throughout development.

## REFERENCES

- Abnet CC, Hemmert W, Tsai BS, Weiss TF (2003) Dynamic material properties of the tectorial membrane: A summary. *Hear Res*, 180(1-2):1-10
- Ahlin G, Hilgendorf C, Karlsson J, Al-Khalili Szigyarto C, Uhlén M, Artursson P (2009) Endogenous gene and protein expression of drug-transporting proteins in cell lines routinely used in drug discovery programs. *Drug Metab Dispos*, 37(12):2275-2283  
doi: 10.1124/dmd.109.028654
- Back JF, Bain JM, Vadehra DV, Burley RW (1982) Proteins of the outer layer of the vitelline membrane of hen's eggs. *Biochim Biophys Acta*, 705(1):12-9.
- Barber RD, Harmer DW, Coleman RA, Clark BJ (2005) *GAPDH* as a housekeeping gene: Analysis of *GAPDH* mRNA expression in a panel of 72 human tissues. *Physiol Genomics*, 21(3):389-95
- Békésy GV (1952) Resting potentials inside the cochlear partition of the guinea pig. *Nature*, 169:241-242.  
doi:10.1038/169241a0
- Bergevin C, Velenovsky DS, Bonine KE (2010) Tectorial membrane morphological variation: Effects upon stimulus frequency otoacoustic emissions. *Biophys J*, 99:1064–1072
- Bissonnette JP, Fekete DM (1996) Standard atlas of the gross anatomy of the developing inner ear of the chicken. *J Comp Neurol*, 368:620-630 (1996)
- Bolt MA, Mahoney PA (1997), High-efficiency blotting of proteins of diverse sizes following sodium dodecyl sulphate-polyacrylamide, gel electrophoresis. *Anal Biochem*, 247:185–192
- Bordeaux J, Welsh AW, Agarwal S, Killiam E, Baquero MT, Hanna JA, Anagnostou VK, Rimm DL (2010) Antibody validation. *BioTechniques*, 48(3):197-209

- Burton, S. Pandya, A, Arnos KS (2006) Genetics and hearing loss: An overview. *ASHA Lead*, 11(1):31-33
- Campbell NA, & Reece JB (2005) *Biology* (Seventh ed.). San Francisco CA: Benjamin Cummings
- Chen Z, Shamsi FA, Li K, Huang Q, Al-Rajhi AA, Chaudhry IA, Wu K (2010) Comparison of camel tear proteins between summer and winter. *Mol Vis*, 17:323-331
- Chiarella G, Saccomanno M, Scumaci D, Gaspari M, Faniello MC, Quaresima B..... Cassandro E (2012) Proteomics in Ménière's disease. *J Cell Physiol*, 227(1):308-312  
doi: 10.1002/jcp.22737
- Chung WH, Lai KM, H KC (2010) Comparative study on histological structures of the vitelline membrane of hen and duck egg observed by cryo-scanning electron microscopy. *J Agric Food Chem*, 58:1794-1799
- Cuchillo CM, Nogués V, Raines§ RT (2011) Bovine pancreatic ribonuclease: 50 years of the first enzymatic reaction. *Mechanism Biochem*, 50(37):7835-7841  
doi: 10.1021/bi201075b
- Cunningham CD, Schulte BA, Bianchi LM, Weber PC, Schmiedt BN (2001) Microwave decalcification of human temporal bones. *Laryngoscope*, 111:278-282
- Daidone I, Di Nola A, Smith CJ (2011) Molecular origin of gerstmann-sträussler-scheinker syndrome: Insight from computer simulation of an amyloidogenic prion peptide. *Biophys J*, 100(12):3000-3007
- Digby JE, Purdy SC, Kelly AS (2012) *Hearing loss in New Zealand children: 2011*, New Zealand Audiological Society, Auckland, New Zealand.
- Don RH, Cox PT, Wainwright BJ, Baker K, Mattick JS (1991) 'Touchdown' PCR to circumvent spurious priming during gene amplification. *Nucleic Acids Res*, 19(14): 4008.

- Dror AA, Avraham KB (2009) Hearing loss: Mechanisms revealed by genetics and cell biology. *Annu Rev Genet*, 43:411-437.  
doi: 10.1146/annurev-genet-102108-134135
- Farrukh A, Shamsi, Chen Z, Liang J, Li K, Al-Rajhi AA, Chaudhry IA, Li M, Wu K (2011) Analysis and comparison of proteomic profiles of tear fluid from human, cow, sheep, and camel eyes. *Invest Ophthalmol Vis Sci*, 52(12):9156-9165
- Feilotter HE, Hannon GJ, Ruddell CJ, Beach D (1994) Construction of an improved host strain for two hybrid screening. *Nucleic Acids Res*, 22(8):1502–1503
- Ferrary, E, Sterkers O (1998) Mechanisms of endolymph secretion. *Kidney Int*, 65:98-103
- Fischer AH, Jacobson KA, Rose J, Zeller R (2008). SOP: Hematoxylin and eosin staining of tissue and cell sections
- Flock A, Scarfone E (2001) Structural relationships of the unfixed tectorial membrane. *Hear Res*, 151(1-2):41-47
- Frank K, Sippl MJ (2008) High-performance signal peptide prediction based on sequence alignment techniques. *Bioinformatics*, 24(19):2172-6  
doi: 10.1093/bioinformatics/btn422
- Freeman DM, Masaki K, McAllister AR, Wei JL, Weiss TF (2003) Static material properties of the tectorial membrane: A summary. *Hear Res*, 180(1-2):11-27.
- Friedman LM, Dror AA, Avraham KB (2007) Mouse models to study inner ear development and hereditary hearing loss. *Int J Dev Biol*, 51(6-7):609-31.
- Friedman TB, Griffith AJ (2003) Human nonsyndromic sensorineural deafness. *Annu Rev Genomics Hum Genet*, 4:341-402
- Gates, G. (2006). Ménière's disease review 2005. *J Am Acad Audiol*, 17(1), 16-26.

- Gavara N, Manoussaki D, Chadwick RS (2011) Auditory mechanics of the tectorial membrane and the cochlear spiral. *Curr Opin Otolaryngol Head Neck Surg*, 19(5):382-387
- Ghaffari R, Aranyosi AJ, Freeman DM (2007) Longitudinally propagating traveling waves of the mammalian tectorial membrane. *PNAS*, 104(42):16510-16515
- Ghaffari R, Page SL, Farrahi S, Sellon JB, Freeman DM (2013) Electrokinetic properties of the mammalian tectorial membrane. *NAS*, 110(11):4279-4284
- Gordon, A. G. (2006). Ménière's disease. *Lancet*, 367(9515):984.  
doi: 10.1016/S0140-6736(06)68419-5
- Greville Consulting. New Zealand deafness detection data January - December 2005. Report prepared for National Audiology Centre, Auckland District Health Board, March 2007
- Greville Consulting. New Zealand vision & hearing screening report July 2005 - June 2006. Report prepared for National Audiology Centre, Auckland District Health Board, November 2006
- Greville, Anne. Hearing impaired and deaf people in New Zealand; an update. Greville Consulting report (March 2005)
- Greville, KA (2001) Hearing impaired and deaf people in New Zealand; population numbers and characteristics. Greville Consulting report (October, 2001)
- Gromiha MM, Selvaraj S (2004) Folding mechanism of all-beta globular proteins. *Prep Biochem Biotechnol*, 34(1):13-23.
- Gu JW, Hemmert W, Freeman DM, Aranyosi AJ (2008) Frequency-dependent shear impedance of the tectorial membrane. *Biophys J*, 95(5): 2529–2538
- Guearin-Dubiard C, Pasco M, Mollea D, Deasert C, Croguennec T, Nau F (2006) Proteomic analysis of hen egg white. *J Agric Food Chem*, 54:3901–3910

- Gueta R, Levitt J, Xia A, Katz O, Oghalai JS, Rousso I (2011) Structural and mechanical analysis of tectorial membrane TECTA Mutants. *Biophys J*, 100:2530-2538
- Gummer AW, Hemmert W, Zenner HP (1996) Resonant tectorial membrane motion in the inner ear: Its crucial role in frequency tuning. *Proc Natl Acad Sci*, 93:8727-8732
- Hanahan D (1985) DNA cloning: A practical approach. Glover, D. M. (ed.), Vol. 1, p. 109, IRL Press, McLean, Virginia.
- Harlow E, Lane D (1999) Using antibodies. Cold Spring Harbor, New York: Cold Spring Harbor Laboratory Press
- Hildebrand MS, Sorensen JL, Jensen M, Kimberling WJ, Smith RJ (2008) Autoimmune disease in a DFNA6/14/38 family carrying a novel missense mutation in WFS1. *Am J Med Genet A*, 146(17):2258-65.  
doi: 10.1002/ajmg.a.32449
- Hilgert N, Smith RJH, Van Camp G (2009) Function and expression pattern of nonsyndromic deafness genes. *Curr Mol Med*, 9(5):546-564
- Huynh ML, Russell P, Walsh B (2009) Tryptic digestion of in-gel proteins for mass spectrometry analysis. *Methods Mol Biol*, 519:507-13.  
doi: 10.1007/978-1-59745-281-6\_34.
- Kanonier G, Fritsch E, Rainer T, Thumfart WF (1996) Radiotherapy in early glottic carcinoma. *Ann Otol Rhinol Laryngol*, 105(10):759-763.
- Karkos PD, Anari S, Johnson IJ (2005). Cochlear implantation in patients with MELAS syndrome. *Eur Arch Otorhinolaryngol*, 262(4):322–324
- Keats, B. (2005). Genetics and hearing loss. *ASHA Leader*, 10(12):15-18.
- Keithley EM, Truong T, Chandronait B, Billings PB (2000). Immunohistochemistry and microwave decalcification of human temporal bones. *Hearing Res*, 148:192-196.
- Khaitlina SY (2007) Mechanisms of spatial segregation of actin isoforms. *Cell and Tissue Biology*, 1(4):293-304

- Kido S, Doi Y (1988) Separation and properties of the inner and outer layers of the vitelline membrane of hen's eggs. *Poult Sci*, 67(3):476-48  
doi: 10.3382/ps.0670476
- Kido S, Doi Y, Kim F, Morishita E, Narita H, Kanaya S, Ohkubo T, Nishikawa K, Yao T, Ooi T (1995) Characterization of vitelline membrane outer layer protein I, VMO-I: Amino acid sequence and structural stability. *J Biochem*, 117(6):1183-91.
- Kido S, Morimoto A, Kim F, Doi Y (1992) Isolation of a novel protein from the outer layer of the vitelline membrane. *J Biochem*, 286(1):17-22.
- Kim SH, Kim KX, Raveendran NN, Wu T, Pondugula SR, Marcus DC (2009) Regulation of ENaC-mediated sodium transport by glucocorticoids in Reissner's membrane epithelium. *Am J Physiol Cell Physiol*, 296:544-557
- Kitajima N, Watanabe Y, Suzuki M (2011) Eustachian tube function in patients with Ménière's disease. *Auris Nasus Larynx*, 38(2):215-219  
doi: 10.1016/j.anl.2010.10.003
- Kraeva RI, Krastev DB, Roguev A, Ivanova A, Nedelcheva-Veleva MN, Stoyanov SS (2007) Stability of mRNA/DNA and DNA/DNA duplexes affects mRNA transcription. *PLOS One*, 2(3):e290  
doi:10.1371/journal.pone.0000290
- Lodish H, Berk A, Zipursky SL, et al. *Molecular Cell Biology*. 4th edition. Section 11.6, Processing of rRNA and tRNA New York: W. H. Freeman; 2000.
- Magariños M, Contreras J, Aburto MR, Varela-Nieto I (2012) Early development of the vertebrate inner ear. *Anatomical Record* 295:1775–1790
- Mann, K. (2008). Proteomic analysis of the chicken egg vitelline membrane. *Proteomics*, 8(11), 2322-2332.  
doi: 10.1002/pmic.200800032
- Marcos HJA, Ferrari CC, Cervino C, Affani JM (2002) Histology, histochemistry and fine structure of the lacrimal and nictitans gland in the south american

armadillo chaetophractus villosus (*Xenarthra, Mammalia*). *Elsevier Science*, 75:731-744.

Masaki K, McAllister AR, Wei JL, Weiss TF (2003) Static material properties of the tectorial membrane: A summary. *Hear Res*, 180(1-2):11-27

Mathers C, Smith A, Concha M: Global burden of hearing loss in the year 2000. Global Burden of Disease 2000 WHO

Mazzoli M, Van Camp G, Newton V, Giarbini N, Declau F, Parving A (2003) Recommendations for the description of genetic and audiological data for families with nonsyndromic hereditary hearing impairment. *Audiol Med*, 1(2):1-3

McLean A, Caudwell L, Greville A. Development and Implementation of a National Funding and Service System for Hearing Aids: Stage One Interim Report. Report for the Ministry of Health, March 2008

Merchant SN, Adams JC, Nadol JB (2005) Pathology and pathophysiology of idiopathic sudden sensorineural hearing loss. *Otol Neurotol*, 26(2):151-60.

Merchant SN, Nadol JB (1993). Schuknecht's pathology of the ear (Third ed.). Shelton CT: People's Medical Pub. House.

Meyer NC, Alasti F, Nishimura CJ, Imanirad P, Kahrizi K, Riazalhosseini Y, Malekpour M, .... Najmabadi H (2007) Identification of three novel TECTA mutations in Iranian families with autosomal recessive nonsyndromic hearing impairment at the DFNB21 locus. *Am J Med Genet*, 143(14):1623-9.

Mikaelian D, Ruben RJ (1965) Development of hearing in the normal CBA-J mouse. *Acta Otolaryngol*, 59:451-461.

Minekawa A, Abe T, Inoshita A, Iizuka T, Kakehata S, Narui Y, Koike T, .... Ikeda K (2009) Cochlear outer hair cells in a dominant-negative connexin26 mutant mouse preserve non-linear capacitance in spite of impaired distortion product otoacoustic emission. *J Neurosci*, 164(3):1312-9



- Morrison AW, Bailey ME, Morrison, G. A. (2009). Familial Ménière's disease: Clinical and genetic aspects. *J Laryngol Otol*, 123(1), 29-37.  
doi: 10.1017/S0022215108002788
- Morsli H, Choo D, Ryan A, Johnson R, Wu DK (1998) Development of the mouse inner ear and origin of its sensory organs. *J Neurosci*, 18(9): 3327-3335
- Murzin AG, Brenner SE, Hubbard T., Chothia C. (1995). SCOP: A structural classification of proteins database for the investigation of sequences and structures. *J. Mol. Biol.* 247, 536-540
- Nadol JB (1996) Techniques for human temporal bone removal: Information for the scientific community. *Otolaryngol Head Neck Surg*, 115(4):298-305.
- Nagalakshmi U, Waern K, Snyder M (2010) RNA-Seq: A Method for Comprehensive Transcriptome Analysis. *Curr Protoc Mol Biol*, 4(11):1-13
- Ohashi Y, Dogru M, Tsubota K, (2006) Laboratory findings in tear fluid analysis. *Clin Chim Acta*, 369(1):17-28.  
doi: 10.1016/j.cca.2005.12.035
- Peters LM, Belyantseva IA, Lagziel A, Battey JF, Friedman TB, Morell RJ (2007). Signatures from tissue-specific MPSS libraries identify transcripts preferentially expressed in the mouse inner ear. *Genomics*, 89(2):197-206.  
doi: 10.1016/j.ygeno.2006.09.006
- Peterson MG (1988) DNA sequencing using *Taq* polymerase. *Nucleic Acids Res*, 16(22)
- Petit C, Levilliers J, Hardelin JP (2001) Molecular genetics of hearing loss. *Annu Rev Genet*, 35:589–646
- Phillips M (2003) Genetics of hearing loss. *Medsurg Nursing*, 12(6):386-411.
- Pirvola U, Zhang X, Mantela J, Ornitz DM, Ylikoski J (2004) Fgf9 signaling regulates inner ear morphogenesis through epithelial–mesenchymal interactions. *Dev Biol*, 273(2):350-360

- Quint E, Steel KP (2003) Use of mouse genetics for studying inner ear development. *Curr Top Dev Biol*, 57:45-83
- Raikos V, Hansen R, Campbell L, Euston SR, (2006) Separation and identification of hen egg protein isoforms using SDS–PAGE and 2D gel electrophoresis with MALDI-TOF mass spectrometry. *Food Chem*, 99(4):702-710.  
doi: 10.1016/j.foodchem.2005.08.047
- Rueda J, Cantos R, Lim DJ (1996) Tectorial membrane-organ of Corti relationship during cochlear development. *Anat Embryol*, 194(5):501-14.
- Rüegg MA, Meinen S (2012) Histopathology in hematoxylin & eosin stained muscle sections. (SOP: MDC1A\_M.1.2.004) University of Basel, Basel, Switzerland
- Salt A (2001) Regulation of endolymphatic fluid volume. *Ann N.Y. Acad Sci*, 942:306–312.  
doi: 10.1111/j.1749-6632.2001.tb03755.x.
- Sambrook J, Russell DW, Adams PD, Ohh M (2005) Identification of associated proteins by coimmunoprecipitation. *Nature Methods* 2, 475-476  
doi:10.1038/nmeth0605-475
- Schaefer BC (1995) Revolutions in rapid amplification of cDNA ends: New strategies for polymerase chain reaction cloning of full-length cDNA Ends. *Anal Biochem*, 227(2):255–273
- Schrijver I (2004) Hereditary Non-Syndromic Sensorineural Hearing Loss: Transforming Silence to Sound. *J Mol Diagn*, 6(4): 275–284
- Shamsi FA, Chen Z, Liang J, Li K, Al-Rajhi AA, Chaudhry Ia, . . . Wu K (2011) Analysis and comparison of proteomic profiles of tear fluid from human, cow, sheep, and camel eyes. *Invest Ophthalmol Vis Sci*, 52(12):9156-9165.  
doi: 10.1167/iovs.11-8301
- Sharma A, Chandran D, Singh DD, Vijayan M, (2007) Multiplicity of carbohydrate-binding sites in beta-prism fold lectins: Occurrence and possible evolutionary implications. *J Biosci*, 32(6):1089-1110.

- Sharma A, Vijayan M, (2011) Quaternary association in beta-prism I2 fold plant lectins: Insights from X-ray crystallography, modelling and molecular dynamics. *J Biosci*, 36(5):793-808  
doi: 10.1007/s12038-011-9166-2
- Sheffield AM (2012) Gene therapy for hereditary hearing loss: Lessons from a mouse model (Dissertation) University of Iowa,  
<http://ir.uiowa.edu/etd/2984>.
- Shimizu T, Morikawa K, (1996) The beta-prism: A new folding motif. *Trends Biochem Sci*, 21(1), 3-6.
- Shimizu T, Morikawa K, Kido S, Doi Y (1994) Crystallization and preliminary crystallographic data of vitelline membrane outer layer protein I, VMO-I. *J Mol Biol*, 235(2):793-4.
- Shimizu T, Vassilyev DG, Kido S, Doi Y, Morikawa K (1994) Crystal structure of Vitelline membrane outer layer protein I (VMO1): A folding protein motif with homologous Greek key structures related by an internal three-fold symmetry. *EMBO J*, 13(5):1003-1010
- Shukla A, Burton NM, Jayaraman PS, Gaston K (2012) The proline rich homeodomain protein PRH/Hhex forms stable oligomers that are highly resistant to denaturation. *PLoS One*, 7(4):35984.  
doi:10.1371/journal.pone.0035984. Epub 2012 Apr 23.
- Silverthorn DU, (2004). Human physiology: An integrated approach (Third ed.). San Francisco, CA: Fox, D.
- Smith RJH, Shearer AE, Hildebrand MS, Van Camp G, (2012). Deafness and hereditary hearing loss overview. Seattle: University of Washington, GeneReviews at GeneTests: Medical genetics information resource (database online). Retrieved January 1, 2013, from: [www.genetests.org](http://www.genetests.org)
- Smith RJH, Van Camp G: Nonsyndromic hearing loss and deafness, DFNB1. GeneReviews™ [Internet]. Pagon RA, Adam MP, Bird TD, et al., editors. Seattle (WA): University of Washington, Seattle; 1993-2013.

- Snoeckx RL, Huygen PL, Feldmann D, Marlin S, Denoyelle F, Waligora J, ...  
Van Camp G (2005) *GJB2* mutations and degree of hearing loss: A multicenter study. *Am J Hum Genet*, 77(6):945-57. Epub 2005 Oct 19.
- Steel KP (2000) A take on the tectorial membrane. *Nature Genetics*, 24.2 :104
- Stegmann BJ, Carey JC (2002) TORCH infections. Toxoplasmosis, other (syphilis, varicella-zoster, parvovirus b19), rubella, cytomegalovirus (CMV), and herpes infections. *Curr Womens Health Rep*, 2(4):253-8.
- Carter R, Aldridge S, Page M, Parker S (2009). The Brain Book: An illustrated guide to its structure, function and disorders. UK:Dorling Kindersly Pub Inc
- Tinling SP, Giberson RT, Kullar RS, (2004) Microwave exposure increases bone demineralization rate independent of temperature. *J Microsc*, 215(3), 230-235.
- Toedling J, Servant N, Ciaudo C, Farinelli L, Voinnet O, Heard E, Barillot E (2012) Deep-sequencing protocols influence the results obtained in small-RNA sequencing. *PLoS One*, 7(2):e32724.  
doi: 10.1371/journal.pone.0032724
- Towbin H, Staehelin T, Gordon J (1979) Electrophoretic transfer of proteins from polyacrylamide gels to nitrocellulose sheets: Procedure and some applications. *Proc Natl Acad Sci*, 76(9):4350-4.
- Tranebaerg L (2008) Genetics of congenital hearing impairment: A clinical approach. *Int J Audiol*, 47:535-545.
- Tsuprun V, Santi P (1996) Crystalline arrays of proteoglycan and collagen in the tectorial membrane. *Matrix Biology*, 15:31-38
- Tubbs RS, Kelly DR, Humphrey ER, Chua GD, Shoja MM, Salter EG, .... Oakes WJ (2007) The tectorial membrane: Anatomical. *Clin Anat*, 20:382–386
- Uyeda A, Inuzuka C, Doi Y, Kido S, Kikuchi M (1994) Cloning and sequencing of hen magnum cDNAs encoding vitelline membrane outer layer protein I (VMO-I). *Gene*, 144(2):311-312

- Valk WL, Wit HP, Albers FW (2006) Rupture of Reissner's membrane during acute endolymphatic hydrops in the guinea pig: A model for Ménière's disease? *Acta Otolaryngol*, 126(10):1030-1035.  
doi:10.1080/00016480600621722
- Van Camp G, Smith RJH. Hereditary hearing loss homepage.  
URL: <http://hereditaryhearingloss.org>  
Retrieved July 2013
- Verhoeven K, Van Laer L, Kirschhofer K, Legan PK, Hughes DC, Schatteman I, ..... Van Camp G (1998) Mutations in the human alpha-tectorin gene cause autosomal dominant non-syndromic hearing impairment. *Nat Genet*, 19(1):60-2.
- Verpy E, Leibovici M, Michalski N, Goodyear RJ, Houdon C, Weil D, Richardson GP, Petit C (2011) Stereocilin connects outer-hair-cell stereocilia to one another and to the tectorial membrane. *J Comp Neurol*, 519(2):194–210
- Vrabec JT, (2003) Herpes simplex virus and Ménière's Disease. *Laryngoscope*, 113
- Vreugde S, Erven A, Kros CJ, Marcotti W, Fuchs H, Kurima K, . . Steel KP (2002) Beethoven, a mouse model for dominant, progressive hearing loss DFNA36. *Nat Genet*, 30(3):257-258.  
doi: 10.1038/ng848
- Wang YL, Tan Y, Satoh Y, Ono K (1995) Morphological changes of myoepithelial cells of mouse lacrimal glands during postnatal development. *Histol Histopathol*, 10:821-827
- Whitton DS, Szakaly R, Greiner MA, (2001) Cryoembedding and sectioning of cochleas for immunocytochemistry and *in situ* hybridization. *Elsevier Science*, 6:159-166.
- Xia A, Gao SS, Yuan T, Osborn A, Bress A, Pfister M, Maricich SM, Pereira FA (2010) Deficient forward transduction and enhanced reverse transduction in the alpha tectorin C1509G human hearing loss mutation. *Dis Model*

*Mech*, 3(3-4):209-23.

doi: 10.1242/dmm.004135. Epub 2010 Feb 8.

Xie XS, Yu J, Yang WY (2006) Living cells as test tubes. *Science*, 312(5771):228-230

doi:10.1126/science.1127566

Yamazaki M, Kim KX, Marcus DC, (2011) Sodium selectivity of Reissner's membrane epithelial cells. *BMC Physiol*, 11(4).

doi: 10.1186/1472-6793-11-4

Yan D, Liu XZ, (2010) Modifiers of hearing impairment in humans and mice. *Curr Genomics*, 11(4):269-278.

Zakzouk S (2002) Consanguinity and hearing impairment in developing countries: A custom to be discouraged. *J Laryngol Otol*, 116(10):811-816

Zdebik AA, Wangemann P, Jentsch TJ (2009) Potassium ion movement in the inner ear: Insights from genetic disease and mouse models. *J Physiol*, 24:307-316.

doi: 10.1152/physiol.00018.2009

Zhang Y, Zhang W, Johnston AH, Newman TA, Pyykkö I, Zou J (2010) Improving the visualization of fluorescently tagged nanoparticles and fluorophore-labeled molecular probes by treatment with CuSO<sub>4</sub> to quench autofluorescence in the rat inner ear. *Hear Res*, 269(1-2):1-11.

doi: 10.1016/j.heares.2010.07.006. Epub 2010 Jul 24.

Zimatore G, Fetoni AR, Paludetti G, Cavagnaro M, Podda MV, Troiani D (2011) Post-processing analysis of transient-evoked otoacoustic emissions to detect 4 kHz-notch hearing impairment – a pilot study. *Med Sci Monit*, 17(6):41-49.

Zine A, Romand R (1996) Development of the auditory receptors of the rat: A SEM study. *Brain Res*, 721:49–58.

Ziyan C, Shamsi FA, Li K, Huang Q, Al-Rajhi AA, Chaudhry IA, Wu K (2011) Comparison of camel tear proteins between summer and winter. *Mol Vis*, 17: 323–331.

## APPENDIX ONE

# BUFFERS AND SOLUTIONS

### 1X PBS – phosphate buffered saline pH 7-7.4

8g	NaCl
0.25g	KCl
0.2g	KH <sub>2</sub> PO <sub>4</sub>
1.15g	Na <sub>2</sub> HPO <sub>4</sub>

Make up to 1L with mQH<sub>2</sub>O.

### 1X PBS-T – phosphate buffered saline + Tween-20 pH 7-7.4

1L	PBS
0.5mL	Tween-20.

Autoclave

### 50X TAE - Tris-acetate EDTA buffer

242g	Tris base dissolved in 800 mL mQH <sub>2</sub> O
57.1mL	Glacial acetic acid
100mL	0.5M EDTA (pH 8.0)

Make up to 1L with mQH<sub>2</sub>O

### 1X TAE running buffer

20mL	50X TAE
980mL	mQH <sub>2</sub> O

### 0.1% DEPC treated water - diethyl pyrocarbonate

2mL	DEPC
-----	------

Make up with 2L mQH<sub>2</sub>O, mix overnight using a magnetic stirrer, then autoclave.

### Eosin (1% solution)

10g	Eosin Y
2.0mL	Acetic acid (5% aqueous)
0.1g	Phloxine B

Make up with 1L mQH<sub>2</sub>O

### Haematoxylin

4.0g	Haematoxylin
0.4g	Sodium iodate
35.2g	Aluminium sulphate
250mL	Ethylene glycol
40mL	Glacial acetic acid

Make up to 1L with mQH<sub>2</sub>O

### Ponceau S stain

0.1g	Ponceau S
0.1g	Acetic acid

Make up to 1L with mQH<sub>2</sub>O

**1X TBS - Tris buffered saline**

50mL 1M Tris  
30mL 5M Sodium chloride  
Make up to 1L with mQH<sub>2</sub>O and autoclave

**1X TBS-T - Tris buffered saline + Tween-20**

999mL TBS  
1mL Tween-20

**6X agarose gel loading buffer**

3mL Glycerol  
25mg Bromophenol Blue  
20µl Xylene Cyanole  
Make up to 10mL with sterile mQH<sub>2</sub>O

**10X PhosSTOP Phosphatase Inhibitor Cocktail**

1mL 1X PBS  
1 PhosSTOP Phosphatase Inhibitor Cocktail Tablet (Roche)

**10X cComplete Protease Inhibitor Cocktail**

1mL 1X PBS  
1 cComplete Protease Inhibitor Cocktail Tablet (Roche)

**Protein lysis buffer**

2.5mL 1M Tris  
1.9mL 4M NaCl  
200µl 0.5M EDTA  
250µl Triton-X 100  
0.5mL 1X PhosSTOP Phosphatase Inhibitor Cocktail  
0.5mL 1X cComplete Protease Inhibitor Cocktail  
Make up to 50mL with sterile mQH<sub>2</sub>O

**2X Protein loading buffer**

2mL 0.5M Tris-HCl pH6.8  
4mL 10% SDS solution  
2mL Glycerol  
1mL 2-mercaptoethanol  
1mL Bromophenol Blue

**SDS Running Buffer**

3.0g Tris  
14.4g Glycine  
1g SDS (or 100mL of 10% SDS solution)  
Make up to 1L with dH<sub>2</sub>O

**37:1 acrylamide:BIS (22%)**

22.2g Acrylamide  
0.6g Bisactylamide  
Make up to 100mL dH<sub>2</sub>O

**10% APS**

0.1g Ammonium persulfate (oxidiser)  
1mL H<sub>2</sub>O



**2X Freezing medium**

6.30g	K <sub>2</sub> HPO <sub>4</sub>
0.45g	Sodium citrate
0.09g	MgSO <sub>4</sub> ·7H <sub>2</sub> O
1.80g	(NH <sub>4</sub> ) <sub>2</sub> SO <sub>4</sub>
44.00mL	Glycerol

Make up to 500mL with mQH<sub>2</sub>O and autoclave

**1M Tris HCL pH 8.0**

500mL	H <sub>2</sub> O
60.5g	Tris

Autoclave

**0.5M EDTA pH 8.0**

93.05g	EDTA
--------	------

Make up to 500mL with mQH<sub>2</sub>O and autoclave

**4% PFA - paraformaldehyde**

4.0g	PFA
10.0μl	10M NaOH

Make up to 50mL with mQH<sub>2</sub>O and heat in 65°C water bath to dissolve

10mL	10X PBS
------	---------

Make up to 100mL with sterile mQH<sub>2</sub>O

**Mounting fluid**

0.036g	NaHCO <sub>3</sub>
0.008g	Na <sub>2</sub> CO <sub>3</sub>
5mL	H <sub>2</sub> O
45mL	Glycerol

**2M MgCl<sub>2</sub>**

31.8g	MgCl <sub>2</sub>
-------	-------------------

Make up to 200mL with mQH<sub>2</sub>O

**TE buffer – Tris EDTA pH 8.0**

10mL	1X Tris-HCl
2mL	0.5M EDTA

**0.9% H<sub>2</sub>O<sub>2</sub>**

16.7mL	H <sub>2</sub> O <sub>2</sub>
--------	-------------------------------

Make up to 500mL with 1X PBS

**Blocking solution**

5g	Low fat milk powder
50mL	1X TBS-T

**Transfer buffer**

3g	25mM Tris
14.4g	Glycine
200mL	Methanol

Make up to 1L using SDS running buffer

**0.5% Triton-X 100**

250µl Triton-X 100  
Make up to 50mL with 1X PBS

**Antigen revival buffer – sodium citrate buffer**

1.47g Tri-sodium citrate (dehydrate)  
Make up to 500mL with mQH<sub>2</sub>O and autoclave  
250µl Tween 20

**Stripping buffer**

0.75g Glycine  
0.05g SDS  
10mL Tween20  
Make up to 50mL with mQH<sub>2</sub>O

**LB broth – Luria Base broth pH 7.0**

10g Bactotryptone  
5g Bacto yeast extract  
10g NaCl  
Make up to 1L with mQH<sub>2</sub>O and autoclave

**LB plates – Luria base agar plates**

1L LB broth  
15g Bactoagar  
Autoclave and pour plates at <60°C add antibiotics at 50°C

**Coomassie blue stain**

0.25g Coomassie blue brilliant stain R-250  
90mL Methanol  
10mL Glacial acetic acid  
Make up to 200mL with dH<sub>2</sub>O

**IPTG – isopropylthiogalactoside**

200mg IPTG  
1mL dH<sub>2</sub>O

**Xgal - 5-bromo-4-chloro-3-indolyl-β-D-galactopyranoside**

20mg Xgal  
1mL Dimethyl formamide

**PEG – polyethyleneglycol potassium hydroxide pH 13.3-13.5**

27mL PEG 200  
465µl 2M KOH  
Make up to 50mL with mQH<sub>2</sub>O

# APPENDIX TWO

## VECTOR MAPS

### 10.1 pET41-a(+)

A cloning and expression vector containing a kanamycin antibiotic resistance gene, an N-Terminal GST-Tag for enhanced production and solubility, and a C-Terminal His Tag for purification of recombinant protein. This was the original vector chosen for VMO1 recombinant protein expression due to the presence of the Terminal GST Tag and C-Terminal His Tag. The vector was not retrievable from storage on Whatmans paper using DNA elution and transformation.

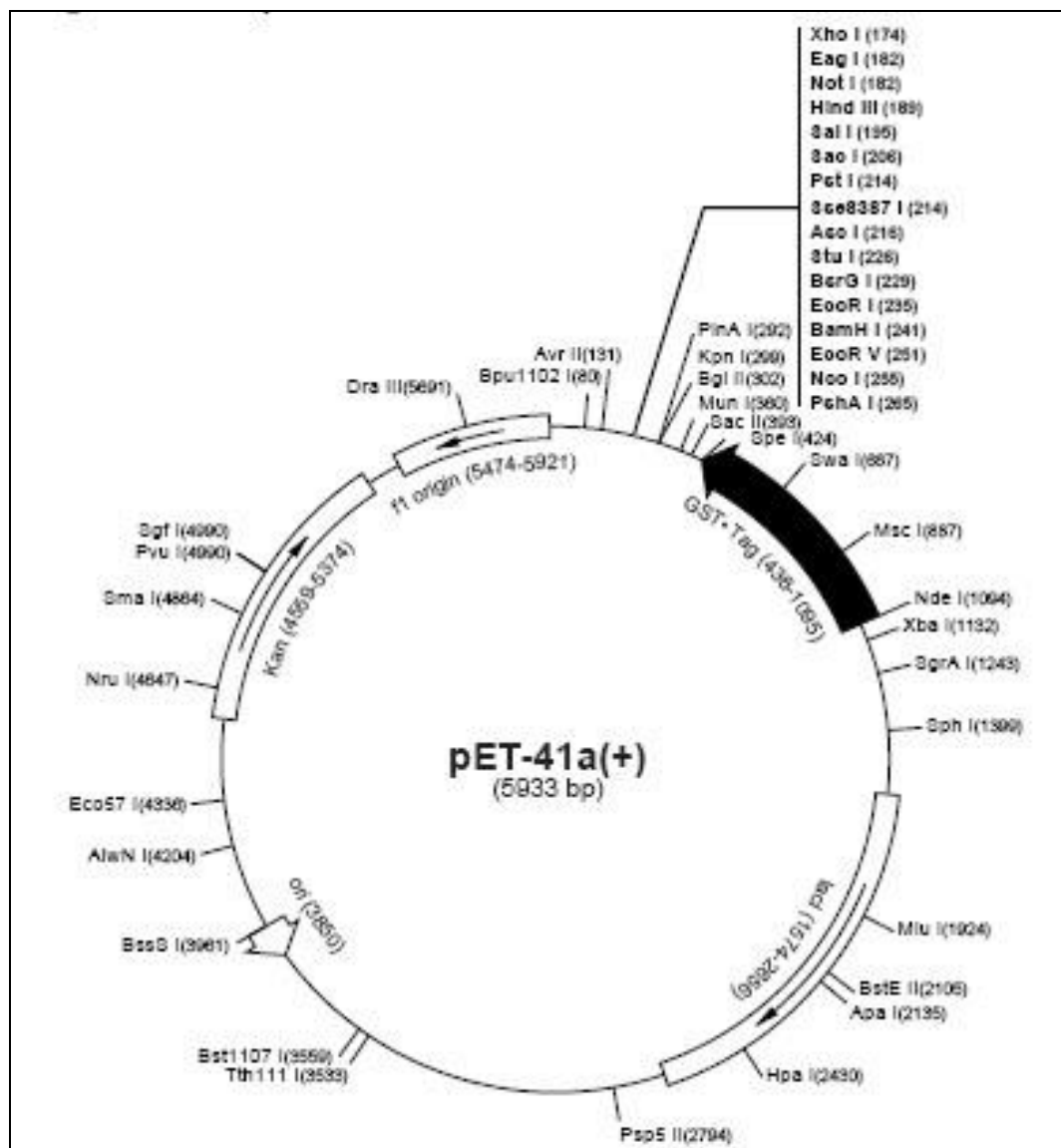


Figure 64: pET-42a(+) vector map showing position of multiple cloning site and Restriction enzyme cut sites (AddGene)

## 10.2 pET-41a(+) vector

A cloning and expression vector with kanamycin resistance, an N-Terminal GST-Tag for enhanced production and solubility, a C-Terminal His-Tag for purification of recombinant protein. This vector was selected because of availability and compatibility with original *Vmo1* primers to produce a recombinant VMO1 protein using BamHI and EcoRI RE and was as alternative when pET41a(+) vector was not retrievable from storage on filter paper.

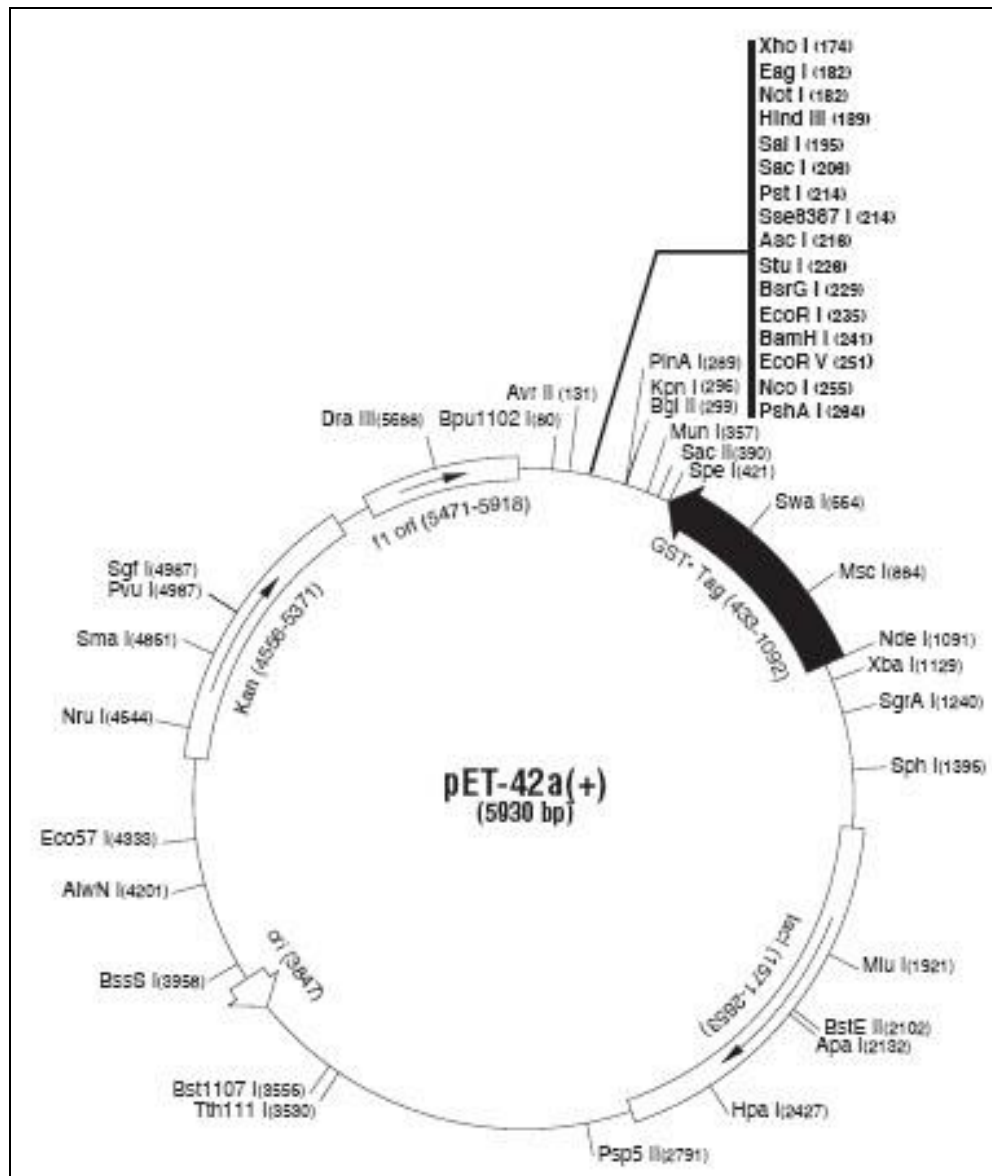


Figure 65: pET-42a(+) vector map showing position of multiple cloning site and Restriction enzyme cut sites (AddGene)

### 10.3 pProEX HTb vector

pProEX HTb is an *E. coli strain* BL21 bacterial protein expression vector used for the expression of recombinant proteins under the trc promoter. In addition, contains an N-terminal His-Tag for purification of recombinant protein, a multiple cloning site and ampicillin resistant. This vector was selected because of availability and primers redesigned for compatibility with *VmoI* ORF using HindIII RE to produce a VMO1 recombinant protein.

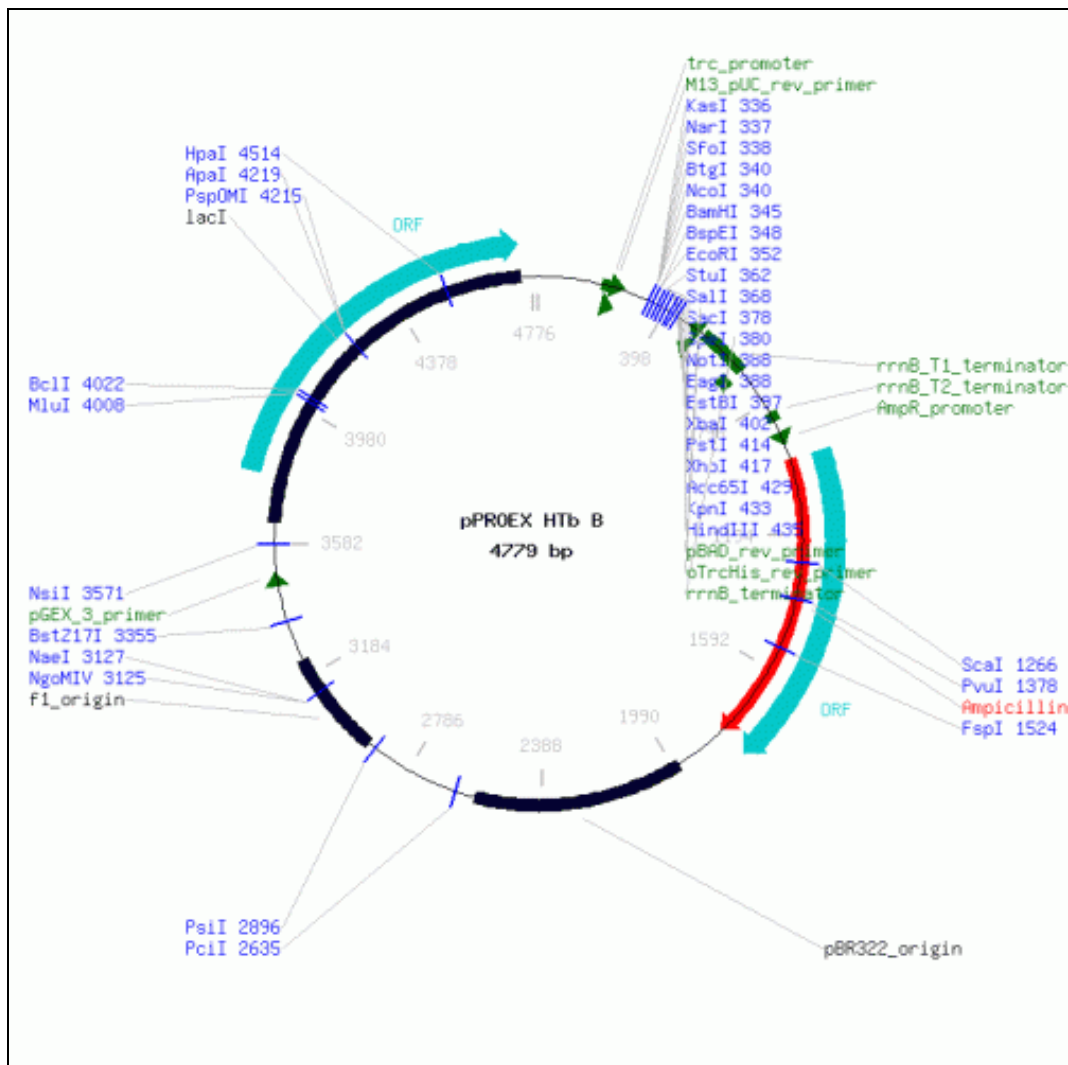


Figure 66: pProEX HTb (Invitrogen) vector map showing position of multiple cloning site and Restriction enzyme cut sites (AddGene)

## 10.4 pBluescript II SK(+)

This cloning vector has blue/white colony screening on Xgal/IPTG plates and ampicillin resistance. This vector was selected because of the lack of success shown with ligation of PCR product directly into expression vectors, its availability and the robust method outlined in the BIOL362 Laboratory Manual, UoW. Excess amounts of EcoRI results in EcoRI prime activity and cleavage at a non-EcoRI site at the 3' end of the f1 intergenic region (Instruction Manual – Agilent Technologies).

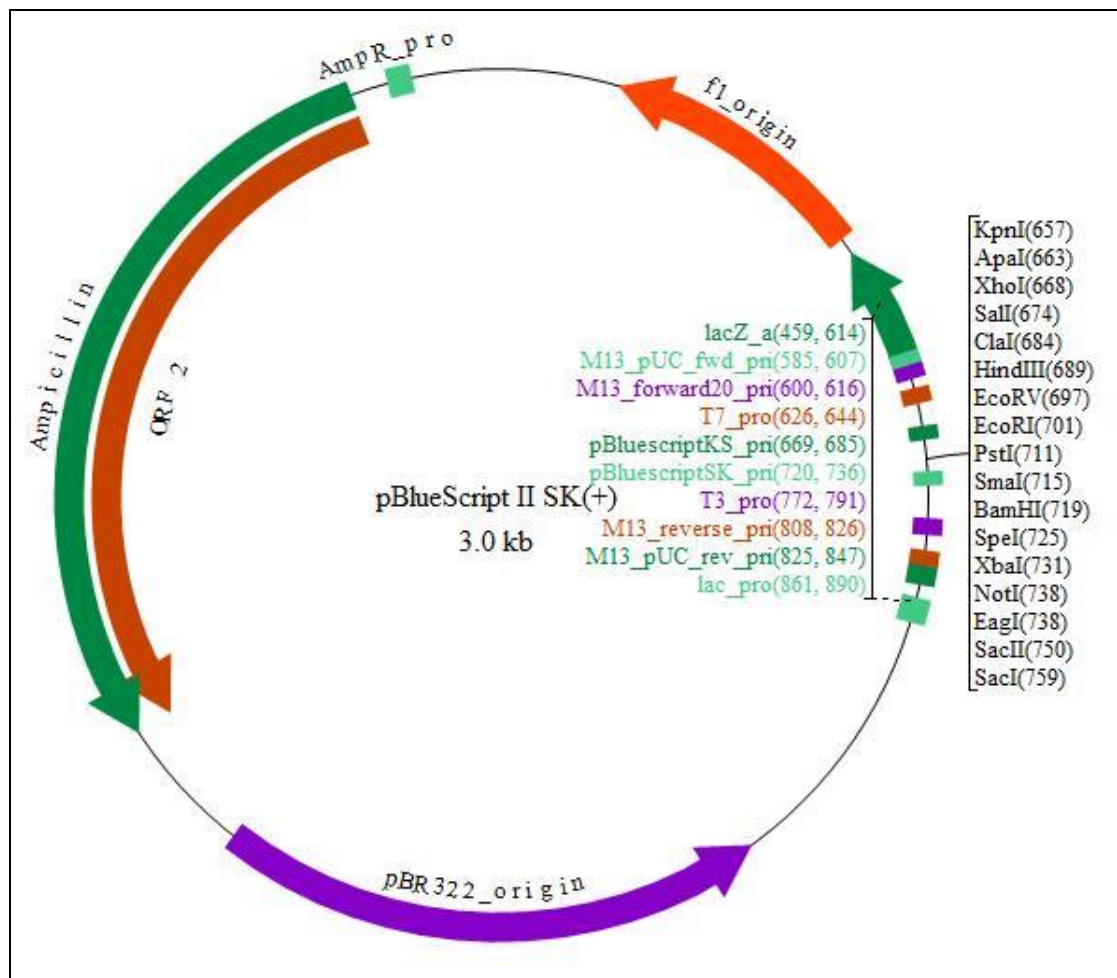


Figure 67: pBluescript II SK(+) vector map showing position of multiple cloning site and Restriction enzyme cut sites (AddGene)

## 10.5 pCR™4-TOPO® TA vector

This cloning vector has ampicillin and kanamycin antibiotic resistance with blue/white colony screening on Xgal/IPTG plates (Adapted from Invitrogen User guide 2012). This vector was selected for ability to directly ligate PCR products into the vector with no additional need for T-tailing, or RE digestion. This vector has an alternative to the pBluescript II SK(+) vector.

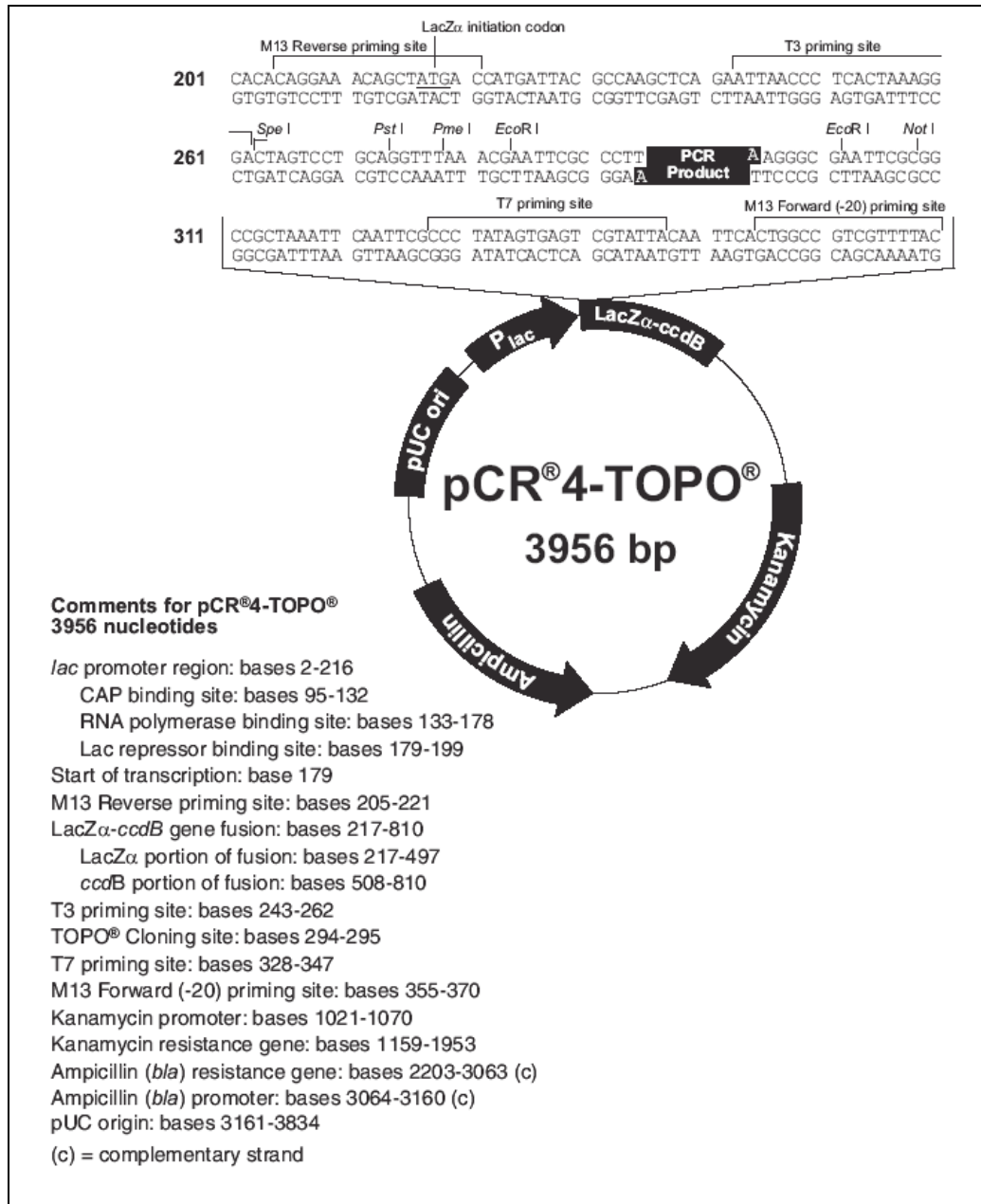
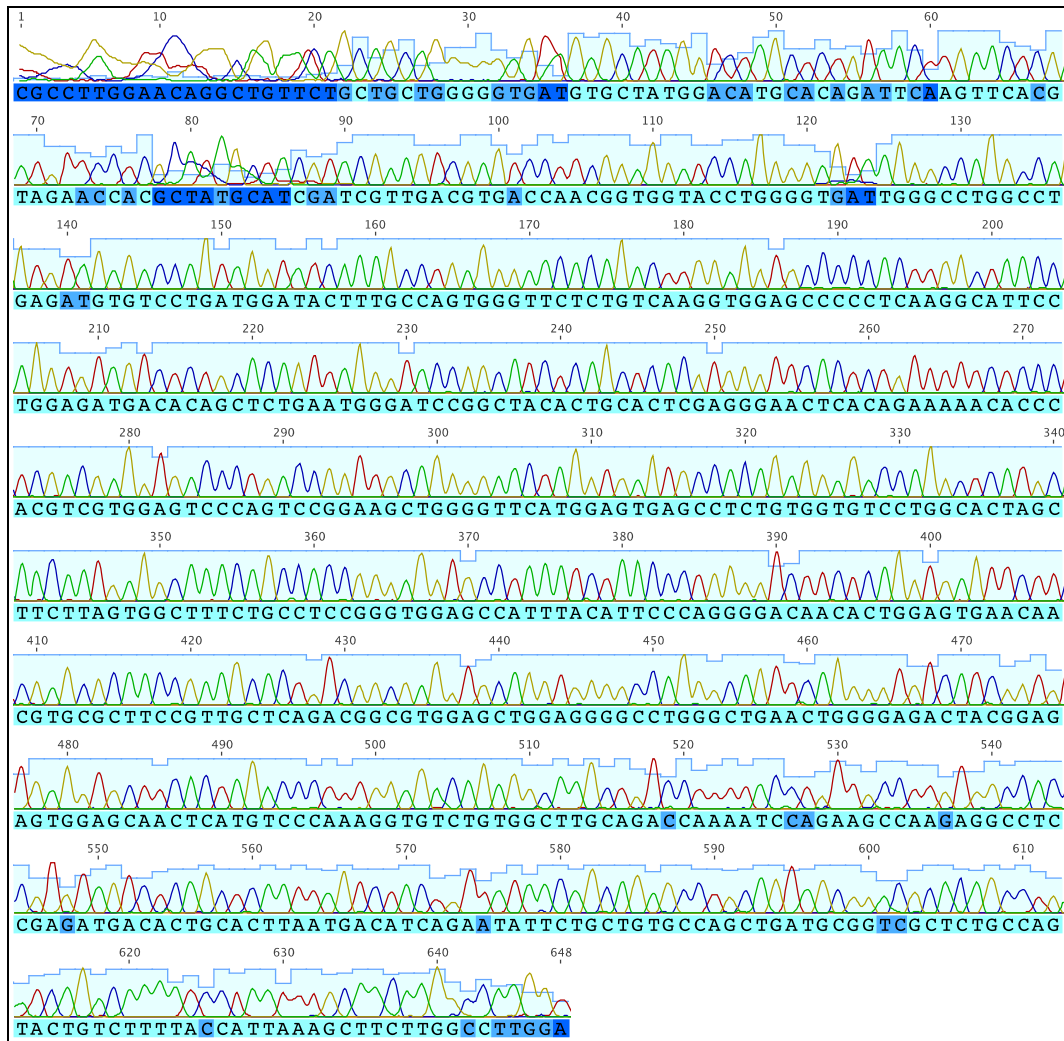


Figure 68: pCR<sup>®</sup>4-TOPO<sup>®</sup> cloning vector 3956bp long showing information from the supplier Invitrogen.

# APPENDIX THREE

## DNA SEQUENCING RESULTS



**Figure 69: Chromatogram of Forward PCR sequence result obtained from the UoW DNA Sequencing Facility (Hamilton, New Zealand) using an Applied Biosystems 3130xl Genetic Sequence Analyzer. The sequence was analysed using Applied Biosystems Software. The PCR product was produced from cDNA synthesized from mouse inner ear RNA using primer set BFG27/28, and purified using the rAPid Alkaline Phosphatase and sequenced using primer BFG27F. Figure shows the nucleotide peaks for each individual basecall from nucleotide 1-648 showing little background noise within the 90-510 base regions. Quality is indicated by the shading of each nucleotide; light blue represents good quality and dark blue, poor quality. Results indicate good quality of DNA sequencing with poor coverage of the 5' end.**



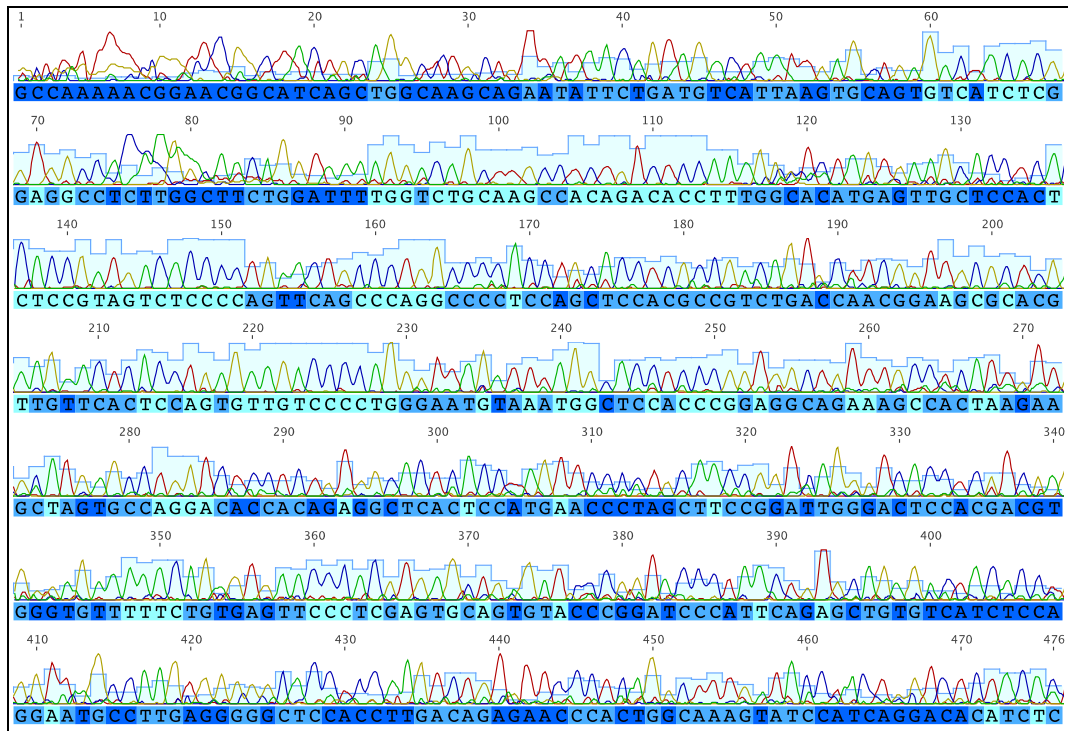


**Figure 70: Chromatogram of Reverse PCR sequence result obtained from the UoW DNA Sequencing Facility (Hamilton, New Zealand) using an Applied Biosystems 3130xl Genetic Sequence Analyzer. The sequence was analysed using Applied Biosystems Software. The PCR product was produced from cDNA synthesized from mouse inner ear RNA using primer set BFG27/28, and purified using the rAPid Alkaline Phosphatase and sequenced using primer BFG28R. Figure shows the nucleotide peaks for each individual basecall from nucleotide 1-475 showing high levels of background noise throughout the sequence. Quality is indicated by the shading of each nucleotide; light blue represents good quality and dark blue, poor quality. Results indicate poor quality of DNA sequencing with only a small amount of the PCR amplicon covered.**

**APPENDIX FOUR**  
**ANIMAL ETHICS APPROVAL**

## THE UNIVERSITY OF WAIKATO

APPLICATION TO THE ANIMAL ETHICS COMMITTEE  
FOR APPROVAL OF EXPERIMENTS ON ANIMALS

ANIMAL SPECIES: Mouse

NUMBER OF ANIMALS: to up to 100

STARTING DATE: May 2012

COMPLETION DATE: March 2013

1. (a) **Name of applicant:** Blaise Forrester-Gauntlett
- (b) **Position:** MSc Student
- (c) **Department:** Biological Sciences  
**/Address for Mailing)** Faculty of Science and Engineering  
Private Bag3105, Hamilton 3240, New Zealand
- (d) **Contact Phone number & email address:** Ext: 5110  
blaise\_erin@hotmail.com
- (e) **Qualifications and Experience:**  
BSc – Biological Sciences, University of Waikato, 2011
- (f) **Have you previously carried out related experiments?** No
- (g) **Other Personnel involved (including titles and roles):**  
  
Dr Linda Peters (MSc Supervisor)  
Mrs Olivia Patty (technician)  
Mr Bruce Patty (technician)  
Dr Seumas McCroskery (Honorary Research Fellow)  
Any changes in staff personal will be notified to the Animal Ethics Committee
2. **Title of Project:** Determine the developmental gene expression profile of vitelline outer membrane layer 1 (*vmo-1*) in the mouse auditory system
3. **Aim of Project (written in terms that people with a non-scientific background will understand):**  
  
The aim of the project is to determine the localization of vitelline membrane outer layer 1 protein (*vmo-1*) in the mouse auditory system. Dissected mouse tissue will be used to determine the presence and positioning of *vmo-1* in different cells at different developmental ages.
4. **Significance of this Project (written in terms that people with a non-scientific background will understand):**  
  
Vitelline membrane outer layer 1 gene (*vmo-1*) expression was discovered to be restricted exclusively to the mouse inner ear (Peters *et al.*, 2007). The function of this gene is currently unknown but is of interest because it is a candidate for being involved in human hearing loss and balance disorders.  
  
The mouse (*Mus musculus*) has been used extensively as an animal model to analyse the genetic and environmental causes of human hearing loss. The mouse ear is similar to that of humans and more easily accessible to study.  
  
Knowledge generated from this preliminary study will demonstrate where *vmo-1* protein is expressed in the auditory system and provide further insight into gene function and the mechanism of hearing.
5. **Is/Has this work already being/been carried out (provide details)**
- (a) **In New Zealand?** No
- (b) **Overseas?** No
6. **Have alternative methods to achieving the aims that do not involve the use of animals been explored?**  
The aims of this research project cannot be achieved without the use of animal tissue.

**7. How will the results of this work be disseminated?**

Through a publication in a scientific journal, conference presentation and MSc Thesis

**Description of Experiments**

**(a) Full details of procedures**

Animals: Male and Female mice of different ages. All animals will be housed in standard mouse housing conditions and fed standard food and water according to the Standard Operating Procedure 5(SOP5). Matings will be established to produce animals of specific developmental ages.

All animals will be sacrificed for dissection of ears and other tissues according to SOP9.

Bruce Patty will provide training with respect to matings, the procedures and how to use the equipment.

All experiments will be carried out on dissected dead tissue in order to extract/localize RNA, DNA or protein.

**(b) The statistical design of the experiments**

The experiments will be qualitative not quantitative.

**8. List the relevant SOP's (number and full title) to be used:**

**Housing/Care:** SOP Number: 5. The housing and care of domestic and wild rodents

**Euthanasia:** SOP Number: 9. Euthanasia of rodents by CO<sub>2</sub> asphyxiation

10. (a) **Where experiments will be conducted:** Rodents will be euthanized in the animal facility in BL05, tissue will be dissected out and then transferred to the C2 containment facility at the University of Waikato for further analysis.

(b) **Where the animals will be housed:** BL05

(c) **Person in immediate charge of laboratory and housing:** Bruce Patty

(d) **Veterinary advisor to the laboratory:** Gwyneth Verkerk

11. **Is there an operational procedure required for the use of a product (drug/chemical) in these experiments?** No

12. (a) **Anaesthetic:**

(b) **Method of Restraint:**

(c) **Will the animal have to recover from anaesthetic?**

(d) **How will you deal with post-operative pain and/or discomfort?**

(e) **What is the fate of the animals at termination of experiment?**

Animals will be euthanized and the tissue dissected for immunohistochemical and genetic analysis

14. **Has this application in whole or in part previously been declined approval by another Animal Ethics Committee?**

No

15. **For experiments to be undertaken at Ruakura or at other facilities under the control of another Animal Ethics Committee, has an application also been made to that Committee:**

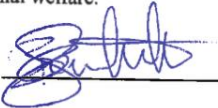
No

If 'YES' state which Committee \_\_\_\_\_

16. **Is any of this work being used in a thesis to be submitted for a degree at The University of Waikato?**

Yes

17. Are any permits (e.g. DOC) or approvals (e.g. Iwi) required? No
18. I have read and understand the conditions outlined in the Code of Ethical Conduct for the Use of Animals for Teaching and Research. Yes  
[http://www.waikato.ac.nz/research/unilink/uow\\_only/Approved%20Code%202010%20-%202014.pdf](http://www.waikato.ac.nz/research/unilink/uow_only/Approved%20Code%202010%20-%202014.pdf)
19. I have read the Good Practice Guide for the Use of Animals in Research, Testing and Teaching Yes  
<http://www.biosecurity.govt.nz/files/regs/animal-welfare/pubs/naeac/guide-for-animals-use.pdf>
20. Further conditions:  
 If this application is approved, I will inform the Committee of any changes in the project or unexpected outcomes affecting animal welfare, and any event (beyond any approved manipulation) impacting adversely on animal welfare.

Signed by the applicant:  Date: 26-3-12

I accept responsibility for this project's compliance with the University's Code of Ethical Conduct for the Use of Animals for Teaching and Research.

Signed by the Supervisor:  Date: 28/3/2012

I accept responsibility for this project's compliance with the University's Code of Ethical Conduct for the Use of Animals for Teaching and Research.

Approved/NOT approved .

Signed on behalf of the Committee:   
 (Chairperson)

Date: 20/04/12

## APPENDIX FIVE

### SPECIMEN AND TISSUES TYPE

**Table 18: Specimen and tissue type of mice used during the course of this research. Mice were euthanised using SOP#9 in the animal house at the UoW. Table shows the date of dissection, the age of the mice, what applications they were used for, whether animal ethics approval was needed and the approval number and the type of tissues extracted. Two ears were extracted from each adult (P28+) mouse unless otherwise stated. Where ethics approval was not required, mice were acquired from another study, in which the ears were donated from a deceased mouse and thus, did not require ethics approval**

<b>Date</b>	<b>Age</b>	<b>Application</b>	<b>Ethics approval needed</b>	<b>Tissue used</b>
7/12/11	P28+	Paraffin IHC	No	One ear, heart, spleen, liver, lung
7/12/11	P28+	Paraffin IHC	No	Ears
7/12/11	P28+	Paraffin IHC and protein extraction	No	Ears and full protein dissection
28/12/11	P28+	Protein extraction	No	Full protein dissection
28/12/11	P28+	Protein extraction	No	Ears, eyes, tear gland
28/12/11	P28+	Protein extraction	No	Ears, eyes, tear gland
28/12/11	P28+	Protein extraction	No	Ears, eyes, tear gland
12/01/12	P28+	Protein extraction	No	Full protein dissection
27/03/12	P28+	Protein extraction	No	Full protein dissection
30/03/12	P28+	Protein extraction	No	Full protein dissection
7/05/12	P28+	Protein extraction	No	Full protein dissection
7/06/12	P28+	RNA extraction	Protocol 853	Ears
7/06/12	P28+	RNA extraction	Protocol 853	Ears
7/06/12	P5	OCT IHC	Protocol 853	Head
7/06/12	P5	OCT IHC	Protocol 853	Head
7/06/12	P5	OCT IHC	Protocol 853	Head
7/06/12	P5	OCT IHC	Protocol 853	Head
8/06/12	P28+	RNA and protein extraction	Protocol 853	Ears and full protein dissection

Tissues dissected for full dissection included: adrenal gland, appendix, bladder, diaphragm, duodenum, gall bladder, heart, hypothalamus, kidney, liver, lumbar lymph node, lung, nose, ovaries, pancreas, small intestine, spleen, stomach, thymus, tongue and uterus.

## APPENDIX SIX

# STANDARD OPERATING PROCEDURE NINE

### UNIVERSITY OF WAIKATO ANIMAL ETHICS COMMITTEE STANDARD OPERATING PROCEDURE

SOP Number: 9

<b>Title:</b> Euthanasia of Rodents by CO <sub>2</sub> Asphyxiation
---

**\*\*Only persons that have received appropriate training and have been approved by the Animal Ethics Committee may perform this euthanasia\*\***

#### **General:**

This procedure outlines the general procedure for euthanizing rodents using CO<sub>2</sub> gas.

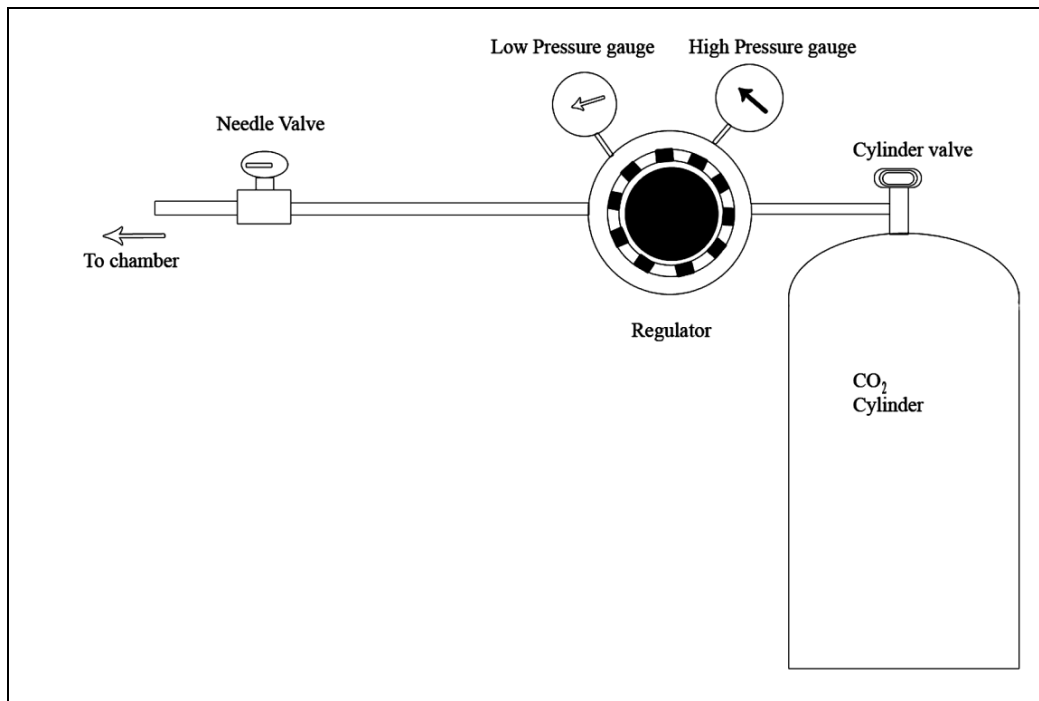
#### **Equipment Required:**

Building Animal House (Glasshouse compound) has a purpose built chamber connected to a CO<sub>2</sub> cylinder.

#### **Setup:**

Check with the Technician if there are any questions or concerns.

- Put the cage still containing the animal(s) directly in chamber. It is recommended that animals be euthanized in their 'home' cages. There has been less stress observed if the animal(s) are with familiar surroundings and smells.
- Ensure that the chamber lid is shut
- It is essential that there is adequate ventilation for the operator.
- Operation (see diagram):
  1. Ensure needle valve is closed
  2. Open cylinder valve one full turn
  3. Turn regulator until low pressure gauge reads "200"
  4. Slowly open needle valve 2 turns



- Once the concentration has caused the animal(s) to stop breathing, the CO<sub>2</sub> may be turned off but the chamber should remain closed for 10 minutes.
  1. Turn off cylinder valve
  2. Wait for pressure to drop
  3. Loosen off the regulator
  4. Close needle valve
- After 10 minutes open the chamber and ensure that the animals are dead. There should be an absence of breathing, no detectable heartbeat and glazed over eyes.

The chamber has a quite large volume and it may take some time for the level of CO<sub>2</sub> to rise up to and into the cage tray.

### **Alternatives:**

#### *Small numbers of animals:*

Where there are small numbers of animals involved, an effective method is to place the cage into a plastic bag and insert the gas hose into the bag and seal it off. Single animals may be euthanized in a clear lidded bucket that has the gas hose inserted. Food wrap or a clear plastic bag over the top works well.

#### *Dealing with large numbers of animals:*

The chamber can only fit a limited number of cages at once.

The operator:

- 1) can rotate the cages through (but chamber must be vented between batches; it is painful for the animals to be dunked straight into high CO<sub>2</sub> concentrations (ANZCART, 2006).
- 2) transfer the animals to as few cages as possible; operator must carefully check that the animals are all dead. Ones at the bottom of the pile may lie in air pockets.



3) let all animals run loose in the chamber (without cages). They will be too busy sniffing each other to notice the effects of the gas. The operator will then have to clean up the chamber afterward.

*Field work with wild animals:*

The chamber in the Animal House is not portable; therefore field euthanasia will have to involve the use of a small CO<sub>2</sub> cylinder, regulator, needle valve and plastic bag or a custom made chamber (or tube). Use a dark bag so not to stress out the animal further. Wild animal respond differently to CO<sub>2</sub> and may take longer to succumb than lab bred animals. **DO NOT** bring wild animals into Animal House for euthanizing without permission from the technician; wild animals carry diseases/parasites which could transmit to lab animals being housed in Animal House.

**Adverse Events and Unexpected Outcomes:** Occasionally animals have recovered consciousness and/or exhibited signs of life sometime after the procedure. They were not fully euthanized but the operator did not observe signs of life (**wait the full 10 minutes**). This possibly is due to the animal(s) being at the bottom of a pile and in a lower (insufficient) concentration of CO<sub>2</sub>. The animal(s) must be returned to the chamber (or bucket) without delay to complete the euthanasia.

**Occupational Safety and Health Considerations:** CO<sub>2</sub> gas is heavier than air. In confined spaces the gas displaces air and could cause asphyxiation to the operator in high concentrations. Ensuring ventilation during these operations is essential (i.e. open the doors and remain away from the chamber when possible, preferably outside). Asphyxiation symptoms may not be apparent and their onset may be quick. Refer to the MSDS for more information.

**Reference:**

ANZCART, 2006. Report of the International Consensus Meeting on Carbon Dioxide Euthanasia of Laboratory Animals. ANZCART News 19:2 1-7 *summarized* from the final report prepared by Hawkins, P *et al.* Copy available from: ([www.nc3rs.org.uk/CO2ConsensusReport](http://www.nc3rs.org.uk/CO2ConsensusReport) ).

**Versions and Reviews:**

<b>Date written:</b>	February 2007
<b>Author:</b>	Bruce Patty
<b>Date approved (AEC):</b>	Feb 2007
<b>Date approved (IDAO Validator):</b>	March 2007
<b>Reviewed:</b>	September 2010
<b>Review date:</b>	September 2013

# APPENDIX SEVEN

## GENETICALLY MODIFIED ORGANISMS

C2 Laboratories, Biological Sciences Department, UoW

Containment Manual, Version 6.5 issued on 17-02-12

### Form for Lab records of New Organisms Register of GMOs

Developed in Facility Number 759

HSNO ACT APPROVAL No. APP201152 UOW Appl. No: GMD101146\_\_\_\_\_

PROJECT: Developmental gene expression profile of *Vmol* in the mouse auditory system

P.C.LEVEL: 1 Additional Controls: \_\_\_\_\_

Researcher: Blaise Forrester-Gauntlett

\*Project Leader/Supervisor: Dr. Linda Peters

Host Species and Strain: *E. coli* strain DH5 $\alpha$

Vector: pBluescript/pProExHtb/pET42a Insert DNA: Mouse *Vmol*

Species of donor of nucleic acids: *Mus musculus*

Note: all records must be dated and initialled. Continue on a new page if necessary.

DATE	NAME OF GMO Assign a code and number	STORAGE DETAILS Specify fridge or freezer	TRANSFER DETAILS Reg. No. of sending/receiving facility	DISPOSAL DETAILS Specify method used
07-08-12	BFG001		NA	Autoclave
15-08-12	BFG002		NA	Autoclave
20-09-12	BFG003		NA	Autoclave
03-10-12	BFG004		NA	Autoclave
24-10-12	BFG005		NA	Autoclave
15-11-12	BFG006 – pProEX Htb in <i>E. coli</i>	4°C fridge plates -20°C glycerol stock	NA	
15-11-12	BFG007– pET42a in <i>E. coli</i>	4°C fridge plates -20°C glycerol stock	NA	
20-11-12	BFG008– pBluescript in <i>E. coli</i>	4°C fridge plates -20°C glycerol stock	NA	

Info transferred to electronic record (date) 26-11-12 by (name) Judith Burrows.

# APPENDIX EIGHT

## COMPARATIVE GENOMICS ANALYSIS

Unless otherwise stated comparative genomic analysis was carried out using Geneious® R6 created by Biomatters. Available online from <http://www.geneious.com/>.

### Sequence Alignments

Multiple and Pairwise alignments were carried out using ClustalW (Kyoto University Bioinformatics Center) and Geneious software <http://www.genome.jp/tools/clustalw/>

### BLAST and Database searching

The following databases were used to investigate the genomics of *Vmo1* and collect information on HL:

- A [BioGPS - http://biogps.org/#goto=welcome](http://biogps.org/#goto=welcome)
- B Chicken Genome –  
<http://www.ncbi.nlm.nih.gov/projects/genome/guide/chicken/>  
<http://genome.ucsc.edu/cgi-bin/hgGateway?clade=vertebrate&org=Chicken&db=0&hgsid=67521880>
- C COSMIC - Catalogue of Somatic Mutations in Cancer  
<http://cancer.sanger.ac.uk/cancergenome/projects/cosmic/>
- D dbSNP - Single nucleotide polymorphism database  
<http://www.ncbi.nlm.nih.gov/projects/SNP/>
- E Ensembl - joint project between EMBL - EBI and the Welcome Trust Sanger Institute  
<http://www.ensembl.org/index.html>
- F EMBL - European Molecular Biology Laboratory  
<http://www.ebi.ac.uk/embl/>
- G GenBank – National institute of health genetic sequence database  
<http://www.ncbi.nlm.nih.gov/>
- H Hereditary hearing loss homepage  
<http://hereditaryhearingloss.org/main.aspx?c=.HHH&n=86162>

- I Human Genome  
<http://www.ncbi.nlm.nih.gov/genome/guide/human/>  
<http://genome.ucsc.edu/cgi-bin/hgGateway?hgsid=346698985&clade=mammal&org=Human&db=0>
- J IKMC - International Knockout Mouse Consortium -  
<http://www.knockoutmouse.org>
- K Mouse Genome –  
<http://www.ncbi.nlm.nih.gov/projects/genome/guide/mouse/>  
<http://genome.ucsc.edu/cgi-bin/hgGateway?clade=vertebrate&org=Mouse&db=0&hgsid=67521880>
- L NCBI - National centre for biotechnology information  
[http://blast.ncbi.nlm.nih.gov/Blast.cgi?CMD=Web&PAGE\\_TYPE=BlastHome](http://blast.ncbi.nlm.nih.gov/Blast.cgi?CMD=Web&PAGE_TYPE=BlastHome)
- M NEB - New England biolabs  
<https://www.neb.com>
- N NHLBI - National Heart, Lung, and Blood Institute  
<http://www.nhlbi.nih.gov>
- O RefSeq - Reference sequence database  
<http://www.ncbi.nlm.nih.gov/RefSeq/>
- P SCOP - Structural classification of proteins  
<http://scop.mrc-lmb.cam.ac.uk/scop/>
- Q Signal peptide  
<http://www.cbs.dtu.dk/services/SignalP/>
- R TPA - Third party annotation database  
<http://www.ncbi.nlm.nih.gov/genbank/tpa/>

### **Molecular weight prediction**

The theoretical molecular weight of proteins was predicted using the Swiss Institute of Bioinformatics Resource Portal (ExPASy) “Compute pI/Mw” tool.  
[http://web.expasy.org/compute\\_pi/](http://web.expasy.org/compute_pi/)

### **mRNA translation**

mRNA transcript translation was carried out using ExPASy and Geneious software

<http://www.expasy.org/tools/dna.html>

### **Primer analysis**

PCR primer analysis was carried out using IDT OligoAnalyzer 3.1 and Oligo-Calc

<http://www.idtdna.com/analyzer/applications/oligoanalyzer/>

<http://www.basic.northwestern.edu/biotools/oligocalc.html>

### **Primer design**

PCR primers were designed using Primer-BLAST on the NCBI website

(<http://www.ncbi.nlm.nih.gov/tools/primer-blast/>)

### **Trypsin Digestion Prediction**

The theoretical digestion of proteins using Trypsin was calculated using the ExPASy “PeptideMass” tool.

[http://web.expasy.org/peptide\\_mass/](http://web.expasy.org/peptide_mass/)